

2002

# High Temperature Compression Testing of an Advanced Carbon-Carbon Composite in an Oxidizing Atmosphere

Joshua C. Walls

Follow this and additional works at: <http://digitalcommons.library.umaine.edu/etd>



Part of the [Mechanical Engineering Commons](#)

---

## Recommended Citation

Walls, Joshua C., "High Temperature Compression Testing of an Advanced Carbon-Carbon Composite in an Oxidizing Atmosphere" (2002). *Electronic Theses and Dissertations*. 296.  
<http://digitalcommons.library.umaine.edu/etd/296>

This Open-Access Thesis is brought to you for free and open access by DigitalCommons@UMaine. It has been accepted for inclusion in Electronic Theses and Dissertations by an authorized administrator of DigitalCommons@UMaine.

HIGH TEMPERATURE COMPRESSION TESTING OF AN  
ADVANCED CARBON-CARBON COMPOSITE IN AN  
OXIDIZING ATMOSPHERE

By

Joshua C. Walls

B.S. University of Maine, 2000

A THESIS

Submitted in Partial Fulfillment of the

Requirements for the Degree of

Master of Science

(in Mechanical Engineering)

The Graduate School

The University of Maine

May, 2002

Advisory Committee:

Vincent Caccese, Associate Professor of Mechanical Engineering, Advisor

Donald Grant, Chairman and Richard C. Hill Professor of Mechanical Engineering

Michael Peterson, Assistant Professor of Mechanical Engineering

Senthil Vel, Assistant Professor of Mechanical Engineering

## LIBRARY RIGHTS STATEMENT

In presenting this thesis in partial fulfillment of the requirements for an advanced degree at The University of Maine, I agree that the Library shall make it freely available for inspection. I further agree that permission for "fair use" copying of this thesis for scholarly purposes may be granted by the librarian. It is understood that any copying or publication of this thesis for financial gain shall not be allowed without my written permission.

Signature:



Date:

5/9/02

# HIGH TEMPERATURE COMPRESSION TESTING OF AN ADVANCED CARBON-CARBON COMPOSITE IN AN OXIDIZING ATMOSPHERE

By Joshua C. Walls

Thesis Advisor: Dr. Vincent Caccese

An Abstract of the Thesis Presented  
in Partial Fulfillment of the Requirements for the  
Degree of Master of Science  
(in Mechanical Engineering)  
May, 2002

Compression testing of an advanced, three-dimensional weave, carbon-carbon composite was performed from room temperature to 2192°F (1200°C) in an oxidizing environment. The material tested is primarily used for missile nose cones and rocket nozzles. A test system and test method was developed for performing high temperature compression testing and techniques were developed for machining the material to minimize fiber damage and maintain accurate tolerances. Test specimens were cut from a block of the test material in the three principal fiber orientations, and off-axis tests were cut at 45° orientations to each principal fiber direction. The specimens were tested by direct end loading using custom made, ceramic test fixtures, permitting the determination of the compressive modulus and ultimate compressive strength for each principal fiber direction and an approximation of the ultimate shear strength based on the off-axis tests. To document the materials oxidation rate an oxidation study was also performed at temperatures in excess of 1112°F (600°C).

The results demonstrate that the structural integrity of the material was maintained from room temperature to 1472°F (800°C), while moderate oxidation was observed from room temperature to 1472°F (800°C) and severe oxidation occurred above 1472°F (800°C). Based on the data from the oxidation results, the compression test data generated for the 1472°F (800°C) tests was corrected to account for material loss during each test due to oxidation. The compression test results also demonstrated material symmetry along two of the principal fiber orientations.

## **ACKNOWLEDGMENTS**

This project would not have been possible without the sponsorship of Applied Thermal Sciences Inc. of Sanford, Maine and funding provided by the Maine Space Grant Consortium. The author would like to thank Dr. Vince Caccese for his support as an advisor, and his graduate committee, Dr. Donald Grant, Dr. Michael Peterson, and Dr. Senthil Vel. The assistance of Arthur Pete, the coordinator for Crosby Lab, is also greatly appreciated. The author would finally like to thank his parents and Rebecca Potter for their enduring support throughout this project.

# TABLE OF CONTENTS

|                      |     |
|----------------------|-----|
| ACKNOWLEDGMENTS..... | ii  |
| LIST OF TABLES.....  | vi  |
| LIST OF FIGURES..... | vii |

## Chapter

|  |    |
|--|----|
| 1. OVERVIEW.....   | 1  |
| 1.1 – Introduction .....   | 1  |
| 1.2 – Objectives.....  | 4  |
| 1.3 – Scope of Work.....   | 4  |
| 1.4 – Literature Review.....   | 5  |
| 1.5 – Review of Pertinent ASTM Standards.....                                    | 14 |
| 2. – TEST METHOD.....  | 23 |
| 2.1 – Test Method Overview.....  | 23 |
| 2.2 – Test Method and Specimen Design.....                                       | 25 |
| 2.3 – Test Specimen Preparation.....   | 27 |
| 2.4 – High Temperature Test Fixtures.....  | 29 |
| 2.4.1 – Alumina Platens.....   | 31 |
| 2.4.2 – Test Fixture Base.....   | 36 |
| 2.4.3 – Procedure for Installing the Test Fixtures in the<br>MTS Load Frame..... | 38 |

|   |     |
|---|-----|
| 2.5 – Furnace and Temperature Control.....          | 40  |
| 2.5.1 – Furnace.....                                | 40  |
| 2.5.2 – Temperature Control.....                    | 41  |
| 2.5.2.1 – Temperature Control Program.....          | 42  |
| 2.5.2.2 – Digital/Analog Interface.....             | 47  |
| 2.6 – Instrumentation and Data Acquisition.....     | 49  |
| 2.7 – Proof Tests.....                              | 52  |
| 2.7.1 – Test Specimens.....                         | 53  |
| 2.7.2 – Proof Test Results.....                     | 56  |
| 2.7.2.1 – Stainless Steel Test Results.....         | 57  |
| 2.7.2.2 – Carbon-Carbon Results.....                | 58  |
| 2.7.2.3 – Summary of Carbon-Carbon Proof Tests..... | 61  |
| 3. – ATS CARBON-CARBON TESTS.....                   | 63  |
| 3.1 – Test Specimens.....                           | 63  |
| 3.2 – Test Procedure.....                           | 71  |
| 3.3 – Oxidation Study.....                          | 74  |
| 3.4 – Test Results.....                             | 82  |
| 3.4.1 – In-Plane Tests.....                         | 85  |
| 3.4.2 – Off-Axis Tests.....                         | 98  |
| 4. – CONCLUSIONS AND RECOMENDATIONS.....            | 104 |
| 4.1 – Conclusions.....                              | 104 |
| 4.2 – Recommendations and Future Work.....          | 107 |
| BIBLIOGRAPHY.....                                   | 108 |



|  |     |
|--|-----|
| APPENDICES.....  | 109 |
| Appendix A. – High Temperature Control Source Code for the ‘Universal<br>Temperature Control Program’ (Delphi 5) ..... | 109 |
| Appendix B. – Temperature Control Box Parts List.....  | 125 |
| Appendix C. – ATS Test Specimen Locations.....   | 126 |
| Appendix D. – Test Specimen Data.....  | 129 |
| Appendix E. – Test Matrix.....   | 132 |
| Appendix F. – Test Data Sheet.....   | 135 |
| Appendix G. – Individual In-Plane Compression Test Results.....  | 136 |
| Appendix H. – Individual Off-Axis Compression Test Results.....  | 160 |
| Biography of the Author .....  | 169 |

## LIST OF TABLES

|  |     |
|--|-----|
| Table 2.1 – Thermal and Mechanical Properties of Rescor 960 .....                  | 31  |
| Table 2.2 – Thermal and Mechanical Properties of the Fully Fired Alumina.....      | 33  |
| Table 2.3 – P.I. Tuning Constants .....  | 46  |
| Table 2.4 – Proof Test Specimen Test Temperatures .....                            | 53  |
| Table 2.5 – Mechanical Properties for the Carbon-Carbon Proof Test Specimens ..... | 55  |
| Table 2.6 – Carbon-Carbon Proof Test Specimen Dimensions .....                     | 55  |
| Table 2.7 – Summary of Proof Test Results .....                                    | 59  |
| Table 3.1 – Preliminary Test Plan .....  | 66  |
| Table 3.2 – X-Direction Test Results .....   | 90  |
| Table 3.3 – Y-Direction Test Results .....   | 91  |
| Table 3.4 – Z-Direction Test Results .....   | 92  |
| Table 3.5 – Summary of the Average In-Plane Results .....                          | 93  |
| Table 3.6 – Summary of the Off-Axis Test Results .....                             | 102 |
| Tables A.1 – Set Point Form Computer Code (Caccese, Walls, 2001).....              | 109 |
| Tables A.2 - Set Point Data Form Computer Code (Caccese, Walls, 2001).....         | 120 |
| Table B.1 – Parts List .....   | 125 |
| Table D.1 – Dimensions, Weight and Density .....                                   | 129 |
| Table E.1 – Test Matrix .....  | 132 |

## LIST OF FIGURES

|   |    |
|---|----|
| Figure 2.1 – Photograph of the Test Setup .....   | 24 |
| Figure 2.2 – Schematic of the Test Setup and Temperature Control Hardware.....                                  | 24 |
| Figure 2.3 – Photograph of the MK Diamond Wet Saw .....   | 28 |
| Figure 2.4 – Photograph of the South Bay Technology Wet Saw .....   | 29 |
| Figure 2.5 – Sketch of High Temperature Test Fixture .....  | 30 |
| Figure 2.6 – One of the Damaged Alumina Platens .....   | 32 |
| Figure 2.7 – Photograph of the Lower Load Platen with the Aremco Insert .....                                   | 33 |
| Figure 2.8 – Photograph of the Upper Load Platen with the Aremco Insert Bonded<br>In Place .....                | 34 |
| Figure 2.9 – Detailed Drawing of the Test Fixture Base .....  | 37 |
| Figure 2.10 – Backside of Furnace with Thermocouples .....  | 41 |
| Figure 2.11 – Screen Capture of the ‘Universal Temperature Control Program’<br>Front End .....                  | 42 |
| Figure 2.12 – Screen Capture of the Input Portion of the ‘Universal Temperature<br>Control Program’ .....       | 43 |
| Figure 2.13 – Screen Capture of the P.I. Tuning Portion of the ‘Universal<br>Temperature Control Program’ ..... | 46 |
| Figure 2.14 – Control Box for the MTS Furnace .....   | 48 |
| Figure 2.15 – Inside of the Control Box .....   | 48 |
| Figure 2.16 – MTS High Temperature Extensometer .....   | 50 |
| Figure 2.17 – Extensometer Affixed to the Alumina Inserts .....   | 51 |
| Figure 2.18 – Extensometer Mounting Configuration .....   | 52 |

|   |    |
|---|----|
| Figure 2.19 – Carbon-Carbon Proof Test Geometry .....   | 55 |
| Figure 2.20 – Fractured Test Fixture .....  | 57 |
| Figure 2.21 – Stainless Steel Test Specimens After Testing .....  | 58 |
| Figure 2.22 – Proof Test Stress-Strain Curves .....   | 59 |
| Figure 2.23 – Linear Stress Strain Relation for CC02-HT .....   | 60 |
| Figure 2.24 – Severe Oxidation of CC01-HT .....   | 61 |
| Figure 3.1 – Test Specimen Geometry .....   | 63 |
| Figure 3.2 – Top Face of the ATS Carbon-Carbon Block .....  | 64 |
| Figure 3.3 – Bottom Face of the ATS Carbon-Carbon Block .....   | 65 |
| Figure 3.4 – Carbon Block Coordinate System and Dimensions .....  | 65 |
| Figure 3.5 – Model for Cutting the Carbon-Carbon Block .....  | 67 |
| Figure 3.6 – Location of Z-Direction Test Specimens .....   | 67 |
| Figure 3.7 – Sections Cut from the ATS Carbon-Carbon Block .....  | 69 |
| Figure 3.8 – Clamp for Cutting the Off-Axis Specimens .....   | 70 |
| Figure 3.9 – Format of the Test Matrix .....  | 71 |
| Figure 3.10 – Specimen Oxidation at 2192°F (1200°C) .....   | 75 |
| Figure 3.11 – Oxidation Test Setup .....  | 76 |
| Figure 3.12 – Percent Loss of Mass, Cross Sectional Area, and Volume Due to<br>Oxidation at 1112°F (600°C) .....  | 78 |
| Figure 3.13 - Percent Loss of Mass, Cross Sectional Area, and Volume Due to<br>Oxidation at 1472°F (800°C) .....  | 79 |
| Figure 3.14 - Percent Loss of Mass, Cross Sectional Area, and Volume Due to<br>Oxidation at 1832°F (1000°C) ..... | 79 |

|   |     |
|---|-----|
| Figure 3.15 – Oxidation Rates for Mass Loss .....                 | 80  |
| Figure 3.16 – Oxidation Rates for Cross Sectional Area Loss ..... | 80  |
| Figure 3.17 – Local and Principal Coordinate System .....         | 83  |
| Figure 3.18 – Typical X-Direction Stress-Strain Curve .....       | 86  |
| Figure 3.19 – Typical Y-Direction Stress-Strain Curve .....       | 86  |
| Figure 3.20 – Typical Z-Direction Stress-Strain Curve .....       | 87  |
| Figure 3.21 – Specimen End Crushing .....                         | 88  |
| Figure 3.22 – Specimen Shear Failure .....                        | 88  |
| Figure 3.23 – X-Direction Modulus, Room Temperature .....         | 94  |
| Figure 3.24 – X-Direction Modulus, 1112°F (600°C) .....           | 94  |
| Figure 3.25 – X-Direction Modulus, 1472°F (800°C) .....           | 95  |
| Figure 3.26 – Y-Direction Modulus, Room Temperature .....         | 95  |
| Figure 3.27 – Y-Direction Modulus, 1112°F (600°C) .....           | 96  |
| Figure 3.28 – Y-Direction Modulus, 1472°F (800°C) .....           | 96  |
| Figure 3.29 – Z Direction Modulus, Room Temperature .....         | 97  |
| Figure 3.30 – Z-Direction Modulus, 1112°F (600°C) .....           | 97  |
| Figure 3.31 – Z-Direction Modulus, 1472°F (800°C) .....           | 98  |
| Figure 3.32 – Typical XY-Plane Stress-Strain Curve .....          | 99  |
| Figure 3.33 – Typical XZ-Plane Stress-Strain Curve .....          | 99  |
| Figure 3.34 – Typical YZ-Plane Stress-Strain Curve .....          | 100 |
| Figure 3.35 – Typical Off-Axis Shear Failure .....                | 101 |
| Figure 3.36 – Typical Matrix Failure .....                        | 101 |
| Figure 3.37 – Shear Strength as a Function of Temperature .....   | 103 |

|  |     |
|--|-----|
| Figure C.1 – X-Direction Test Specimens .....      | 126 |
| Figure C.2 – Y-Direction Test Specimens .....      | 126 |
| Figure C.3 – Z-Direction Test Specimens .....      | 127 |
| Figure C.4 – XZ-Plane Test Specimens .....         | 127 |
| Figure C.5 – YZ-Plane Test Specimens .....         | 128 |
| Figure C.6 – XY-Plane Test Specimens .....         | 128 |
| Figure G.1 – X-Direction Stress-Strain Curves..... | 136 |
| Figure G.2 – Y-Direction Stress-Strain Curves..... | 144 |
| Figure G.3 – Z-Direction Stress-Strain Curves..... | 152 |
| Figure H.1 – XZ-Plane Stress-Strain Curves.....    | 160 |
| Figure H.2 – YZ-Plane Stress-Strain Curves.....    | 163 |
| Figure H.3 – XY-Plane Stress-Strain Curves.....    | 166 |

## **1. OVERVIEW**

### **1.1 Introduction**

The popularity of advanced carbon-carbon composites for engineering design continues to increase as improvements in the manufacturing processes and material properties are made, and the price of the material continues to decrease. A few applications of carbon-carbon composites include commercial aircraft brake components, racecar brake components, missile nose cones, rocket nozzles, high temperature fasteners, and even biomedical devices. One of the attributes of carbon-carbon composites is the material's ability to maintain excellent mechanical properties at temperatures in excess of 5432°F (3000°C) in a non-oxidizing environment or when protected from oxidation by coating the outer surface (Peters, 1998). As a comparison, superalloys can only withstand temperatures of around 2190°F (1200°C) (Chung, 1994).

As the use and applications of carbon-carbon composites increases, the need for characterizing the mechanical properties of the material through testing also increases, which necessitates testing at high temperatures to evaluate the materials performance. One of the most common tests used for evaluating the high temperature performance of carbon-carbon composites is the flexure test. This is primarily because of the relatively simple test specimen geometry and test fixture design that permits ceramics to be used in the construction of the test fixtures. However, the flexure test cannot be used to determine the strength and stiffness data required for design purposes. The uniaxial tensile test is the optimum test for determining the mechanical properties of carbon-carbon at high temperature. However, the major disadvantage of high temperature tensile

testing is the extreme difficulty in applying a tensile load to the material. Many of the gripping systems that have been developed for high temperature testing utilize cylindrical test specimens and are not suitable for laminated composites (Savage, 1993). Gripping inside of the furnace is not normally feasible because there are very few materials that can maintain structural integrity in tension at the temperatures that carbon-carbon composites can withstand. Tests have been performed at temperatures as high as 3632°F (2000°C), which is well beyond what most alloys can withstand. Cold gripping outside of the furnace with liquid cooled grips is much more feasible, but requires specimens long enough to extend outside of the furnace. The major problem with this method is that a large temperature gradient is induced in the specimen and great care must be taken to prevent failure in the temperature transition region (Savage, 1993).

A viable alternative to high temperature tensile testing is the uniaxial compression test. Inexpensive and readily available ceramic materials can be used to construct test fixtures, similar to the flexure test, because the test fixtures can be designed to only sustain compressive loads. Ceramics tend to exhibit excellent high temperature characteristics and compressive properties, but are typically poor in tension due to their brittle nature. Though the compression test may be markedly more simple at high temperatures than the tension test, difficulties still arise. Achieving a uniform load distribution in the test specimen, accurate strain measurement, and, as with any high temperature testing, equipment cooling and durability are just a few of the issues that must be addressed for successfully conducting high temperature compression testing.



#### **1.4 Literature Review**

A literature review was performed to investigate current techniques for testing advanced composite materials at high temperature, and room temperature. Particular issues of interest for this review include test specimen geometry, cutting and machining techniques, and test fixture design and configuration. The review includes journal articles, handbooks, and other reference books relative to the objectives of this effort.

Savage (1993) gives an overview of the entire engineering spectrum of carbon-carbon composites. The topics covered in his text include: an introduction to carbon materials; manufacturing processes including the gas phase impregnation of carbon-carbon, thermosetting matrix resin procedures, thermoplastic matrix procedures and oxidation protection; mechanical testing of carbon-carbon materials; test sample preparation; and applications of carbon-carbon materials.

Carbon-carbon composites and polymer matrix composites are susceptible to fiber damage during machining. To avoid fiber damage composites should be machined using water-cooled, high-speed diamond-impregnated grinding wheels. Savage (1993) stresses that great care must also be taken to align the specimen properly when cutting since the mechanical properties of composites are highly dependent on fiber orientation. If the test specimen requires the use of bonded end-tabs, Savage (1993) recommends that the tabs should be affixed prior to any cutting or machining.

Methods summarized by Savage (1993) for static testing of carbon-carbon composites include: the tensile test, flexure test, and interlaminar shear strength test. A short section on high temperature mechanical testing is also included. The tensile test is used for determining the principal engineering properties of a carbon-carbon laminate. Straight-sectioned specimens with bonded end-tabs are often used to prevent failure at the grip interface. The stress-strain curve for carbon-carbon can sometimes be non-linear. Therefore the tensile modulus is calculated at a specific strain value,

$$E_{11} = \text{secant modulus at } S\% \text{ longitudinal strain.}$$

The major Poisson's ratio may be defined as,

$$\nu = \text{transverse strain/longitudinal strain at } S\% \text{ longitudinal strain.}$$

To evaluate the flexural properties of a composite laminate, a three or four point flexure test is performed. Savage (1993) recommends using the three-point flexure test when testing high modulus materials such as carbon-carbon. Flat specimens should be used with a span/depth ( $l/d$ ) ratio high enough to ensure a failure in bending and to reduce the effects of interlaminar shear deformation. Savage provides a table of the minimum  $l/d$  for three different fiber orientations. The flexural modulus,  $E_f$ , and the flexural stress,  $\sigma_f$ , for the three point bending test is defined as:

$$\sigma_f = 3Pl/2bd^2 \quad (1)$$

$$E_f = l^3m/4bd^3 \quad (2)$$

Where  $P$  is the applied load,  $l$  is the length between the two lower load heads,  $b$  is the width of the test specimen,  $d$  is the thickness of the specimen, and  $m$  is the slope of the tangent to the initial straight line portion of the load deflection curve. The flexural modulus for the four point bending test is defined as:

$$\sigma_f = 3Pl/4bd^2 \quad (3)$$

$$E_f = 0.21l^3m/bd^3 \quad (4)$$

The major disadvantage of the flexure test for composite materials is that it is possible to have several failure modes; compression, tension, shear, or a combination of failure modes. Flexure testing is also more susceptible to surface flaws, which typically will result in conservative results.

The interlaminar shear strength of composite materials is an important life-limiting failure mode to consider in the design process. Savage (1993) recommends using a shortened span, three point bending test as one method to evaluate the interlaminar shear strength. The details of this test are described in ASTM D2344. The interlaminar shear strength (ILS) is defined as:

$$ILS = 3P/4bd \quad (5)$$

The failure mode for this test must be single or multiple shear or plastic deformation with evidence of shear for the test to be valid. However, Savage (1993) also points out that the validity of this will be questionable because carbon-carbon composites usually contain numerous flaws.

Adams (1998) provides a detailed guide of various test methods and fixtures for mechanical testing of composite materials including tension, compression and shear testing. Summarized are the three current compressive loading techniques in use today include: shear loading through end tabs; direct end loading; and flexural loading of a

sandwich beam. All of the test methods that Adams discusses are for room temperature testing. However, many of the ideas presented are relevant to high temperature testing.

Compression testing by shear loading is usually accomplished by using inverted wedge grips. ASTM D3410 describes two test fixtures for use with shear loading; the Celanese and IITRI test fixtures. The Celanese test fixture utilizes conical wedge grips while the IITRI test fixture employs rectangular wedge grips. With both test fixtures it is important to maintain the proper slenderness ratio of the test specimens. If the test specimen is too thick the bonded taps may shear off or the specimen may slip in the wedge grip. If the specimen is too thin column buckling will likely occur. ASTM D3410 provides all necessary guidelines for test specimen configuration.

The major disadvantage to the Celanese fixture is that it is inherently unstable. This is because the test fixture utilizes two split cones at each end of the test fixture to generate the necessary clamping force. The fixture may become unstable due to seating problems of the conical wedges in the test fixture base if the specimen is slightly too thin or slightly too thick. The IITRI test fixture eliminates the instability problem associated with the Celanese fixture by using rectangular wedge grips. The disadvantage to this fixture is that it must be much more massive than the Celanese fixture because of the less efficient stress transfer from the fixture base to the wedge grips.

Adams (1998) also introduces a modified Celanese test fixture developed by Wyoming Test Fixtures that is not covered in any of the ASTM standards. The modified fixture

was developed as a compromise between the unstable, but lightweight Celanese fixture and the more versatile, but heavy IITRI test fixture. The fixture utilizes a flat wedge face similar to the IITRI fixture but also incorporates tapered cylindrical wedges. This combination still allows for the surface contact area between the fixture base and the wedges to be independent of the specimen thickness. The result is a test fixture that has the versatility of the IITRI fixture with size and weight characteristics similar to that of the Celanese fixture.

Perhaps the simplest method of applying a compressive load to a test specimen is by directly loading the specimen through its ends. Adams (1998) suggests that this method is feasible for materials of relatively low compressive strengths of 100-ksi (700-Mpa) or less. For stronger or brittle materials end crushing may result. The specimens should also have a constant cross section because any attempt to dog-bone or taper the specimens in the center of the gage length to induce failure will likely result in shear off of the enlarged section of the specimen; reducing the specimen to a constant cross sectional specimen. Adams (1998) suggests that it may be possible to slightly dog-bone some materials, but as the material becomes more highly orthotropic the tendency for shear off of the enlarged ends increases.

For materials with a compressive strength less than 100-ksi (700-Mpa) Adams recommends using the Wyoming end-loaded, side-supported compression test fixture. The fixture is designed to apply a compressive stress to the specimen by direct end loading of a relatively thin, straight-sided specimen. The test specimens for this test are

typically only 0.040-in (1-mm) thick and have a gage length of only 0.188-in (4.8-mm) to prevent column buckling. The use of such a small test specimen combined with bonded end tabs does not allow enough space for strain gages or other instrumentation. To alleviate this problem two tests are typically conducted; one using the bonded end tabs to obtain the ultimate strength and a second test without the end tabs to allow enough space to affix a strain gage, or other strain measuring device.

Another method in current use is to bond the test specimen to a core material of relatively low compressive stiffness. The bonded core material provides lateral stiffness to prevent column buckling of the specimen and allow for a specimen gage length of sufficient size for instrumentation. However, this method may not be feasible for elevated temperature testing.

The last test method Adams discusses for compression testing is the sandwich beam flexure test. In this test a compressive failure is achieved by making the tension side of the panel significantly stronger than the compressive side. This test method is not commonly used due to the large size and cost associated with the test specimens. Another concern with this test method is that the core may artificially increase the compressive strength of the material being tested.

Gyekenesi (1998) discuss the steps undertaken to create a high temperature material testing facility at NASA Lewis Research Center. Two systems were developed, one for testing in atmospheric conditions at temperatures up to 1550°C (2820°F), and a second

system for testing materials in an inert atmosphere at temperatures up to 1700°C (3100°F). Both systems consist of a 22 kip screw actuated universal tensile testing frame, a resistance element-heated furnace, pneumatic grips isolated outside of the furnace environment and water cooled, a mechanical extensometer to measure strain, and thermocouples to monitor temperature.

The high temperature testing facility at the NASA Lewis Research Center was constructed and used to study uniaxial silicon carbide fiber reinforced reaction bonded silicon nitride (SiC/RBSN) and an enhanced tri-axially woven silicon carbide fiber reinforced silicon carbide. The materials were exposed to high temperatures in air for up to four hours, but they showed negligible changes in moduli. Young's modulus showed an overall decrease as the temperature rose, with its slowest decrease between 800°C (1470°F) and 1400°C (2550°F). The first matrix cracking stress decreased from 600°C (1110°F) to 800°C (1470°F), and then showed a very small change to 1400°C (2550°F).

Singh (1993) reports the results of testing a monolithic zircon ceramic, a zircon ceramic matrix uniaxially reinforced with continuous SiC fibers, and a zircon ceramic matrix uniaxially reinforced with continuous BN-coated SiC fibers, over a temperature range of 25°C to 1500°C (77°F to 2732°F). The tests were performed using a three-point bending test fixture constructed from a thoriated-tungsten material. The tests were conducted using a high-temperature furnace in a flowing Ar-2%H<sub>2</sub> atmosphere. Temperatures were measured using a W-Re thermocouple placed near the specimen and the temperature of the furnace was controlled by the use of a programmable digital controller. The tests

were performed. A universal testing machine was used with a crosshead travel rate of  $0.0127\text{-cm min}^{-1}$ . In each case, four samples were tested at room temperature to establish baseline properties. Subsequently, high temperature tests were conducted and the results compared to the room temperature tests. After testing, failed specimens were examined using a scanning electron microscope.

The report details many of the ideas involved in failure theory of composites. An important idea investigated is the first-matrix cracking stress. The first-matrix cracking stress is the stress at which the composite's matrix exhibits the first sign of cracking, and is typically used for the design stress. Any stress at or beyond this point can cause irreversible damage to the composite. One method to investigate the first-matrix cracking phenomenon is mechanical testing.

Kuramada and Sato (1989) discuss the results obtained from testing two kinds of carbon felt reinforced carbon composites containing pitch carbon fibers and PAN carbon fibers. Tensile tests and fracture toughness tests were performed from room temperature up to  $2400^{\circ}\text{C}$  ( $4352^{\circ}\text{F}$ ). Thermal shock tests were also performed on a disk specimen (30-mm diameter and 3-mm thickness) to measure the thermal shock resistance.

The tests were conducted using an Instron load frame, with a high temperature furnace with graphite coil heaters. The furnace had an outer diameter of 300-mm (11.8-in), height of 600-mm (23.6-in), and power 30 kW. Type CA thermocouples were used at temperatures less than  $1000^{\circ}\text{C}$  ( $1832^{\circ}\text{F}$ ) to monitor the temperature of the test specimens.



Above 1000°C (1832°F) the temperature of the test specimens was measured using optical high-temperature and radiation thermometers from outside of the furnace through an aperture of the high temperature coils. The type of atmosphere the tests were conducted in was not specified.

The test specimens consisted of a dog-boned geometry for both the tensile test and the fracture toughness test with an overall length of 150-mm (5.90-in). The enlarged ends of the test specimens were 30-mm (1.18-in) wide with 12-mm (0.472-in) holes drilled at the enlarged ends for applying the load. The gage length for the tensile test specimens was 15-mm (0.591-in) with a gage thickness of 5-mm (0.197-in), while the gage length for the fracture toughness specimens was 30-mm (1.18-in) with a gage thickness of 15-mm (0.591-in). A small notch with a radius less than 0.2-mm (0.008-in) was made in the gage length of the fracture toughness specimen. The test fixtures were constructed of graphite MF306-3, and PAN-series carbon-carbon composite was used for the pins.

Senet (1991) presents testing of 2-D discontinuous carbon-carbon composites from room temperature to 1650°C (3002°F) in an argon atmosphere to investigate the materials fracture toughness. The tests were conducted to develop isothermal crack growth resistance and fracture toughness as a function of temperature. The carbon-carbon examined in this study was designed for high performance aircraft brakes. A three-point bending test fixture constructed of SiC was used to apply load to the test specimens in conjunction with a screw driven load frame. The test specimens consisted of both single-edge notch beam and chevron-notch beam specimen geometry with a length of

60-mm (2.362-in), and a square cross section of 10-mm (0.394-in). Room temperature modulus of rupture tests were also conducted using unnotched specimens.

Tests were performed at room temperature 650°C (1202°F), 1050°C (1922°F), 1400°C (2552°F), and 1650°C (3002°F) with an argon backfilled furnace. To minimize the oxidation of the specimen the argon inlet tubes were directed toward the loading surfaces and the notch.

### **1.5 Review of Pertinent ASTM Standards**

Though there are no ASTM standards that apply directly to the testing of carbon-carbon composites, or that apply to compression testing at elevated temperatures, there are several ASTM standards that are relevant to this effort:

- ASTM D 695 – 96 Standard Test Method for Compressive Properties of Rigid Plastics
- ASTM 3410/D3410M – 95 Standard Test Method for Compressive Properties of Polymer Matrix Composite Materials with Unsupported Gage Section by Shear Loading
- ASTM 3518M-94 Standard Test Method for In-Plane Shear Response of Polymer Matrix Composite Materials by Tensile Test of a  $\pm 45^\circ$  Laminate
- C 1359-96 Standard Test Method for Monotonic Tensile Strength Testing of Continuous Fiber-Reinforced Advanced Ceramics with solid rectangular Cross-Section Specimens at Elevated Temperatures
- E 1319-89 (Reapproved 1996) Standard Practice for High Temperature Strain Measurement

## **ASTM D 695 – 96 Standard Test Method for Compressive Properties of Rigid**

### **Plastics**

This standard details the test method for determining the compressive properties of rigid plastics and high modulus composites. The significance of this standard for this effort are the specifications for applying a compressive load by means of direct end loading, and the recommendations for test specimen geometry, size and dimension tolerances. ASTM recommends that the compression tool used for applying the load should be constructed to axially load the test specimen within 1:1000 and surfaces of the test fixture should be flat within 0.001-in and parallel to each other normal to the loading axis. A supporting jig is also recommended for thin specimens.

The test specimens shall have the geometry of a right cylinder or prism having a length of twice the principal width or diameter. Additional geometries are also recommended for testing of rod material, tubes, and laminates in the form of sheets, but are not relative to this effort. The ends of the test specimens where the load is applied should be flat and parallel within 0.001-in. and have sharp, clean edges.

The number of test specimens recommended by ASTM is five for each sample for an isotropic material and five specimens for each axis of anisotropy. Specimens that fail at obvious flaws should be discarded.

**ASTM D 3410/3410M – 95 Standard Test Method for Compressive Properties of Polymer Matrix Composite Materials with Unsupported Gage Section by Shear**

**Loading**

This standard details the test method for determining the in-plane compressive properties of polymer matrix composite materials and is limited to composites that are orthotropic in nature with respect to the load axis of the material. The procedures outlined in this standard are for using wedge grips to apply a compressive load through shear using specimens with or without tabs.

Two test procedures are described in this standard; procedure 'A' employs conical wedge grips and procedure 'B' employs rectangular wedge grips. The test fixture in procedure 'A' is much smaller, but is prone to seating problems between the conical wedges and the fixture base. Procedure 'B' eliminates the seating problems of procedure 'A' but is substantially larger in size.

The test specimens for this procedure should have a constant rectangular cross section with a width variation of no more than  $\pm 1\%$  and a thickness variation of no more than  $\pm 4\%$ . The width and thickness of the test specimens are specified according to two different procedures; one for using conical wedge grips and one for using rectangular wedge grips. The specimen dimensions for use with the conical wedge grips must have a thickness of 0.15-in. and a width of 0.25-in. The rectangular wedge grips allow for variations in the width and thickness of the test specimen. Bonded resistance strain gages or extensometers are recommended for measuring the strain. ASTM recommends

measuring strain in the axial direction on opposite faces of the specimen to allow for the detection of column buckling. At least five specimens should be tested for each test condition unless valid results can be obtained using fewer specimens.

**ASTM D 3518M-94 Standard Test Method for In-Plane Shear Response of Polymer Matrix Composite Materials by Tensile Test of a  $\pm 45^\circ$  Laminate**

This standard details the test method for determining the in-plane shear response of polymer matrix composites with fibers oriented at  $\pm 45^\circ$  with respect to the load direction. Because there is in-plane normal stress component is present with this test, a pure state of shear is not possible. Therefore the true shear strength values can not be obtained from this test.

The shear stress is calculated using the following equation:

$$\tau_{12} = \frac{P}{2 \cdot A} \quad (7)$$

Where P is the applied axial tension load and A is the cross sectional area. The corresponding shear strain,  $\gamma_{12}$ , is determined by:

$$\gamma_{12} = \epsilon_x - \epsilon_y \quad (8)$$

Where  $\epsilon_x$  is the axial strain and  $\epsilon_y$  is the lateral strain. The chord shear modulus of elasticity can be determined over the lower, strain range of 1500-2500  $\mu\epsilon$  and is determined by:

$$G_{12\text{chord}} = \frac{\Delta\tau_{12}}{\Delta\gamma_{12}} \quad (9)$$

**ASTM C 1359 - 96 Standard Test Method for Monotonic Tensile Strength Testing of Continuous Fiber-Reinforced Advanced Ceramics with solid rectangular Cross-Section Specimens at Elevated Temperatures**

This standard details the test method for determining the tensile properties of continuous fiber, reinforced advanced ceramic composites at elevated temperature. This test method applies to uni-directional, bi-directional, tri-directional and other multi directional reinforcements as well as glass matrix composites. There are no temperature limitations presented for the application of this standard.

ASTM suggests that the tests be performed in an inert environment or at a sufficiently high loading rate so as to minimize the effects of slow crack growth. They also emphasize the importance of testing materials in an atmosphere similar to operating conditions. If testing is conducted in an ambient air atmosphere, the relative humidity should be monitored throughout the test.

Data acquisition is also addressed in the standard. The recording devices must be accurate to within plus or minus one percent of the selected range for the testing system including the readout unit. The data acquisition system should have a sample rate of 10 Hz with a response of 50 Hz.

The dimensions of the test specimen should be measured to within plus or minus 0.02 mm and they have to be measured by a device with an accuracy of plus or minus 0.01

mm. A minimum of five test specimens is needed for the statistical purpose of calculating means.

If thermocouples are used to monitor the temperature, ASTM suggests that for a specimen gage length of 25-50 mm, at least two should be used. One should be positioned at each end of the gage length. If the gage length is greater than 50 mm, a third thermocouple should be placed near the center of the specimen.

Once the furnace has been brought up to the operating temperature, the test should not commence until the engineer is sure that the test specimen has reached equilibrium. This could also be thought of as the time necessary for the strain measuring devices to stabilize. This “hold time” should not be greater than thirty minutes. As with any tensile testing of a material, the load cell and extensometer must be zeroed before the test begins.

**ASTM E 1319-89(Reapproved 1996) Standard practice for High Temperature Strain Measurement**

This standard covers the use of strain gages for the measurement of strain at temperatures ranging from 425 to 650°C (800 to 1200°F). The techniques described in this standard may be applicable to temperatures outside of the specified temperature range. Several factors must be considered when selecting a high temperature strain gage including operating temperature, strain range, strain rate, test duration, test environment, strain gradient, uncertainty factor, space requirement, and the effects of the strain gage on the test article. No one particular gage may meet all the requirements of a certain test,

therefore certain test objectives may have to be compromised. ASTM provides guidelines in this standard for evaluating uncertainties due to gage selection.

Strain gage selection for a particular application must meet the specified conditions of the test. ASTM describes the capability of four types of currently available strain gages, namely wire and foil free-filament gages, weldable resistance strain gages, differential capacitance strain gages, and variable capacitance strain gages.

Wire and foil free-filament gages have a temperature limit of approximately 400°C (750°F) for static conditions and approximately 1250°C (2280°C) for certain dynamic conditions. Problems with bonding of these strain gages may arise for certain specimens and structures.

Weldable resistance strain gages generally employ an active wire strain element sealed inside of a steel tube with a highly compacted ceramic powder to transfer the strain energy from the tube to the active gage. To attach the strain tube to a test specimen a mounting flange is welded to the strain tube and then welded to the test specimen. The temperature limit for these gages is typically 500°C (932°F).

Differential capacitance strain gages measure the strain in the test specimen by changes in capacitance. To compensate for temperature changes a compensating rod is used which has similar thermal expansion characteristics to those of the test specimen. Thermocouples are connected to both the test specimen and the gage to allow for



computing correction factors if there is a difference between the temperature of the compensating rod and the temperature of the surface of the test specimen. Differential capacitance strain gages are generally designed to operate over the full temperature range of this standard, 425°C to 650°C (800°F to 1200°F).

Variable capacitance strain gages are a single capacitor, variable capacitance instrument that measures strain in the test specimen by the relative movement of two electrodes. This type of gage produces a nonlinear output with respect to strain and typically has a working range of 10 micro-strain. To reduce error caused by thermal expansion, the thermal expansion coefficients of the gage and the specimen should be matched as closely as possible. Variable capacitance strain gages also generally operate over the full temperature range of this standard.

Due to the temperature limitations of commercially available high temperature strain gages, these gages are not a viable means of measuring strain for this effort. Other limitations, such as the physical size of most commercially available strain gages and the method of attaching these gages, also prohibits the use of high temperature strain gages in this effort.

The literature review and ASTM Standard review provides an essential background of current techniques associated with this effort for developing high temperature testing techniques. Though many of the techniques and methods currently in use do not directly apply to this effort, the methods and standards presented provide a useful guide to determine the best methods for testing carbon-carbon at high temperatures such as: load rate, loading techniques, strain measurement, and test specimen geometry.

## **2. TEST METHOD**

### **2.1 Test Method Overview**

This section presents the design and development of a high temperature test setup for compression testing from room temperature to 1200°C (2282°F). Conducting compression tests at high temperatures presents several problems: constructing test fixtures that can withstand both high temperatures and high compressive stresses, accurate strain measurement, equipment cooling, and accurate temperature control. Furthermore, there are considerations that must be made with regard to the material being tested, such as manufacturing of the test specimens and potential loss of material due to oxidation.

All tests are performed using a 110,000-lb capacity, MTS load frame in conjunction with a 22,000-lb load cell. Figure 2.1 is a photograph of the high temperature test setup with the furnace open to display the complete test fixtures and Figure 2.2 is a schematic of the test apparatus. The test fixtures required for these tests utilize two forms of alumina, which is a high strength ceramic, and water cooling for the base of the fixtures to maintain a safe operating temperature of the load frame grips. The strain measurement is accomplished using a high temperature extensometer that incorporates quartz extension rods and air-cooling. A computer program written with Delphi 5 was developed specifically for controlling the temperature of the MTS furnace, and is used in conjunction with a Daqbook and custom-made control box.

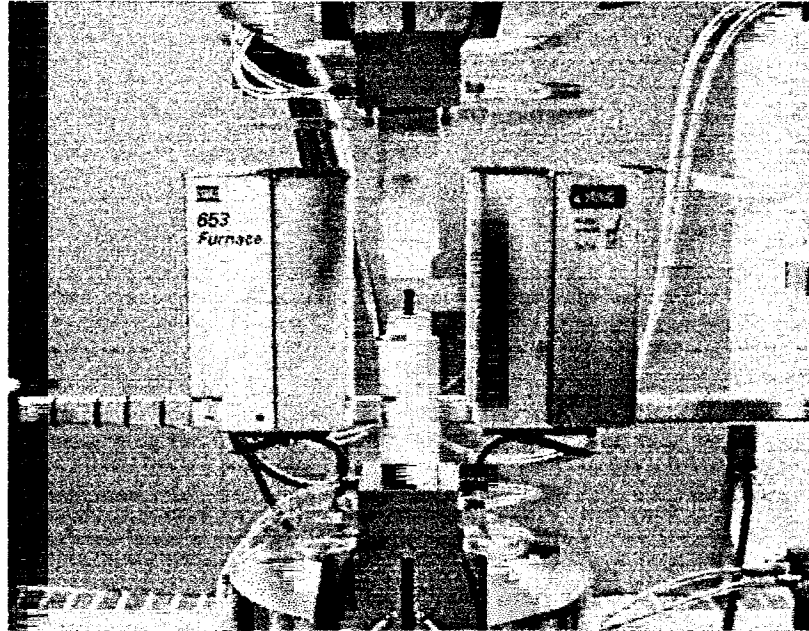


**Figure 2.1 – Photograph of The Test Setup**

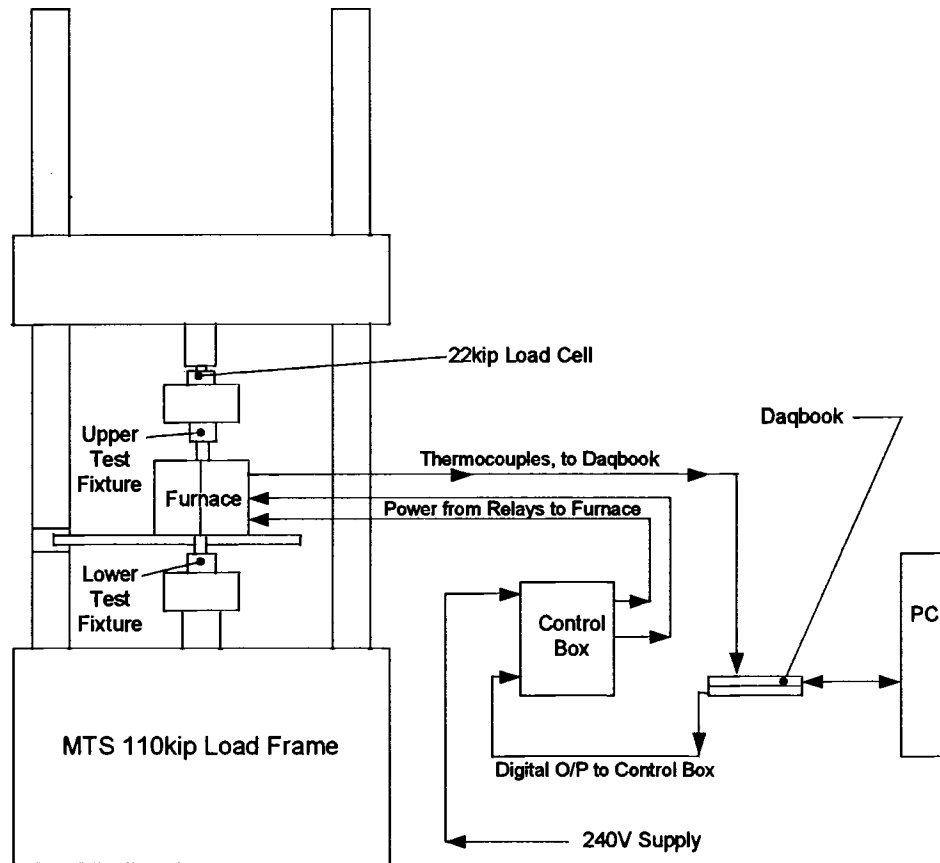


**Figure 2.2 – Schematic of The Test Setup and Temperature Control Hardware**

## **2.2 Test Method and Specimen Design**

Test method and specimen design plays a crucial role in obtaining accurate compression test results. There are no direct standardized testing procedures for carbon-carbon composites. However, there are numerous references in the form of journal articles, conferences, books, and several ASTM standards that can be used as a guide for developing a successful test specimen design and test procedure, as discussed in Sections 1.4 and 1.5.

For the test specimen geometry a rectangular, constant cross section design is chosen. The primary reason for using a constant cross sectional specimen is because with a highly orthotropic material any effort made to dog-bone or reduce the area of the specimen in the center to induce failure will likely result in shear-off of the enlarged ends (Adams, 1998). The shear off reduces the specimen to a straight-sided specimen; therefore it makes sense to start with a straight-sided specimen. ASTM D 695 standard for end-loaded compression testing of rigid plastics is used as a reference for determining the appropriate length of the test specimen. This standard specifies a length for cylindrical and prismatic specimens of twice the specimen's principal width or diameter.

There are several different methods for applying a compressive load that are currently used: shear loading through end tabs, direct end loading, a combination of both shear loading and end loading, and sandwich-beam flexure loading (Adams, 1998). The combination of both end loading and shear loading through tabs achieves the most favorable stress distribution (Peters, 1998) however, the high temperature testing

conditions for this effort prohibit any practical means of affixing tabs to the test specimen. The method of sandwich-beam flexure loading is also impractical due to the large specimen size, and complexity of fabrication. After considering all of the common methods for compressive loading, the most practical method for this effort is determined to be direct end loading.

Direct end loading is, by far, the simplest method for applying a compressive load. However, great care must be taken in preparing the test specimen and constructing the test fixtures to achieve a uniform stress state. ASTM D 695 is the only standard that is suitable for end loaded compressive testing. The standard specifies that the loading be applied axially within 0.001-in. and that the loading surfaces be flat and parallel within 0.001-in. Section 2.4 describes in detail how the compression test fixture is designed, and aligned in the load frame to meet these specifications. ASTM D 695 also specifies that the test specimen ends be smooth, flat, and parallel within 0.001-in.

A consideration for determining the load rate for this effort is oxidation at high temperatures. If a load rate that is too slow is used, the time required to run the test may be long enough to allow a substantial amount of oxidation to occur. Based on experience with working with and testing composite materials and recommendations from ASTM standards and Savage (1993), an initial load rate of 0.005 in/min is chosen for the proof test specimens.

ASTM D 695, for compression testing of rigid plastics, specifies a load rate of 0.01 in/min and ASTM D 3410, for compression testing by shear loading of polymer matrix composites, specifies a load rate of 0.05 in/min. Both of these standards are relevant to this effort however, the standards do not directly address testing of carbon-carbon composites. Subsequently, the load rates defined are too high. Savage (1993) recommends a strain rate of 0.5% per minute for tensile testing of carbon-carbon composites, which is a more reasonable recommendation for carbon-carbon. To determine if the chosen load rate of 0.005 in/min is comparable to Savage's recommendations, the results of the proof test specimens are used to calculate a strain rate. For the proof test specimens the load rate of 0.005 in/min resulted in a strain rate of approximately 0.3 – 0.7% strain per minute. The strain rate was also verified for the ATS test specimens and averaged 0.3 – 1.0% strain per minute.

### **2.3 Test Specimen Preparation**

To avoid fiber damage when cutting the test specimens, all specimen preparation is done using water lubricated, diamond impregnated wheel saws. Figure 2.3 is a photograph of the MK Diamond model MK-101 professional series tile saw used for making the initial rough cuts of the tests specimens. The MK Diamond is a high speed, 10-in diameter wheel saw that operates at a constant speed of 1450 RPM. Though a fairly high level of precision can be obtained with this saw, it cannot achieve the stringent tolerances required for the load surfaces of the test specimens. The finish cuts for the test specimens are made using a high precision, low speed diamond wheel saw. Figure 2.4 is a

photograph of the South Bay Technology model 650 wheel saw. The saw incorporates a variable speed motor, which permits a wheel speed range of 0 – 300 RPM. The cutting wheel used in conjunction with the South Bay saw was a four-inch diameter, 0.012-inch thick, high concentration diamond wheel. Precise specimen positioning in the saw is accomplished by an integrated micrometer with increments of 0.001-in. After each test specimen is cut the length and cross sectional dimensions are measured using a pair of dial Vernier calipers incremented to 0.001-in. Each test specimen is also weighed using an Acculab Pocket Pro model 250-B digital scale with a readout of  $\pm 0.1$ -g.

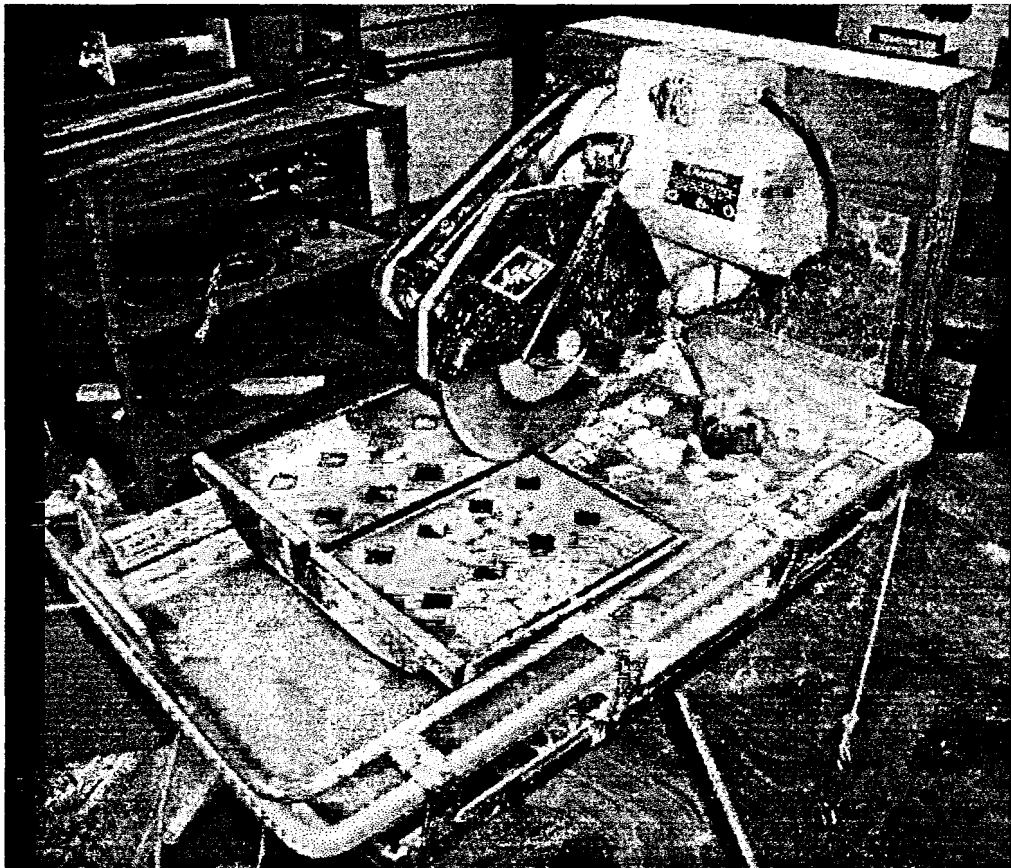


**Figure 2.3 – Photograph of the MK Diamond Wet Saw**



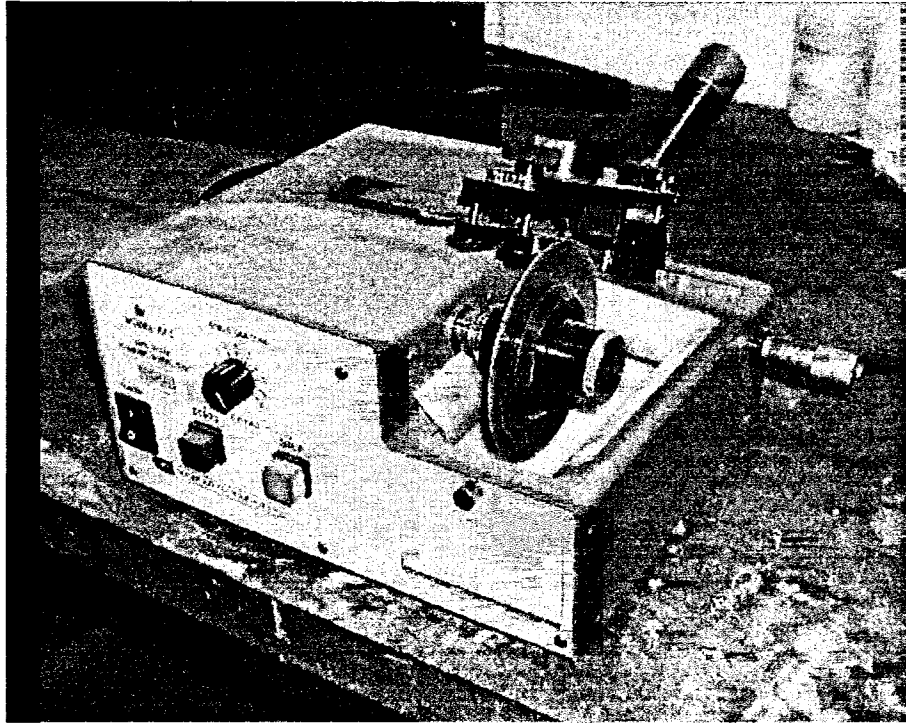


**Figure 2.4 – Photograph of the South Bay Technology Wet Saw**

#### **2.4 High Temperature Test Fixtures**

A sketch of the high temperature test fixtures is shown in Figure 2.5. To apply a compressive load to the test specimens at high temperatures the fixtures must exhibit high compressive strength from room temperature to 1200°C (2192°F). Temperatures this high do not allow for the use of steel or other common structural alloys. However, many ceramic materials exhibit excellent high temperature characteristics and compressive properties.

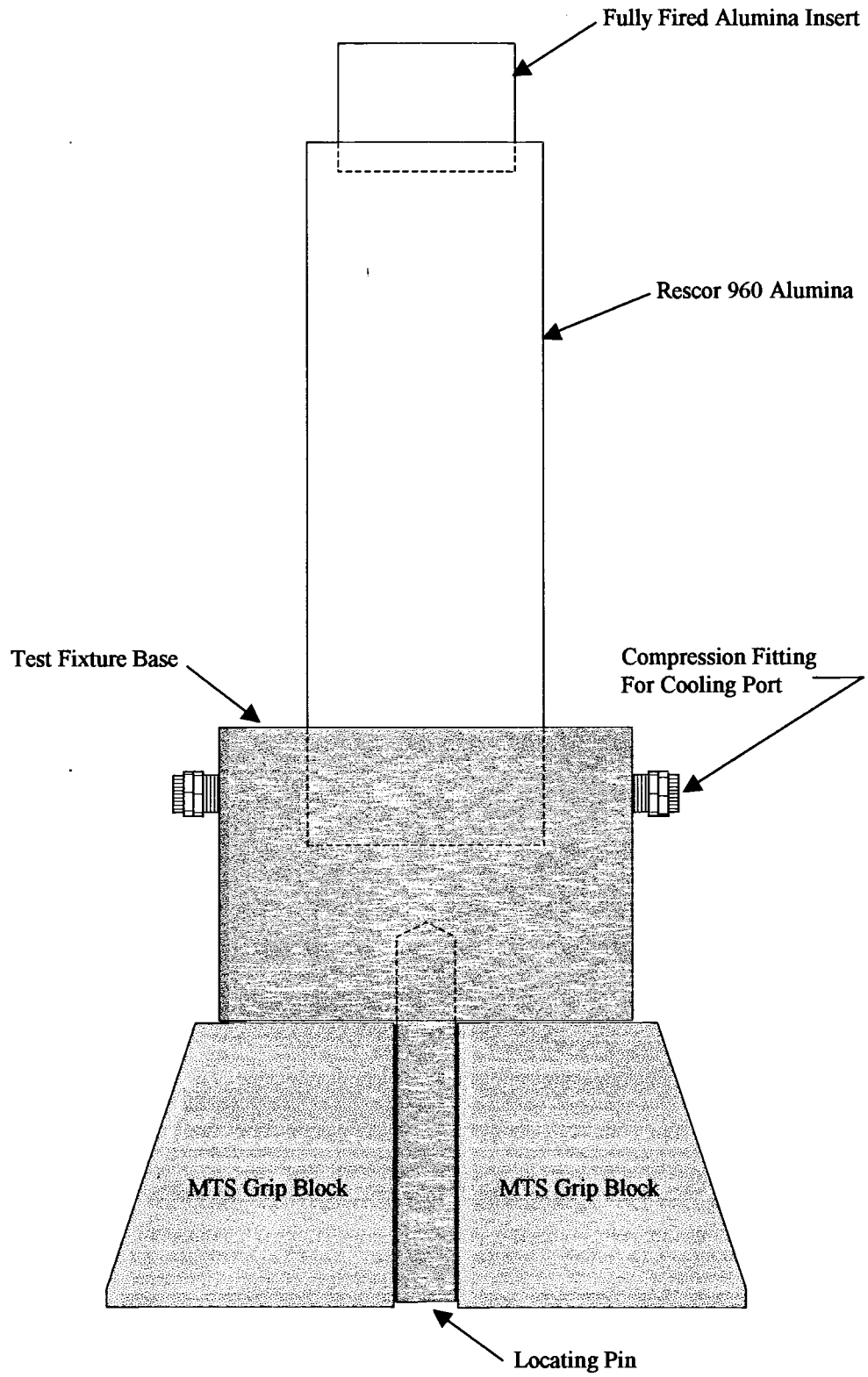


**Figure 2.5 – Sketch of High Temperature Test Fixture**

### 2.4.1 Alumina Platens

The load platens for the test fixtures are fabricated from two-inch diameter, solid rod, Rescor 960 alumina manufactured by Cotronics Corporation. Rescor 960 can be easily machined with carbide tooling and exhibits excellent mechanical and thermal properties, with a summary given in Table 2.1.

**Table 2.1 – Thermal and Mechanical Properties of Rescor 960**

|  |              |
|--|--------------|
| Max Operating Temp, °F (°C)                              | 3000 (1649)  |
| Melting Point, °F (°C)                                   | 3400 (1871)  |
| Thermal Expansion $\times 10^{-6}/^{\circ}\text{F}$ (°C) | 4.3 (7.7)    |
| Compressive Strength, psi (Mpa)                          | 60,000 (414) |
| Flexural Strength, psi (Mpa)                             | 38,000 (262) |

Though Rescor 960 exhibits excellent compressive properties, it was found to be too soft during one of the carbon-carbon proof tests (CC01-HT) at 1000°C (1832°F). The proof test specimen heavily oxidized during the warm-up period of the furnace and by the time the test was begun only a small amount of the original material remained. When a load was applied to the specimen, small impressions 0.120-in. deep by 0.175-in. in diameter were made in the alumina platens. A picture of the damaged lower platen is shown in Figure 2.6. It was determined that the damage occurred because the Rescor 960 is not a fully fired ceramic with a porosity of around 10%.

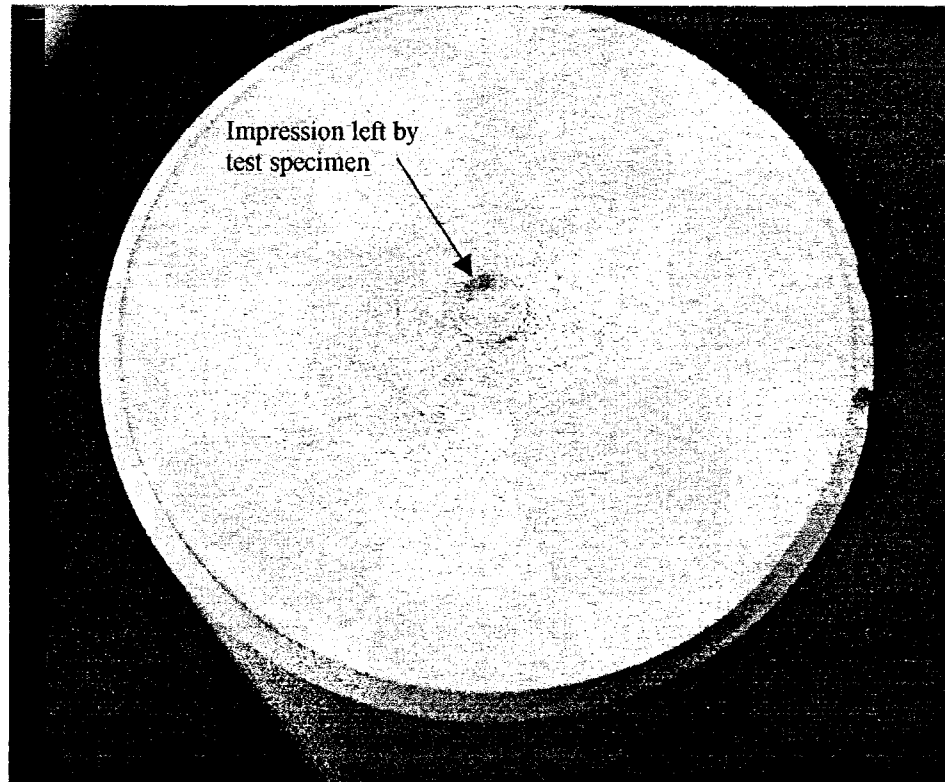


**Figure 2.6 – One of the Damaged Alumina Platens**

To solve the problem of the alumina becoming too soft at elevated temperatures, fully fired alumina inserts with 0% porosity are used at the end of each platen. Aremco Products Inc. fabricated the inserts, with the specifications for the material summarized in Table 2.2. When alumina is fully fired its density, hardness and compressive strength increases substantially; the compressive strength of the Aremco alumina is 340,000-psi where the Rescor alumina has a compressive strength of 60,000- psi The fully fired, alumina inserts are a 1.50-in. diameter solid cylinder by 1.00-in. high and rest in a bored hole at the end of each of the alumina platens. Figure 2.7 is a photograph of the Aremco alumina insert positioned on the Rescor alumina rod of the lower test fixture. For the upper test fixture, the insert must be bonded to the Rescor alumina rod to prevent the

insert from falling out when there is no load on the test fixture. Figure 2.8 is a photograph of the upper platen with the insert bonded in place. The adhesive used to bond the insert to the upper platen is Thermeez Ceramic Putty produced by Cotronics. The adhesive putty is rated for continuous use up to 2300°F (1260 °C) and has a melting point of 3200°F (1760 °C).

**Table 2.2 – Thermal and Mechanical Properties of the Fully Fired Alumina**

|  |                |
|--|----------------|
| Max Operating Temp, °F (°C)                              | 3000 (1649)    |
| Thermal Expansion $\times 10^{-6}/^{\circ}\text{F}$ (°C) | 3.5 (6.3)      |
| Compressive Strength, psi (Mpa)                          | 340,000 (2344) |
| Flexural Strength, psi (Mpa)                             | 46,000 (317)   |
| Hardness, Moh's Scale                                    | 9.0            |

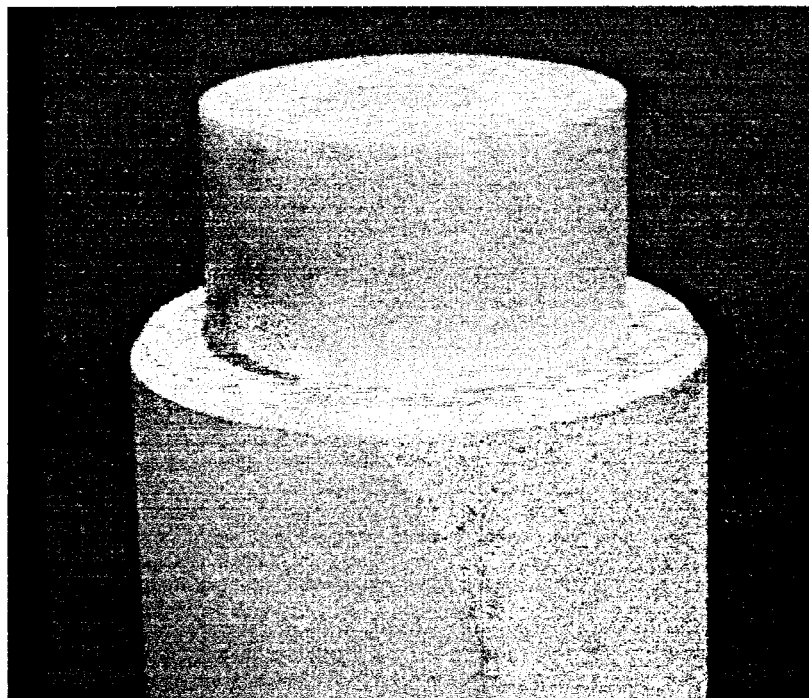


**Figure 2.7 – Photograph of the Lower Load Platen with the Aremco Insert**



**Figure 2.8 – Photograph of the Upper Load Platen with the Aremco Insert Bonded In Place**

To insure that the adhesive putty does not effect the axial and parallel alignment of the Aremco inserts, and to insure that a secure bond is achieved the following procedure is used:

1. With both test fixtures secured in the MTS load frame, place one of the fully fired alumina inserts into the bored hole on top of the lower platen.
2. Place the second insert on top of the first insuring that both of the extensometer slots are properly lined up. (Section 2.6)
3. Turn on the MTS hydraulics and set the control mode to 'Force.' It is also recommended that the upper compressive limit is set to 1000 – 1500 lbs to avoid

accidental damage to the alumina platens in the event that one of the inserts is misaligned.

4. Adjust the crosshead of the load frame so that the end of the upper alumina platen is close enough to the lower platen to allow contact when the actuator is moved upward.
5. Slowly turn the Actuator Positioning Control (APC) knob until the actuator begins to move upward.
6. As the lower platen continues to move upward, guide the insert for the upper test fixture into the bored hole of the upper test fixture and increase the load to approximately 500-lbs.
7. With the two alumina inserts correctly positioned, apply the Cotronics Thermeez Ceramic Putty to the end of the upper platen and the sides of the insert. Insure that the putty is spread around the entire insert and platen end.
8. The MTS machine must be left on while the putty cures to insure that the upper insert does not fall out. The cure time is approximately 8 – 12 hours however; the cure time can be shortened to about two hours if the furnace is closed around the test fixtures and used to slowly heat up the platens. A warm up procedure that works well is setting the furnace control to ramp up to 200°C (392°F) in 30-minutes, holding this temperature for one hour, and then letting the furnace cool down for 30-minutes.

#### **2.4.2 Test Fixture Base**

The purpose of the test fixture base is to couple the alumina load platens to the MTS 810 hydraulic wedge grips. The bases of the fixtures are made of 4140 cold-rolled steel and were made by Lane Supply Company in Brewer Maine. A detailed drawing of the test fixture base is shown in Figure 2.9. The fixtures are held in the wedge grips by threading a 4-inch by 9/16-inch diameter stud into the bottom of each test fixture. Using the largest set of V-shaped wedge blocks available for the MTS load frame the studs at the bottom of each test fixture can be securely gripped and axially located in the load frame. A detailed procedure on how to properly grip, locate, and align the test fixtures in the MTS load frame is discussed in Section 2.4.3; *Procedure for Installing the Test Fixtures in the MTS Load Frame*.

The two-inch diameter alumina platens are affixed to the steel bases by using a light drive, interference fit. The alumina platens are pressed into the approximately two-inch diameter bored hole in the test fixture bases. To aid in the removal and installation of the alumina rods, the steel base is placed on a hot plate and allowed to expand until the alumina platens easily pull out of the test fixture base or drop easily into the bored holes in the steel bases. This procedure is most important when removing the alumina platens from the base. Ceramics are poor in tension and the alumina platen would not be able to withstand the force required to be pulled out of the pressed fit in the steel base without the aid of heating.



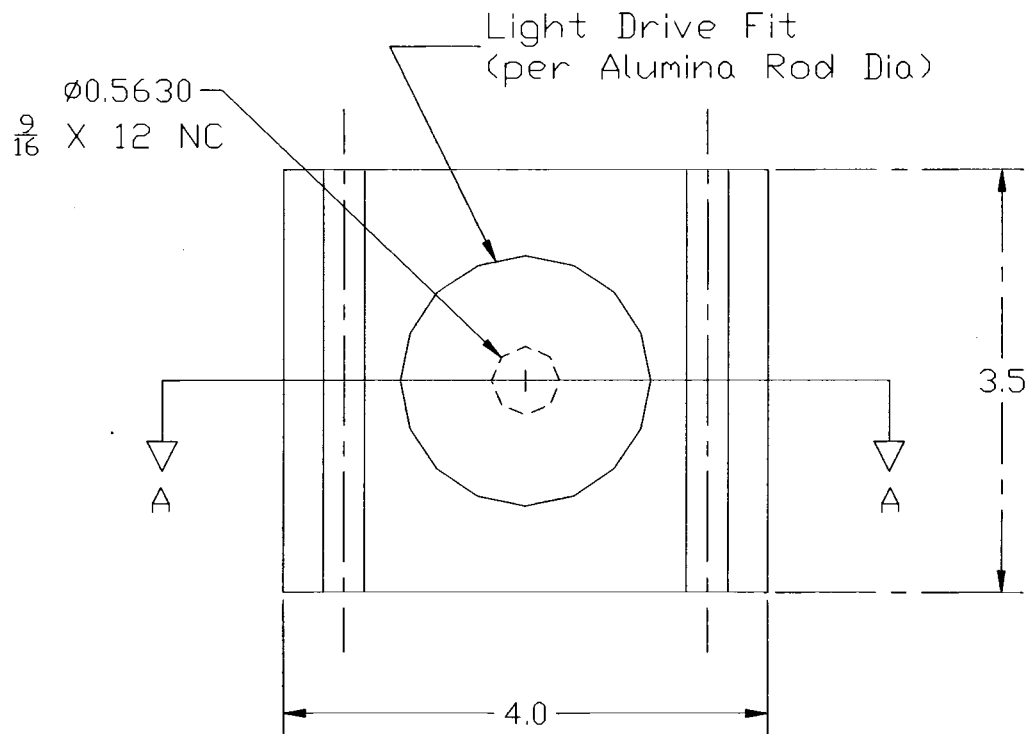
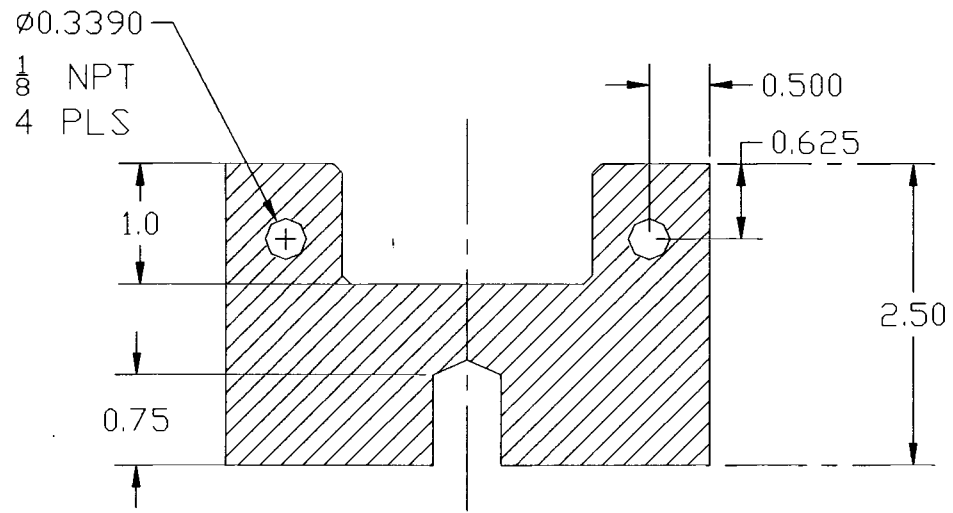


**Figure 2.9 – Detailed Drawing of Test Fixture Base**

During operation of the furnace the steel test fixture bases require cooling because each test fixture base is in close proximity to the furnace, and the alumina platens that extend into the furnace conduct a sufficient amount of heat into the steel bases. To satisfy the cooling needs, two cooling ports are drilled through each test fixture base and threaded at each end with 1/8-inch pipe thread as shown in Figure 2.9. Cooling lines are then connected to each port and cold water is circulated through the bases while the furnace is in use. Each base has its own throttling valve, which allows for independent control of the coolant flow.

To further prevent the hydraulic wedge grips from overheating a stainless steel, 24 gauge, 12-inch square heat shield is attached to the upper test fixture base. The reason this heat shield is required on the top test fixture is because through natural convection a large amount of heat is released through the vents on top of the furnace and cause the upper wedge grip to heat up considerably. To prevent oxidation of the steel test fixture bases several coats of high temperature paint was applied to each test fixture base. The paint selected was Steel It, which is rated for temperatures up to 1200°F (650°C) and available from McMaster-Carr.

#### **2.4.3 Procedure for Installing the Test Fixtures in the MTS Load Frame**

The procedure for installing the test fixtures into the MTS grips is very important. Incorrect installation could result in the misalignment of the fixtures, causing improper loading of the test specimens. This procedure should only be performed after the

Aremco alumina inserts are in place, and also assures that the alumina platens are fully pressed into the steel test fixture bases.

1. Install the largest set of V-shaped grip blocks in both upper and lower wedge grips.
2. Turn the hydraulic pressure down to 1500 psi or as low as it will go for the hydraulic wedge grips. The reason a low pressure is required is because the steel studs that screw into the bottom of each test fixture are a mild-steel and the grips will crush them if the pressure is too high.
3. With the grips open and the steel studs screwed into the base of each fixture place the fixtures in the grips so that the studs are centered in the wedge blocks and close each grip. There should be no gap between the bottom of each test fixture base and the top of the wedge blocks.
4. The V-shaped grip blocks assure that the platens will be aligned in the axial direction of the load frame. However, to insure that the load face of each platen is parallel it is necessary to load each platen with the grips in the open position:
  - a. With both upper and lower fixtures in place turn on the hydraulics for the MTS load frame, and switch the control mode to 'Force'. It is recommended at this point to change the load limit to 5,000 lbs in compression to avoid overloading the fixtures. The fixtures can withstand far more load than 5,000-lbs, but this is a good safety precaution for this procedure.
  - b. Adjust the crosshead of the load frame so that the end of the upper alumina platen is close enough to the lower platen to allow contact when the actuator is moved upward.

- c. Slowly increase the load until the actuator begins to move upward and the lower platen contacts the upper platen. Slowly increase the load to 2000-2500lbs.
  - d. With the platens now loaded and the MTS still in load control, open each grip separately and then close it. By opening the grips while a compressive load is applied to the fixtures the test fixture bases will seat properly against the tops of the wedge blocks and will not lift up when the grips are closed.
6. At this point it is important to check that there are no gaps between where the upper and lower platens are in contact. A 0.001-inch feeler gauge can be used to check for any gaps between the platens. If the gauge can slide in-between the platen ends at any point then the fixtures are not properly aligned.

## **2.5 Furnace and Temperature Control**

### **2.5.1 Furnace**

The furnace used for conducting the high temperature tests is a MTS model 653 furnace with a temperature range from room temperature to 1400°C (2552°F). The furnace has three heating zones, upper, middle, and lower, each with two-120V graphite heating elements. A two-inch diameter hole is located at the top and bottom that allows for the two-inch diameter alumina platens to extend inside the furnace. Figure 2.10 shows the backside of the furnace where the thermocouples are mounted. Five type R thermocouples, with a temperature range of 0 to 1450°C (32 to 2642°F), are used to monitor temperature.

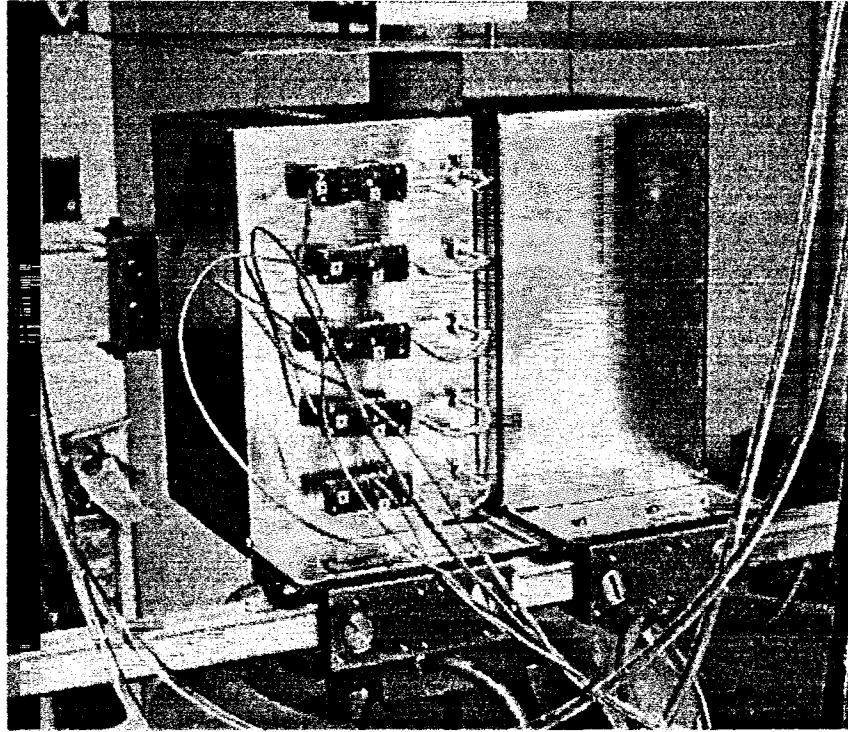


**Figure 2.10 – Backside of Furnace with Thermocouples**

### **2.5.2 Temperature Control**

The temperature controller supplied with the MTS 653 furnace proved to be insufficient for the needs of this project. An effort was made to interface the MTS controller with the software Itools™, produced by Eurotherm, to communicate with the three Eurotherm temperature control modules incorporated in the MTS temperature control system. Itools™ was designed to work in conjunction with the Eurotherm software Set Point Editor to allow for multiple set points to be programmed into each controller. An RS-232 to RS-485 serial communication converter was also purchased to allow communication between a PC and the Eurotherm temperature control modules. However, the software did not function as needed and a decision was made to design a custom temperature control system with existing equipment on hand in Crosby Lab at The University of Maine.

### 2.5.2.1 Temperature Control Program

A computer program written in Delphi 3 (Caccese, Malm & Walls - 1999) for controlling an existing oven in Crosby Laboratory at The University of Maine was used as a building block to develop a temperature control program for the high temperature MTS 653 furnace. The existing program was modified to allow for control of the existing oven and also allow for control of the high temperature furnace. A screen capture of the front end of the new program, 'Universal Temperature Control Software', is shown in Figure 2.11. The high temperature portion of the program was developed to allow the user to enter in a series of set point temperatures and corresponding times in a spreadsheet form. A screen capture of this portion of the program is shown in Figure 2.12.

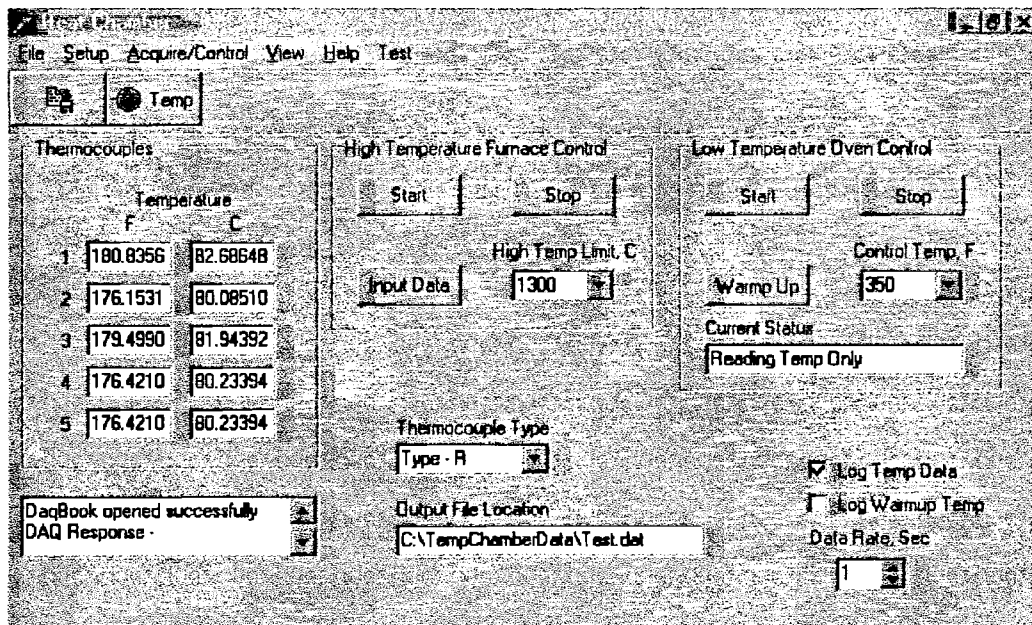
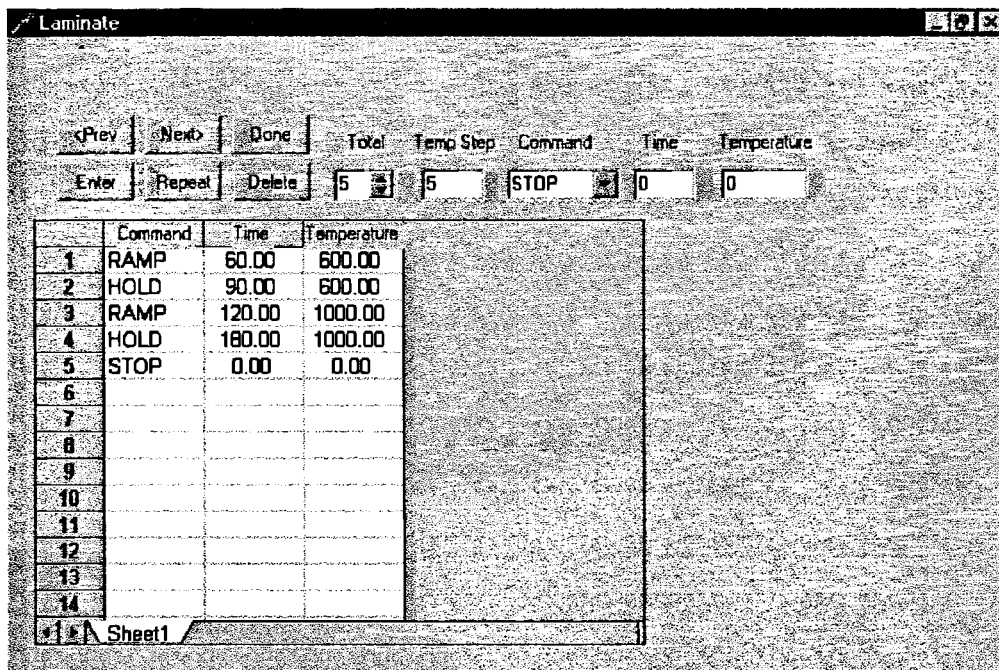


Figure 2.11 – Screen Capture of the 'Universal Temperature Control Program' Front End

The user can select three different commands for developing a temperature control routine: RAMP, HOLD, and STOP. The 'RAMP' command is used to ramp the

temperature up from whatever the current temperature is to a new temperature, specified by the user, in a time frame that is also specified by the user. The 'HOLD' command is used to hold a specified temperature for a specified time, and the 'STOP' command is used to specify the end of the temperature control routine. The screen capture in Figure 2.12 also illustrates a sample input routine with the time in minutes and the temperature in Celsius.



**Figure 2.12 – Screen Capture of the Input Portion of the ‘Universal Temperature Control Program’**

To develop an accurate temperature control program that minimizes overshoot and maintains a consistent temperature, a feedback control algorithm was developed. A typical feedback control system implements P.I.D. (Proportional, Integral, Derivative) control. This form of control is designed to accurately control a system by monitoring the system input and adjusting the system output accordingly. The proportional band is a band centered around the desired setpoint with a range from 0% to 100%. With only

proportional control the setpoint will generally be located at the center of the control band. Mathematically, the proportional band looks like this:

$$\text{Output} = K_p \cdot \text{error} \quad (1)$$

$$\text{error} = \text{input} - \text{setpoint} \quad (2)$$

Where  $K_p$  is a gain constant that can be changed to properly tune the control system. The Integral band of the P.I.D. control algorithm is designed to automatically shift the Proportioning band by monitoring the error over time between the setpoint and the input. Adding the integral band to the proportional band generates the following expression:

$$\text{Output} = K_p \cdot \text{error} + K_i \int \text{error} \, dt \quad (3)$$

Where the integral of the error with respect to time represents a summation of the error over a given time period and  $K_i$  is a gain constant. The last part of the P.I.D. control algorithm is the Differential Band. The differential band examines at the rate of change of the input and adjusts the output accordingly. The purpose of the derivative band is to prevent excessive overshoot on system startups and systems upsets. The complete P.I.D. algorithm looks like this:

$$\text{Output} = K_p \cdot \text{error} + K_i \left( \int \text{error} \, dt + K_d \frac{d}{dt} \text{error} \right) \quad (4)$$

Where  $K_d$  is another gain constant that is used to tune the control system.

For the control requirements of the MTS furnace, only the proportional and integral control bands are used. The differential control band control was not implemented, but could easily be added to the control algorithm if necessary. The primary reason for not



implementing the differential control band is that the sampling rate of the input, the thermocouples, could not practically be set high enough to make the differential band effective. For an explanation of how the P.I. algorithm functions for the 'Universal Temperature Control Program' only zone 1 is illustrated. However, each of the three zones in the furnace has independent P.I. control algorithms.

The proportional portion of the control algorithm is the error generated by the difference between current set point and the actual temperature, multiplied by a gain constant:

$$\text{zone1Pterm} = \text{zone1Kp} \cdot \text{zone1Error} \quad (5)$$

Where zone1Pterm is the proportional term for zone 1 of the furnace (upper zone), zone1Kp is the gain constant, and zone1Error is equal to the set point temperature minus the current temperature. The integral portion of the control algorithm is the sum of the error over time multiplied by a gain constant,

$$\text{zone1Iterm} = \text{zone1Ki} \cdot \text{zone1SumError} \quad (6)$$

Where zone1Iterm is the integral term for zone 1 of the furnace, zone1Ki is the gain constant, and zone1SumError is the zone1Error summed up over time. To prevent the integral term from "blowing up" during start up or other unforeseen variables that may occur, the integral term is bounded between zero and one. The final output for each zone is the summation of both the proportional term and the integral term,

$$\text{zone1PercentGain} = \text{zone1Pterm} + \text{zone1Iterm} \quad (7)$$

To tune the P.I. control algorithm to specific operating parameters, the constants zone1Kp and zone1Ki can be altered by the user. A screen capture of the portion of the program that allows the user to tune the P.I. control is shown in Figure 2.13. The tuning constants that were used for all of the testing done in this study are listed in Table 2.3 and were primarily determined by trial and error.

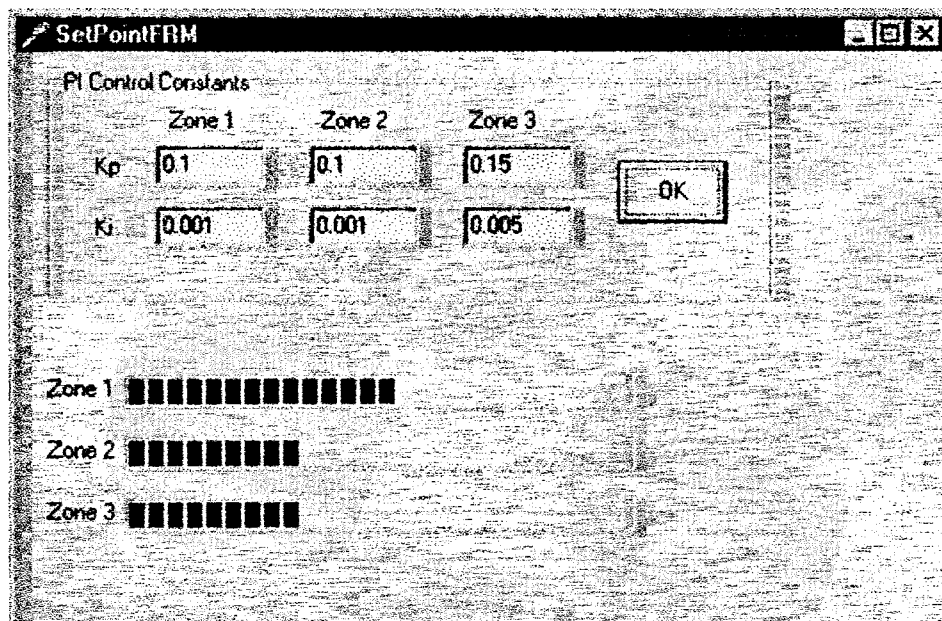


**Figure 2.13 – Screen Capture of the P.I. Tuning Portion of the ‘Universal Temperature Control Program’**

**Table 2.3 – P.I. Tuning Constants**

|           | <b>Zone 1</b> | <b>Zone 2</b> | <b>Zone 3</b> |
|-----------|---------------|---------------|---------------|
| <b>Kp</b> | 0.15          | 0.15          | 0.18          |
| <b>Ki</b> | 0.001         | 0.001         | 0.002         |

The heating elements for the MTS furnace can either be turned ‘on’ or ‘off’, but the voltage applied to the heating elements can not be varied to allow for any gain control.

For a P.I.D. algorithm (P.I in this case) to function, a method of gain control must be developed. To accomplish this with heating elements that can only be turned 'on' or 'off' a duty cycle was implemented. The duty cycle works by only allowing the heating elements to be on for a percentage of a prescribed period of time. For this program a period of five seconds is used; If a gain of 100% is returned from the P.I. algorithm, the heaters remain on for the full 5-seconds, if a gain of 25% is returned the heaters only turn on for 1.25-seconds. Figure 2.13 also shows three progress bars below the input section for the P.I. tuning constants. The progress bars are used to display the percent gain for each zone for the purpose of giving a visual idea of how the P.I. algorithm is performing, and to aid in tuning. A print out of the source code for the high temperature portion of the computer program is available in Appendix A.

#### **2.5.2.2 Digital/Analog Interface**

The interface between the PC used to run the temperature control software, and the MTS furnace consists of two parts: an Iotech Daqbook 100 and thermocouple card, and a custom-built control box. The Daqbook is connected to the PC using the parallel port and allows the output from the five thermocouples to be read into the program and allows a digital output to be sent to the control box. Figures 2.14 and 2.15 show the control box built for the MTS furnace. The control box utilizes three Omega relays to switch the heating elements on or off by a digital signal generated by the Daqbook of either +5V or 0V. A complete parts list with pricing for the control box is available in Appendix B.

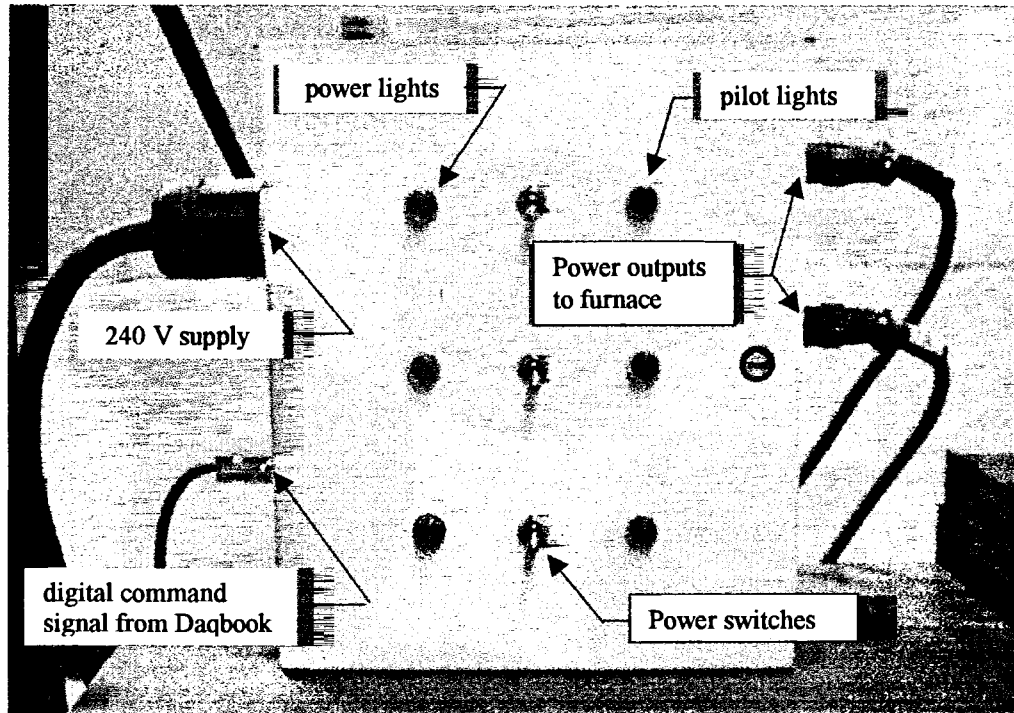


**Figure 2.14 – Control Box for the MTS Furnace**

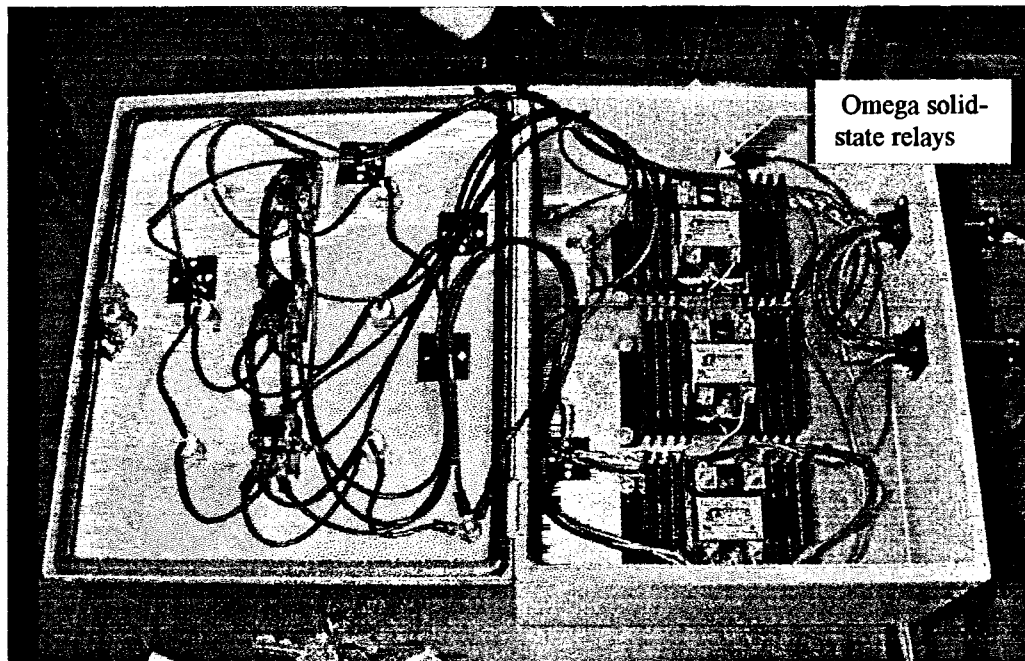


**Figure 2.15 – Inside of the Control Box**

## **2.6 Instrumentation and Data Acquisition**

For all of the data acquisition needs of this project the MTS software Teststar II is used to record time, displacement, load, and strain. A data-sampling rate of 0.5 Hz is used for the proof test specimens and a sampling rate of 1.5Hz is used for the ATS test specimens. The full capacity of the 110,000-lb load frame is not necessary for the tests conducted for this effort. To improve resolution in the data a 22,000-lb load cell is connected in series to the existing 110,000-lb capacity load cell.

Some of the most common methods for measuring strain for mechanical testing are the use of bonded strain gages, measuring crosshead or actuator displacement of the load frame, and using an extensometer. For this project two methods of strain measurement are employed: the actuator displacement on the MTS 810 load frame and a high temperature extensometer. The primary method of strain measurement is the high temperature extensometer and the strain values calculated by using the actuator displacement are used as a comparison to verify the somewhat non-traditional method of using the extensometer. The reason for not relying solely on the MTS actuator displacement to measure strain is that small deflections in the load train could skew the results. Carbon-carbon generally exhibits low strain to failure characteristics and small deflections in the load train of the testing equipment may be significant when compared to the deflections of the test specimens.

The MTS model 632-54E-11 high temperature extensometer is shown in Figure 2.16. The gauge length of the extensometer is 1.000-in and it has a range of +10% and -5%.

For the extensometer to withstand being in close proximity to the furnace the extension rods are quartz, and the transducer portion of the extensometer is located behind a heat shield. To avoid error as a result of temperature changes, air-cooling is used to keep the transducer portion of the extensometer at a constant temperature.

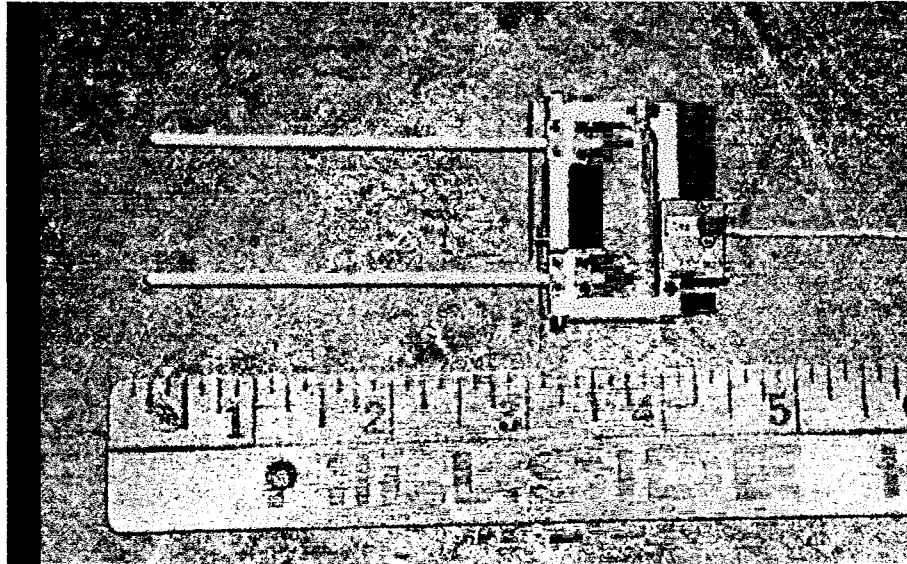


**Figure 2.16 – MTS High Temperature Extensometer**

Due to the geometry of the test specimens it is not feasible to connect the extensometer directly to the test specimen and measure the strain over a 1-inch gage length. However, if the test specimens are cut to be slightly shorter than the gage length of the extensometer, the entire test specimen can serve as the gage length and strain can be measured off the platen ends. Figure 2.17 is a photograph that shows how the extensometer is configured to measure strain off the Aremco alumina insert ends. The furnace has been swung out of the way and the air-cooling diffuser has been removed for clarity. Though this procedure is a non-traditional method for using an extensometer, it is

perfectly valid providing the alumina platens are significantly more stiff than the test specimens. Considering that the inserts exhibit a compressive strength of 360,000-psi, and hardness of 9.0 on the Moh scale, deflection at the surface of the inserts is insignificant.

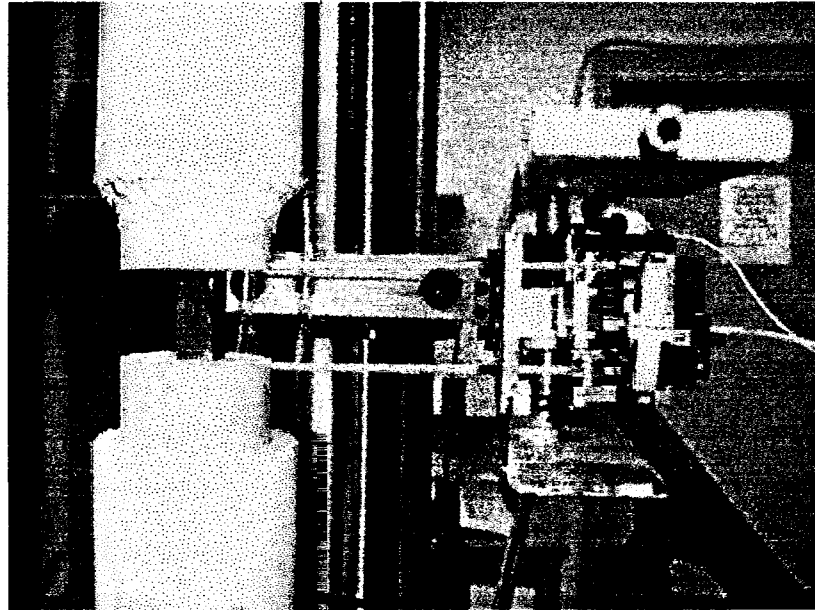


**Figure 2.17 – Extensometer Affixed to the Alumina Inserts**

The extensometer ends maintain contact with the alumina inserts by means of a spring-loaded connection to the extensometer-mounting arm. A small slot is cut on both alumina inserts 0.125-in from the load face of each insert. To precisely cut these slots the South Bay Technology diamond wheel saw, described in Section 2.3, is used. Together with the axial force applied to both of the quartz extension rods, and two small slots in the alumina inserts, the extensometer extension rods can be securely held in place against the inserts. Figure 2.18 is a photograph that shows the extensometer properly attached to the mounting arm.

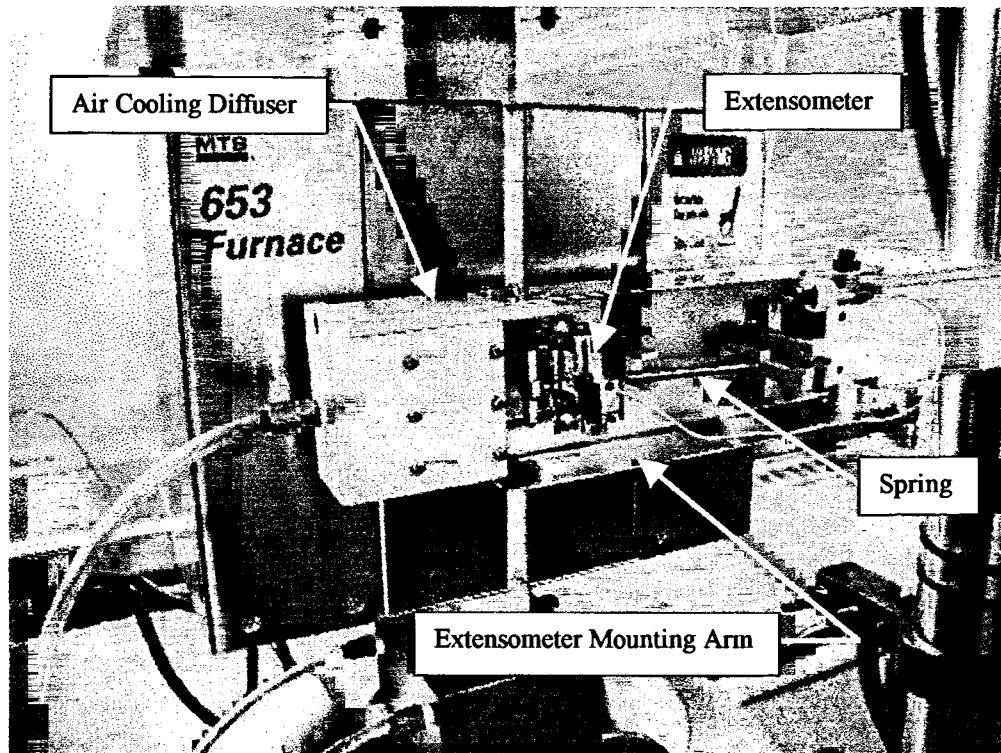


**Figure 2.18 – Extensometer Mounting Configuration**

## **2.7 Proof Tests**

To develop an accurate testing procedure and to insure that the test apparatus would function correctly, proof tests were performed on stainless steel specimens and carbon-carbon specimens with known mechanical properties. The compressive modulus and ultimate compressive strength is determined experimentally for the carbon-carbon proof test specimens at various temperatures and compared to the provided mechanical properties of the material.



### 2.7.1 Test Specimens

Table 2.4 is a list of all the proof test specimens used and the corresponding testing temperature. For the proof test specimens the nomenclature aa##-bb, is used to identify the test specimens. The first two letters are the material identification, and are either SS for stainless Steel or CC for carbon-carbon. The two numbers that follow the material identification are for identifying the test number. The last two letters are either HT or RT, and stand for room temperature or high temperature respectfully. The 'I' used in the nomenclature for the last two carbon-carbon test specimens in Table 2.4 indicate that these proof tests were performed using the fully fired, alumina inserts.

**Table 2.4 – Proof Test Specimen Test Temperatures**

| Test Specimen | Test Temperature<br>°C, (°F) |
|---------------|------------------------------|
| SS01-HT       | 800 (1472)                   |
| SS02-HT       | 1000 (1832)                  |
| SS03-RT       | Room Temp                    |
| CC01-RT       | Room Temp                    |
| CC02-RT       | Room Temp                    |
| CC01-HT       | 1000 (1832)                  |
| CC02-HT       | 200 (392)                    |
| CC03-HT       | 400 (752)                    |
| CC04-HT       | 600 (1112)                   |
| CC05-HT-I     | 800 (1472)                   |
| CC06-HT-I     | 800 (1472)                   |

The first proof tests were the three stainless steel specimens and were cut from ½ -in. diameter 316 annealed and cold drawn stainless steel. Each specimen was cut slightly longer than one inch and was then faced in a lathe to achieve flat, parallel surfaces on each end with a finish length of one inch. These tests were performed early in the

development of the test apparatus and were only performed to insure that the alumina platens would withstand a compressive load at high temperature without fracturing. All three tests were conducted in load control with a load rate of 100-lbf/min. The two high temperature tests were stopped at 4000-lbf, while the third test was performed at room temperature and was stopped at 10,000-lbf. A technique for measuring strain had not yet been developed and problems with the MTS Testware software configuration resulted in invalid data files.

The carbon-carbon proof test specimens are cut from a block, approximately 2-in. by 2-in. by 0.375-in thick, of commercial carbon-carbon. The material was ordered from Goodfellow, item number C413100 from the 2000/2001 catalog, and is made from a thick cloth weave with liquid impregnation of the carbon matrix. Table 2.5 is a list of the material properties supplied by Goodfellow. Before the specimens are cut from the block the edges are trimmed with the MK Diamond wet saw to insure that all the edges are square. Rectangular prisms with a square cross section are cut approximately 0.875-in long are cut from the block of carbon-carbon. This length closely resembles the aspect ratio specified in ASTM D 695, and the specimen length permits strain measurement from the platen ends. The dimensions for each specimen are listed in Table 2.6 and the specimen geometry is shown in Figure 2.19. The 'a' dimension and the 'L' dimension are parallel to the fiber plane while the 'b' dimension is perpendicular to the fiber plane.

**Table 2.5 – Mechanical Properties for the Carbon-Carbon Proof Test Specimens**

|   |                         |
|---|-------------------------|
| Compressive Strength - parallel to plane, psi (Mpa) | 17,400-29,000 (120-200) |
| Compressive Strength - perp. to plane, psi (Mpa)    | 8,700-21,800 (60-150)   |
| Flexural Modulus - parallel to plane, Msi (Gpa)     | 1.45-2.90 (10-20)       |
| Flexural Strength - parallel to plane, psi (Mpa)    | 11,600-29,000 (80-200)  |
| Shear Strength - in-plane, psi (Mpa)                | 2900-4350 (20-30)       |
| Tensile Modulus - parallel to plane; Msi (Gpa)      | 2.90-4.35 (20-30)       |
| Tensile Strength - parallel to plane, psi (Mpa)     | 5800-10100 (40-70)      |
| Tensile Strength - perp. To plane, psi (Mpa)        | <1450 (10)              |

**Table 2.6 – Carbon-Carbon Proof Test Specimen Dimensions**

| Test Specimen | Dimension, in (mm) |               |               |
|---------------|--------------------|---------------|---------------|
|               | a                  | b             | L             |
| CC01-RT       | 0.374 (9.50)       | 0.395 (10.03) | 0.870 (22.10) |
| CC02-RT       | 0.358 (9.09)       | 0.395 (10.03) | 0.881 (22.38) |
| CC01-HT       | 0.374 (9.50)       | 0.395 (10.03) | 0.855 (21.72) |
| CC02-HT       | 0.357 (9.07)       | 0.395 (10.03) | 0.870 (22.10) |
| CC03-HT       | 0.395 (10.03)      | 0.395 (10.03) | 0.857 (21.77) |
| CC04-HT       | 0.367 (9.32)       | 0.395 (10.03) | 0.865 (21.97) |
| CC05-HT-I     | 0.395 (10.03)      | 0.395 (10.03) | 0.876 (22.25) |
| CC06-HT-I     | 0.368 (9.35)       | 0.395 (10.03) | 0.858 (21.79) |

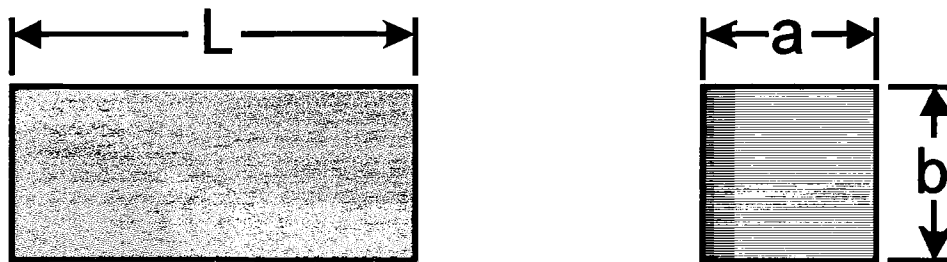


**Figure 2.19 – Carbon-Carbon Proof Test Specimen Geometry**

### **2.7.2 Proof Test Results**

The results of the proof tests identified several flaws in the test setup and procedure. The first major flaw was the Rescor 960 alumina platens becoming too soft at high temperatures (Section 2.4.1). This problem prevented any form of accurate strain measurement and could potentially result in the test specimen becoming unstable in the test fixtures. The upper platen also failed while the furnace was heating up prior to the first stainless steel test, SS01-HT. A picture of the fractured platen is shown in Figure 2.20. The failure appeared to originate as a small crack that propagated from the steel test fixture base down the length of the platen. The interference fit for the upper platen was substantially tighter than the lower platen, which was likely the cause of the failure; As the alumina was heated, consequently expanding, the steel base was prevented from expanding due to the water-cooling. The result was a high enough stress level in the platen to cause failure. When the platen was replaced the diameter of the end pressed into the steel base was reduced slightly with fine, 200-grit sandpaper to alleviate the stresses at the confined end. Problems with the extensometer were also discovered when the Aremco alumina inserts were incorporated in the test fixtures. During the last two proof tests the extensometer slipped, invalidating the strain data for these tests. This problem was rectified prior to conducting the ATS tests by creating deeper groves in the inserts where the extensometer extension rods attached to the inserts. Another flaw found was in the preparation of the test specimen load surfaces. All of the carbon-carbon test specimens were prepared using the MK Diamond wet saw, which could not maintain the stringent tolerances required for the load surfaces. This problem was solved by the purchase of the South Bay Technology precision diamond wheel saw. Software and data

acquisition problems were also found and fixed accordingly. Several bugs were discovered in the 'Universal Temperature Control Program', and configuration issues with the MTS Testware software were also resolved.

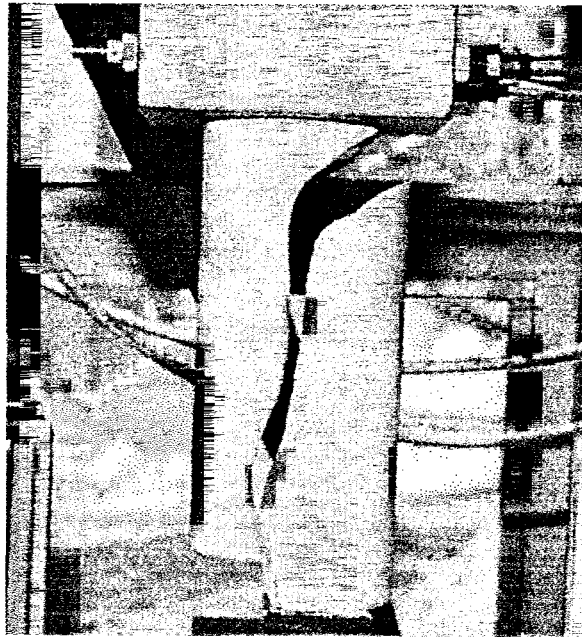


**Figure 2.20 – Fractured Test Fixture**

#### **2.7.2.1 Stainless Steel Test Results**

The results of the stainless steel tests demonstrated that the test fixtures could withstand a compressive load of at least 4000-lbf, or approximately 20,000-psi at temperatures as high as 1000°C (1832°F) and compressive loads as high as 10,000-lbf, or approximately 51,000-psi at room temperature. Higher temperature tests could not be achieved with the stainless steel specimens because the material began to melt at 1000°C. Figure 2.21 is a photograph of the two high temperature stainless steel specimens after the tests were

completed. The specimen on the left is SS01-HT, which was tested at 1000°C; the test specimen on the right is SS02-HT, which was tested at 800°C. Severe deformation of SS01-HT clearly shows that 1000°C exceeded the temperature limitations of 316 stainless steel.

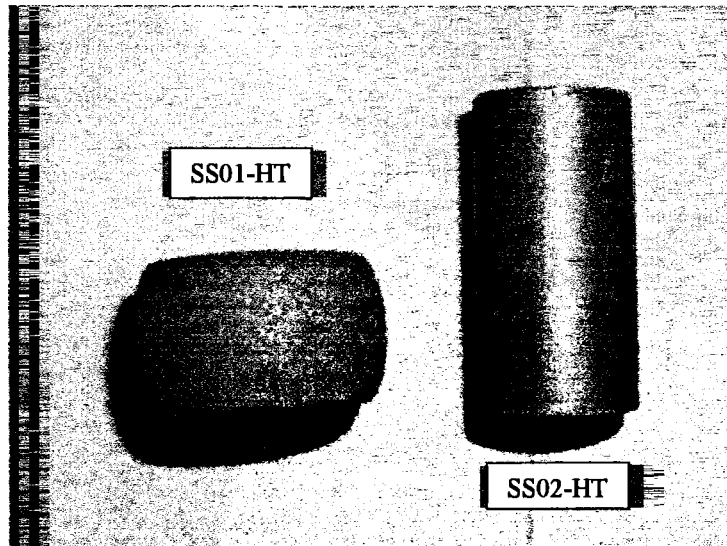


**Figure 2.21 – Stainless Steel Test Specimens After Testing**

### **2.7.2.2 Carbon-Carbon Results**

The stress-strain curves for five of the eight carbon-carbon proof tests are shown in Figure 2.22 and the compressive modulus and ultimate compressive stress results are summarized in Table 2.7. The modulus for each test was determined by plotting only the linear portion of the stress strain curve in Microsoft Excel and fitting a trendline to the data. Figure 2.23 shows the linear portion of the stress-strain curve for test specimen CC02-RT. To determine the strength of the linear relationship of the modulus, the correlation coefficient was calculated using statistical analysis tools in Excel.

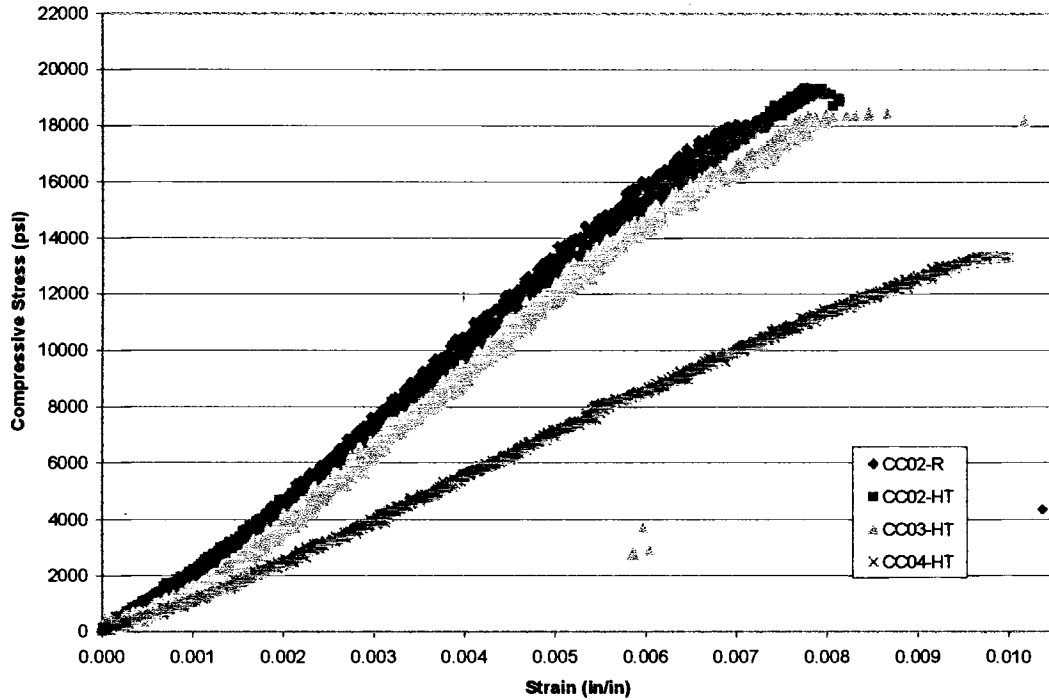


**Figure 2.22 – Proof Test Stress-Strain Curves**

**Table 2.7 – Summary of Proof Test Results**

| Test Specimen | Test Temperature<br>°C, (°F) | Compressive Strength<br>psi (MPa) | Compressive Modulus<br>Msi (GPa) | Correlation Coefficient |
|---------------|------------------------------|-----------------------------------|----------------------------------|-------------------------|
| CC01-RT       | Room Temp                    | 14,178 (97.75)                    | invalid                          | ---                     |
| CC02-RT       | Room Temp                    | 18,092 (124.74)                   | 2.796 (19.27)                    | 0.9994                  |
| CC01-HT       | 1000 (1832)                  | invalid                           | invalid                          | ---                     |
| CC02-HT       | 200 (392)                    | 19,351 (133.42)                   | 2.604 (17.81)                    | 0.9984                  |
| CC03-HT       | 400 (752)                    | 18,433 (127.09)                   | 2.726 (18.80)                    | 0.9951                  |
| CC04-HT       | 600 (1112)                   | 13,336 (91.95)                    | 1.506 (10.38)                    | 0.9964                  |
| CC05-HT-I     | 800 (1472)                   | 9,198 (63.42)                     | invalid                          | ---                     |
| CC06-HT-I     | 800 (1472)                   | 11,855 (81.74)                    | invalid                          | ---                     |

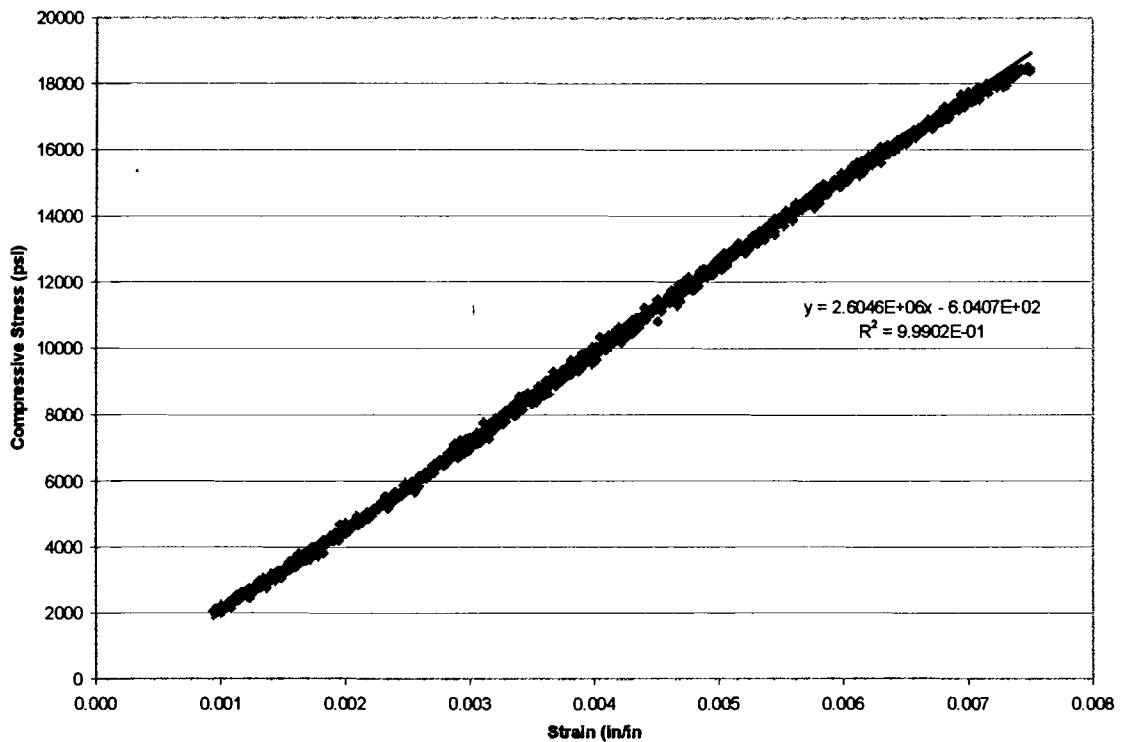


**Figure 2.23 – Linear Stress Strain Relation for CC02-HT**

Three of the tests, CC01-RT, CC01-HT, and CC05-HT are not shown due to problems that developed during the tests, which invalidated the results. For CC01-RT, CC05-HT, and CC06-HT the extensometer slipped off of one of the load platens, thus invalidating the strain data. CC01-HT was the one proof test conducted at 1000°C (1832°F) and caused damage to the alumina platens, as described in Section 2.4.1. Figure 2.24 is a photograph of the test specimen CC01-HT after the test was complete, and clearly shows how severely the test specimen oxidized.



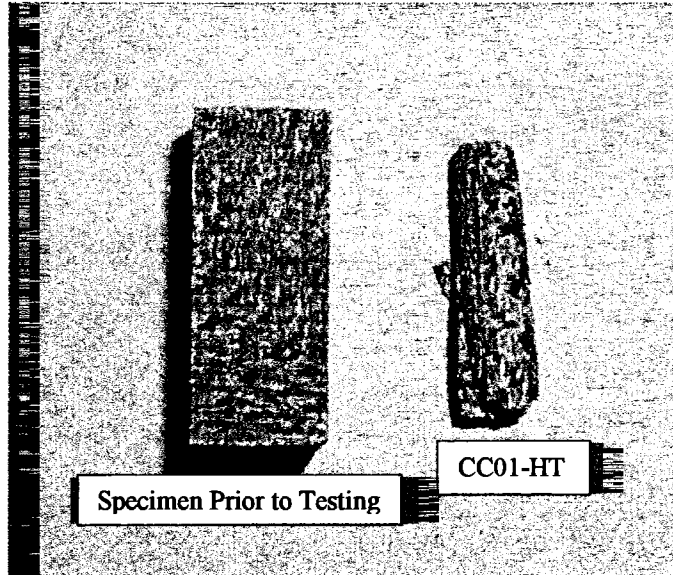


**Figure 2.24 – Severe Oxidation of CC01-HT**

The failure mode for all of the carbon-carbon proof test specimens was consistently the same with the exception of CC01-HT, which oxidized too heavily to determine the failure mode. The remaining specimens all exhibited shear failure with no evidence of end crushing.

### **2.7.2.3 Summary of Carbon-Carbon Proof Tests**

The results of the carbon-carbon tests identified problems with the test apparatus and test method and, for the tests that were successfully completed, demonstrated an acceptable correlation with the mechanical properties supplied by Goodfellow. The compressive strength parallel to the fiber plane provided by Goodfellow is 17,400 – 29,000 psi (120 - 200 MPa), compared to the experimental compressive strength results of 11,855 – 19,351 psi (81.74 – 133.42 MPa). The lower compressive strengths, with the exception of CC01-RT, all occurred at test temperatures of 1112°F (600°C) to 1472°F (800°C). The

higher temperature tests all exhibited moderate oxidation causing conservative ultimate stress values. Three of the four lower temperature ultimate strength values fell within the specifications provided by Goodfellow. However, the results were on the lower end of the specified ultimate strength. The likely cause of this phenomenon was most likely insufficient preparation of the test specimen load surfaces. This problem was rectified for the ATS tests with the use of the South Bay Technology wet saw. The compressive modulus ranged from 1.506 to 2.796-Msi (10.31 to 19.27-Gpa) with the lowest value occurring at 1112°F (600°C) and the highest value occurring at room temperature. Goodfellow did not provide a compressive modulus for the material, which is likely because the material exhibits similar stiffness characteristics in both tension and compression. The compressive modulus results were just below the tensile modulus range of 2.90 to 4.35 Msi (20-30-Gpa) and are close to the lower range of the tensile modulus provided by Goodfellow, indicating that the modulus results of the proof tests are conservative. The conservative results are likely due to insufficient load surface preparation, or the material could exhibit a slightly lower stiffness in compression than tension.

### 3. ATS CARBON-CARBON TESTS

High temperature tests in an oxidizing environment were conducted to evaluate the compressive properties of a three-dimensional weave carbon-carbon composite. The material is used primarily for missile nose cones and was provided by ATS. Testing summarized in this section consist of 66 tests conducted from room temperature to 2192°F (1200°C). The test specimens were cut at six different orientations; three along the principal fiber orientations, and three off-axis orientations cut 45° to the fiber direction. The purpose of the off-axis tests was to evaluate the interlaminar shear strength. All tests were conducted using the test method described in Chapter 2. Further testing was conducted to determine the sensitivity of the material to oxidation. These tests were conducted from 1112°F (600°C) to 1832°F (1000°C).

#### 3.1 Test Specimens

The geometry for the three-dimensional carbon-carbon test specimens is the same as the geometry used for the proof test specimens. Each test specimen is cut to form a rectangular prism, with the geometry illustrated in Figure 3.1. The average length,  $L$ , of each test specimen is 0.875-in and the base dimensions, 'B1' and 'B2', averaged 0.375-in. Unlike the proof test specimens the base dimensions are arbitrary and not relative to the fiber orientation.

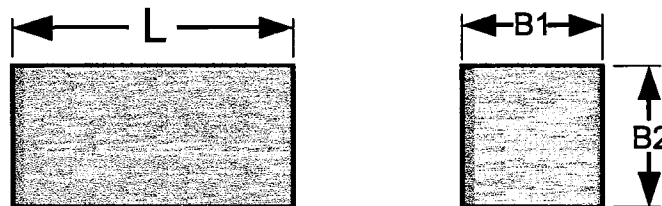
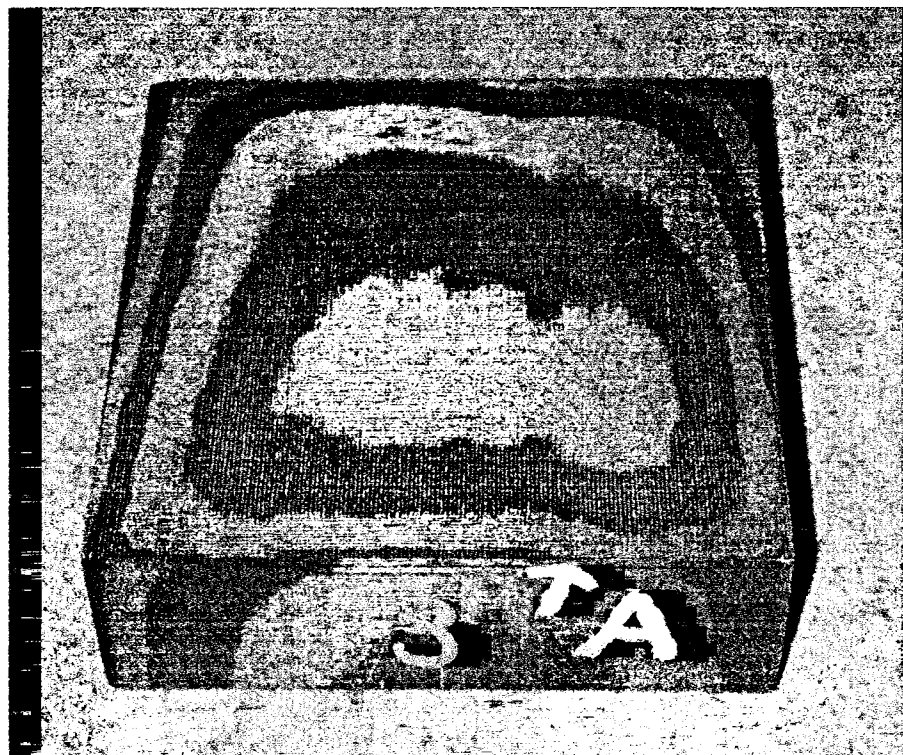
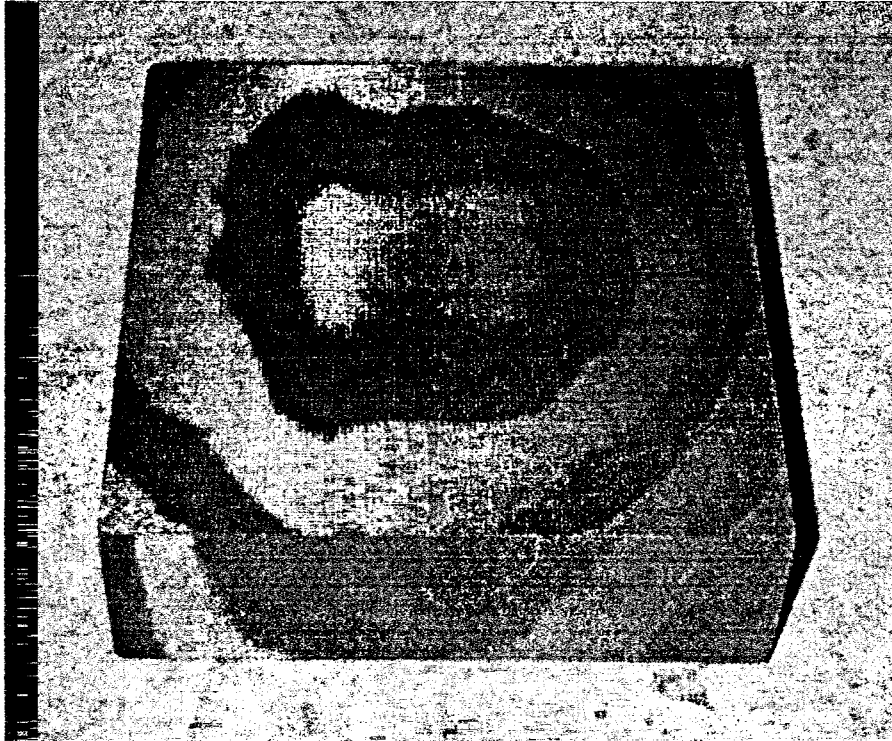


Figure 3.1 – Test Specimen Geometry

The test specimens are cut from a large block of carbon-carbon approximately 4.85-in square by 1.59-in thick. Figures 3.2 and 3.3 are photographs of the carbon-carbon block before the test specimens were cut. A reference face was arbitrarily chosen for the purpose of establishing a global coordinate system and marked with the letter 'A'. To accurately map out the location of each test specimen a three dimensional model of the carbon-carbon block was created in AutoCAD and the location of each specimen was laid out prior to any cutting. Figure 3.4 is a three-dimensional wire frame drawing of the block that depicts the chosen coordinate system and the original dimensions of the block. The letter 'A' on the front face of the block in Figure 3.4 corresponds to the same face marked with the letter 'A' on the carbon-carbon block



**Figure 3.2 – Top Face of the ATS Carbon-Carbon Block**



**Figure 3.3 – Bottom Face of the ATS Carbon-Carbon Block**

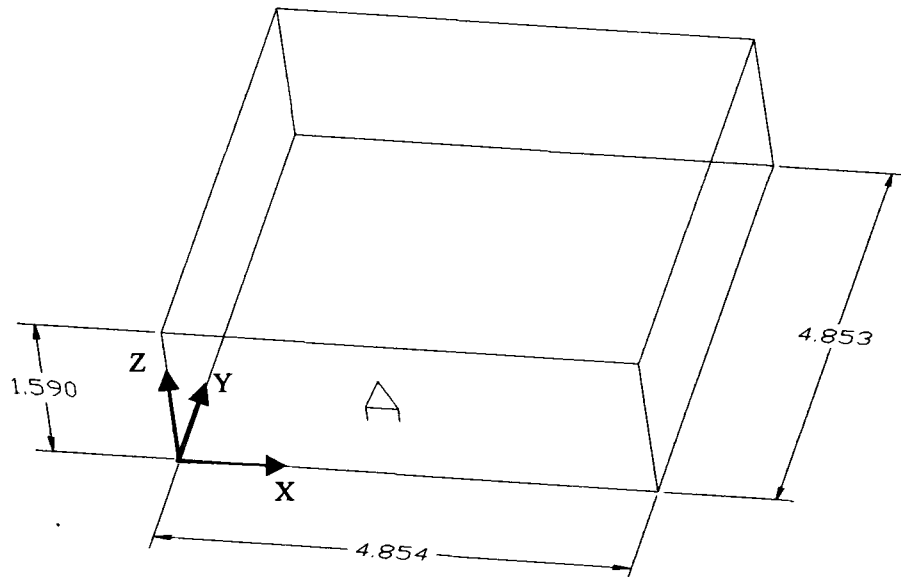


**Figure 3.4 – Carbon Block Coordinate System and Dimensions**

Before the test specimen map is generated, a test plan was developed to determine how many specimens are required for each orientation. Table 3.1 summarizes the number of test specimens required for each test. Based on ASTM D695, which recommends five specimens for each axis of anisotropy, five test specimens are chosen for each of the three principal fiber orientations and test temperatures. Only two specimens for each test temperature are chosen for the off-axis test specimens due to the significant amount of waste material generated by cutting these specimens. The determination of where the specimens were to be cut from the block was determined by optimizing the number of specimens that could be cut from the block yielding the least amount of scrap material. The final map of where each specimen was cut from the carbon-carbon block is shown in Figure 3.5. The scale used to create the model is 1:1, though Figure 3.5 is not shown to scale. The 0.060-in thickness for the width of the cutting wheel of the MK Diamond wet saw is also accounted for in the model. Every test specimen is labeled, though not shown in Figure 3.5, and each group of test specimens is created in separate layers to allow for one group of test specimens to be displayed at a time for clarity. Figure 3.6 illustrates only the Z-direction specimens with corresponding labels. Any significant size scrap pieces are also labeled and marked after cutting to allow for the use of the scrap for future testing. Individual printouts of all the specimen orientation groups are available in Appendix C.

**Table 3.1 – Preliminary Test Plan**

| Orientation | Number of Tests for Each Test Temperature<br>°C |     |     |      | Total #<br>of Tests |
|-------------|---|-----|-----|------|---------------------|
|             | Room Temp                                       | 600 | 800 | 1200 |                     |
| X-direction | 5   | 5   | 5   | 5    | 20                  |
| Y-direction | 5   | 5   | 5   | 5    | 20                  |
| Z-direction | 5   | 5   | 5   | 5    | 20                  |
| XY-plane    | 2   | 2   | 2   | 2    | 8                   |
| XZ-plane    | 2   | 2   | 2   | 2    | 8                   |
| YZ-plane    | 2   | 2   | 2   | 2    | 8                   |

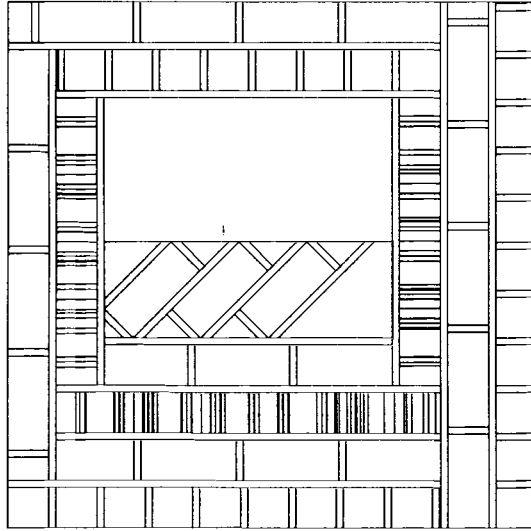


**Figure 3.5 – Model for Cutting the Carbon-Carbon Block**

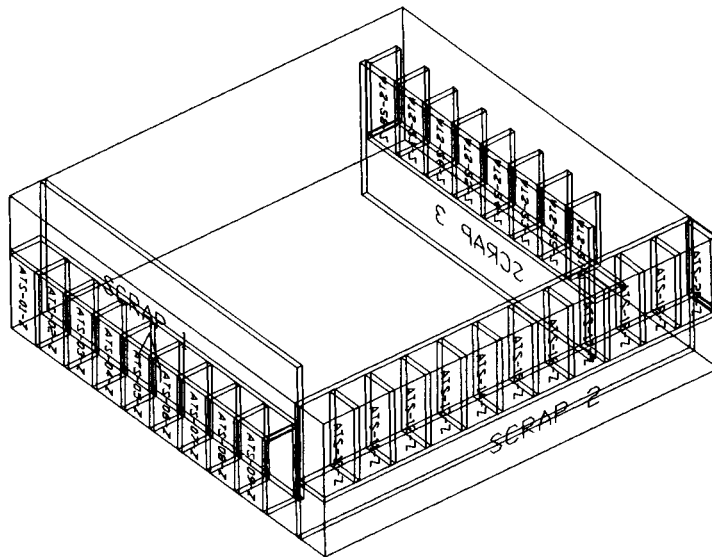


**Figure 3.6 – Location of Z-Direction Test Specimens**

The initial cuts made on the carbon-carbon block were performed with the MK Diamond wet saw described in Section 2.3. Figure 3.7 is a photograph of three sections cut from the block. Each section that is cut is labeled, and the reference face is marked to document the orientation of the section with respect to the established global coordinate system. Whenever possible the high precision, South Bay Technology wet saw is used to make the remaining cuts however, for several of the section orientations it is necessary to use the MK Diamond to further reduce the size of the larger sections. Regardless of which saw is used, the final finish cuts for the length, L, of the specimen are made using the South Bay Technology saw. As discussed in Section 2.3, the critical dimensions for the test specimens are the overall length and the two load surfaces. To insure that the two load surface are parallel both ends of the specimen are cut without removing the specimen from the saw. After the first cut is made the position of the second cut is dialed in using the micrometer that is incorporated in the saw. This method insures that the two surfaces are parallel, and also permits a tolerance of  $\pm 0.003$ -in from the specified length of 0.875-in.



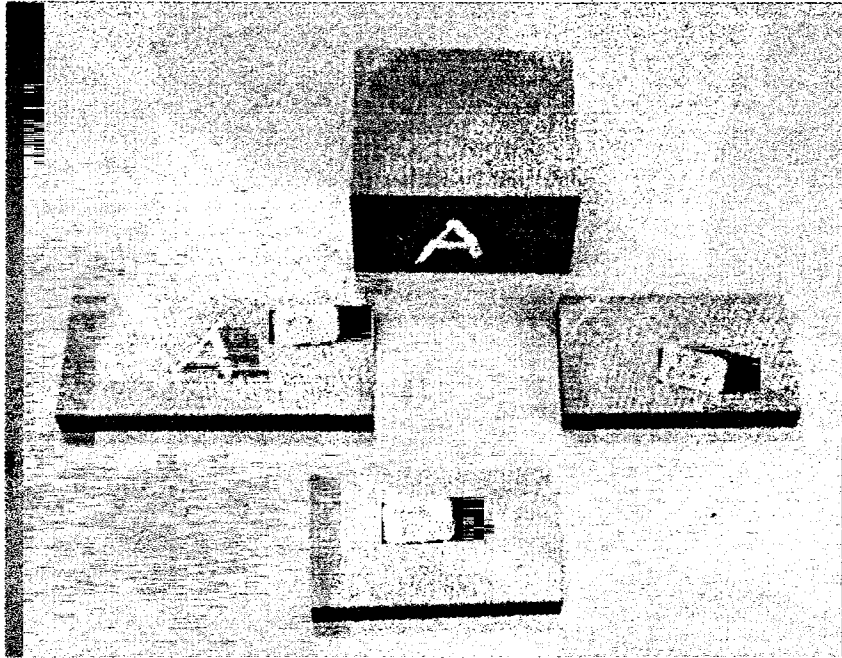


**Figure 3.7 – Sections Cut from the ATS Carbon-Carbon Block**

The in-plane test specimens were cut with little difficulty however; cutting the off-axis specimens at a  $45^\circ$  angle to the principal axis presented a problem; The MK Diamond was too large and too awkward for making the  $45^\circ$  cuts, and the clamping fixture supplied with the South Bay Technology wheel saw was too small to clamp the larger sections at a  $45^\circ$  orientation. To solve the problem a larger, custom-made clamp was constructed that could be used in place of the original clamp. Figure 3.8 illustrates a section of carbon-carbon clamped in the saw with the new clamp, and how the carbon-carbon sections were aligned in the clamp using a Starrett<sup>R</sup> Combination Square.

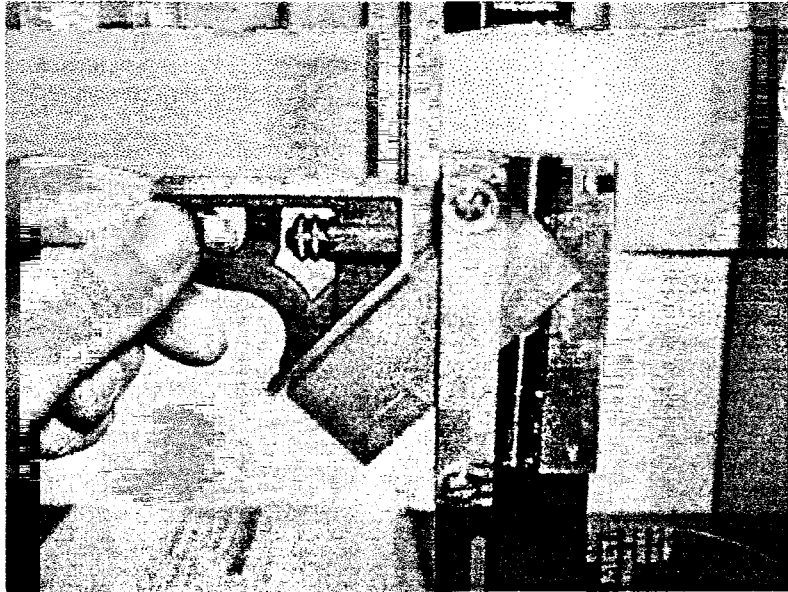


**Figure 3.8 – Clamp for Cutting the Off-Axis Specimens**

After each specimen is cut from the carbon-carbon block the dimensions are measured using a pair of dial Vernier calipers with a precision of 0.001-in., and the weight of each specimen is recorded to the nearest one-hundredth of an ounce. Each specimen is placed in a small zip-lock bag and labeled. The test specimen data is logged in a spreadsheet, and the density of each specimen is calculated, with the final test specimen data available in Appendix D.

Once all of the test specimen data is compiled, the final test matrix is developed. For each test temperature and test orientation five specimens are chosen based on the density of the specimens; for any group of five specimens a density range of the higher density specimens to lower density specimens is attained. The purpose of this is to insure that a distribution of specimens is achieved for each group of tests that is representative of the entire block of carbon-carbon. Figure 3.9 illustrates a small portion of the test matrix to

demonstrate the format used. The complete test matrix is available in Appendix E. For clarity each temperature group is shaded a different color. The temperature column is left blank for any extra specimens that are not tested.

| Specimen | Temperature<br>°C | Density<br>lb/in <sup>3</sup> | Comments |
|----------|-------------------|-------------------------------|----------|
| ATS-01-X | room temp         | 0.0652                        |          |
| ATS-02-X |                   | 0.0663                        |          |
| ATS-03-X | 1200              | 0.0662                        |          |
| ATS-04-X | 600               | 0.0688                        |          |
| ATS-05-X | room temp         | 0.0696                        |          |
| ATS-06-X | 800               | 0.0693                        |          |
| ATS-07-X |                   | 0.0664                        |          |
| ATS-08-X | 800               | 0.0654                        |          |
| ATS-09-X | 600               | 0.0696                        |          |

**Figure 3.9 – Format of the Test Matrix**

### 3.2 Test Procedure

Chapter 2 presented the steps taken to develop a successful test method for high temperature testing however, a detailed testing procedure was not presented. This is primarily because the proof tests were used to develop a successful procedure to be used for the three-dimensional carbon-carbon tests. This section details the refined procedure used to conduct all of the three-dimensional carbon-carbon tests.

The documentation of each test included filling out a test data sheet to record all of the relevant test parameters and uploading the raw data files into Microsoft Excel. A sample test data sheet is available in Appendix E. After each test was completed a stress-strain curve was created in Excel to ascertain if problems with the data acquisition developed during the test. This procedure enabled any problems to be rectified prior to conducting subsequent tests. The only problem encountered was the extensometer slipping during a

few of the tests. In most cases small alignment adjustments could be made to solve the problem prior to the next test.

The relevant parameters for all of the tests conducted include: test specimen orientation, test temperature, furnace warm-up rate, load rate, and data sampling rate. Test temperature and specimen orientation are the variables of interest, therefore the remaining variables are held constant for all of the tests. The warm-up rate for the furnace was set to approximately 7°C per minute (12.8°F per minute). The primary reason a fairly slow warm up rate was chosen was to prevent the alumina platens from cracking due to stresses developed from the large temperature gradient created by having one end of the platen at room temperature and one end inside the furnace. After several tests were successfully completed it was discovered that the furnace tuning constants were not optimally adjusted, and the actual warm-up rate was determined to be around 12°C per minute (24.8°F per minute). This rate did not appear to have any ill effects on the test equipment; subsequently the test parameters were not changed in an effort to maintain consistent testing parameters for the remaining tests. After the furnace reached the desired temperature, five minutes was allowed for the temperature in the furnace to equilibrate and to insure that the test specimen reached the desired test temperature. The load rate, as described in Section 2.2, was 0.005-in/min for the in-plane tests. A significant decrease in stiffness for the off-axis test specimens resulted in a change in the load rate from 0.005-in/min to 0.01-in/min.

The step-by-step procedure used to conduct all of the tests is as follows:

1. Enter the required parameters into the 'Universal Temperature Control Program'.
2. Start the MTS Teststar software and open the C-C Compression template.
3. Zero the displacement and load channels on the MTS control pod.
4. Center a test specimen on the lower alumina platen and slowly raise the actuator, using load control, until the specimen contacts the upper platen. Adjust the load to apply approximately 50-lbf of load to the specimen.
5. Carefully swing the extensometer arm into position and attach the extensometer extension arms to the alumina platens by securing the pointed ends in the small groves cut in the platens.
6. Tighten the two bolts that clamp the extensometer mounting arm to the MTS load frame and insure that equal pressure is applied to each extension rod to prevent the extensometer from slipping during the test.
7. Close the furnace, turn on the air-cooling and water-cooling and start the temperature control program.
8. After the furnace has reached temperature, wait five minutes to insure that the test specimen has reached the desired test temperature before starting the test. It is important to allow the same amount of time for the furnace and test specimen to equilibrate due to the time dependent oxidation of the specimen.
9. Insure that the compressive load on the specimen is no more then approximately 50-lbs and adjust accordingly. Zero the displacement, force and extensometer channels, and switch the pod to displacement control.
10. Turn off the Actuator Positioning Control and begin the test.

11. After the test is complete remove the extensometer from the furnace prior to unloading or lowering the actuator. Failure to do this may snap the quartz extension rods on the extensometer.
12. Stop the temperature control program and wait until the temperature of the furnace has cooled to approximately 200°F (93°C) before opening the furnace and removing the test specimen. Allowing adequate cooling time is critical to the service life of the graphite heating elements, the alumina insulation, and the load platens.

### **3.3 Oxidation Study**

An oxidation study was performed to determine the rate at which the test specimens oxidized from 1112°F (600°C) to 1832°F (1000°C). The test specimens exhibited less than 5% mass loss and less than 1% loss in cross sectional area during the 1112°F (600°C) tests however, more extensive oxidation was observed for all of the 1472°F (800°C) tests and severe oxidation occurred for the three 2192°F (1200°C) tests. Figure 3.10 illustrates the extent of the oxidation at 2192°F (1200°C) compared to an untested specimen. Due to the severe oxidation no further compression tests were conducted at 2192°F (1200°C) and an emphasis was placed on characterizing the oxidation rate from 1112°F (600°C) to 1832°F (1000°C).

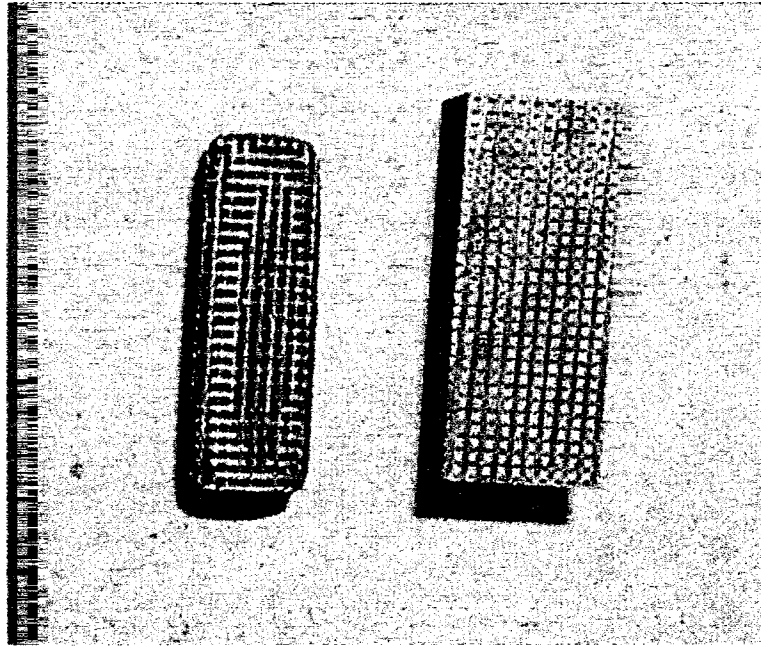


**Figure 3.10 – Specimen Oxidation at 2192°F (1200°C)**

To characterize the oxidation rate of the test specimens, six tests were conducted using extra test specimens from the y-direction orientation. Actual test specimens were used for the tests instead of scrap material because the oxidation rate is dependent on both temperature and surface area. All the specimens were taken from the same material orientation for consistency however; the difference in fiber orientation is not expected to have any significant effect on the oxidation rate. Tests were conducted at constant temperatures of 1112°F (600°C), 1472°F (800°C) and (1000°C). To fully characterize the oxidation rate of the test specimens, specific to the compression test method used, it was also necessary to measure the amount of oxidation that occurred between the temperatures of 1112°F (600°C) and 1472°F (800°C) while the furnace was warming up. To characterize this one test was conducted by ramping the temperature of the furnace

from room temperature to 1472°F (800°C) at the same rate used for conducting the high temperature compression testing.

The oxidation tests were performed using a similar equipment set-up described in Chapter 2 however, the upper load platen was removed and the two-inch diameter hole in the top of the furnace was filled with alumina insulation. Figure 3.11 is a photograph of the furnace positioned in the MTS load frame with the MTS high temperature furnace.

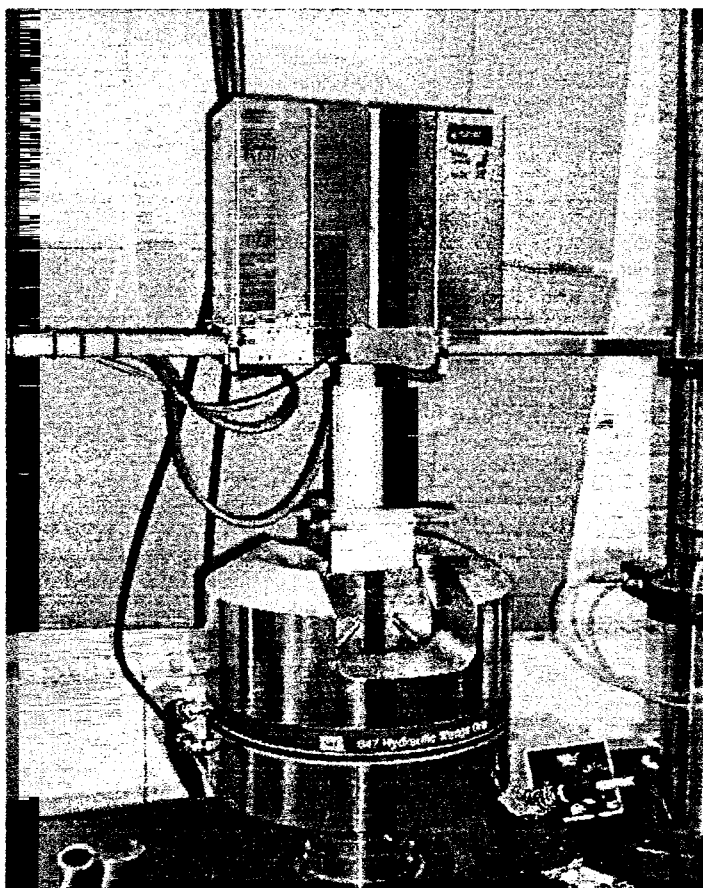


**Figure 3.11 – Oxidation Test Setup**



The warm-up test was performed by placing a test specimen, ATs-26-y, on the lower alumina load platen, raising the actuator of the MTS load frame to position the specimen in the center of the furnace, and then letting the furnace warm up to 1472°F (800°C) at a rate of 13°F per minute (7°C per minute). Once the furnace reached 1472°F (800°C) the lower test fixture was lowered out of the furnace and the weight, length and base dimensions were measured. The specimen exhibited a 7.7% loss in mass, and 2.8% decrease in cross sectional area.

The remaining five tests conducted were used to develop an oxidation rate at a constant temperature. The tests were conducted by warming up the furnace and lower load platen to the desired test temperature, lowering the load platen and placing a test specimen on the platen, inserting the specimen in the furnace by raising the MTS actuator, and then removing the specimen every 10-minutes to measure the weight and dimensions. The first two tests were performed at 1472°F (800°C) using a scale with a precision of 0.1-g, and subsequently did not provide satisfactory resolution. As a result, these test results were discarded. The remaining tests were conducted using a precision digital scale, Mettler PC220, with 0.001-g resolution. Figures 3.12–3.14 illustrates the percent loss in mass, volume and cross sectional area for tests specimens ATs-23-y, ATs-12-y and ATs-20-y. Fewer data points exist for the volume and cross sectional area because after approximately 35% loss of volume and cross sectional area the test specimens no longer closely resembled a prismatic cross section; therefore making calculations of the cross sectional area and volume erroneous. Figure 3.15 is a plot of the percent loss in mass for ATs-23-y, ATs-12-y and ATs-20-y and illustrates the increase in oxidation with

temperature. Figure 3.16 represents the percent loss in cross sectional area for the three oxidation test temperatures. A second order polynomial is fit to the data generated with the ATS-12-y test for the purpose of developing a relation for correcting the compressive stress results for the 1472°F (800°C) tests. To illustrate how well the equation approximates the data, the  $R^2$  value is also shown with the equation.

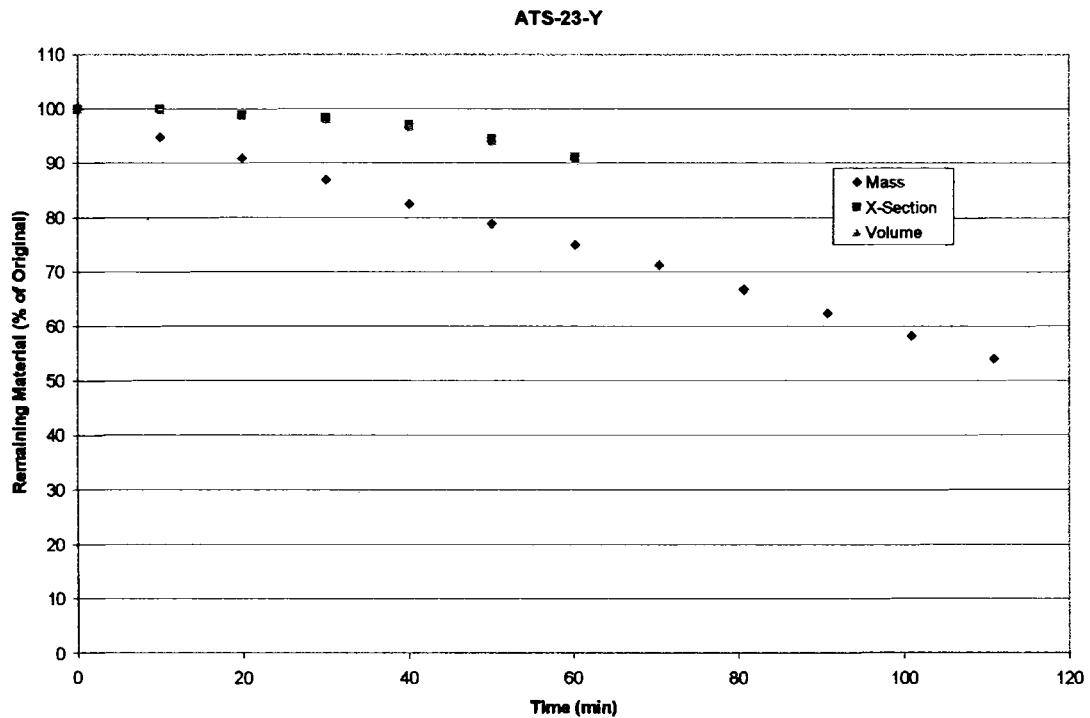


**Figure 3.12 - Percent Loss of Mass, Cross Sectional Area, and Volume Due to Oxidation at 1112°F (600°C)**

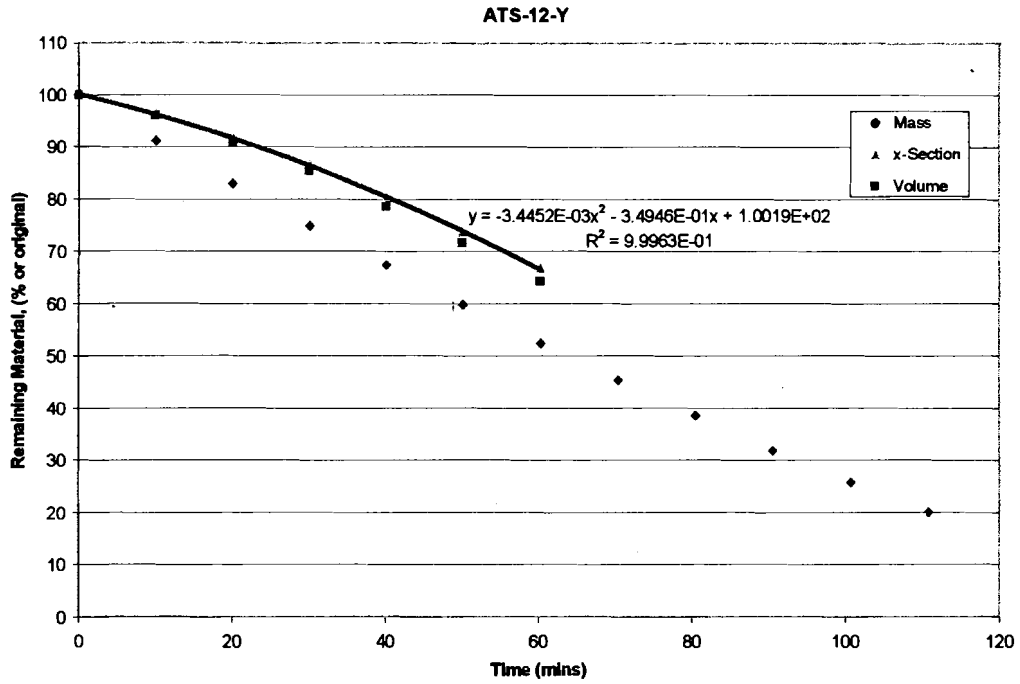


**Figure 3.13 - Percent Loss of Mass, Cross Sectional Area, and Volume Due to Oxidation at 1472°F (800°C)**

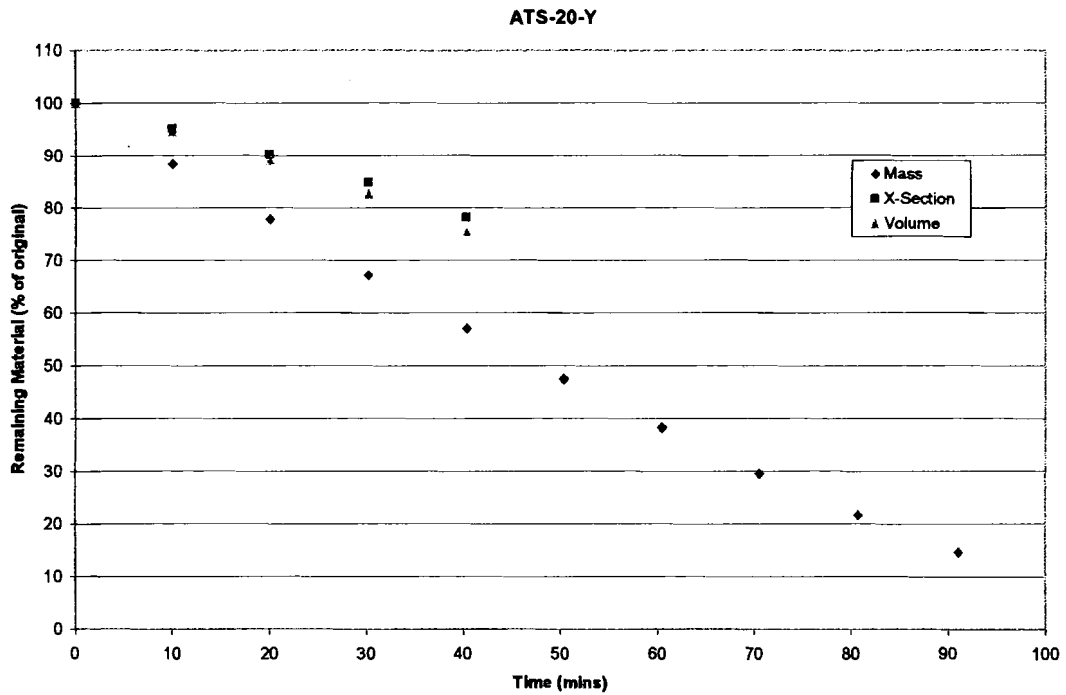


**Figure 3.14 – Percent Loss of Mass, Cross Sectional Area, and Volume Due to Oxidation at 1832°F (1000°C)**

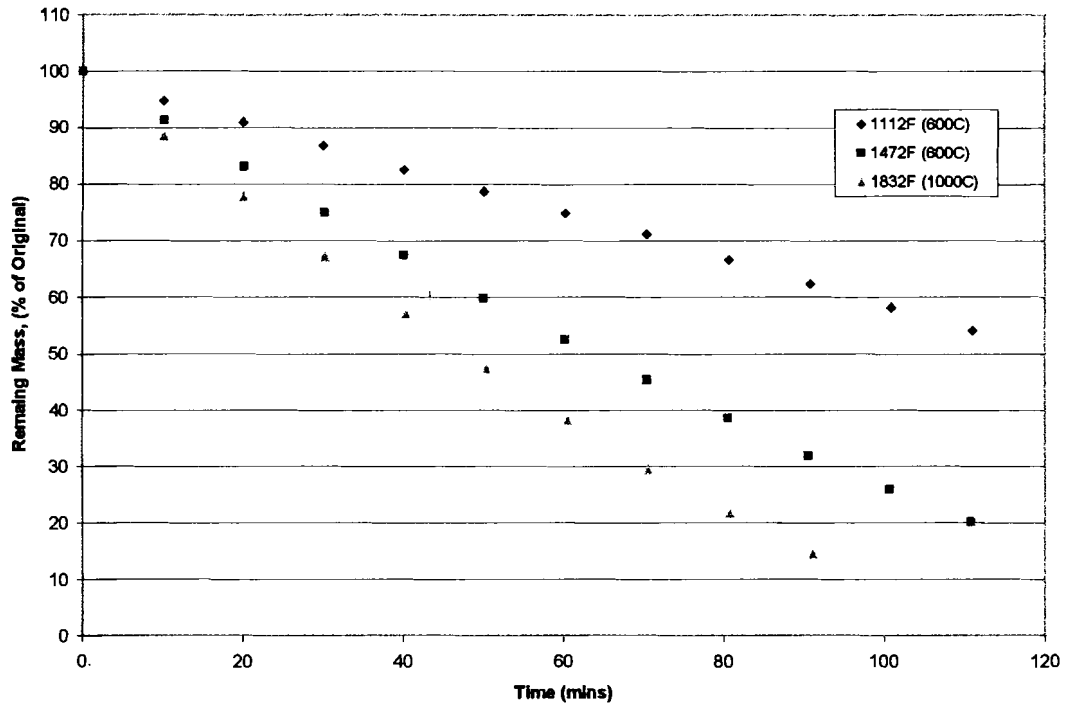


**Figure 3.15 – Oxidation Rates for Mass Loss**

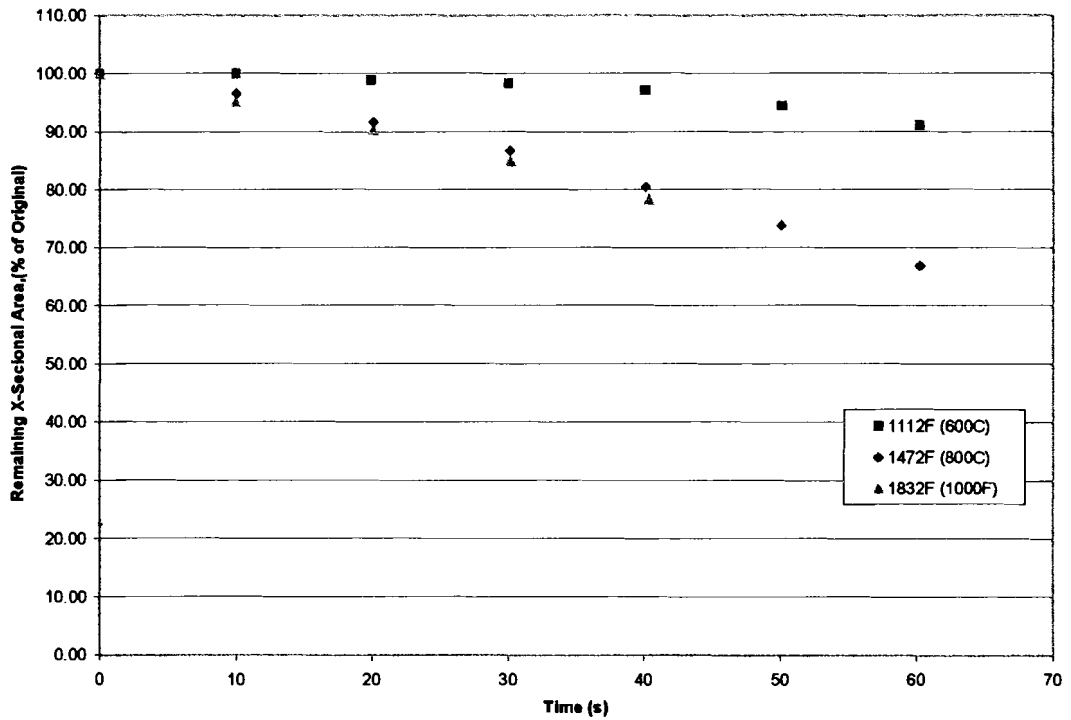


**Figure 3.16 – Oxidation Rates for Cross Sectional Area Loss**

The compressive stress is determined for each data point by dividing the applied load measured with the MTS load frame by the cross sectional area of each test specimen. For the 1472°F (800°C) tests, the stress data is corrected by developing an equation that represents the decrease in cross sectional area as a function of time. For all of the compression tests the time is recorded for every data point, allowing for the calculation of the material loss once the test has begun. This equation is simply the polynomial shown in Figure 3.13,

$$y = -9.5699 \cdot 10^{-7} t^2 - 5.8244 \times 10^{-3} t + 100 \quad (1)$$

Where 't' is the time in seconds and y is the percent of the original cross sectional area remaining. The equation is expressed in terms of minutes in Figure 3.13 however; for the purpose of this analysis the equation is converted to seconds. The oxidation that occurs during the warm up period of each test must also be accounted for. Subtracting the percent decrease in cross sectional area of 2.8% from Equation 1 accounts for the loss that occurs during the warm up period. For each high temperature compression test five minutes was allowed from the time the furnace reached temperature to the time the test was started. This is accounted for by adding five minutes, or 300-seconds, to every time increment. The final equation representing the percent cross sectional area remaining as a function of time becomes,

$$y = -9.5699 \cdot 10^{-7} (t+300)^2 - 5.8244 \times 10^{-3} (t+300) + 97.2 \quad (2)$$

This equation allows for the compressive stress to be adjusted, compensating for the decreasing cross sectional area during each test. Using this relation, a percent loss in cross sectional area of approximately 4.6% occurs prior to initiation of each test, and a

percent loss of approximately 7-9% by the completion of each test. Any remaining oxidation occurred while the furnace was cooling down.

### **3.4 Test Results**

A total of 48 in-plane tests and 18 off-axis tests were conducted. Problems with the extensometer slipping, that were not discovered until after all the tests were complete, resulted in invalid strain measurement for three of the in-plane tests. The three tests conducted at 1200°C (2192°F) experienced severe oxidation, which prohibited accurate calculation of the compressive stress. The 800°C (1472°C) tests also exhibited oxidation however; the amount of oxidation was small enough that the results could be adjusted, per Section 3.3, to account for oxidation. The modulus of elasticity was determined for each in-plane test specimen and the ultimate compressive strength is also examined however; problems with end crushing of the specimens may provide a conservative ultimate compressive strength. Though most of the test specimens exhibited end crushing as the failure mode, several specimens ultimately failed in shear. The off-axis tests provided useful data on how the material behaved at 45° orientations from the X, Y, and Z-directions and allowed for an approximation of the ultimate shear strength. The stress transformation used to determine the ultimate shear stress from the applied axial stress is shown in Equation 3 below. Figure 3.17 illustrates the local coordinate system used to define the load direction and principal material orientation for each off-axis test specimen. The principal coordinate system is oriented 45° from the X-axis about the Z-axis, which is positive out of the page. Though the test specimens were cut from three

different planes with respect to the global material coordinate system, as shown in Figure 3.4, the local and principal coordinate systems shown in Figure 3.17 remain the same.

$$\begin{pmatrix} \sigma_1 \\ \sigma_2 \\ \sigma_3 \\ \tau_{23} \\ \tau_{13} \\ \tau_{12} \end{pmatrix} = \begin{pmatrix} \cos^2 \theta & \sin^2 \theta & 0 & 0 & 0 & 2 \cdot \cos \theta \cdot \sin \theta \\ \sin^2 \theta & \cos^2 \theta & 0 & 0 & 0 & -2 \cdot \cos \theta \cdot \sin \theta \\ 0 & 0 & 1 & 0 & 0 & 0 \\ 0 & 0 & 0 & \cos \theta & -\sin \theta & 0 \\ 0 & 0 & 0 & \sin \theta & \cos \theta & 0 \\ -\cos \theta \cdot \sin \theta & \cos \theta \cdot \sin \theta & 0 & 0 & 0 & \cos^2 \theta - \sin^2 \theta \end{pmatrix} \begin{pmatrix} \sigma_x \\ \sigma_y \\ \sigma_z \\ \tau_{yz} \\ \tau_{xz} \\ \tau_{xy} \end{pmatrix} \quad (3)$$

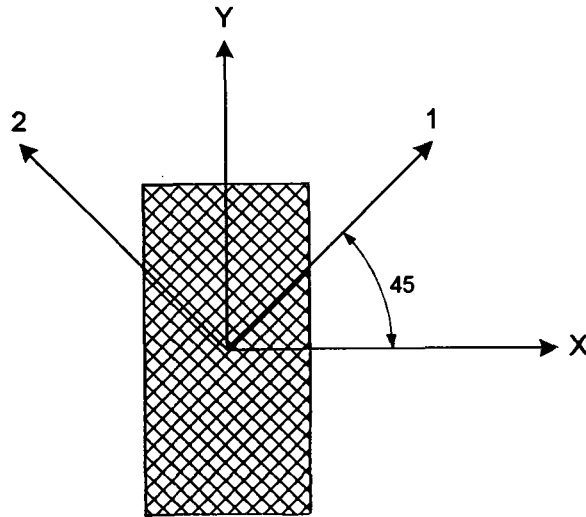


**Figure 3.17 – Local and Principal Coordinate System**

The load is applied in the negative Y-direction for all of the tests,  $\sigma_y$ , and all other stresses in the local coordinate system;  $\sigma_x$ ,  $\sigma_z$ ,  $\tau_{yx}$ ,  $\tau_{xz}$ , and  $\tau_{xy}$ , are assumed to be negligible compared to  $\sigma_y$ . With this assumption, the only non-zero terms are  $\sigma_1$ ,  $\sigma_2$ , and

$\tau_{12}$ . The shear stress,  $\tau_{12}$ , is the term of interest, and when substituting  $45^\circ$  into equation 3 the resulting expression is,

$$\tau_{12} = \frac{\sigma_y}{2} \quad (4)$$

Subsequently, the ultimate shear stress results presented in Section 3.4.2 are determined by Equation 4.

To fully characterize the shear modulus of the material the strain in the x and y-direction must be simultaneously measured during the test. The shear modulus,  $G_{12}$ , is defined as,

$$G_{12} = \frac{\tau_{12}}{\gamma_{12}} \quad (5)$$

Where  $\gamma_{12}$  is the shear strain and is defined as,

$$\gamma_{12} = \varepsilon_x - \varepsilon_y \quad (6)$$

Combining Equations 4, 5, and 6 an expression for  $G_{12}$  can be formulated in terms of the axially applied compressive stress,  $\sigma_y$ ,  $\varepsilon_x$  and  $\varepsilon_y$ :

$$G_{12} = \frac{\sigma_y}{2 \cdot (\varepsilon_x - \varepsilon_y)} \quad (7)$$

Equation 7 illustrates that two strain components must be measured during the test to enable the determination of the shear modulus  $G_{12}$ . Due to the nature of the test apparatus, which employs a single extensometer for axial strain measurement, it is not possible to measure  $\varepsilon_x$ .



### **3.4.1 In-Plane Tests**

A total of 48 in-plane tests were conducted, and 48 individual stress strain curves were developed. The tests exhibited similar stress-strain curves for each group of specimens from a given material orientation; therefore a representative plot for each testing orientation is presented in Figures 3.18-3.20. The plots for the remaining tests are available in Appendix G. The two curves in each plot represent the two different methods used for measuring strain; the MTS displacement transducer (LVDT) and the MTS extensometer. The plots clearly illustrate the compliance of the testing apparatus was a factor in the LVDT strain measurement taken from the load frame however; in some of the tests the extensometer slipped before the test was complete and the LVDT strain measurements provided a good representation of the specimens response for the remainder of the test. For determination of the modulus, only the strain data from the extensometer is used.

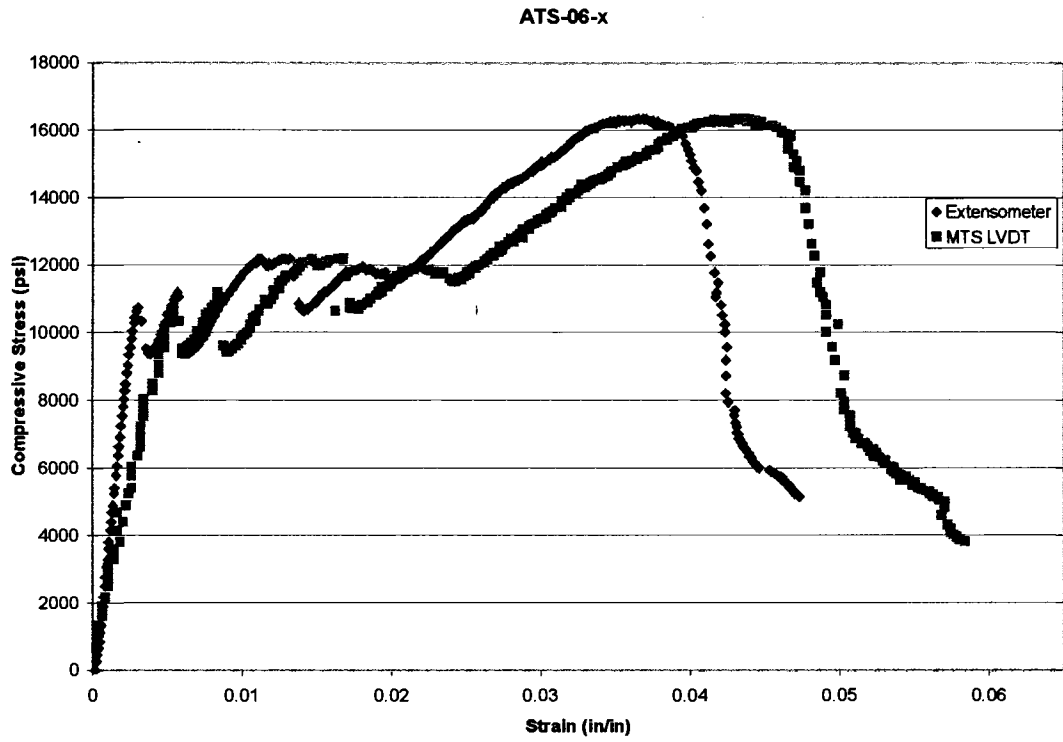


**Figure 3.18– Typical X-Direction Stress-Strain Curve**

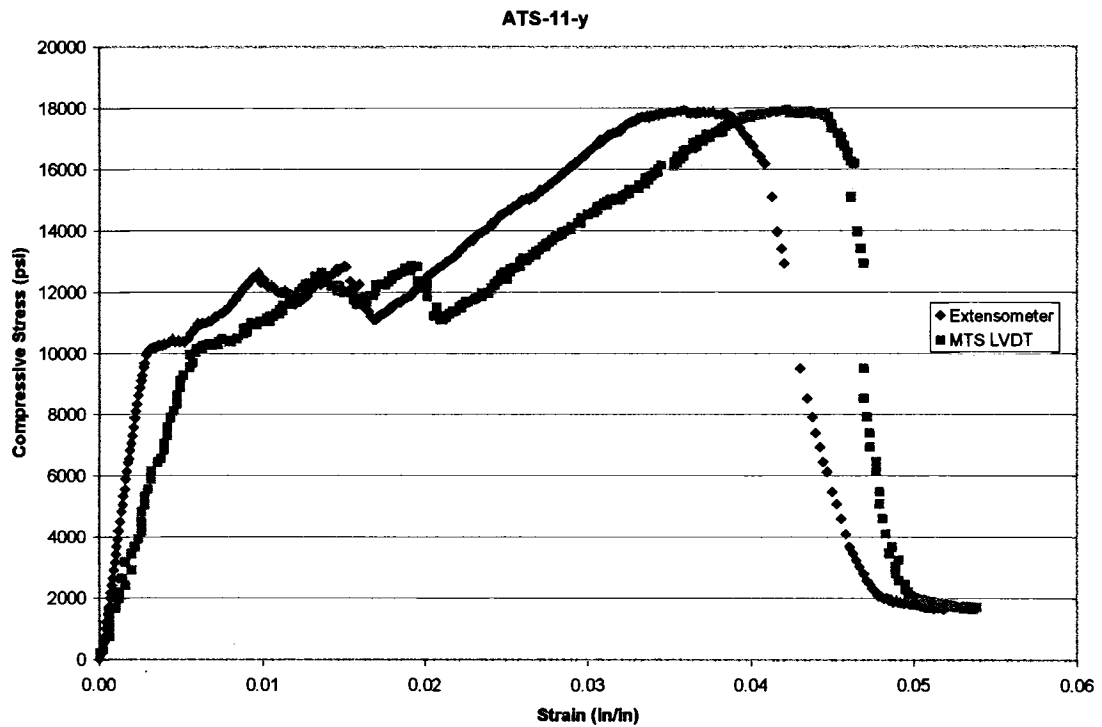


**Figure 3.19 – Typical Y-Direction Stress-Strain Curve**

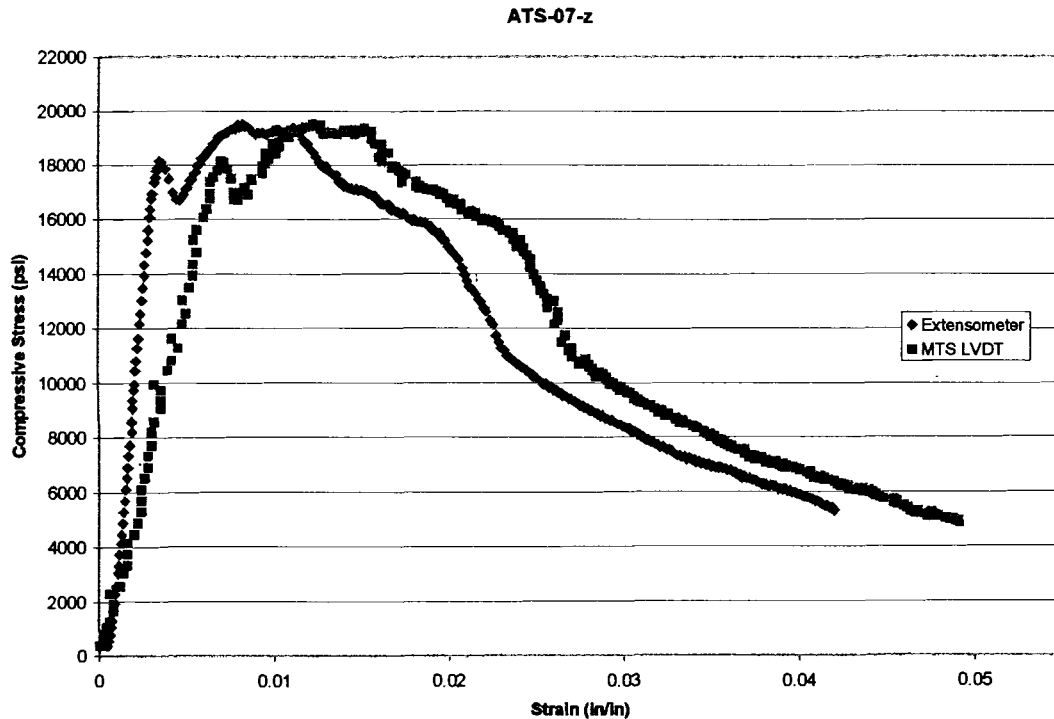


**Figure 3.20 – Typical Z-Direction Stress Strain Curve**

Each point on the plots in Figures 3.18-3.20 where a sharp drop in load occurs indicates where end crushing occurred during the test. Eventually, the specimen ends crushed sufficiently to cause instability of the test specimen in the test fixture, inhibiting the specimen from carrying any further load. Figure 3.21 is a photograph that illustrates a typical specimen failure by end crushing. Though end crushing was the predominant failure mode, eleven of the in-plane specimens, seven x-direction, four y-direction, and one z-direction, ultimately failed in shear. Figure 3.22 illustrates the shear failure of ATS-23-x, which was tested at 1112°F (600°C). Only one of the specimens that failed in shear failed at room temperature, the remaining all failed at either 1112°F (600°C) or 1472°F (800°C).

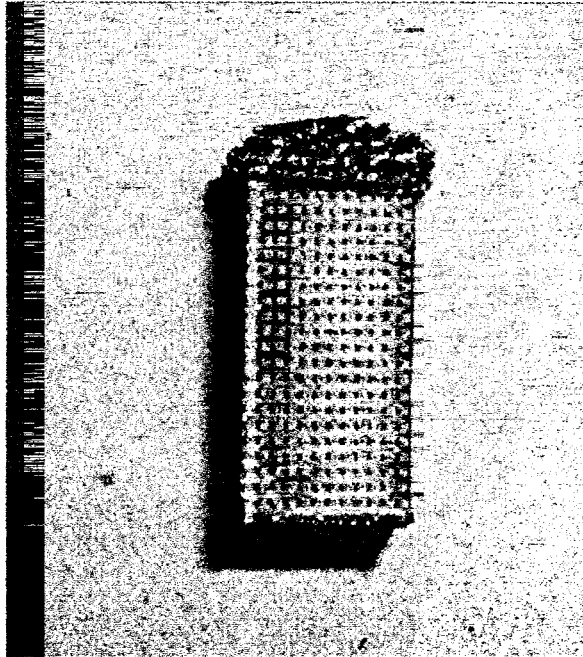


**Figure 3.21 – Specimen End Crushing**



**Figure 3.22 – Specimen Shear Failure**

Table 3.2-3.4 lists the results at various test temperatures for each test and includes the compressive modulus, correlation coefficient, ultimate compressive strength, percent deviation from the average compressive strength, density and failure mode. The correlation coefficient was computed on the data in the linear portion of the stress-strain curves. The 'invalid' entries for the modulus indicate that the extensometer slipped during the test, invalidating the strain measurements. It is noted that the compressive strength of the test specimens that failed in shear was not significantly higher than the specimens that failed by end crushing. For test specimen ATS-16-y the ultimate compressive strength is not presented because the test was terminated prematurely due to a hydraulic problem with the test equipment.

Table 3.5 summarizes the average compressive modulus and ultimate strength results for the in-plane tests. The average modulus for the X, Y, and Z-direction specimens exhibited a decrease of 6 – 10% from room temperature to 1112°F (600°C). The average modulus from room temperature to 1472°F (800°C) exhibited little change for the x-direction tests, an increase of 5.6% for the z-direction tests, and a slight decrease of 1.4% for the y-direction tests. However, the variation in the modulus for each group of five specimens at a given test temperature and material orientation was as high as 53%, for the room temperature x-direction tests, and as low as 3.5%, for the x-direction 1472°F (800°C) tests. With a significant variation in the individual tests results, the relatively small variation in the average modulus, of no more than 10%, demonstrates that the change in modulus from room temperature to 1472°F (800°C) is negligible. The deviation in the ultimate compressive strength from the average compressive strength

was no more than 10% for all of the tests. The average compressive strength was also observed to increase approximately 5-7% from room temperature to 1112°F (600°C) and 3-7% from room temperature to 1472°F (800°C). However, with a deviation of 0-10%, the increases in compressive strength are insignificant.

**Table 3.2 – X-Direction Test Results**

| Room Temperature |                                  |                         |                                   |                          |                               |              |
|------------------|----------------------------------|-------------------------|-----------------------------------|--------------------------|-------------------------------|--------------|
| Test Specimen    | Compressive Modulus<br>Msi (GPa) | Correlation Coefficient | Compressive Strength<br>psi (MPa) | Deviation from Mean<br>% | Density<br>lb/in <sup>3</sup> | Failure Mode |
| ATS-01-x         | 6.501 (44.82)                    | 0.9983                  | 16,800 (115.8)                    | -8.93                    | 0.0652                        | end crushing |
| ATS-05-x         | 3.787 (26.11)                    | 0.9994                  | 18,700 (128.9)                    | 2.14                     | 0.0696                        | end crushing |
| ATS-10-x         | 3.023 (20.84)                    | 0.9985                  | 18,400 (126.9)                    | 0.54                     | 0.0630                        | end crushing |
| ATS-16-x         | 3.925 (27.06)                    | 0.9991                  | 17,900 (123.4)                    | -2.23                    | 0.0662                        | end crushing |
| ATS-25-x         | 3.843 (26.50)                    | 0.9976                  | 19,700 (135.8)                    | 0.71                     | 0.0677                        | shear        |
| 1112°F (600°C)   |                                  |                         |                                   |                          |                               |              |
| Test Specimen    | Compressive Modulus<br>Msi (GPa) | Correlation Coefficient | Compressive Strength<br>psi (MPa) | Deviation from Mean<br>% | Density<br>lb/in <sup>3</sup> | Failure Mode |
| ATS-04-x         | 5.217(35.970)                    | 0.9983                  | 17,800 (122.7)                    | -9.55                    | 0.0688                        | end crushing |
| ATS-09-x         | invalid                          | ---                     | 19,200 (132.4)                    | -1.56                    | 0.0696                        | end crushing |
| ATS-12-x         | 3.873(26.703)                    | 0.9995                  | 20,000 (137.9)                    | 2.50                     | 0.0638                        | end crushing |
| ATS-23-x         | 3.554(24.504)                    | 0.9984                  | 20,700 (142.7)                    | 5.80                     | 0.0663                        | shear        |
| ATS-27-x         | 3.162(21.801)                    | 0.9991                  | 20,000 (137.9)                    | 2.50                     | 0.0654                        | shear        |
| 1472°F (800°C)   |                                  |                         |                                   |                          |                               |              |
| Test Specimen    | Compressive Modulus<br>Msi (GPa) | Correlation Coefficient | Compressive Strength<br>psi (MPa) | Deviation from Mean<br>% | Density<br>lb/in <sup>3</sup> | Failure Mode |
| ATS-06-x         | 4.432 (30.56)                    | 0.9994                  | 18,100 (124.8)                    | -4.97                    | 0.0693                        | end crushing |
| ATS-08-x         | invalid                          | ---                     | 18,600 (128.3)                    | -2.15                    | 0.0654                        | shear        |
| ATS-11-x         | 3.676 (25.35)                    | 0.9982                  | 18,200 (125.5)                    | -4.40                    | 0.0645                        | end crushing |
| ATS-18-x         | invalid                          | ---                     | 19,200 (132.4)                    | 1.04                     | 0.0662                        | end crushing |
| ATS-21-x         | 4.592 (31.66)                    | 0.9977                  | 20,900 (144.1)                    | 9.09                     | 0.0670                        | end crushing |

**Table 3.3 – Y-Direction Test Results**

| Room Temperature |                                  |                         |                                   |                          |                               |              |
|------------------|----------------------------------|-------------------------|-----------------------------------|--------------------------|-------------------------------|--------------|
| Test Specimen    | Compressive Modulus<br>Msi (GPa) | Correlation Coefficient | Compressive Strength<br>psi (MPa) | Deviation from Mean<br>% | Density<br>lb/in <sup>3</sup> | Failure Mode |
| ATS-02-y         | 5.115 (35.27)                    | 0.9991                  | 17,300 (119.2)                    | -3.61                    | 0.0624                        | end crushing |
| ATS-08-y         | 3.700 (25.51)                    | 0.9995                  | 18,000 (124.1)                    | 0.42                     | 0.0689                        | end crushing |
| ATS-14-y         | 3.628 (25.01)                    | 0.9989                  | 18,100 (124.8)                    | 0.97                     | 0.0647                        | end crushing |
| ATS-16-y         | 4.255 (29.34)                    | 0.9976                  | invalid                           | ---                      | 0.0679                        | end crushing |
| ATS-18-y         | 4.544 (31.33)                    | 0.9981                  | 18,300 (126.2)                    | 2.05                     | 0.0707                        | end crushing |
| 1112°F (600°C)   |                                  |                         |                                   |                          |                               |              |
| Test Specimen    | Compressive Modulus<br>Msi (GPa) | Correlation Coefficient | Compressive Strength<br>psi (MPa) | Deviation from Mean<br>% | Density<br>lb/in <sup>3</sup> | Failure Mode |
| ATS-01-y         | 3.787 (26.11)                    | 0.9987                  | 19,100 (131.7)                    | 0.73                     | 0.0634                        | end crushing |
| ATS-03-y         | 4.983 (34.35)                    | 0.9984                  | 18,200 (125.5)                    | -4.18                    | 0.0680                        | end crushing |
| ATS-06-y         | 3.405 (23.48)                    | 0.9991                  | 21,100 (145.5)                    | 10.14                    | 0.0660                        | shear        |
| ATS-07-y         | 2.901 (20.00)                    | 0.9987                  | 18,700 (128.9)                    | -1.39                    | 0.0698                        | end crushing |
| ATS-24-y         | 3.914 (26.99)                    | 0.9990                  | 17,700 (128.9)                    | -7.12                    | 0.0655                        | end crushing |
| 1472°F (800°C)   |                                  |                         |                                   |                          |                               |              |
| Test Specimen    | Compressive Modulus<br>Msi (GPa) | Correlation Coefficient | Compressive Strength<br>psi (MPa) | Deviation from Mean<br>% | Density<br>lb/in <sup>3</sup> | Failure Mode |
| ATS-11-y         | 3.966 (27.35)                    | 0.9993                  | 19,200 (132.4)                    | 0.21                     | 0.0652                        | end crushing |
| ATS-13-y         | 3.997 (27.56)                    | 0.9980                  | 19,300 (137.1)                    | 0.73                     | 0.0656                        | shear        |
| ATS-17-y         | 4.083 (28.15)                    | 0.9990                  | 19,400 (133.8)                    | 1.24                     | 0.0672                        | end crushing |
| ATS-22-y         | 4.380 (30.20)                    | 0.9988                  | 18,200 (125.5)                    | -5.27                    | 0.0690                        | shear        |
| ATS-25-y         | 4.511 (31.10)                    | 0.9990                  | 19,700 (126.9)                    | 2.74                     | 0.0644                        | end crushing |

**Table 3.4 – Z-Direction Test Results**

| Room Temperature |                                  |                         |                                   |                          |                               |              |
|------------------|----------------------------------|-------------------------|-----------------------------------|--------------------------|-------------------------------|--------------|
| Test Specimen    | Compressive Modulus<br>Msi (GPa) | Correlation Coefficient | Compressive Strength<br>psi (MPa) | Deviation from Mean<br>% | Density<br>lb/in <sup>3</sup> | Failure Mode |
| ATS-05-z         | 9.244 (63.73)                    | 0.9993                  | 21,100 (145.5)                    | 9.38                     | 0.0625                        | end crushing |
| ATS-06-z         | 6.212 (42.83)                    | 0.9960                  | 18,000 (124.1)                    | -6.22                    | 0.0643                        | end crushing |
| ATS-13-z         | 7.236 (49.89)                    | 0.9990                  | 18,600 (128.2)                    | -2.80                    | 0.0677                        | end crushing |
| ATS-19-z         | 5.648 (38.94)                    | 0.9992                  | 18,300 (126.2)                    | -4.48                    | 0.0676                        | end crushing |
| ATS-21b-z        | 5.558 (38.32)                    | 0.9988                  | 19,600 (135.1)                    | 2.45                     | 0.0698                        | end crushing |
| 1112°F (600oC)   |                                  |                         |                                   |                          |                               |              |
| Test Specimen    | Compressive Modulus<br>Msi (GPa) | Correlation Coefficient | Compressive Strength<br>psi (MPa) | Deviation from Mean<br>% | Density<br>lb/in <sup>3</sup> | Failure Mode |
| ATS-07-z         | 7.226 (49.82)                    | 0.9993                  | 19,500 (134.4)                    | -3.49                    | 0.0633                        | end crushing |
| ATS-09-z         | 6.131 (42.27)                    | 0.9996                  | 19,300 (133.1)                    | -4.56                    | 0.0674                        | end crushing |
| ATS-16-z         | 6.690 (46.13)                    | 0.9995                  | 20,100 (138.6)                    | -0.38                    | 0.0689                        | end crushing |
| ATS-22-z         | 6.000 (41.37)                    | 0.9991                  | 22,100 (152.3)                    | 8.69                     | 0.0652                        | end crushing |
| ATS-28-z         | 5.117 (35.28)                    | 0.9997                  | 19,900 (137.2)                    | -1.41                    | 0.0666                        | shear        |
| 1472°F (800oC)   |                                  |                         |                                   |                          |                               |              |
| Test Specimen    | Compressive Modulus<br>Msi (GPa) | Correlation Coefficient | Compressive Strength<br>psi (MPa) | Deviation from Mean<br>% | Density<br>lb/in <sup>3</sup> | Failure Mode |
| ATS-01-z         | 6.302 (43.45)                    | 0.9995                  | 18,900 (124.1)                    | -4.34                    | 0.0685                        | end crushing |
| ATS-08-z         | 7.435 (51.26)                    | 0.9997                  | 19,400 (133.8)                    | -1.65                    | 0.0635                        | end crushing |
| ATS-11-z         | 6.300 (43.44)                    | 0.9994                  | 19,000 (131.0)                    | -3.79                    | 0.0668                        | end crushing |
| ATS-15-z         | 7.240 (49.92)                    | 0.9984                  | 19,900 (137.2)                    | 0.90                     | 0.0659                        | end crushing |
| ATS-27-z         | 8.525 (58.78)                    | 0.9946                  | 21,400 (147.5)                    | 7.85                     | 0.0662                        | end crushing |



**Table 3.5 – Summary of the Average In-Plane Results**

X-Direction

| Temperature<br>°F (°C) | Compressive<br>Modulus<br>Msi (GPa) | Ultimate<br>Strength<br>psi (MPa) |
|------------------------|-------------------------------------|-----------------------------------|
| room temp              | 4.216 (29.07)                       | 18,300 (126.2)                    |
| 1112 (600)             | 3.952 (27.24)                       | 19,500 (134.7)                    |
| 1472 (800)             | 4.233 (29.19)                       | 19,000 (131.0)                    |

Y-Direction

| Temperature<br>°F (°C) | Compressive<br>Modulus<br>Msi (GPa) | Ultimate<br>Strength<br>psi (MPa) |
|------------------------|-------------------------------------|-----------------------------------|
| room temp              | 4.248 (29.29)                       | 17,925 (123.6)                    |
| 1112 (600)             | 3.798 (26.19)                       | 18,960 (130.7)                    |
| 1472 (800)             | 4.187 (28.87)                       | 19,160 (132.1)                    |

Z-Direction

| Temperature<br>°F (°C) | Compressive<br>Modulus<br>Msi (GPa) | Ultimate<br>Strength<br>psi (MPa) |
|------------------------|-------------------------------------|-----------------------------------|
| room temp              | 6.780 (46.74)                       | 19,120 (131.8)                    |
| 1112 (600)             | 6.233 (42.97)                       | 20,180 (139.1)                    |
| 1472 (800)             | 7.160 (49.37)                       | 19,720 (136.0)                    |

The linear portions of the stress-strain curves for each group of tests are presented in Figures 3.23-3.31. Each plot illustrates the modulus for each specimen tested at a given material orientation and test temperature. The plots further demonstrate the large variation in the modulus for each group of five tests under the same test parameters. However, no correlation could be found between the variation in the modulus and test specimen density, and test specimen location in the original block of carbon-carbon.

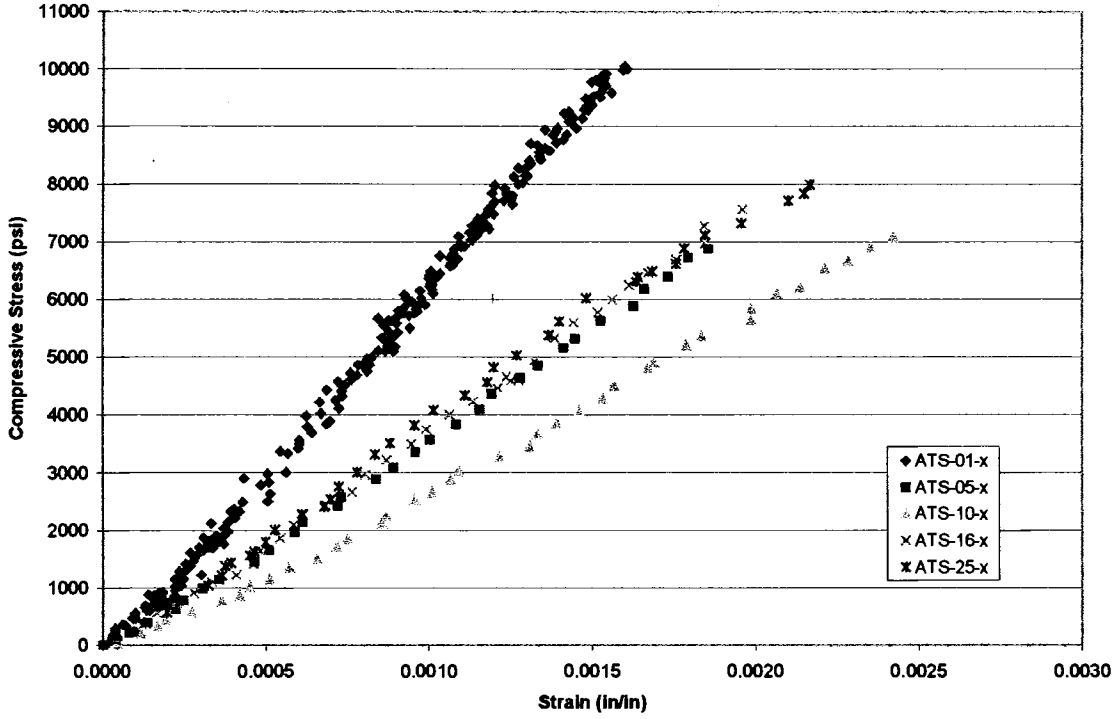


**Figure 3.23 – X-Direction Modulus, Room Temperature**

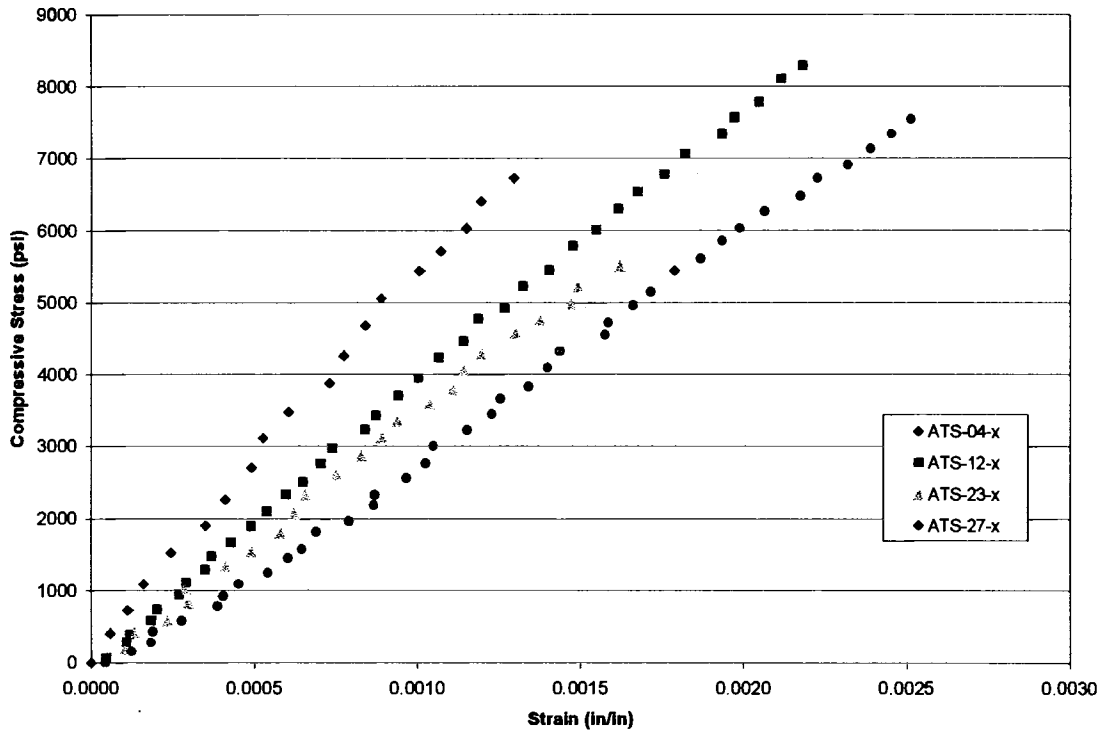


**Figure 3.24 – X-Direction Modulus, 1112°F (600°C)**

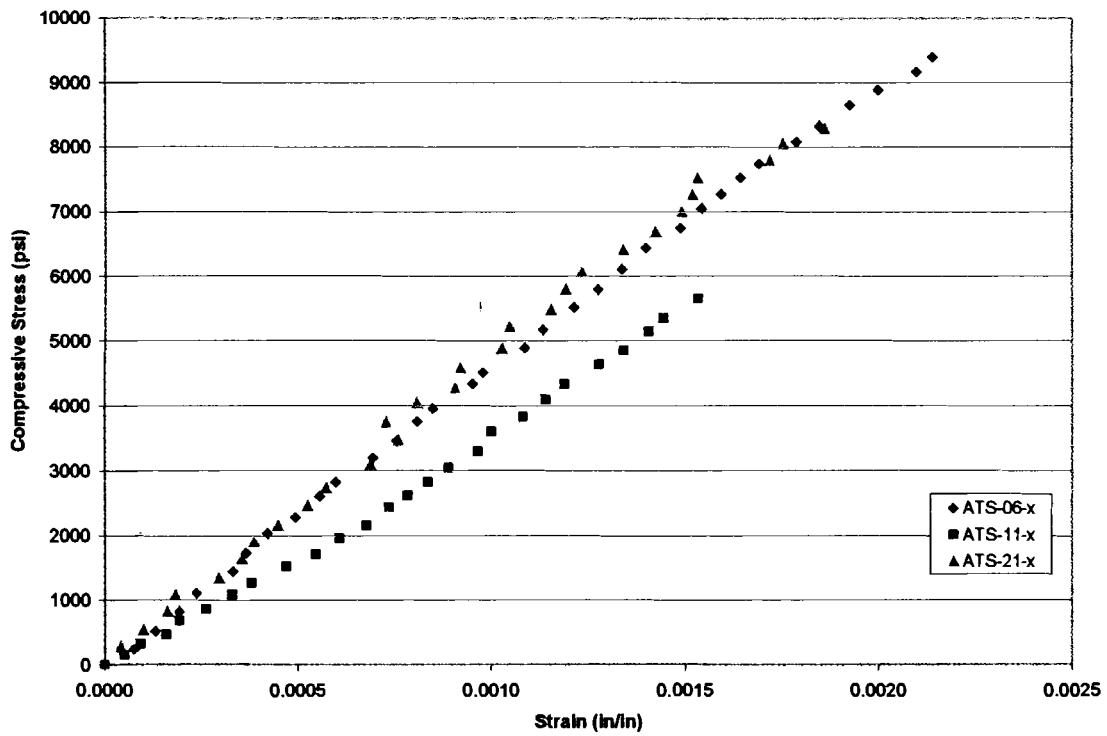


Figure 3.25 – X-Direction Modulus, 1472°F (800°C)

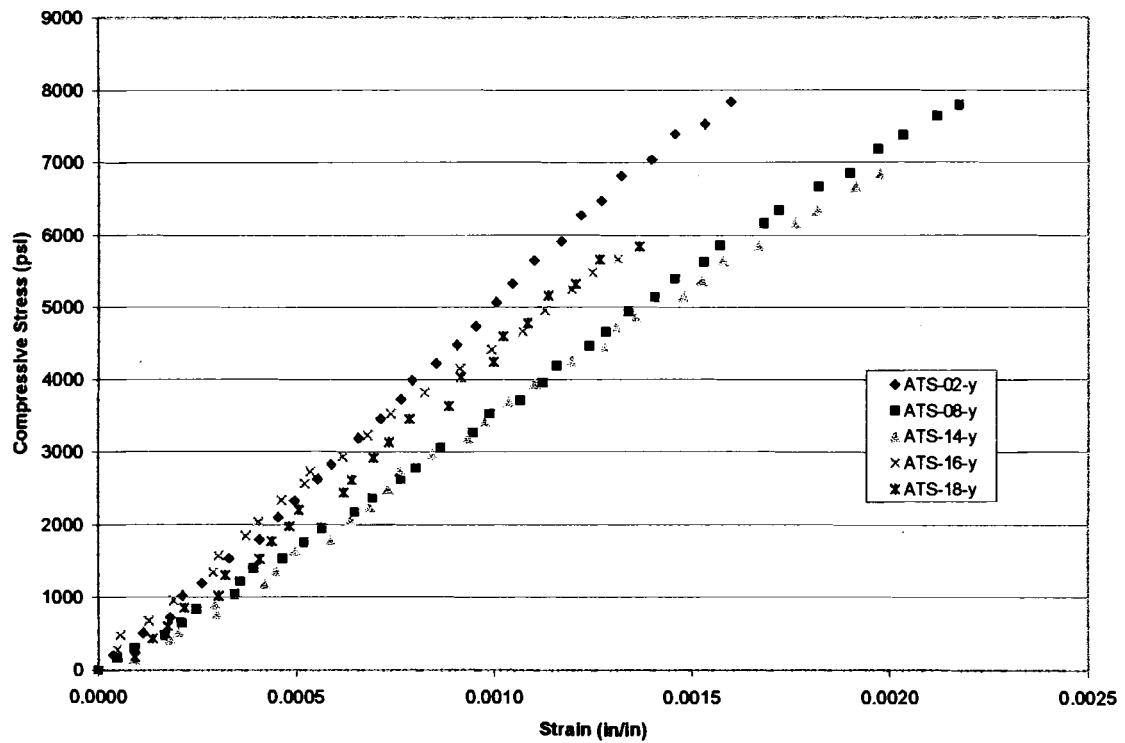


Figure 3.26 – Y-Direction Modulus, Room Temperature

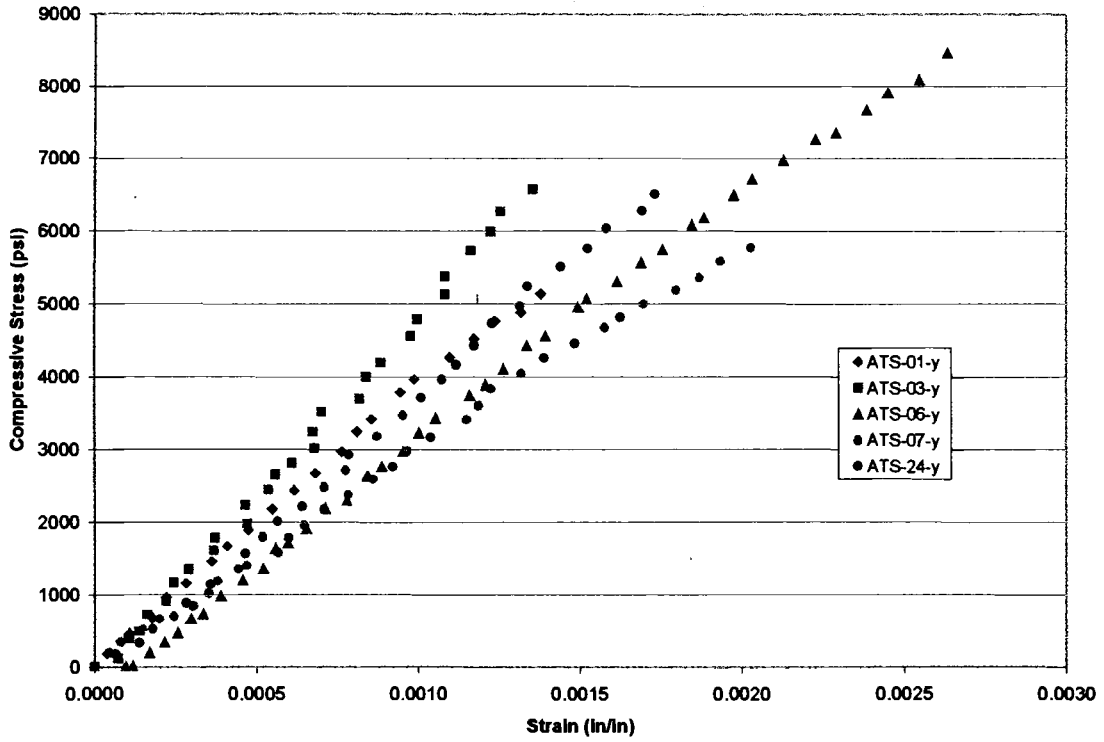


Figure 3.27 – Y-Direction Modulus, 1112°F (600°C)

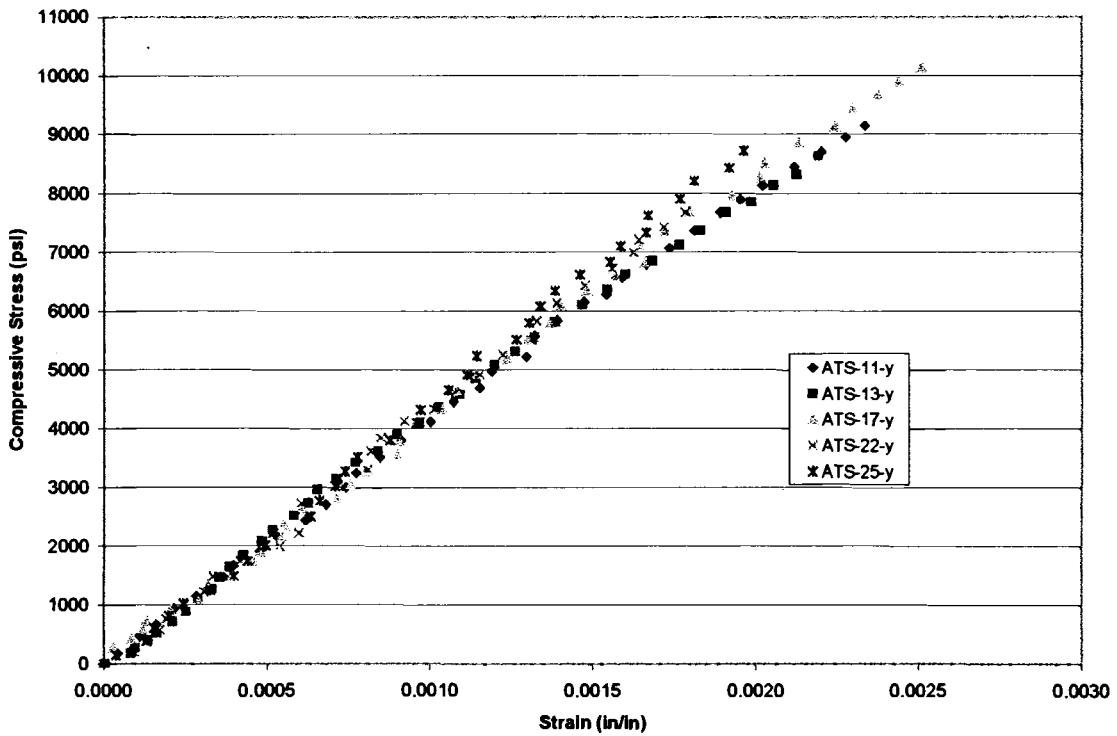
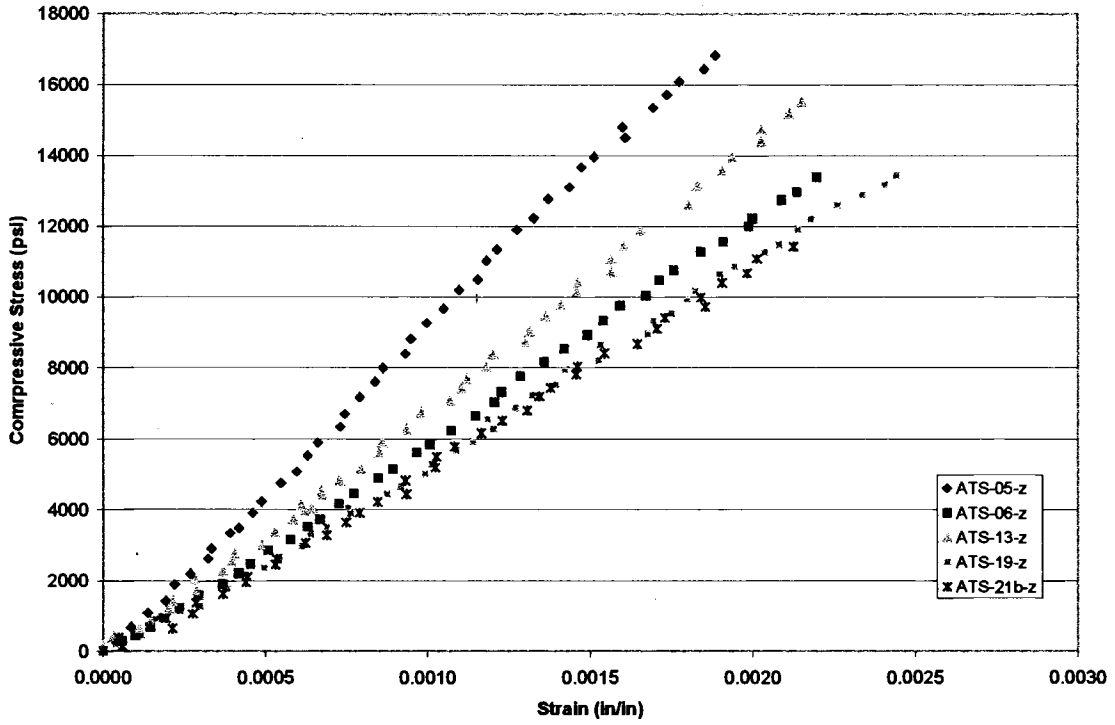
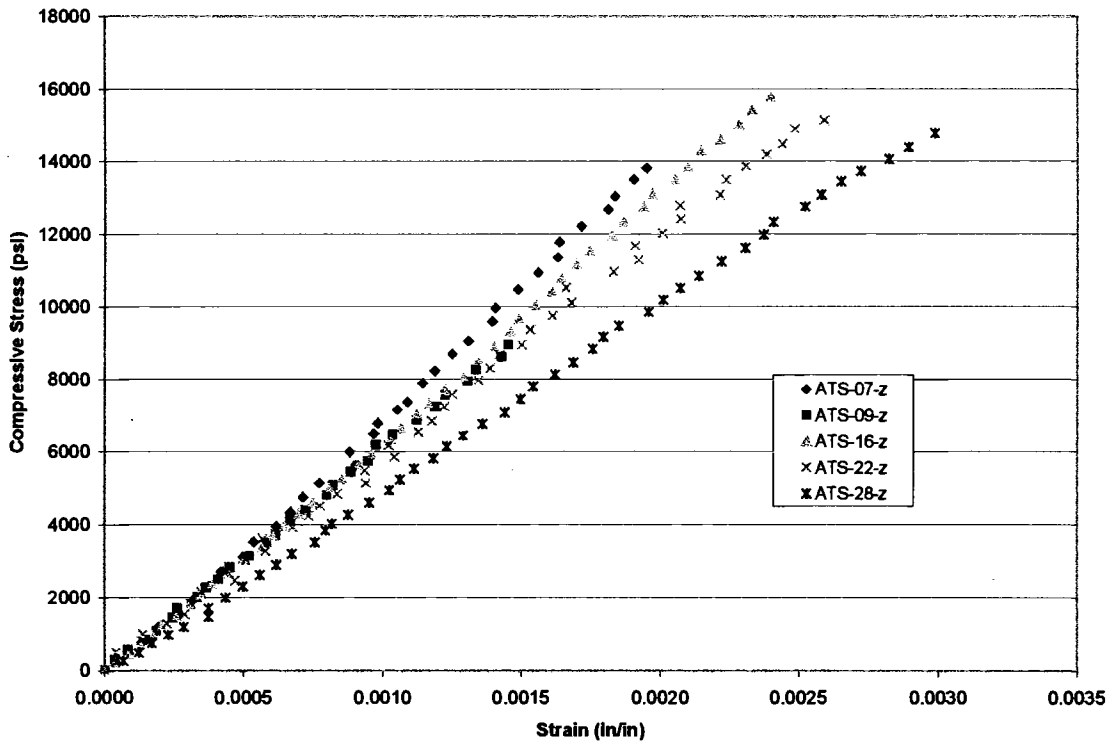


Figure 3.28 – Y-Direction Modulus, 1472°F (800°C)



**Figure 3.29 – Z-Direction Modulus, Room Temperature**



**Figure 3.30 – Z-Direction Modulus, 1112°F (600°C)**

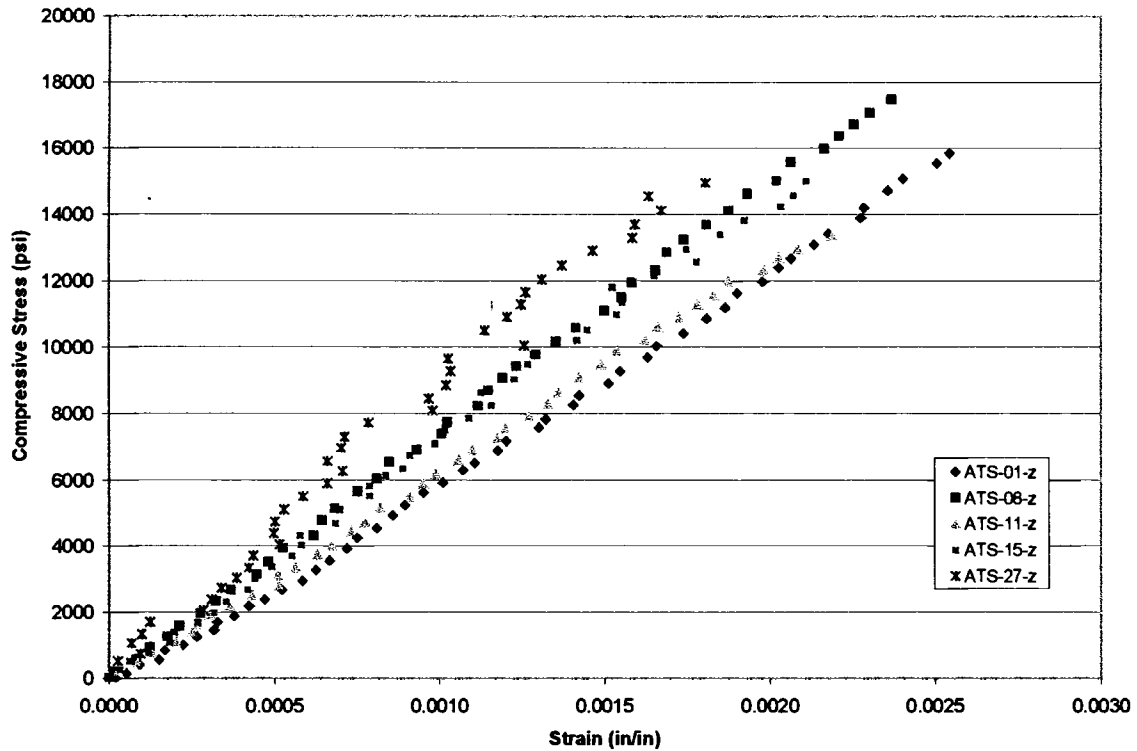


**Figure 3.31 – Z-Direction Modulus, 1472°F (800°C)**

### 3.4.2 Off-Axis Tests

A total of 18 off-axis tests were conducted; six tests at each off-axis orientation in the xy, xz, and yz-planes. One stress-strain plot is selected from each off-axis orientation, as shown in Figure 3.32-3.34, to illustrate the general behavior of the material. The plots for the remaining tests are available in Appendix H. As discussed in Section 3.4.1, each plot contains two stress-strain curves; one developed with the MTS LVDT and one with the MTS high temperature extensometer. The off axis tests exhibited significantly higher strain values than the in-plane tests and exceeded the strain range of 5% in compression for the extensometer. However, the stress-strain curves demonstrate that using the MTS LVDT to calculate the strain is sufficient for all of the off-axis tests because the stiffness of the specimens is sufficiently less than the stiffness of the load frame and test fixtures.

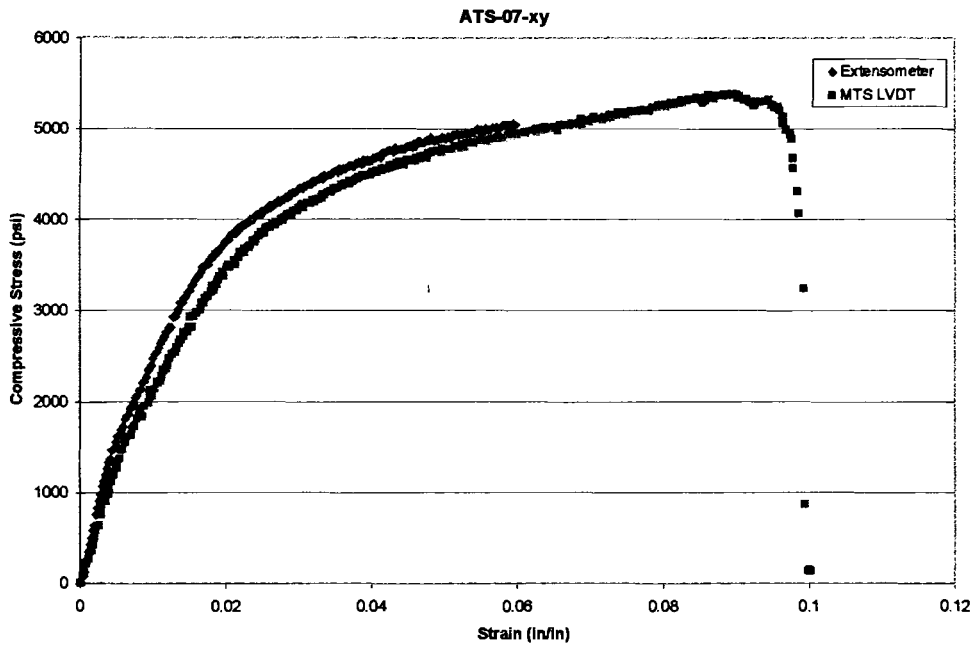


**Figure 3.32 – Typical XY-Plane Stress-Strain Curve**

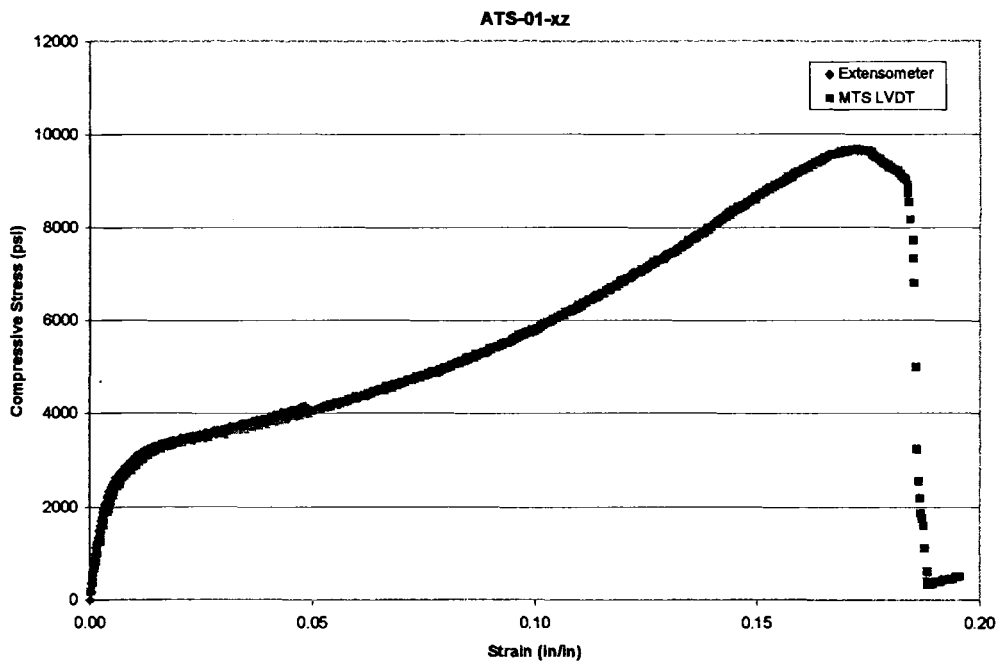


**Figure 3.33 – Typical XZ-Plane Stress-Strain Curve**

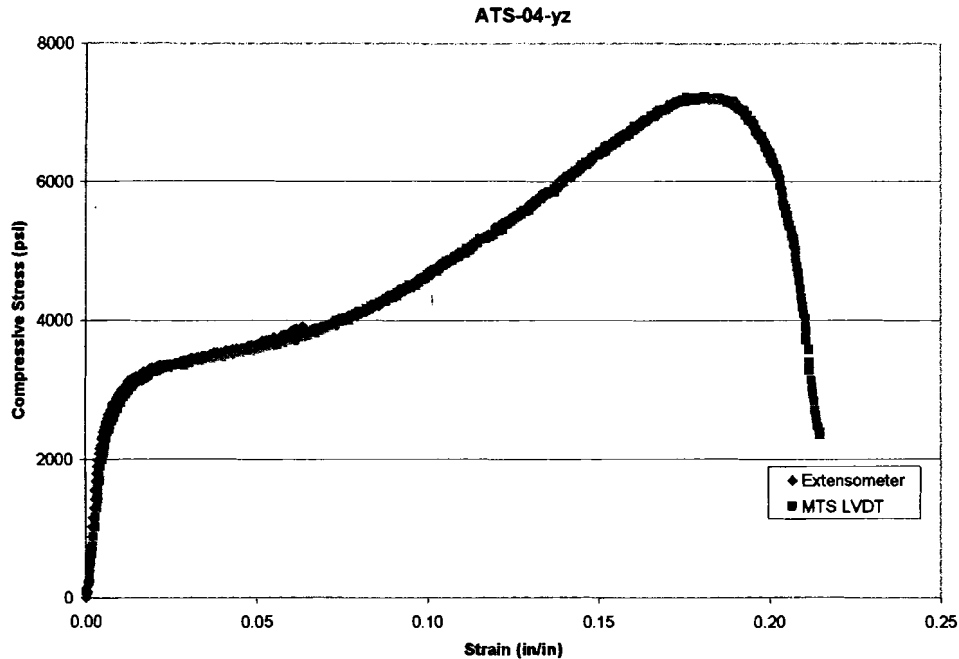


**Figure 3.34 - Typical YZ-Plane Stress-Strain Curve**

Two modes of failure were observed for the off-axis tests; shear failure along one of the fiber planes and matrix crushing however, no end crushing was observed for any of the test specimens. All of the specimens taken from the xy-plane failed in shear, while only two failed in shear from the xz-plane and four from the yz-plane. All of the xz and yz-plane test specimens that failed in shear were conducted at 1112°F (600°C) or 1472°F (800°C), no shear failures occurred with these specimens at room temperature. Figure 3.35 illustrates a typical shear failure of one of the test specimens and Figure 3.36 illustrates a typical matrix failure. For reference, an untested specimen is shown with the failed matrix specimen to illustrate the extent of the specimen failure. Though some of test specimens failed by matrix crushing instead of shear failure, the results demonstrate no significant difference in the ultimate failure stress between the two failure modes. Therefore the failure stress for all of the specimens that exhibited a matrix failure is used to approximate the ultimate shear stress.





**Figure 3.35 – Typical Off-Axis Shear Failure**

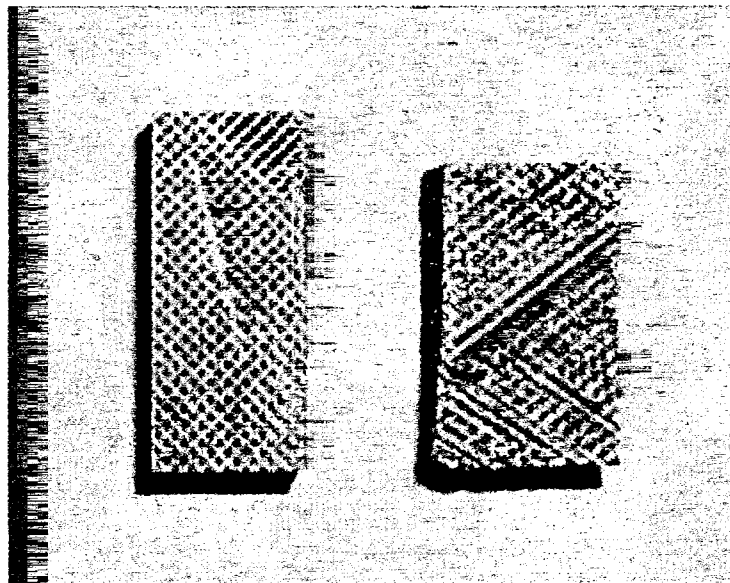


**Figure 3.36 – Typical Matrix Failure**

Table 3.6 summarizes the off axis results and Figure 3.37 illustrates the ultimate shear strength as a function of temperature for each off-axis testing orientation. The ultimate interlaminar shear strength exhibited a slight decrease from room temperature to 1472°F (800°C) for the xz and yz-plane tests, and exhibited no significant change for the xy tests. Figure 3.37 also demonstrates a strong correlation in the response of the ultimate shear strength to temperature for the xz and yz-plane tests. The ultimate shear stress is not available for ATS-yz-01 because the test was terminated prematurely due to test equipment problems.

**Table 3.6 – Summary of the Off-Axis Test Results**

| xy-plane      |                          |                                   |                                 |                            |              |
|---------------|--------------------------|-----------------------------------|---------------------------------|----------------------------|--------------|
| Test Specimen | Test Temperature °F (°C) | Ultimate Failure Stress psi (Mpa) | Ultimate Shear Stress psi (Mpa) | Density lb/in <sup>3</sup> | Failure Mode |
| ATS-xy-04     | room temp                | 4,940 (34.06)                     | 2,470 (17.03)                   | 0.0663                     | shear        |
| ATS-xy-08     | room temp                | 4,200 (28.96)                     | 2,100 (14.48)                   | 0.0697                     | shear        |
| ATS-xy-03     | 1112 (600)               | 4,680 (32.27)                     | 2,340 (16.13)                   | 0.0691                     | shear        |
| ATS-xy-07     | 1113 (600)               | 5,370 (37.02)                     | 2,685 (18.51)                   | 0.0672                     | shear        |
| ATS-xy-05     | 1472 (800)               | 4,370 (31.13)                     | 2,185 (15.07)                   | 0.0691                     | shear        |
| ATS-xy-09     | 1473 (800)               | 4,240 (29.23)                     | 2,120 (14.62)                   | 0.0658                     | shear        |
| xz-plane      |                          |                                   |                                 |                            |              |
| ATS-xz-05     | room temp                | 10,540 (72.67)*                   | 5,270 (36.34)                   | 0.0690                     | matrix       |
| ATS-xz-06     | room temp                | 11,450 (78.94)*                   | 5,725 (39.47)                   | 0.0680                     | matrix       |
| ATS-xz-01     | 1112 (600)               | 9,100 (62.74)                     | 4,550 (31.37)                   | 0.0688                     | shear        |
| ATS-xz-03     | 1113 (600)               | 9,660 (66.60)*                    | 4,830 (33.30)                   | 0.0679                     | matrix       |
| ATS-xz-02     | 1472 (800)               | 8,600 (59.29)                     | 4,300 (29.65)                   | 0.0686                     | shear        |
| ATS-xz-09     | 1473 (800)               | 8,800 (60.67)*                    | 4,400 (30.34)                   | 0.0658                     | matrix       |
| yz-plane      |                          |                                   |                                 |                            |              |
| ATS-yz-01     | room temp                | N/A *                             | N/A                             | 0.0691                     | matrix       |
| ATS-yz-07     | room temp                | 11,370 (78.39)*                   | 5,685 (39.20)                   | 0.0660                     | matrix       |
| ATS-yz-05B    | 1112 (600)               | 9,700 (66.88)                     | 4,850 (33.44)                   | 0.0659                     | shear        |
| ATS-yz-6      | 1113 (600)               | 10,500 (72.39)                    | 5,250 (36.20)                   | 0.0685                     | shear        |
| ATS-yz-04     | 1472 (800)               | 7,200 (49.64)                     | 3,600 (24.82)                   | 0.0656                     | shear        |
| ATS-yz-09     | 1473 (800)               | 9,450 (65.16)                     | 4,725 (32.58)                   | 0.0681                     | shear        |

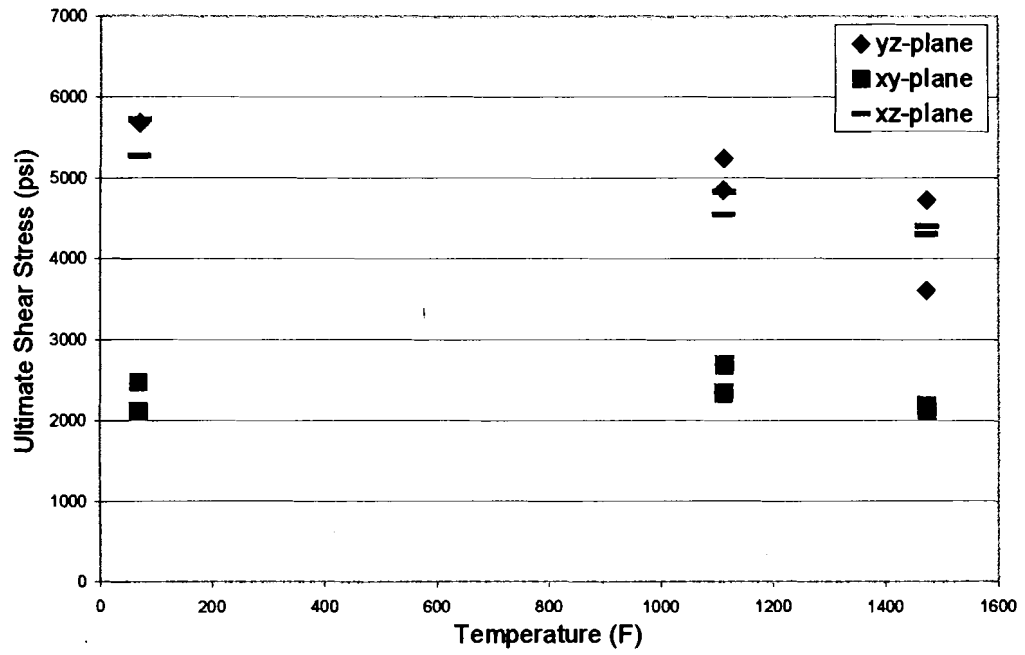


**Figure 3.37 – Shear Strength as a Function of Temperature**

## **4. CONCLUSIONS AND RECOMMENDATIONS**

### **4.1 Conclusions**

A high temperature, compression testing system was developed to evaluate the compressive properties of an advanced, three-dimensional carbon-carbon composite in an oxidizing environment from room temperature to 2192°F (1200°C). A large part of the test apparatus was designed and built at The University of Maine. The test fixtures were custom designed and incorporate two types of alumina ceramic and a water-cooled base to enable the fixtures to withstand high temperatures and high compressive stresses. A custom temperature control system was also developed to control the MTS high temperature furnace. This system included a computer program written with Delphi 5 that incorporates feedback control logic and allows the end user to tailor the time-temperature response of the furnace, an Iotech Daqbook 100 was used for the digital/analog interface, and a custom-built control box provided power to the heating elements. Accurate strain measurement was achieved by using a high temperature extensometer affixed to the platen load ends. Incorporating the high temperature test system with an MTS 110-kip load load frame, and 22kip load cell permitted high resolution, accurate test data to be obtained.

Taking into account the variability of the test results, the in-plane tests demonstrated that the modulus and ultimate compressive strength exhibited little change from room temperature to 1472°F (800°C). The results also indicate symmetry of the material properties in the x and y-directions with the average compressive modulus and ultimate compressive strength consistently equal. The average, ultimate compressive strength in

the z-direction was only 4-7% higher than the average compressive strength in the x and y-direction however; the average z-direction modulus was significantly higher than the average modulus in the x and y-direction, exhibiting a 58-71% increase. The shear strength in the XY-plane,  $\tau_{xy}$ , exhibited an approximate 10% increase from room temperature to 1112°F (600°C) and a decrease of approximately 6% from room temperature to 1472°F (800°C). The off axis results further identified symmetry in the material, demonstrating that the ultimate shear strength in the xz and yz-planes,  $\tau_{xz}$  and  $\tau_{yz}$ , were approximately equal. Both exhibited an 11-15% decrease from room temperature to 1112°F (600°C) and 21-27% decrease from room temperature to 1472°F (800°C). The three 2192°F (1200°C) tests exhibited over 60% mass loss by oxidation over the duration the tests, which prevented the determination of the compressive stress. However, the tests did demonstrate the limitations of the material in an oxidizing environment and, together with the oxidation observed with the 1472°F (800°C) tests, prompted an investigation to quantify the oxidation rate of the tests specimens.

The oxidation study provided useful information on the materials oxidation rate and permitted the correction of the 1472°F (800°C) compressive stress calculations. The specimens exhibited minor oxidation at 1112°F (600°C); over the duration of the tests less than 5% mass loss was observed and less than 1% loss in volume was observed. Over the 120-minute duration of the oxidation test 50% loss in mass was observed. Loss in volume was only recorded up to 60-minutes, and the material exhibited only 10% loss in volume. At 1472°F (800°C) the oxidation rate was significantly higher and the material exhibited an 80% loss in mass by the end of the 120-minute test. The last

1832°F (1000°C) test was stopped at only 90 minutes because at this point 85% loss in mass had occurred. The mode of oxidation also differed from 1112°F (600°C) to 1832°F (1000°C). At 1112°F (600°C) only the matrix oxidized causing the fibers to slowly separate from the specimen. At 1472°F (800°C) and 1832°F (1000°C) both the matrix and fibers oxidized, leaving no fibers behind.

Overall, the material exhibited excellent high temperature mechanical properties that closely resembled those at room temperature. Oxidation was the major limiting factor for testing this material, preventing practical testing above 1472°F (800°C). However, the materials response in an oxidizing environment is important to characterize because, in practice, the material is typically used for missile nose cones and rocket engines that operate in an oxidizing environment. The results of this effort also demonstrate that successful techniques for conducting high temperature testing was developed which can be used as a foundation for future high temperature testing and research at The University of Maine.

## 4.2 Recommendations and Future Work

Based on the results of this study, it is apparent that further testing in an inert atmosphere could provide valuable information that would compliment the results of this effort. Testing in an inert atmosphere would allow for much higher testing temperatures to be achieved. Ideally, testing up to 5432°F (3000°C) to characterize the materials response over the entire temperature spectrum that is typically feasible with carbon-carbon composites. Developing a method for tensile testing at high temperatures would also be beneficial, though it is likely that a cold gripping technique would have to be employed.

Determining the shear modulus,  $G_{xy}$ ,  $G_{xz}$  and  $G_{yz}$ , would also be beneficial to fully characterize the elastic properties of the material. It was demonstrated that determining the shear modulus by a method similar to ASTM D3518M-94 is not practical for high temperature testing. To successfully determine the shear modulus a high temperature test fixture for shear loading would need to be developed similar to the Iosipescu shear test or the double-notch compression test. Both of these techniques are covered in ASTM C1292 however, the standard is only designed for uni-directional or bi-directional fiber orientations.

## BIBLIOGRAPHY

- Adams, D.F., *Mechanical Test Fixtures* in Jenkins, C.H., (ed.), Manual on Experimental Methods for Mechanical Testing of Composites, 1998, The Fairmont Press
- Adams, D.F.(2), *Test Methods for Composite Materials Seminar Notes*, 1995, Technomic Publishing Company
- Chung, D.L., Carbon Fiber Composites, 1994, Butterwoth-Heinemann
- Gyekenyesi, J. Z., *High Temperature Mechanical Characterization of Ceramic Composites*, 1998, NASA/CR-1998-206611
- Herakovich, Carl T., Mechanics of Fibrous Composites, 1998, John Wiley & Sons, Inc.
- Hyer, M. W., Stress Analysis of Fiber-Reinforced Composite Materials, 1998, McGraw Hill Company, Inc.
- Kurumada, A. and Sato, A., *Tensile Properties and Fracture Toughness of Carbon-Fiber Felt Reinforced Carbon Composites at High Temperature*, Carbon, vol. 27, 1989
- Lab 11: PID Control Systems* (12/00), <http://www-gateway.eng.ohio-state.edu/labs/PIDcontrolsystems.html>
- Peters, S.T., ed., Handbook of Composites, 2<sup>nd</sup> edition, 1998, Chapman & Hall
- PID Technical Notes*, <http://instserv.com/pid.htm>
- Savage, G., Carbon-Carbon Composites, 1993, Chapman & Hall
- Senet, S., Grimes, R.E., Hunn, D.L., & White, K.W., *Elevated Temperature Fracture Behavior of a 2-D Discontinuous Fiber Reinforced Carbon-Carbon Composite*, Carbon, vol. 29, 1991
- Shaw, J A., *The PID Control Algorithm*, <http://www.jashaw.com/pid/description.htm>
- Singh, R. N., *Interfacial Properties and High Temperature Mechanical Behavior of Fiber-Reinforced Ceramic Composites*, Materials Science and Engineering, vol. A166, July 15, 1993
- Wescot, T, *PID Without a PhD* (10/00), <http://www.embedded.com/2000/0010/0010/feet3.htm>



## **Appendix A – High Temperature Control Source Code for the ‘Universal Temperature Control Program’ (Delphi 5)**

Only the source code developed specifically for the high temperature portion of the ‘Universal Temperature Control Program’ is presented in this appendix, and consists of two parts; The ‘Set Point Form’ is the main portion of the program and the ‘Set Point Data Form’ is the portion of the program that reads in the time, temperature and command data.

**Table A.1 Set Point Form Computer Code (Caccese, Walls, 2001)**

```
unit SetPoint;

interface

uses
    Windows, Messages, SysUtils, Classes, Graphics, Controls,
    Forms, Dialogs,
    StdCtrls, HeatChamberC, DAQ32Interface,
    Daqfi32Main, SetPointDataForm,
    ExtCtrls, Grids, ComCtrls;

Const
    Deltat = 0.1;
    IntervalTime = 1; {Gain Timer Interval}
    Period = 5;

type
    TSetPointFRM = class(TForm)
        Timer1: TTimer;
        Timer2: TTimer;
        zone3DutyCycleBar: TProgressBar;
        GroupBox1: TGroupBox;
        Label1: TLabel;
        Label2: TLabel;
        Label3: TLabel;
        Label4: TLabel;
        Label5: TLabel;
        zone1DutyCycleBar: TProgressBar;
        Label6: TLabel;
        zone2DutyCycleBar: TProgressBar;
```

```

Label7: TLabel;
Label8: TLabel;
Edit1: TEdit;
Edit2: TEdit;
Edit3: TEdit;
Button1: TButton;
Label9: TLabel;
Label10: TLabel;
zone1KpED: TEdit;
zone1KiED: TEdit;
zone2KpED: TEdit;
zone2KiED: TEdit;
zone3KpED: TEdit;
zone3KiED: TEdit;
Label11: TLabel;
Edit4: TEdit;
Label12: TLabel;
procedure TemperatureControlData;
procedure TurnElementOn(ElementNo: integer);
procedure TurnElementOff(ElementNo: integer);
procedure Hold(TimeIncr: integer);
procedure Timer1Timer(Sender: TObject);
procedure SetPointControl(Incr: integer);
Procedure CheckTemperature(Temp: real);
procedure FormCreate(Sender: TObject);
procedure Timer2Timer(Sender: TObject);
procedure Zone1Gain(GainTimeIncr1: integer);
procedure Zone2Gain(GainTimeIncr2: integer);
procedure Zone3Gain(GainTimeIncr3: integer);
procedure PControl;
procedure PControlParameters;
procedure Button1Click(Sender: TObject);

private
  {StepNo,} TimeStepNo, Command: integer;
  Gain1StepNo, Gain2StepNo, Gain3StepNo: integer;
  HoldTime, PreviousError1, PreviousError2, PreviousError3:
real;
  zone1Ki, zone2Ki, zone3Ki, zone1Kp, zone2Kp, zone3Kp : real;
  HoldTemp, StopInc, Zone1, Zone2, Zone3 : boolean;
  CalculateGain1, CalculateGain2, CalculateGain3 : boolean;
  ResetZone1, ResetZone2, ResetZone3 : boolean;
  PreviousTargetTemp : real;
  { Private declarations }
public
  { Public declarations }
end;

```

```

var
  SetPointFRM: TSetPointFRM;

implementation
  {$R *.DFM}

  {*****Heating Element Control-ON/OFF*****}
  procedure TSetPointFRM.TurnElementOn(ElementNo: integer);
  var
    zone1,zone2,zone3,ALL : integer ;
  begin
    zone1 := Heat_Ch1;
    zone2 := Heat_Ch2;
    zone3 := Heat_Ch4;    {Channel three on DaqBook does not
work}
    ALL := Heat_ALL;
    Case ElementNo of
      1 : TempControl.TurnHeatOn(zone1);
      2 : TempControl.TurnHeatOn(zone2);
      3 : TempControl.TurnHeatOn(zone3);
      4 : TempControl.TurnHeatOn(ALL);
    end; {Case}
  end;

  procedure TSetPointFRM.TurnElementOff(ElementNo: integer);
  var
    zone1,zone2,zone3,All : integer ;
  begin
    zone1 := Heat_Ch1;
    zone2 := Heat_Ch2;
    zone3 := Heat_Ch4;    {Channel three on DaqBook does not
work}
    ALL := Heat_ALL;
    Case ElementNo of
      1 : TempControl.TurnHeatOff(zone1);
      2 : TempControl.TurnHeatOff(zone2);
      3 : TempControl.TurnHeatOff(zone3);
      4 : TempControl.TurnHeatOFF(ALL);
    end; {Case}
  end;

  {*****Reads Input Data From SetPointDataForm*****}
  procedure TSetPointFRM.TemperatureControlData;
  Var
    i : integer;
    PreviousTime : real;

```

```

begin
for i:=1 to TotalTempSteps do
begin
  PreviousTime := SetpointDataFRM.ControlData[i-1].Time;
  Control_Temp[i].Temperature:=
SetpointDataFRM.ControlData[i].Temperature;
  Control_Temp[i].Time:=
SetpointDataFRM.ControlData[i].Time-PreviousTime;

Control_Temp[i].CommandType:=SetpointDataFRM.ControlData[i]
.CommandType;
end
end;

{*****Set Point Temperature Control*****}
procedure TSetPointFRM.SetPointControl(incr: integer);
var
Temp1,Temp2,Temp3,Temp4,Temp5,StepTemp,StepTime : Real;
PreviousTemp,CurrentTemp: Real;
slope: Real;
Intervall : cardinal;

begin
Intervall := round(Deltat*60*1000);  {Timer1 Interval}
Timer1.Interval := intervall;
Timer1.Enabled := true;

Temp1 := Temperature[1]; {Temp1 Corresponds To Themocouple
1 on Frunace}
Temp2 := Temperature[2];
Temp3 := Temperature[3];
Temp4 := Temperature[4];
Temp5 := Temperature[5];
CurrentTemp := (Temp1+Temp3+Temp5)/3;

StepTemp := Control_Temp[incr].Temperature ;
StepTime := Control_Temp[incr].Time ;
Command := Control_Temp[incr].CommandType;
HoldTime := StepTime;  {Used for Hold Procedure Only}

If StepNo = 1 then
  PreviousTemp := InitialTemp
else
  PreviousTemp := Control_Temp[incr-1].Temperature ;
{Calculate Temperature Step}
slope:= (StepTemp-PreviousTemp)/StepTime;
TargetTemp:= slope*deltat + CurrentTemp ;

```

```

If TargetTemp < PreviousTargetTemp then
    TargetTemp:=PreviousTargetTemp;
PreviousTargetTemp:= TargetTemp;

{Temperature Control Commands}
If Command = CM_Stop then
    begin
        Timer1.Enabled    := false ;
        Timer2.Enabled    := false ;
        StartSetpoint     := false ;
        Go                 := false ;
        TurnElementOff(4);
        showmessage('PROGRAM COMPLETE');
    end
else
If (Command = CM_HOLD) and not HoldTemp then
    begin
        HoldTemp := True ;
        TimeStepNo:= 0;
    end
else
If Command = CM_HOLD then
    begin
        CurrentSetPoint := StepTemp;
        SetPointFRM.Hold(TimeStepNo);
    end
else
If Command = CM_Ramp then
    begin
        CurrentSetPoint := TargetTemp;
        If (TargetTemp >= StepTemp) then
            Inc(StepNo);
        end;
    end;
end;
{*****Time Counter For Hold Command*****}
procedure TsetPointFRM.Hold(TimeIncr: integer);
var
ElapsedTime : real;
begin
If HoldTemp then
    begin
        ElapsedTime := Deltat*TimeIncr;
        if ElapsedTime >= HoldTime then
            begin
                HoldTemp := false;
                Inc(StepNo);
            end;
        end;
    end;
end;

```

```

end;
end;

{*****Timer For Set Point Temperature Control*****}
procedure TSetPointFRM.Timer1Timer(Sender: TObject);
begin
  If StartSetpoint then
    begin
      SetPointFRM.TemperatureControlData;
      SetPointFRM.SetPointControl(StepNo);
      if Holdtemp = true then
        Inc(TimeStepNo)
      end
    end;
  {*****Check FurnaceTemperature*****}
  Procedure TSetPointFRM.CheckTemperature(Temp: real);
  var
    zone1Temp, zone2Temp, zone3Temp, AveTemp, HTOverShoot : real;
  begin
    Timer2.Enabled := true;
    zone1Temp := Temperature[1];
    zone2Temp := Temperature[3];
    zone3Temp := Temperature[5];
    AveTemp := (zone1Temp+zone2Temp+zone3Temp)/3 ;
    HTOverShoot := 10;
    If AveTemp >= HighTempLimit Then
      begin
        TurnElementOff(4);
        Go := false ;
        StartSetpoint := false ;
        showmessage('TooHot');
      end
    else
      If (zone1Temp < Temp) and not Zone1 then
        begin
          TurnElementON(1);
          Zone1:= true;
        end;
      If (zone2Temp < Temp) and not Zone2 then
        begin
          TurnElementON(2);
          Zone2:= true;
        end;
      If (zone3Temp < Temp) and not Zone3 then
        begin
          TurnElementON(3);
          Zone3:= true;
        end;
    end;
  end;
end;

```

```

        end
    else
    {Prevents excessive overshoot in the event that the PI
control is incorrectly tuned}
    If (zone1Temp >= (Temp + HTOverShoot)) then
        begin
            TurnElementOFF(1);
            zone1DutyCycleBar.Position := 0;
        end;
    If (zone2Temp >= (Temp + HTOverShoot)) then
        begin
            TurnElementOFF(2);
            zone2DutyCycleBar.Position := 0;
        end;
    If (zone3Temp >= (Temp + HTOverShoot)) then
        begin
            TurnElementOFF(3);
            zone3DutyCycleBar.Position := 0;
        end;
    end;
    end;
    {*}
    {*****PI ControlParameters*****}
    {*}
    procedure TSetPointFRM.PIControlParameters;
    begin
        zone1Kp:= StrToFloat(zone1KpED.text);
        zone2Kp:= StrToFloat(zone2KpED.text);
        zone3Kp:= StrToFloat(zone3KpED.text);
        zone1Ki:= StrToFloat(zone1KiED.text);
        zone2Ki:= StrToFloat(zone2KiED.text);
        zone3Ki:= StrToFloat(zone3KiED.text);
    end;
    {*****PI Algorithm*****}
    Procedure TSetPointFRM.PIControl;
    var

    zone1Temp, zone2Temp, zone3Temp, zone1Error, zone2Error, zone3Er
ror: real;

    zone1Pterm, zone2Pterm, zone3Pterm, zone1sumError, Zone2sumErro
r: real;
    Zone3sumError, zone1Iterm, zone2Iterm, zone3Iterm: real;
    TempCommand: real;
    begin
        SetPointFRM.PIControlParameters;
        Edit4.Text := FloatToStr(CurrentSetPoint);
        zone1Temp := Temperature[1];

```

```

zone2Temp := Temperature[3];
zone3Temp := Temperature[5];
TempCommand:=CurrentSetPoint;
{Zone 1}
zone1Error    := TempCommand-zone1Temp;
zone1SumError := PreviousError1+zone1Error;
If ResetZone1 then
    PreviousError1:=0
else
    PreviousError1:= zone1SumError;
zone1Pterm :=zone1Kp*Zone1Error;
zone1Iterm :=zone1Ki*zone1SumError;
ResetZone1 :=false;
    If zone1Iterm < 0 then {Bounds the Integral term in
the event of Integral Wind up}
        begin
            zone1Iterm:=0;
            ResetZone1:= true;
        end;
    If zone1Iterm > 1 then
        begin
            zone1Iterm:=1;
            ResetZone1:= true;
        end;
    Edit1.Text:= FloatToStr(zone1Iterm);
    If CalculateGain1 then
        zone1PercentGain:=zone1Pterm + zone1Iterm ;
{Zone 2}
zone2Error    :=TempCommand-zone2Temp;
zone2SumError :=PreviousError2+zone2Error;
If ResetZone2 then
    PreviousError2 :=0
else
    PreviousError2 :=zone2SumError;
zone2Pterm :=zone2Kp*Zone2Error;
zone2Iterm :=zone2Ki*zone2SumError;
ResetZone2 :=false;
    If zone2Iterm < 0 then {Bounds the Integral term in
the event of Integral Wind up}
        begin
            zone2Iterm :=0;
            ResetZone2 :=true;
        end;
    If zone2Iterm > 1 then
        begin
            zone2Iterm :=1;
            .ResetZone2 :=true

```



```

        end;
    Edit2.Text:= FloatToStr(zone2Iterm);
    If CalculateGain2 then
        zone2PercentGain:=zone2Pterm + zone2Iterm;
{Zone 3}
    zone3Error      :=TempCommand-zone3Temp;
    zone3SumError  :=PreviousError3+zone3Error;
    If ResetZone3 then
        PreviousError3 :=0
    else
        PreviousError3 :=zone3SumError;
        zone3Pterm :=zone3Kp*zone3Error;
        zone3Iterm :=zone3Ki*zone3SumError;
        ResetZone3 :=False;
        If zone3Iterm < 0 then {Bounds the Integral term in
the event of Integral Wind up}
            begin
                zone3Iterm :=0;
                ResetZone3 :=true;
            end;
        If zone3Iterm > 1 then
            begin
                zone3Iterm :=1;
                ResetZone3 :=true;
            end;
        Edit3.Text:= FloatToStr(zone3Iterm);
        If CalculateGain3 then
            zone3PercentGain:=zone3Pterm + zone3Iterm;
end;

{*****Gain Control*****}
{Zone1}
procedure TSetPointFRM.Zone1Gain(GainTimeIncr1: integer);
var
    Z1ElapsedTime: real;
begin
    CalculateGain1 := false;
    If Zone1 = true then
        begin
            zone1DutyCycleBar.Position :=
Round(zone1PercentGain*100);
            Z1ElapsedTime:= GainTimeIncr1*IntervalTime;
        end;
    If Z1ElapsedTime >= Period*zone1PercentGain then
        begin
            TurnElementOff(1);
            zone1DutyCycleBar.Position := 0;

```

```

    end;
    If Z1ElapsedTime >= Period then
    begin
        CalculateGain1:= true;
        Zone1:= false;
        Gain1StepNo:= 0;
    end
end;
{Zone 2}
procedure TSetPointFRM.Zone2Gain(GainTimeIncr2: integer);
var
    Z2ElapsedTime: real;
begin
    CalculateGain2 := false;
    If Zone2 = true then
        zone2DutyCycleBar.Position :=
Round(zone2PercentGain*100);
        Z2ElapsedTime:= GainTimeIncr2*IntervalTime;
    If Z2ElapsedTime >= Period*zone2PercentGain then
    begin
        TurnElementOff(2);
        zone2DutyCycleBar.Position := 0;
    end;
    If Z2ElapsedTime >= Period then
    begin
        CalculateGain2:= true;
        Zone2:= false;
        Gain2StepNo:= 0;
    end
end;
{Zone3}
procedure TSetPointFRM.Zone3Gain(GainTimeIncr3: integer);
var
    Z3ElapsedTime : real;
begin
    CalculateGain3 := false;
    If Zone3= true then
        zone3DutyCycleBar.Position :=
Round(zone3PercentGain*100);
        Z3ElapsedTime:= GainTimeIncr3*IntervalTime;
    If Z3ElapsedTime >= Period*zone3PercentGain then
    begin
        TurnElementOff(3);
        zone3DutyCycleBar.Position := 0;
    end;
    If Z3ElapsedTime >= Period then
    begin

```

```

        CalculateGain3:= true;
        Zone3:= false;
        Gain3StepNo:= 0;
    end
end;
{*****GainTimer*****}
procedure TSetPointFRM.Timer2Timer(Sender: TObject);
begin
    SetPointFRM.PIControl;
    If Zone1 = true then
    begin
        Inc(Gain1StepNo);
        SetPointFRM.Zone1Gain(Gain1StepNo);
    end;
    If Zone2 = true then
    begin
        Inc(Gain2StepNo);
        SetPointFRM.Zone2Gain(Gain2StepNo);
    end;
    If Zone3 = true then
    begin
        Inc(Gain3StepNo);
        SetPointFRM.Zone3Gain(Gain3StepNo);
    end;
end;

{*****}
procedure TSetPointFRM.FormCreate(Sender: TObject);
var
Interval2: cardinal;
begin
    TakeThermo      := true;
    Timer1.Enabled:= false;
    Timer2.Enabled:= false;
    StartSetpoint  := false;
    Go              := false;
    HoldTemp       := false;
    Zone1          := false;
    Zone2          := false;
    Zone3          := false;
    CalculateGain1:= true;
    CalculateGain2:= true;
    CalculateGain3:= true;
    ResetZone1     := false;
    ResetZone2     := false;
    ResetZone3     := false;
    StepNo         :=1;

```

```

TimeStepNo      :=0;
Gain1StepNo     :=0;
PreviousError1  :=0;
PreviousError2  :=0;
PreviousError3  :=0;
PreviousTargetTemp:=0;
Interval2       := round(IntervalTime*1000);   {Gain
Timer Interval}
Timer2.Interval := Interval2;
end;
procedure TSetPointFRM.Button1Click(Sender: TObject);
begin
    HeatChamberMainFrm.show;
end;

end.

```

**Table A.2 Set Point Data Form Computer Code (Caccese, Walls, 2001)**

```

unit SetPointDataForm;

interface

uses
    Windows, Messages, SysUtils, Classes, Graphics, Controls,
    Forms, Dialogs,
    OleCtrls, vcfl, ComCtrls, Tabnotbk, StdCtrls, AxCtrls,
    Spin, Buttons,
    Grids, HeatChamberC ;

Const
MaxRecords = 200;

type
    TSetPointDataFRM = class(TForm)
        PrevBTN: TButton;
        NextBTN: TButton;
        EnterBTN: TBitBtn;
        RepeatBTN: TBitBtn;
        DeleteBTN: TBitBtn;
        TotalSpin: TSpinEdit;
        TempStepED: TEdit;
        TimeED: TEdit;
        TemperatureED: TEdit;
        Label4: TLabel;
        Label3: TLabel;
    end;

```

```

Label2: TLabel;
Label1: TLabel;
Label5: TLabel;
LayerGrid: TFlBook;
Done: TButton;
CommandCombo: TComboBox;
StaticText1: TStaticText;
StaticText2: TStaticText;
StaticText3: TStaticText;
procedure PrevBTNClick(Sender: TObject);
procedure FormCreate(Sender: TObject);
procedure GetTempStepData(TempStep: integer);
procedure SetTempStepData(TempStep: integer);
procedure EnterBTNClick(Sender: TObject);
procedure WriteGridData(CurrentLayer: integer);
procedure NextBTNClick(Sender: TObject);
procedure RepeatBTNClick(Sender: TObject);
procedure TotalSpinChange(Sender: TObject);
procedure DoneClick(Sender: TObject);
private
  { Private declarations }
public
  CurrentTempStep : integer;
  { TotalTempSteps : integer; }
  ControlData      : array[1..MaxRecords] of
ControlTempRec;
  procedure ShowListBox;
  { Public declarations }
end;

var
  SetPointDataFRM: TSetPointDataFRM;

implementation

uses Daqfi32Main, SetPoint;
procedure TSetPointDataFRM.ShowListBox;
var
  i,ssError : integer;
  pShown : SmallInt;
  pX,pY,pCX,PCy: integer;
  ThisWidth, ThisHeight : integer;
  nRow1,nCol1,nRow2, nCol2 : integer;
  List1 : TList;
  Txt : String;
  PTxt : PChar;
begin

```

```

For i:=0 to 3 do
begin
  Txt := Inttostr(i);
  StrPCopy(PTxt,Txt);
  List1.Add(PTxt);
end;
{
F1Book1.RangeToTwips(nRow1, nCol1, nRow2, nCol2, pX, pY,
pCX, pCY, pShown);
List1.M .Move((F1Book1.Left + pX), (F1Book1.Top + yOffset),
(F1Book1.Left + 2 * thisWidth), (F1Book1.Top + 5 *
thisHeight));
List1.Visible := True;
}
(*
' Set position and size of the listbox, move to click
location and make it visible
List1.Move (F1Book1.Left + xOffset), (F1Book1.Top +
yOffset), (F1Book1.Left + 2 * thisWidth), (F1Book1.Top + 5
* thisHeight)
List1.Visible = True

End Sub
' Set the current selection to the specified font. Default
height is 10 and the other attributes are not set.
Sub List1_Click ()

F1Book1.SetFont List1.List(List1.ListIndex), 10, False,
False, False, False, False, False)
' Make listbox invisible now that we are done with it.
List1.Visible = False

End Sub

*)
end;
{$R *.DEM}

procedure TSetPointDataFRM.PrevBTNClick(Sender: TObject);
begin
  If CurrentTempStep > 1 then
  begin
    dec(CurrentTempStep);
    GetTempStepData(CurrentTempStep);
  end;
end;

```

```

procedure TSetPointDataFRM.GetTempStepData (TempStep:
integer);
begin
    TempStepED.Text := IntToStr (CurrentTempStep);
    CommandCombo.ItemIndex :=
ControlData [TempStep].CommandType;
    TimeED.text := Floattostr (ControlData [TempStep].Time);
    TemperatureED.text :=
Floattostr (ControlData [TempStep].Temperature);
end;

procedure TSetPointDataFRM.SetTempStepData (TempStep:
integer);
begin
    ControlData [TempStep].CommandType :=
CommandCombo.ItemIndex;
    ControlData [TempStep].Command :=
CommandCombo.Items [CommandCombo.ItemIndex];
    ControlData [TempStep].Time :=
StrToFloat (TimeED.text);
    ControlData [TempStep].Temperature :=
StrToFloat (TemperatureED.text);
end;

procedure TSetPointDataFRM.FormCreate (Sender: TObject);
begin
    CurrentTempStep :=1;
    TotalTempSteps :=1;
    CommandCombo.ItemIndex := CM_RAMP;
end;

procedure TSetPointDataFRM.EnterBTNClick (Sender: TObject);
begin
    SetTempStepData (CurrentTempStep);
    WriteGridData (CurrentTempStep);
end;

procedure TSetPointDataFRM.WriteGridData (CurrentLayer:
integer);
var
pText : String;
begin
    LayerGrid.SetActiveCell (CurrentTempStep,1);
    pText := ControlData [CurrentTempStep].Command;
    LayerGrid.Text := pText;
end;

```

```

    LayerGrid.SetactiveCell(CurrentTempStep,2);
    pText := Format('%*.*f', [8, 2,
ControlData[CurrentTempStep].Time]);
    LayerGrid.Text := pText;

    LayerGrid.SetactiveCell(CurrentTempStep,3);
    pText := Format('%*.*f', [8, 2,
ControlData[CurrentTempStep].Temperature]);
    LayerGrid.Text := pText;

end;

procedure TSetPointDataFRM.NextBTNClick(Sender: TObject);
begin
    If CurrentTempStep < TotalTempSteps then
    begin
        inc(CurrentTempStep);
        GetTempStepData(CurrentTempStep);
    end;
end;

procedure TSetPointDataFRM.RepeatBTNClick(Sender: TObject);
begin
    if CurrentTempStep < TotalTempSteps then
    begin
        inc(CurrentTempStep);
        SetTempStepData(CurrentTempStep);
        WriteGridData(CurrentTempStep);
    end;
end;

procedure TSetPointDataFRM.TotalSpinChange(Sender:
TObject);
begin
    TotalTempSteps := TotalSpin.Value;
end;

procedure TSetPointDataFRM.DoneClick(Sender: TObject);
begin
HeatChamberMainFrm.show;
end;

end.

```



## Appendix B – Temperature Control Box Parts List

**Table B.1 – Parts List**

| Quantity | Item  | Manufacturer   | Price Each   | Total Price     |
|----------|---|----------------|--------------|-----------------|
| 3        | relay, model # SSR240DC25                         | Omega          | \$29.00      | \$87.00         |
| 3        | finned heat sink, model # FHS-1                   | Omega          | \$13.00      | \$39.00         |
| 3        | 277V, 10A, double pole single throw toggle switch | Gardber Bender | \$4.19       | \$12.57         |
| 3        | 250V, amber neon pilot light                      | Linrose        | \$4.99       | \$14.97         |
| 3        | 250V, green neon pilot light                      | Linrose        | \$4.99       | \$14.97         |
| 1        | electrical enclosure box                          | Hofman         | \$61.93      | \$61.93         |
| 1        | L6-20, 250V, 20A, turn-lock receptacle            | NEMA           | \$12.79      | \$12.79         |
| 2        | 13A, 7 pin receptacle, part # 211398-1            | AMP            | \$2.91       | \$5.82          |
| 2        | 13A, 7 pin plug, part # 211400-1                  | AMP            | \$3.54       | \$7.08          |
| 1        | multimate contacts, finish pins (bag of 100)      | AMP            | \$20.40      | \$20.40         |
| 1        | multimate contacts, finish sockets (bag of 100)   | AMP            | \$24.00      | \$24.00         |
| 1        | contact extractor tool                            | AMP            | \$21.00      | \$21.00         |
| 3        | glass tube fuse blocks                            | BUSS           | \$0.86       | \$2.58          |
| 1        | D-subminiature connector, 9 pin male              | Radioshack     | \$0.99       | \$0.99          |
| 1        | D-subminiature connector, 9 pin female            | Radioshack     | \$1.29       | \$1.29          |
|          |   |                | <b>Total</b> | <b>\$326.39</b> |

## Appendix C – ATS Test Specimen Locations

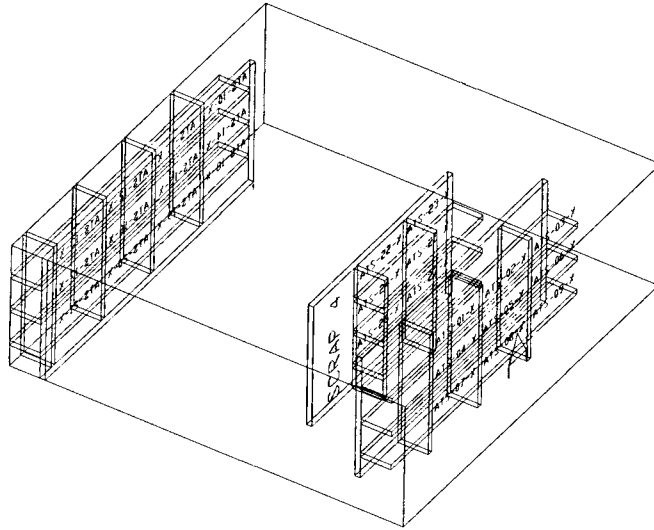


**Figure C.1 - X-Direction Test Specimens**

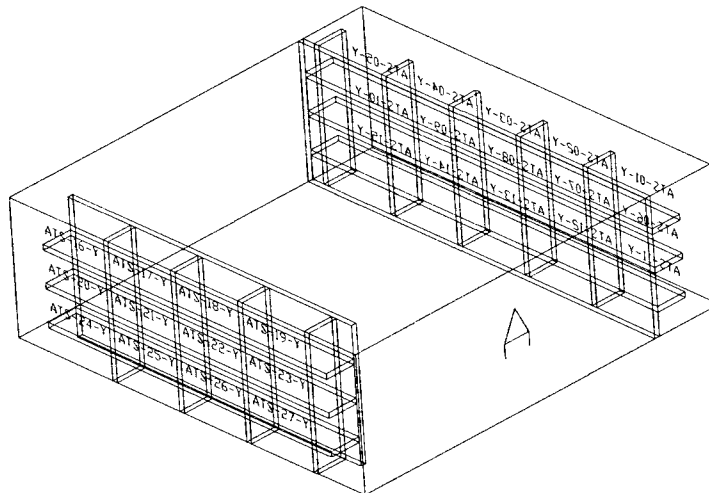


**Figure C.2 - Y-Direction Test Specimens**

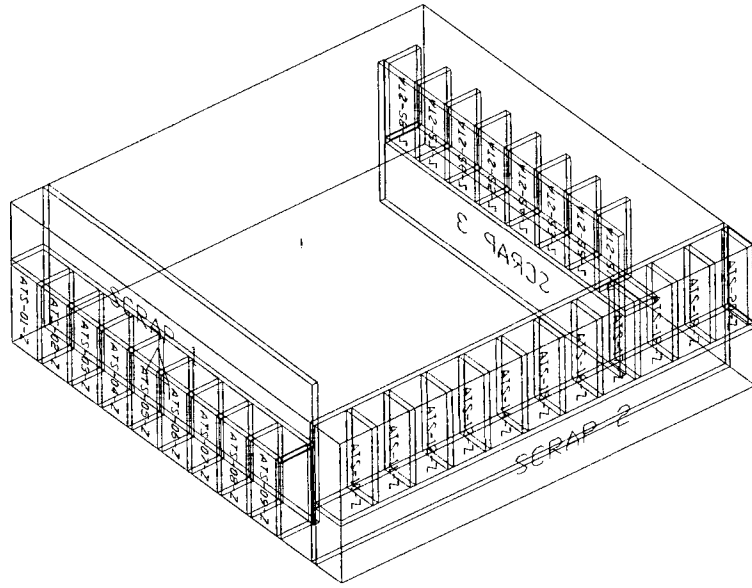


**Figure C.3 - Z-Direction Test Specimens**

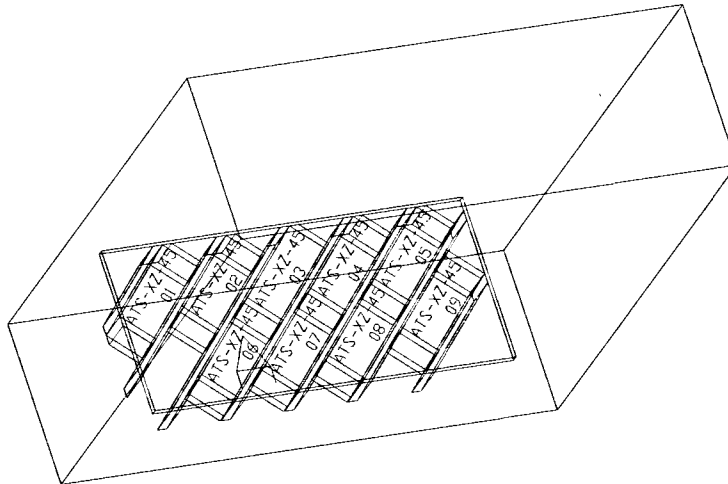


**Figure C.4 - XZ-Plane Test Specimens**

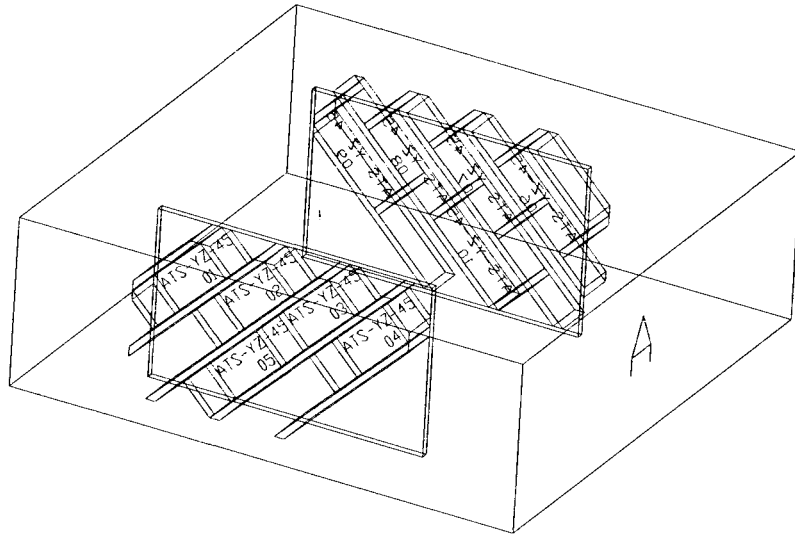


**Figure C.5 - YZ-Plane Test Specimens**

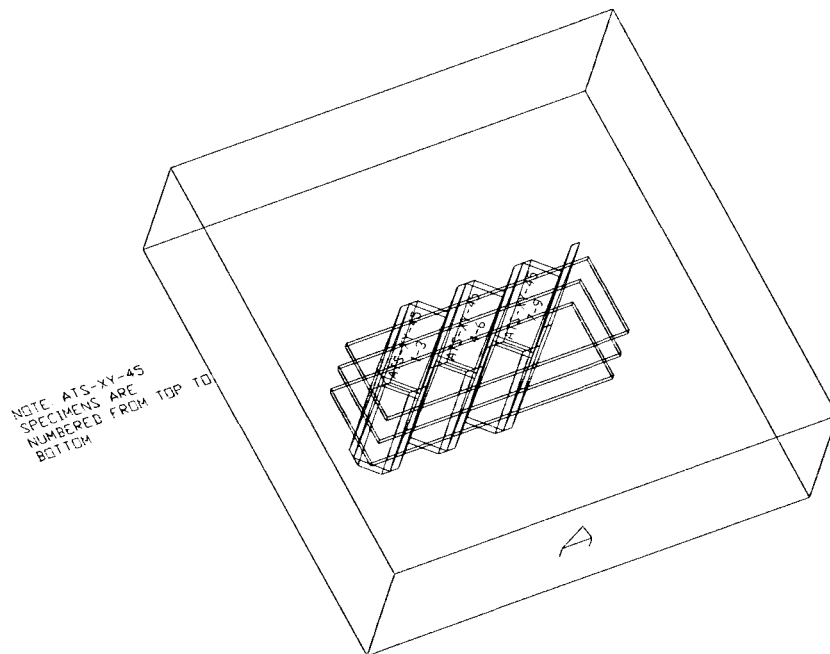


**Figure C.6 - XY-Plane Test Specimens**

**Appendix D – Test Specimen Data**

**Table D.1 – Dimensions, Weight and Density**

| Specimen | Length<br>in | B1<br>in | B2<br>in | Weight<br>oz | X-sect. area<br>in <sup>2</sup> | Density            |                    |
|----------|--------------|----------|----------|--------------|---------------------------------|--------------------|--------------------|
|          |              |          |          |              |                                 | oz/in <sup>3</sup> | lb/in <sup>3</sup> |
| ATS-01-X | 0.875        | 0.390    | 0.365    | 0.13         | 0.142                           | 1.044              | 0.0652             |
| ATS-02-X | 0.874        | 0.384    | 0.365    | 0.13         | 0.140                           | 1.061              | 0.0663             |
| ATS-03-X | 0.874        | 0.386    | 0.364    | 0.13         | 0.141                           | 1.059              | 0.0662             |
| ATS-04-X | 0.875        | 0.370    | 0.365    | 0.13         | 0.135                           | 1.100              | 0.0688             |
| ATS-05-X | 0.874        | 0.366    | 0.365    | 0.13         | 0.134                           | 1.113              | 0.0696             |
| ATS-06-X | 0.873        | 0.368    | 0.365    | 0.13         | 0.134                           | 1.109              | 0.0693             |
| ATS-07-X | 0.875        | 0.384    | 0.364    | 0.13         | 0.140                           | 1.063              | 0.0664             |
| ATS-08-X | 0.875        | 0.389    | 0.365    | 0.13         | 0.142                           | 1.046              | 0.0654             |
| ATS-09-X | 0.874        | 0.391    | 0.368    | 0.14         | 0.144                           | 1.113              | 0.0696             |
| ATS-10-X | 0.875        | 0.380    | 0.358    | 0.12         | 0.136                           | 1.008              | 0.0630             |
| ATS-11-X | 0.874        | 0.376    | 0.354    | 0.12         | 0.133                           | 1.032              | 0.0645             |
| ATS-12-X | 0.875        | 0.374    | 0.359    | 0.12         | 0.134                           | 1.021              | 0.0638             |
| ATS-13-X | 0.875        | 0.371    | 0.355    | 0.12         | 0.132                           | 1.041              | 0.0651             |
| ATS-14-X | 0.875        | 0.383    | 0.378    | 0.14         | 0.145                           | 1.105              | 0.0691             |
| ATS-15-X | 0.874        | 0.380    | 0.377    | 0.13         | 0.143                           | 1.038              | 0.0649             |
| ATS-16-X | 0.875        | 0.375    | 0.374    | 0.13         | 0.140                           | 1.059              | 0.0662             |
| ATS-17-X | 0.874        | 0.371    | 0.368    | 0.13         | 0.137                           | 1.089              | 0.0681             |
| ATS-18-X | 0.874        | 0.397    | 0.381    | 0.14         | 0.151                           | 1.059              | 0.0662             |
| ATS-19-X | 0.873        | 0.401    | 0.379    | 0.14         | 0.152                           | 1.055              | 0.0659             |
| ATS-20-X | 0.875        | 0.402    | 0.375    | 0.14         | 0.151                           | 1.061              | 0.0663             |
| ATS-21-X | 0.875        | 0.401    | 0.372    | 0.14         | 0.149                           | 1.073              | 0.0670             |
| ATS-22-X | 0.875        | 0.392    | 0.374    | 0.14         | 0.147                           | 1.091              | 0.0682             |
| ATS-23-X | 0.875        | 0.392    | 0.385    | 0.14         | 0.151                           | 1.060              | 0.0663             |
| ATS-24-X | 0.875        | 0.395    | 0.376    | 0.14         | 0.149                           | 1.077              | 0.0673             |
| ATS-25-X | 0.875        | 0.392    | 0.377    | 0.14         | 0.148                           | 1.083              | 0.0677             |
| ATS-26-X | 0.874        | 0.395    | 0.378    | 0.14         | 0.149                           | 1.073              | 0.0671             |
| ATS-27-X | 0.875        | 0.395    | 0.387    | 0.14         | 0.153                           | 1.047              | 0.0654             |
| ATS-01-Y | 0.875        | 0.368    | 0.367    | 0.12         | 0.135                           | 1.015              | 0.0635             |
| ATS-02-Y | 0.875        | 0.374    | 0.367    | 0.12         | 0.137                           | 0.999              | 0.0624             |
| ATS-03-Y | 0.875        | 0.372    | 0.367    | 0.13         | 0.137                           | 1.088              | 0.0680             |
| ATS-04-Y | 0.875        | 0.372    | 0.364    | 0.13         | 0.135                           | 1.097              | 0.0686             |
| ATS-05-Y | 0.875        | 0.373    | 0.361    | 0.13         | 0.135                           | 1.103              | 0.0690             |
| ATS-06-Y | 0.873        | 0.381    | 0.370    | 0.13         | 0.141                           | 1.056              | 0.0660             |
| ATS-07-Y | 0.875        | 0.383    | 0.374    | 0.14         | 0.143                           | 1.117              | 0.0698             |
| ATS-08-Y | 0.875        | 0.388    | 0.374    | 0.14         | 0.145                           | 1.103              | 0.0689             |
| ATS-09-Y | 0.875        | 0.383    | 0.374    | 0.13         | 0.143                           | 1.037              | 0.0648             |
| ATS-10-Y | 0.876        | 0.380    | 0.374    | 0.13         | 0.142                           | 1.044              | 0.0653             |
| ATS-11-Y | 0.875        | 0.383    | 0.372    | 0.13         | 0.142                           | 1.043              | 0.0652             |
| ATS-12-Y | 0.875        | 0.385    | 0.371    | 0.13         | 0.143                           | 1.040              | 0.0650             |
| ATS-13-Y | 0.874        | 0.379    | 0.374    | 0.13         | 0.142                           | 1.049              | 0.0656             |
| ATS-14-Y | 0.874        | 0.383    | 0.375    | 0.13         | 0.144                           | 1.036              | 0.0647             |
| ATS-15-Y | 0.875        | 0.385    | 0.374    | 0.13         | 0.144                           | 1.032              | 0.0645             |
| ATS-16-Y | 0.875        | 0.381    | 0.359    | 0.13         | 0.137                           | 1.086              | 0.0679             |
| ATS-17-Y | 0.874        | 0.381    | 0.363    | 0.13         | 0.138                           | 1.075              | 0.0672             |
| ATS-18-Y | 0.875        | 0.357    | 0.368    | 0.13         | 0.131                           | 1.131              | 0.0707             |

**Table D.1 (Continued)**

| Specimen  | Length<br>in | B1<br>in | B2<br>in | Weight<br>oz | X-sect. area<br>in <sup>2</sup> | Density            |                    |
|-----------|--------------|----------|----------|--------------|---------------------------------|--------------------|--------------------|
|           |              |          |          |              |                                 | oz/in <sup>3</sup> | lb/in <sup>3</sup> |
| ATS-19-Y  | 0.874        | 0.385    | 0.373    | 0.13         | 0.144                           | 1.036              | 0.0647             |
| ATS-20-Y  | 0.875        | 0.368    | 0.358    | 0.12         | 0.132                           | 1.041              | 0.0651             |
| ATS-21-Y  | 0.874        | 0.371    | 0.363    | 0.12         | 0.135                           | 1.020              | 0.0637             |
| ATS-22-Y  | 0.874        | 0.371    | 0.363    | 0.13         | 0.135                           | 1.104              | 0.0690             |
| ATS-23-Y  | 0.875        | 0.371    | 0.372    | 0.13         | 0.138                           | 1.077              | 0.0673             |
| ATS-24-Y  | 0.875        | 0.398    | 0.356    | 0.13         | 0.142                           | 1.049              | 0.0655             |
| ATS-25-Y  | 0.875        | 0.397    | 0.363    | 0.13         | 0.144                           | 1.031              | 0.0644             |
| ATS-26-Y  | 0.874        | 0.393    | 0.367    | 0.13         | 0.144                           | 1.031              | 0.0645             |
| ATS-27-Y  | 0.875        | 0.385    | 0.372    | 0.13         | 0.143                           | 1.037              | 0.0648             |
| ATS-01-Z  | 0.875        | 0.382    | 0.355    | 0.13         | 0.136                           | 1.096              | 0.0685             |
| ATS-02-Z  | 0.875        | 0.382    | 0.354    | 0.13         | 0.135                           | 1.099              | 0.0687             |
| ATS-03-Z  | 0.875        | 0.365    | 0.352    | 0.12         | 0.128                           | 1.067              | 0.0667             |
| ATS-04-Z  | 0.875        | 0.368    | 0.351    | 0.12         | 0.129                           | 1.062              | 0.0664             |
| ATS-05-Z  | 0.875        | 0.360    | 0.349    | 0.11         | 0.126                           | 1.001              | 0.0625             |
| ATS-06-Z  | 0.875        | 0.353    | 0.346    | 0.11         | 0.122                           | 1.029              | 0.0643             |
| ATS-07-Z  | 0.874        | 0.361    | 0.344    | 0.11         | 0.124                           | 1.013              | 0.0633             |
| ATS-08-Z  | 0.875        | 0.361    | 0.343    | 0.11         | 0.124                           | 1.015              | 0.0635             |
| ATS-09-Z  | 0.875        | 0.372    | 0.342    | 0.12         | 0.127                           | 1.078              | 0.0674             |
| ATS-10-Z  | ---          | ---      | ---      | ---          | ---                             | ---                | ---                |
| ATS-11-Z  | 0.875        | 0.395    | 0.379    | 0.14         | 0.150                           | 1.069              | 0.0668             |
| ATS-12-Z  | 0.872        | 0.389    | 0.375    | 0.13         | 0.146                           | 1.022              | 0.0639             |
| ATS-13-Z  | 0.875        | 0.395    | 0.374    | 0.14         | 0.148                           | 1.083              | 0.0677             |
| ATS-14-Z  | 0.875        | 0.395    | 0.374    | 0.14         | 0.148                           | 1.083              | 0.0677             |
| ATS-15-Z  | 0.875        | 0.392    | 0.387    | 0.14         | 0.152                           | 1.055              | 0.0659             |
| ATS-16-Z  | 0.875        | 0.391    | 0.371    | 0.14         | 0.145                           | 1.103              | 0.0689             |
| ATS-17-Z  | 0.874        | 0.390    | 0.384    | 0.14         | 0.150                           | 1.070              | 0.0668             |
| ATS-18-Z  | 0.874        | 0.388    | 0.388    | 0.14         | 0.151                           | 1.064              | 0.0665             |
| ATS-19-Z  | 0.875        | 0.388    | 0.381    | 0.14         | 0.148                           | 1.082              | 0.0676             |
| ATS-20-Z  | ---          | ---      | ---      | ---          | ---                             | ---                | ---                |
| ATS-21A-Z | 0.873        | 0.375    | 0.374    | 0.13         | 0.140                           | 1.062              | 0.0664             |
| ATS-21B-Z | 0.875        | 0.382    | 0.375    | 0.14         | 0.143                           | 1.117              | 0.0698             |
| ATS-22-Z  | 0.875        | 0.380    | 0.375    | 0.13         | 0.143                           | 1.043              | 0.0652             |
| ATS-23-Z  | 0.875        | 0.374    | 0.372    | 0.13         | 0.139                           | 1.068              | 0.0667             |
| ATS-24-Z  | 0.873        | 0.377    | 0.372    | 0.13         | 0.140                           | 1.062              | 0.0664             |
| ATS-25-Z  | 0.875        | 0.371    | 0.366    | 0.13         | 0.136                           | 1.094              | 0.0684             |
| ATS-26-Z  | 0.875        | 0.382    | 0.367    | 0.13         | 0.140                           | 1.060              | 0.0662             |
| ATS-27-Z  | 0.875        | 0.382    | 0.367    | 0.13         | 0.140                           | 1.060              | 0.0662             |
| ATS-28-Z  | 0.875        | 0.382    | 0.365    | 0.13         | 0.139                           | 1.066              | 0.0666             |
| ATS-XY-01 | 0.873        | 0.396    | 0.375    | 0.14         | 0.149                           | 1.080              | 0.0675             |
| ATS-XY-02 | 0.875        | 0.380    | 0.375    | 0.13         | 0.143                           | 1.043              | 0.0652             |
| ATS-XY-03 | 0.874        | 0.415    | 0.374    | 0.15         | 0.155                           | 1.106              | 0.0691             |
| ATS-XY-04 | 0.875        | 0.382    | 0.395    | 0.14         | 0.151                           | 1.060              | 0.0663             |
| ATS-XY-05 | 0.874        | 0.383    | 0.379    | 0.14         | 0.145                           | 1.104              | 0.0690             |
| ATS-XY-06 | 0.875        | 0.415    | 0.375    | 0.15         | 0.156                           | 1.102              | 0.0688             |
| ATS-XY-07 | 0.875        | 0.395    | 0.377    | 0.14         | 0.149                           | 1.074              | 0.0672             |
| ATS-XY-08 | 0.874        | 0.383    | 0.348    | 0.13         | 0.133                           | 1.116              | 0.0697             |
| ATS-XY-09 | 0.875        | 0.415    | 0.366    | 0.14         | 0.152                           | 1.053              | 0.0658             |

**Table D.1 (Continued)**

| Specimen    | Length<br>in | B1<br>in | B2<br>in | Weight<br>oz | X-sect. area<br>in <sup>2</sup> | Density            |                    |
|-------------|--------------|----------|----------|--------------|---------------------------------|--------------------|--------------------|
|             |              |          |          |              |                                 | oz/in <sup>3</sup> | lb/in <sup>3</sup> |
| ATS-45-01   | 0.874        | 0.388    | 0.375    | 0.14         | 0.146                           | 1.101              | 0.0688             |
| ATS-45-02   | 0.875        | 0.389    | 0.375    | 0.14         | 0.146                           | 1.097              | 0.0686             |
| ATS-45-03   | 0.874        | 0.394    | 0.374    | 0.14         | 0.147                           | 1.087              | 0.0679             |
| ATS-45-04   | 0.878        | 0.395    | 0.370    | 0.14         | 0.146                           | 1.091              | 0.0682             |
| ATS-45-05   | 0.874        | 0.392    | 0.370    | 0.14         | 0.145                           | 1.104              | 0.0690             |
| ATS-45-06   | 0.875        | 0.392    | 0.375    | 0.14         | 0.147                           | 1.088              | 0.0680             |
| ATS-45-07   | 0.875        | 0.394    | 0.372    | 0.14         | 0.147                           | 1.092              | 0.0682             |
| ATS-45-08   | 0.875        | 0.396    | 0.375    | 0.14         | 0.149                           | 1.077              | 0.0673             |
| ATS-45-09   | 0.875        | 0.393    | 0.377    | 0.14         | 0.148                           | 1.080              | 0.0675             |
| ATS-45-01   | 0.875        | 0.388    | 0.373    | 0.14         | 0.145                           | 1.106              | 0.0691             |
| ATS-YZ-02   | 0.874        | 0.391    | 0.351    | 0.13         | 0.137                           | 1.084              | 0.0677             |
| ATS-YZ-02-B | 0.876        | 0.390    | 0.356    | 0.13         | 0.139                           | 1.069              | 0.0668             |
| ATS-YZ-03   | 0.875        | 0.393    | 0.355    | 0.13         | 0.140                           | 1.065              | 0.0666             |
| ATS-YZ-04   | 0.875        | 0.394    | 0.359    | 0.13         | 0.141                           | 1.050              | 0.0656             |
| ATS-YZ-04-B | 0.875        | 0.395    | 0.361    | 0.13         | 0.143                           | 1.042              | 0.0651             |
| ATS-YZ-05   | 0.874        | 0.392    | 0.355    | 0.13         | 0.139                           | 1.069              | 0.0668             |
| ATS-YZ-05-B | 0.874        | 0.393    | 0.359    | 0.13         | 0.141                           | 1.054              | 0.0659             |
| ATS-YZ-06   | 0.874        | 0.392    | 0.373    | 0.14         | 0.146                           | 1.096              | 0.0685             |
| ATS-YZ-07   | 0.875        | 0.393    | 0.358    | 0.13         | 0.141                           | 1.056              | 0.0660             |
| ATS-YZ-08   | 0.875        | 0.395    | 0.352    | 0.13         | 0.139                           | 1.069              | 0.0668             |
| ATS-YZ-09   | 0.875        | 0.397    | 0.370    | 0.14         | 0.147                           | 1.089              | 0.0681             |
| ATS-YZ-10   | 0.874        | 0.392    | 0.354    | 0.13         | 0.139                           | 1.072              | 0.0670             |

Appendix E – Test Matrix

Table E.1 – Test Specimen Test Temperature

| Specimen | Temperature<br>°C | Density<br>lb/in <sup>3</sup> | Comments |
|----------|-------------------|-------------------------------|----------|
| ATS-01-X | room temp         | 0.0652                        |          |
| ATS-02-X |                   | 0.0663                        |          |
| ATS-03-X | 1200              | 0.0662                        |          |
| ATS-04-X | 600               | 0.0688                        |          |
| ATS-05-X | room temp         | 0.0696                        |          |
| ATS-06-X | 800               | 0.0693                        |          |
| ATS-07-X |                   | 0.0664                        |          |
| ATS-08-X | 800               | 0.0654                        |          |
| ATS-09-X | 600               | 0.0696                        |          |
| ATS-10-X | room temp         | 0.0630                        |          |
| ATS-11-X | 800               | 0.0645                        |          |
| ATS-12-X | 600               | 0.0638                        |          |
| ATS-13-X |                   | 0.0651                        |          |
| ATS-14-X | 1200              | 0.0691                        |          |
| ATS-15-X | 1200              | 0.0649                        |          |
| ATS-16-X | room temp         | 0.0662                        |          |
| ATS-17-X | 1200              | 0.0681                        |          |
| ATS-18-X | 800               | 0.0662                        |          |
| ATS-19-X |                   | 0.0659                        |          |
| ATS-20-X |                   | 0.0663                        |          |
| ATS-21-X | 800               | 0.0670                        |          |
| ATS-22-X |                   | 0.0682                        |          |
| ATS-23-X | 600               | 0.0663                        |          |
| ATS-24-X | 1200              | 0.0673                        |          |
| ATS-25-X | room temp         | 0.0677                        |          |
| ATS-26-X |                   | 0.0671                        |          |
| ATS-27-X | 600               | 0.0654                        |          |
| ATS-01-Y | 600               | 0.0635                        |          |
| ATS-02-Y | room temp         | 0.0624                        |          |
| ATS-03-Y | 600               | 0.0680                        |          |
| ATS-04-Y | 1200              | 0.0686                        |          |
| ATS-05-Y | 1200              | 0.0690                        |          |
| ATS-06-Y | 600               | 0.0660                        |          |
| ATS-07-Y | 600               | 0.0698                        |          |
| ATS-08-Y | room temp         | 0.0689                        |          |
| ATS-09-Y | 1200              | 0.0648                        |          |
| ATS-10-Y |                   | 0.0653                        |          |
| ATS-11-Y | 800               | 0.0652                        |          |
| ATS-12-Y |                   | 0.0650                        |          |
| ATS-13-Y | 800               | 0.0656                        |          |
| ATS-14-Y | room temp         | 0.0647                        |          |
| ATS-15-Y |                   | 0.0645                        |          |
| ATS-16-Y | 1200              | 0.0679                        |          |
| ATS-17-Y | 800               | 0.0672                        |          |
| ATS-18-Y | room temp         | 0.0707                        |          |
| ATS-19-Y |                   | 0.0647                        |          |



**Tables E.1 (Continued)**

| Specimen  | Temperature<br>°C | Density<br>lb/in <sup>3</sup> | Comments |
|-----------|-------------------|-------------------------------|----------|
| ATS-20-Y  |                   | 0.0651                        |          |
| ATS-21-Y  | 1200              | 0.0637                        |          |
| ATS-22-Y  | 800               | 0.0690                        |          |
| ATS-23-Y  |                   | 0.0673                        |          |
| ATS-24-Y  | 600               | 0.0655                        |          |
| ATS-25-Y  | 800               | 0.0644                        |          |
| ATS-26-Y  |                   | 0.0645                        |          |
| ATS-27-Y  | room temp         | 0.0648                        |          |
| ATS-01-Z  | 800               | 0.0685                        |          |
| ATS-02-Z  |                   | 0.0687                        |          |
| ATS-03-Z  | 1200              | 0.0667                        |          |
| ATS-04-Z  |                   | 0.0664                        |          |
| ATS-05-Z  | room temp         | 0.0625                        |          |
| ATS-06-Z  | room temp         | 0.0643                        |          |
| ATS-07-Z  | 600               | 0.0633                        |          |
| ATS-08-Z  | 800               | 0.0635                        |          |
| ATS-09-Z  | 600               | 0.0674                        |          |
| ATS-10-Z  |                   | ---                           |          |
| ATS-11-Z  | 800               | 0.0668                        |          |
| ATS-12-Z  | 1200              | 0.0639                        |          |
| ATS-13-Z  | room temp         | 0.0677                        |          |
| ATS-14-Z  | 1200              | 0.0677                        |          |
| ATS-15-Z  | 800               | 0.0659                        |          |
| ATS-16-Z  | 600               | 0.0689                        |          |
| ATS-17-Z  |                   | 0.0668                        |          |
| ATS-18-Z  |                   | 0.0665                        |          |
| ATS-19-Z  | room temp         | 0.0676                        |          |
| ATS-20-Z  |                   | ---                           |          |
| ATS-21A-Z |                   | 0.0664                        |          |
| ATS-21B-Z | room temp         | 0.0698                        |          |
| ATS-22-Z  | 600               | 0.0652                        |          |
| ATS-23-Z  |                   | 0.0667                        |          |
| ATS-24-Z  |                   | 0.0664                        |          |
| ATS-25-Z  | 1200              | 0.0684                        |          |
| ATS-26-Z  | 1200              | 0.0662                        |          |
| ATS-27-Z  | 800               | 0.0662                        |          |
| ATS-28-Z  | 600               | 0.0666                        |          |
| ATS-XY-01 |                   | 0.0675                        |          |
| ATS-XY-02 | 1200              | 0.0652                        |          |
| ATS-XY-03 | 600               | 0.0691                        |          |
| ATS-XY-04 | room temp         | 0.0663                        |          |
| ATS-XY-05 | 800               | 0.0690                        |          |
| ATS-XY-06 | 1200              | 0.0688                        |          |
| ATS-XY-07 | 600               | 0.0672                        |          |
| ATS-XY-08 | room temp         | 0.0697                        |          |
| ATS-XY-09 | 800               | 0.0658                        |          |

**Tables E.1 (Continued)**

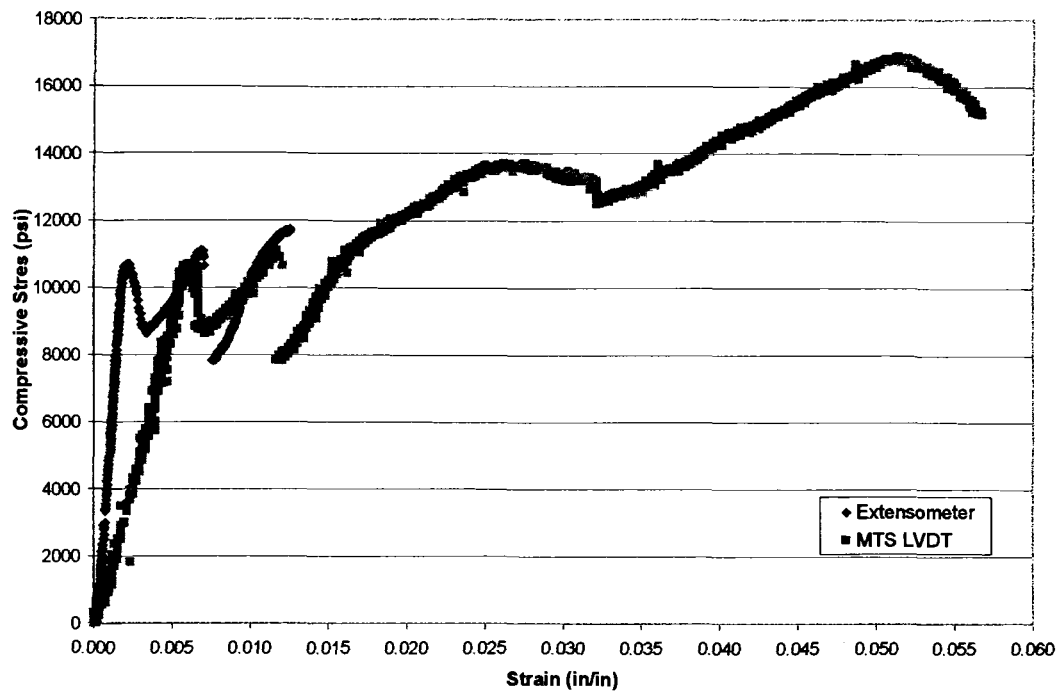
| <b>Specimen</b> | <b>Temperature<br/>°C</b> | <b>Density<br/>lb/in<sup>3</sup></b> | <b>Comments</b> |
|-----------------|---------------------------|--------------------------------------|-----------------|
| ATS-XZ-01       | 600                       | 0.0688                               |                 |
| ATS-XZ-02       | 800                       | 0.0686                               |                 |
| ATS-XZ-03       | 600                       | 0.0679                               |                 |
| ATS-XZ-04       |                           | 0.0682                               |                 |
| ATS-XZ-05       | room temp                 | 0.0690                               |                 |
| ATS-XZ-06       | room temp                 | 0.0680                               |                 |
| ATS-XZ-07       | 1200                      | 0.0682                               |                 |
| ATS-XZ-08       | 1200                      | 0.0673                               |                 |
| ATS-XZ-09       | 800                       | 0.0675                               |                 |
| ATS-YZ-01       | room temp                 | 0.0691                               |                 |
| ATS-YZ-02       | 1200                      | 0.0677                               |                 |
| ATS-YZ-45-B     |                           | 0.0668                               |                 |
| ATS-YZ-03       |                           | 0.0666                               |                 |
| ATS-YZ-04       | 800                       | 0.0656                               |                 |
| ATS-YZ-45-B     | 1200                      | 0.0651                               |                 |
| ATS-YZ-05       |                           | 0.0668                               |                 |
| ATS-YZ-45-B     | 600                       | 0.0659                               |                 |
| ATS-YZ-06       | 600                       | 0.0685                               |                 |
| ATS-YZ-07       | room temp                 | 0.0660                               |                 |
| ATS-YZ-08       |                           | 0.0668                               |                 |
| ATS-YZ-09       | 800                       | 0.0681                               |                 |
| ATS-YZ-10       |                           | 0.0670                               |                 |

## Appendix F – Test Data Sheet

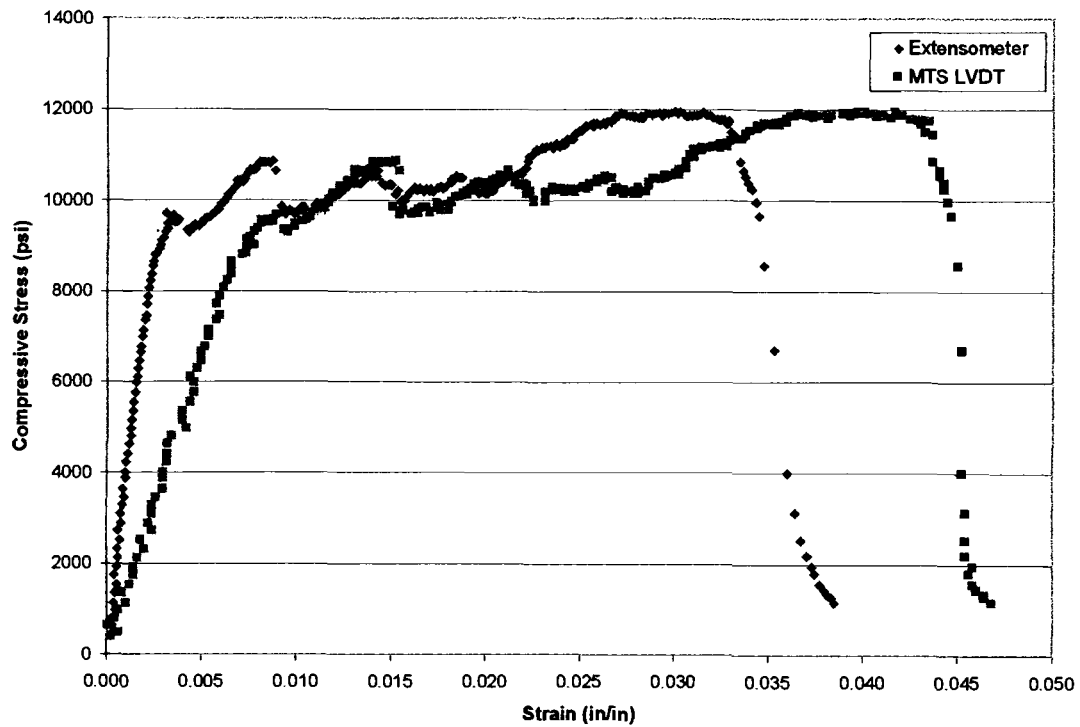
|                            |        |
|----------------------------|--------|
| Test Specimen #            | Date - |
| Test Temperature-          | Time - |
| Warm Up Rate-              |        |
| Load Cell -                |        |
| Load Rate -                |        |
| Data Sampling Rate -       |        |
| Approximate Failure Load - |        |
| Comments-                  |        |

## Appendix G – Individual In-Plane Compression Test Results

### Figure G.1 – X-Direction Stress-Strain Curves

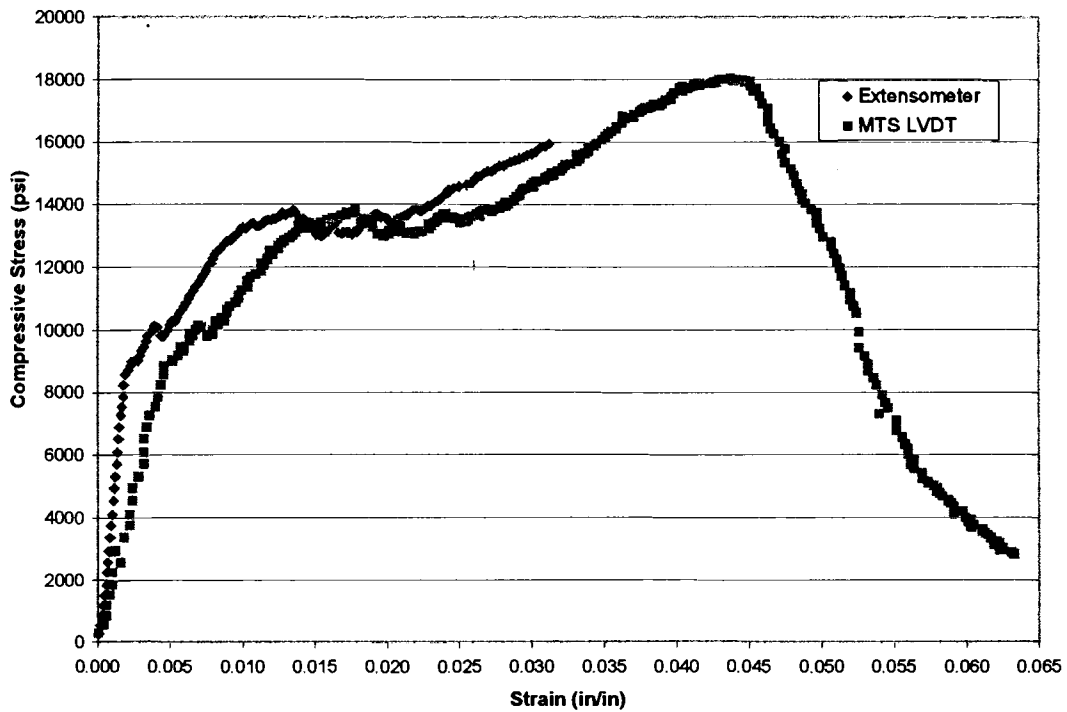


a. Test Specimen ATS-01-X

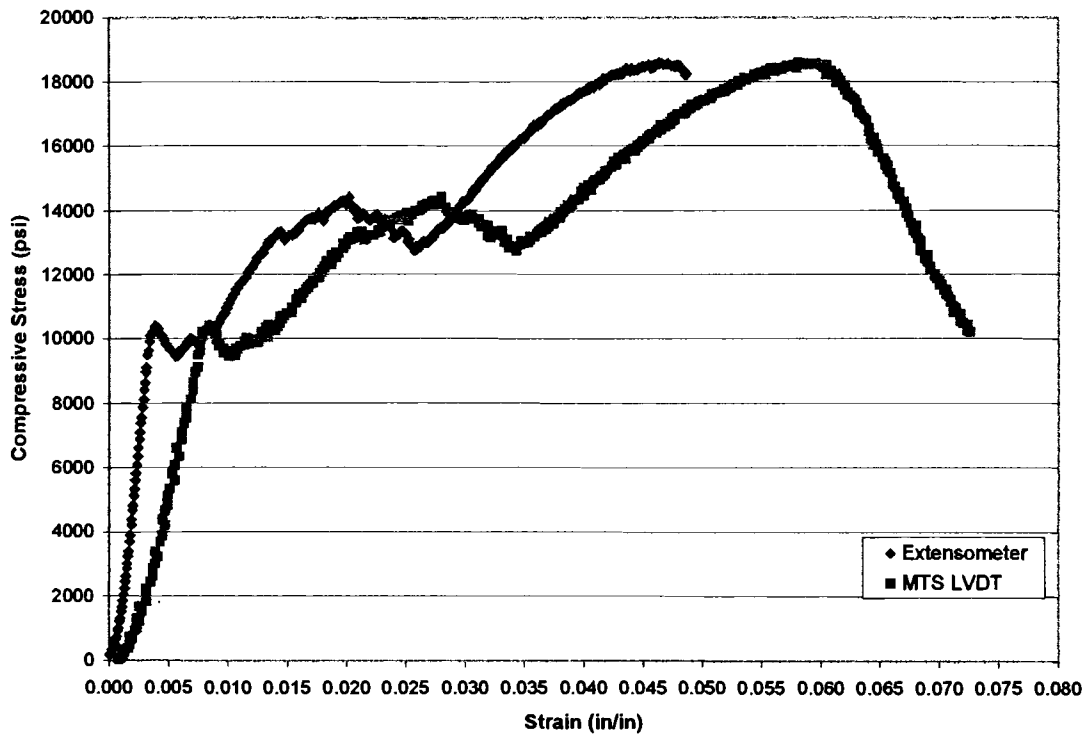


b. Test Specimen ATS-03-x

**Figure G.1 – X-Direction Stress-Strain Curves (Continued)**

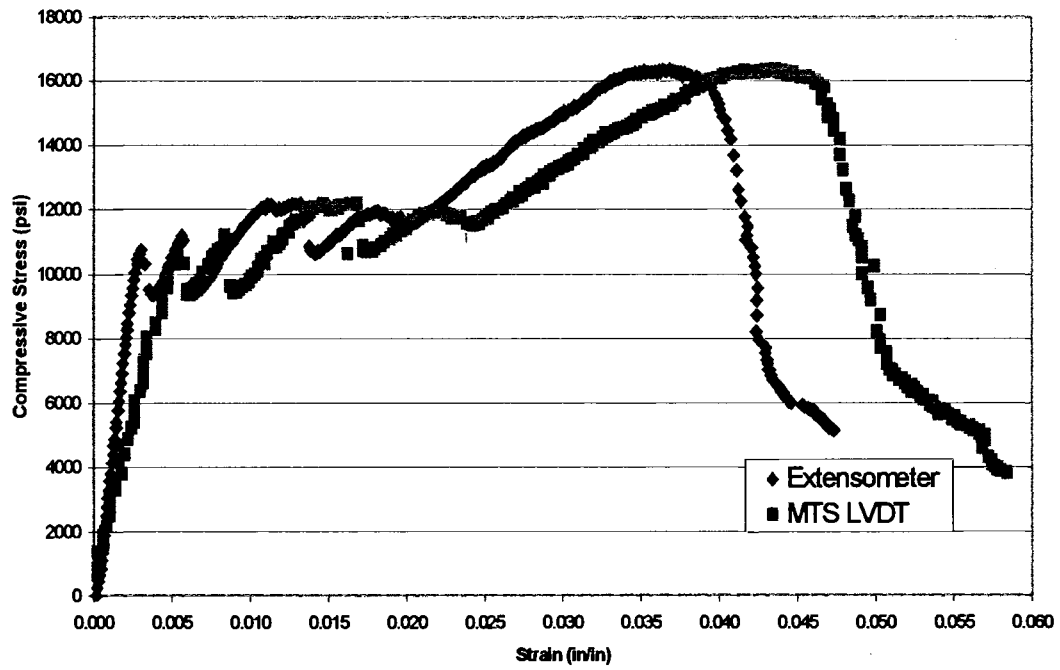


**c. Test Specimen ATS-04-x**

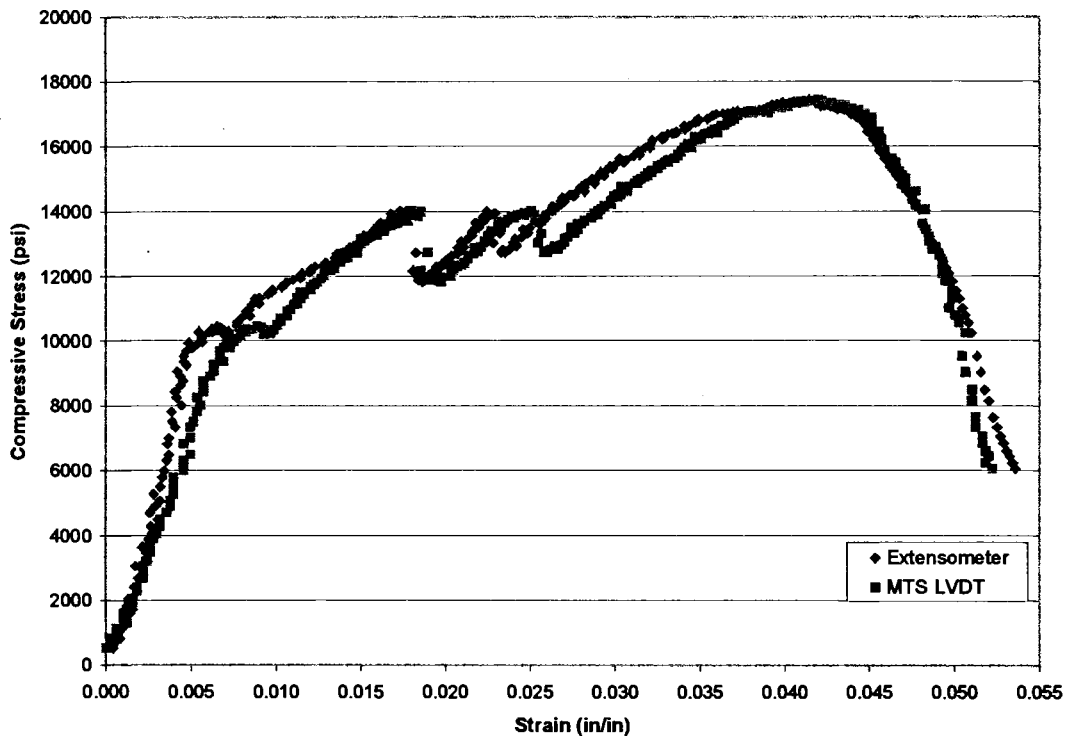


**d. Test Specimen ATS-05-x**

Figure G.1 – X-Direction Stress-Strain Curves (Continued)

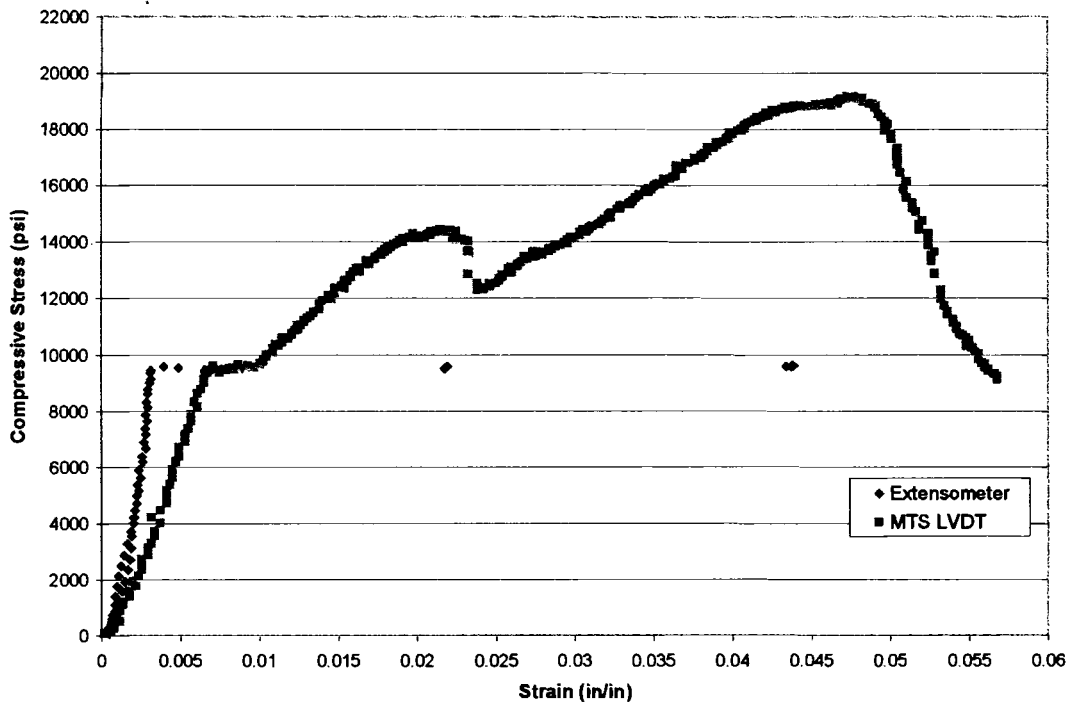


e. Test Specimen ATS-06-x

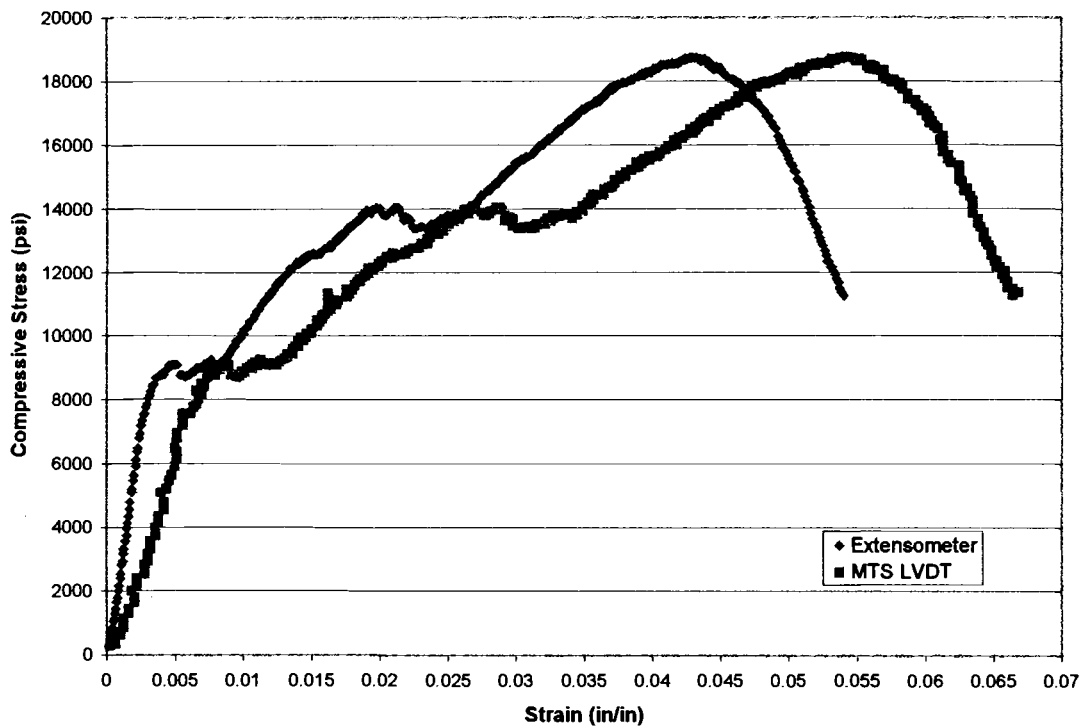


f. Test Specimen ATS-08-x

**Figure G.1 – X-Direction Stress-Strain Curves (Continued)**

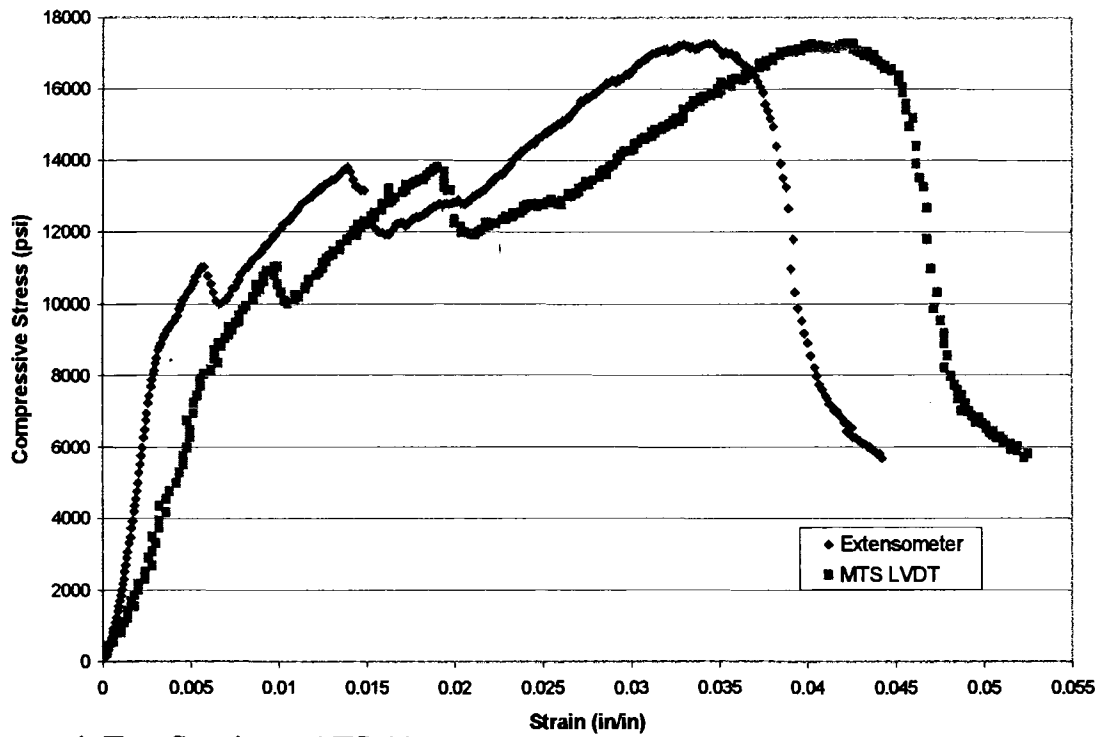


**g. Test Specimen ATS-09-x**

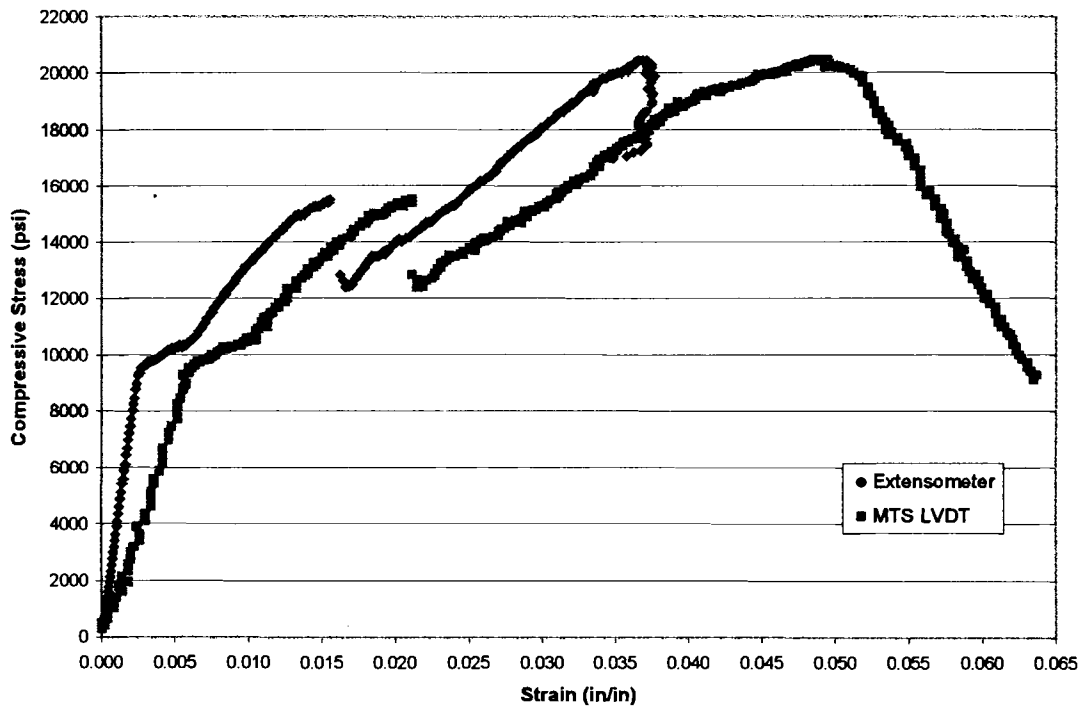


**h. Test Specimen ATS-10-x**

Figure G.1 – X-Direction Stress-Strain Curves (Continued)



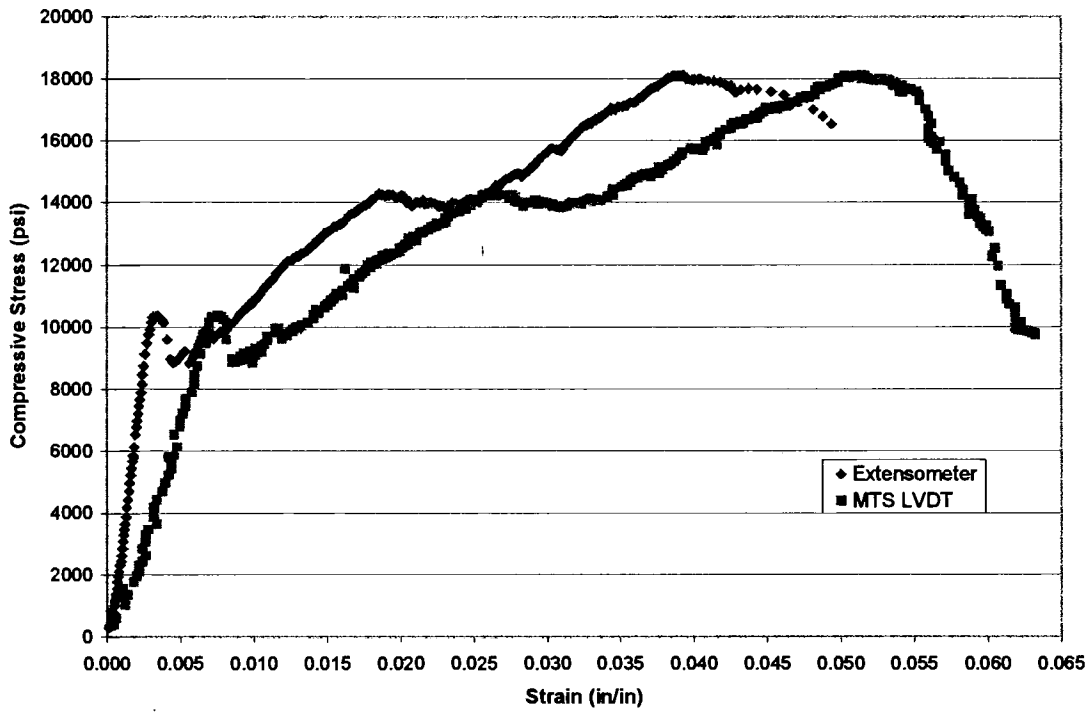
i. Test Specimen ATS-11-x



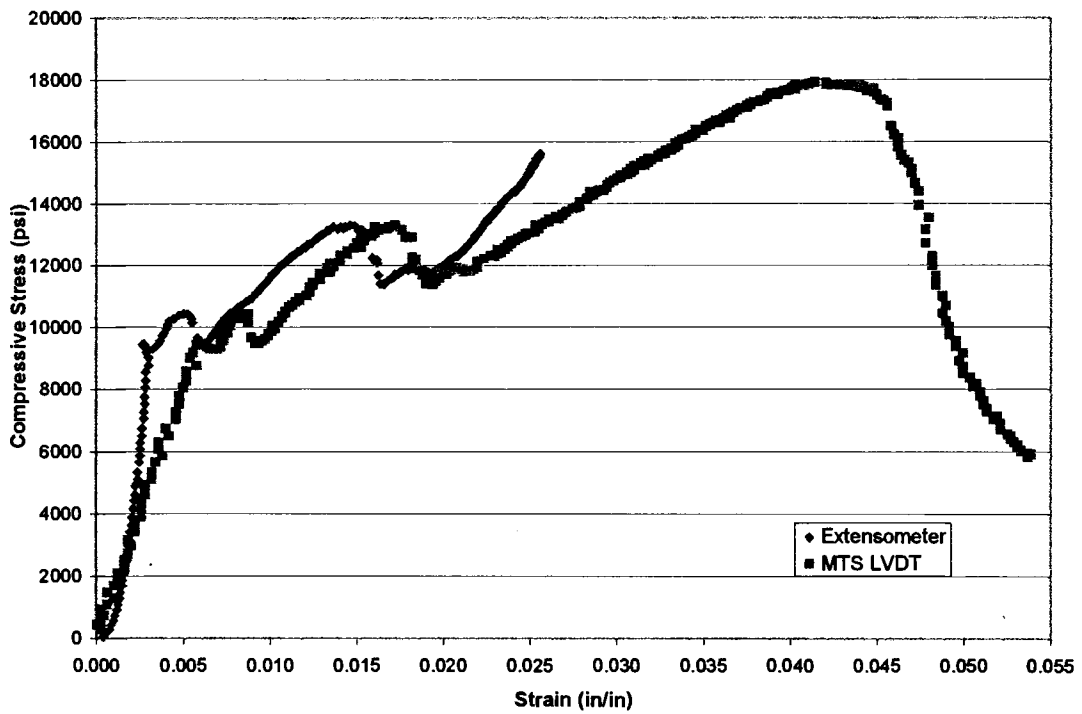
j. Test Specimen ATS-12-x



Figure G.1 – X-Direction Stress-Strain Curves (Continued)

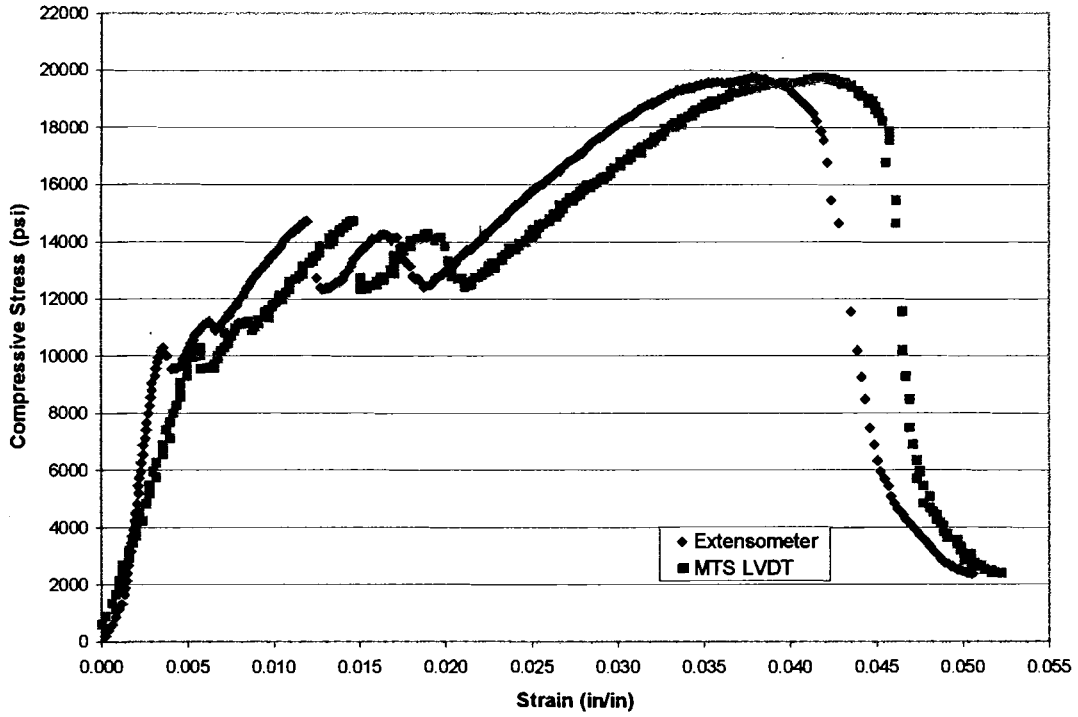


k. Test Specimen ATS-16-x

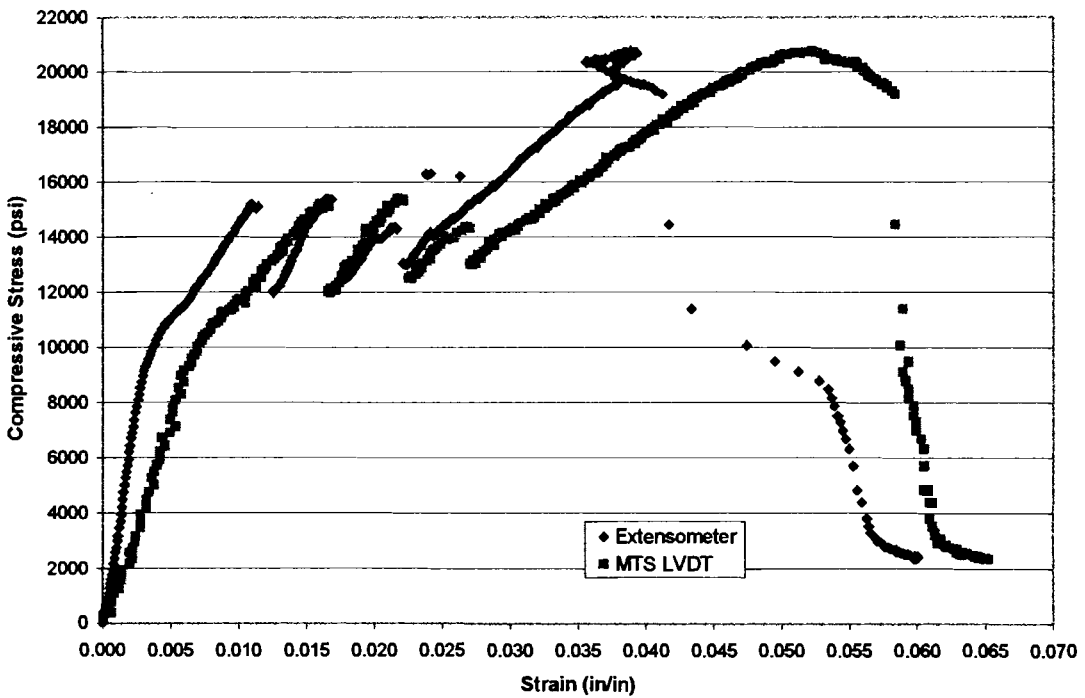


l. Test Specimen ATS-18-x

**Figure G.1 – X-Direction Stress-Strain Curves (Continued)**

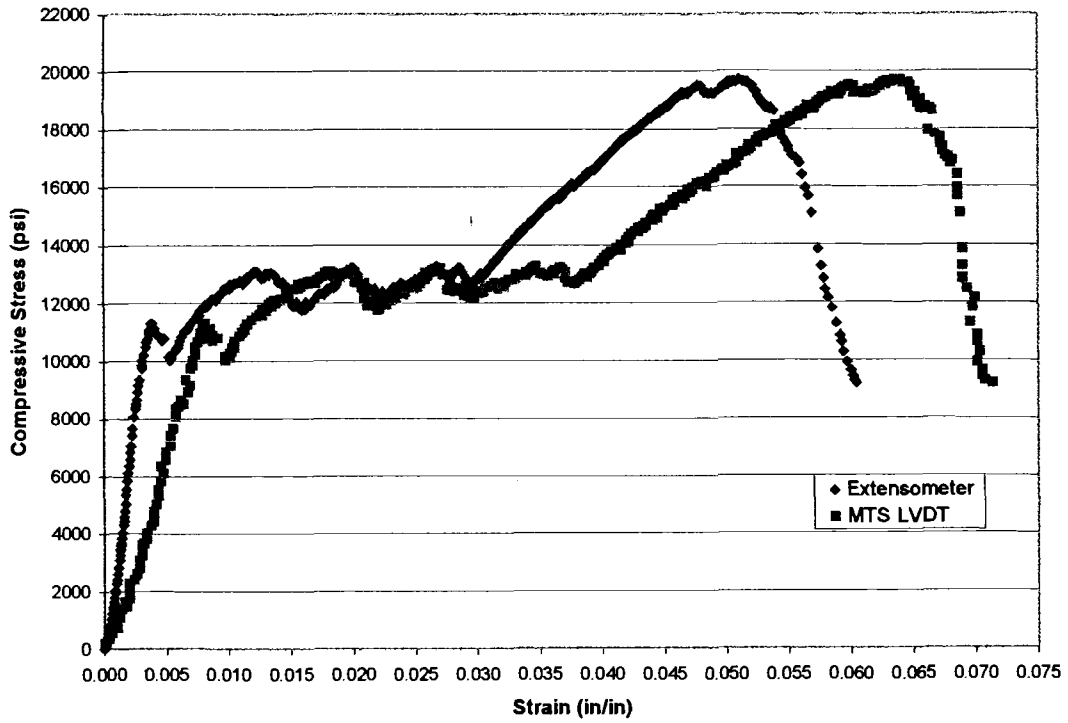


**m. Test Specimen ATS-21-x**

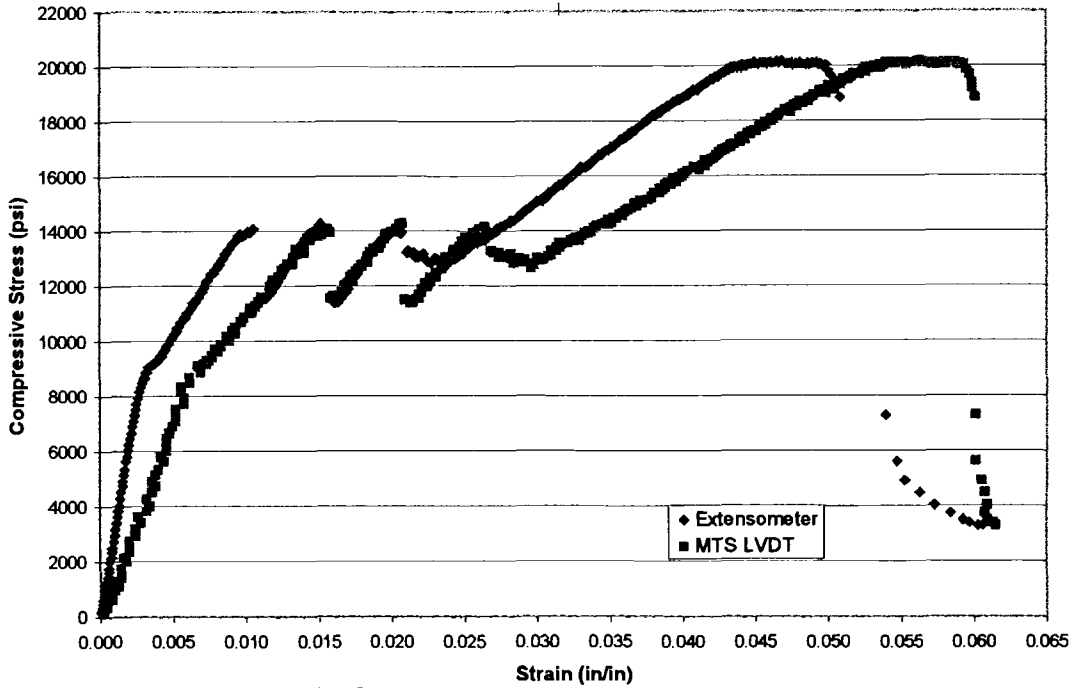


**n. Test Specimen ATS-23-x**

**Figure G.1 – X-Direction Stress-Strain Curves (Continued)**

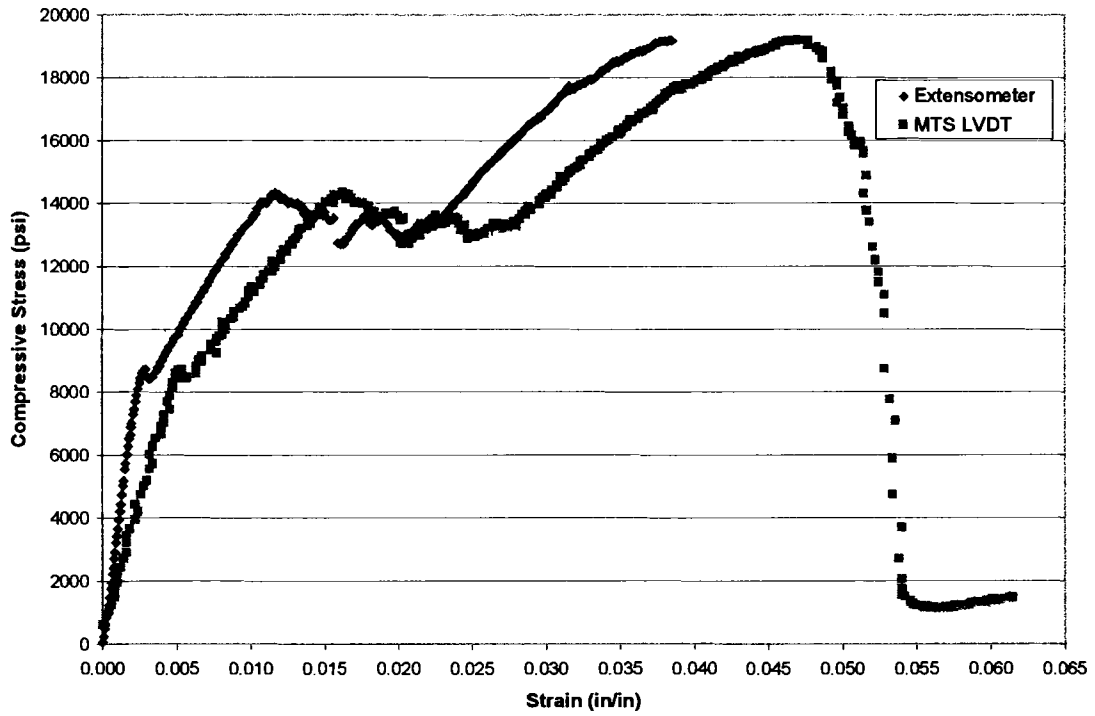


**o. Test Specimen ATS-25-x**

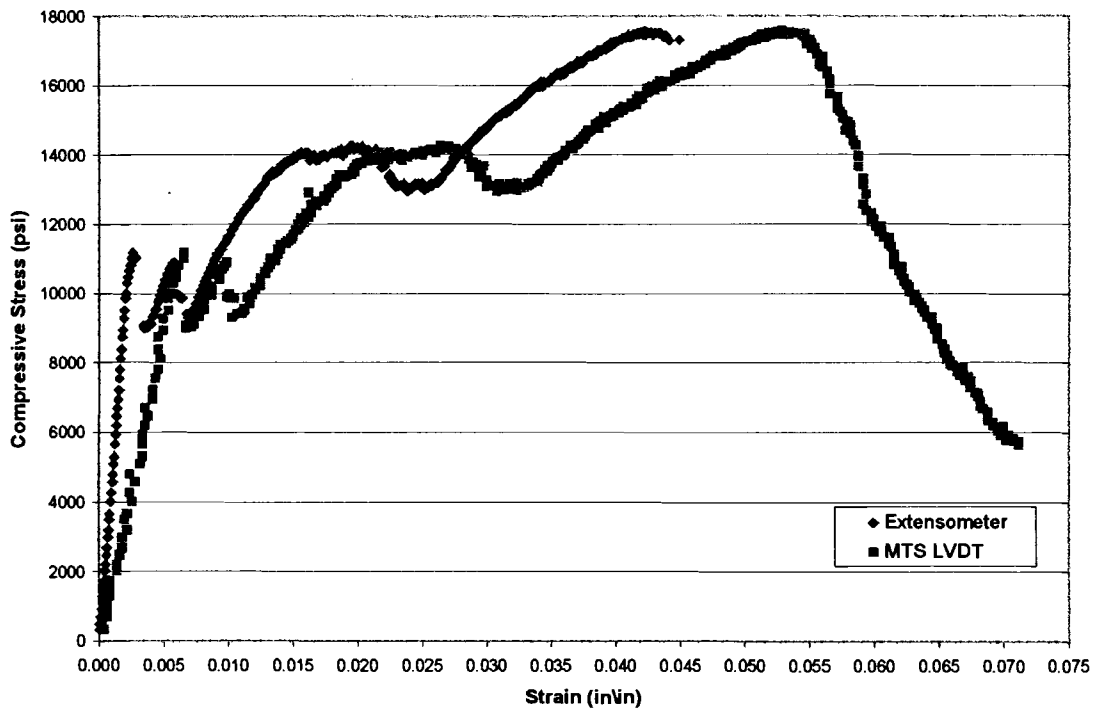


**p. Test Specimen ATS-27-x**

**Figure G.2 – Y-Direction Stress-Strain Curves**

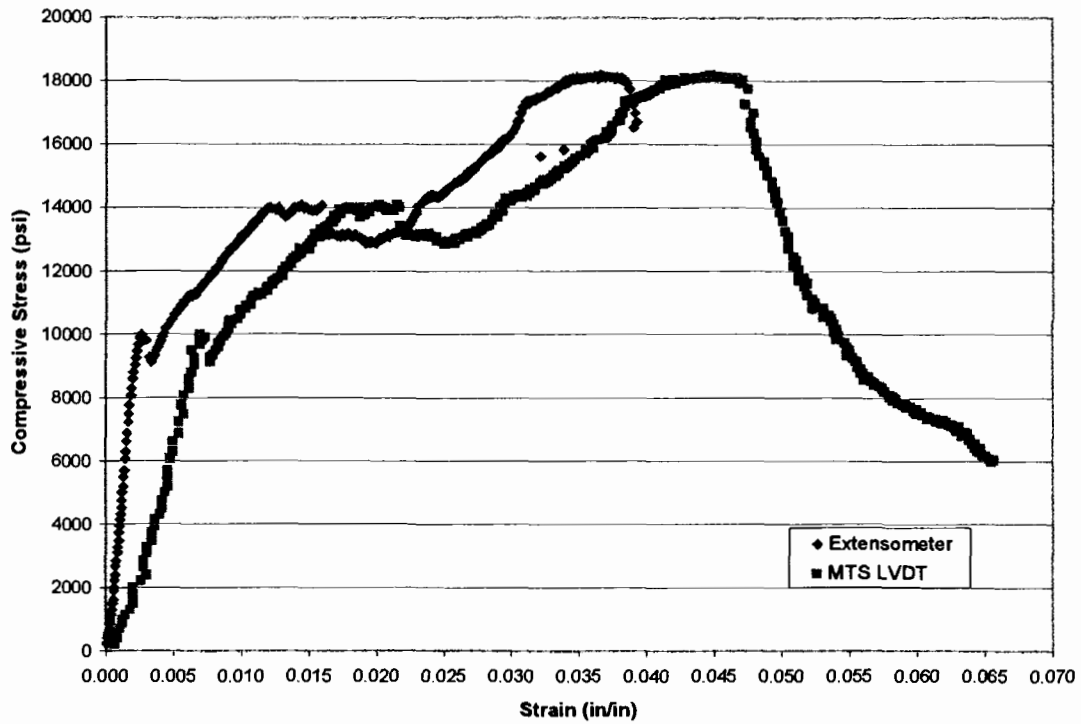


**a. Test Specimen ATS-01-y**

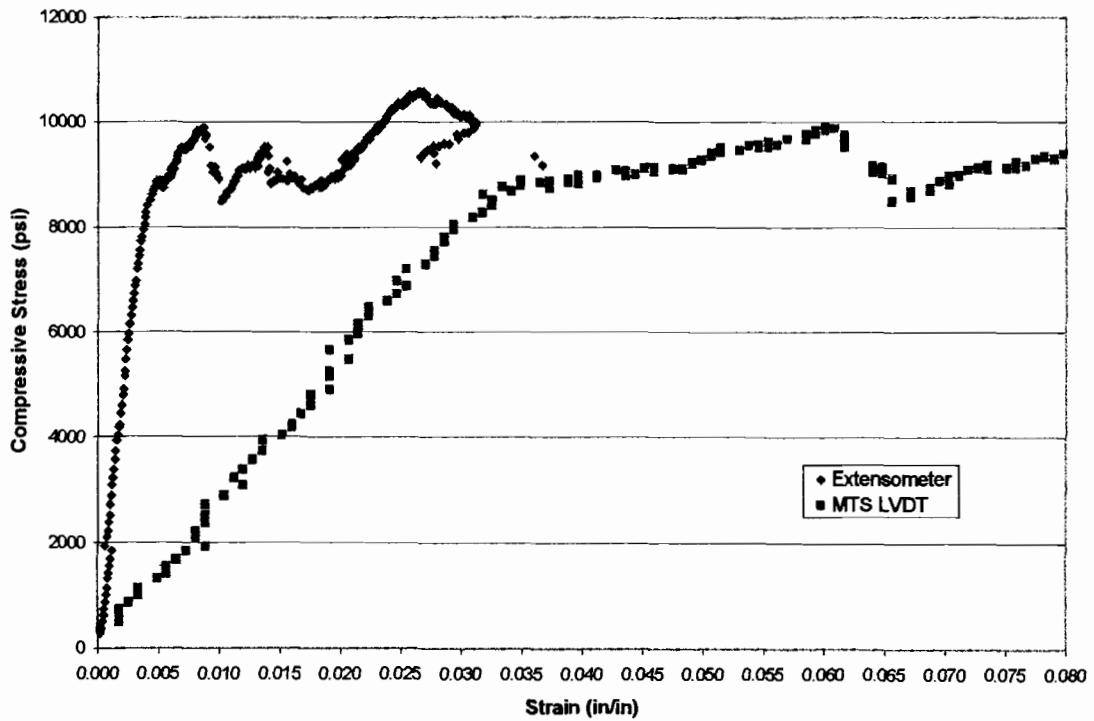


**b. Test Specimen ATS-02-y**

Figure G.2 – Y-Direction Stress-Strain Curves (Continued)

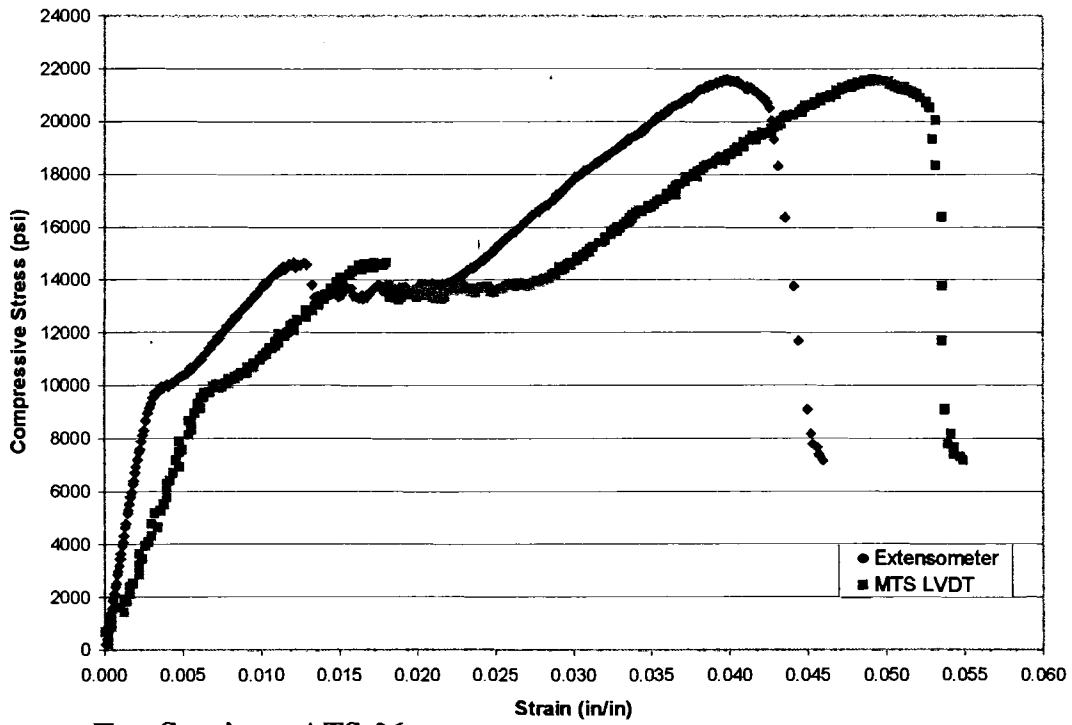


c. Test Specimen ATS-03-Y

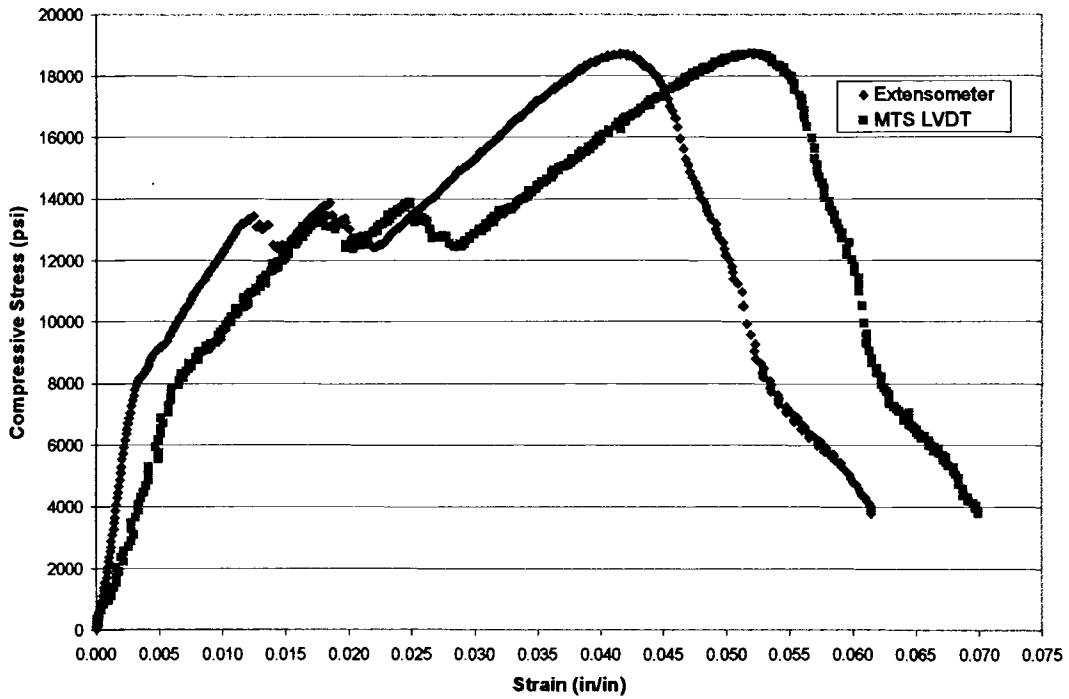


d. Test Specimen ATS-04-y

**Figure G.2 – Y-Direction Stress-Strain Curves (Continued)**

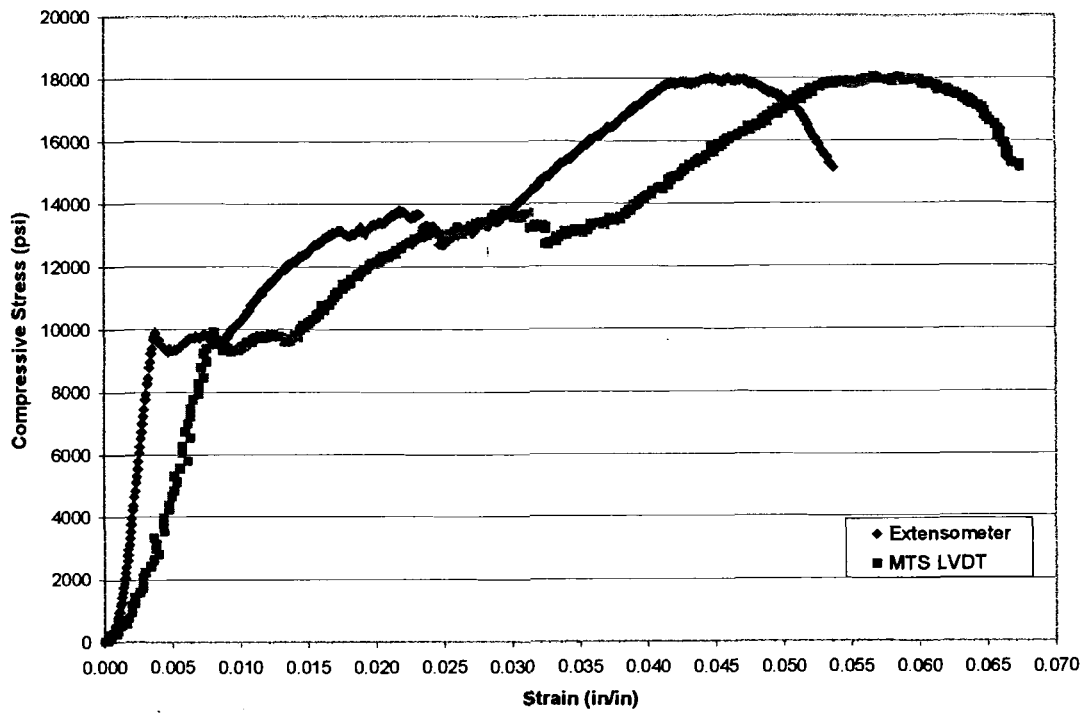


**e. Test Specimen ATS-06-y**

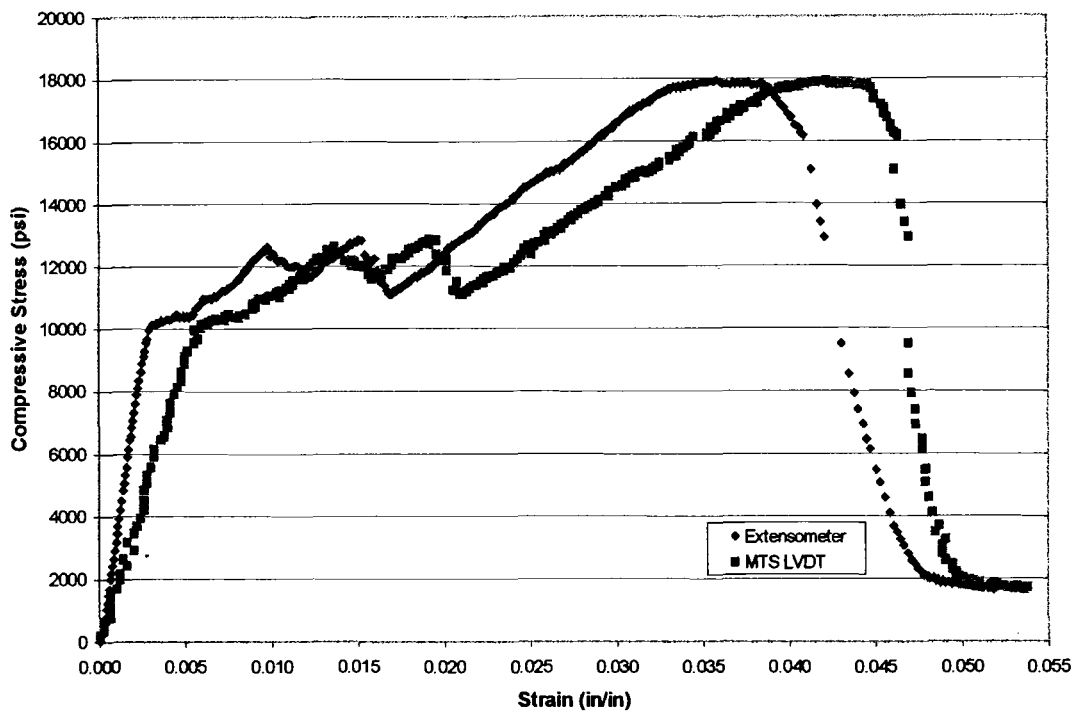


**f. Test Specimen ATS-07-y**

**Figure G.2 – Y-Direction Stress-Strain Curves (Continued)**

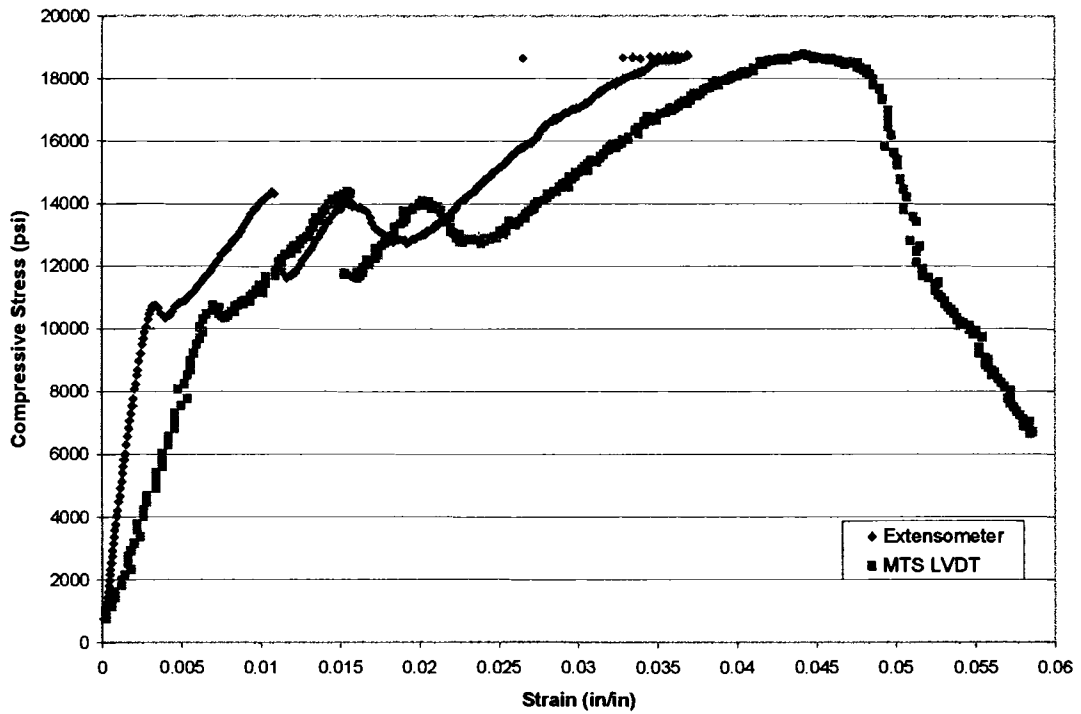


**g. Test Specimen ATS-08-y**

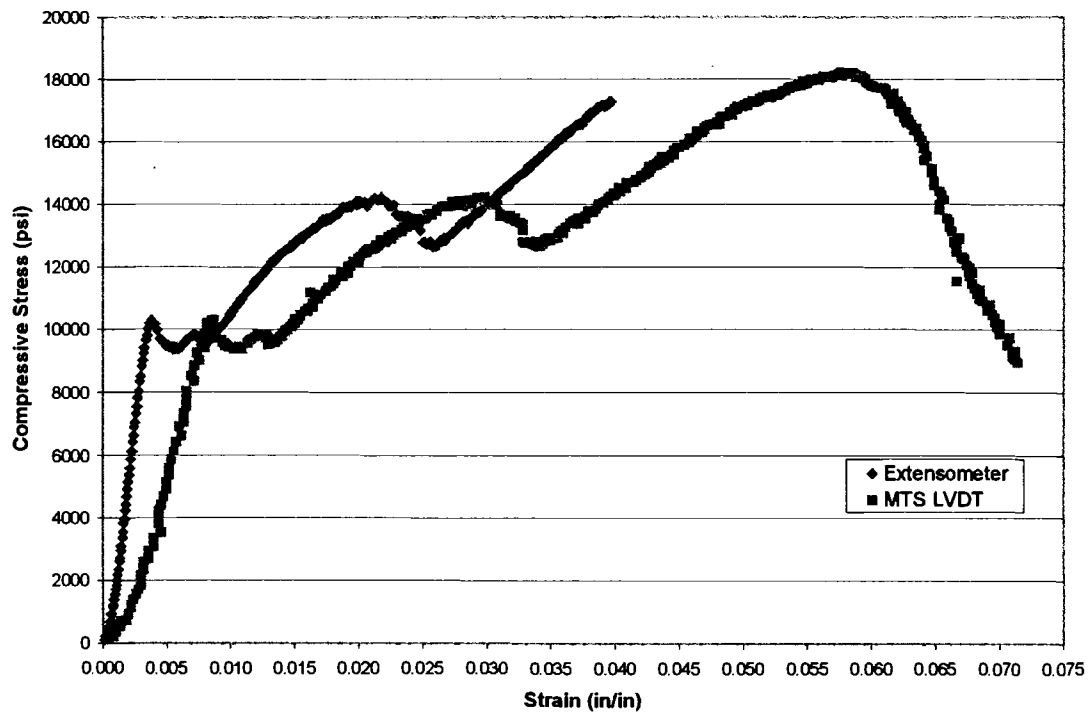


**h. Test Specimen ATS-11-y**

**Figure G.2 – Y-Direction Stress-Strain Curves (Continued)**



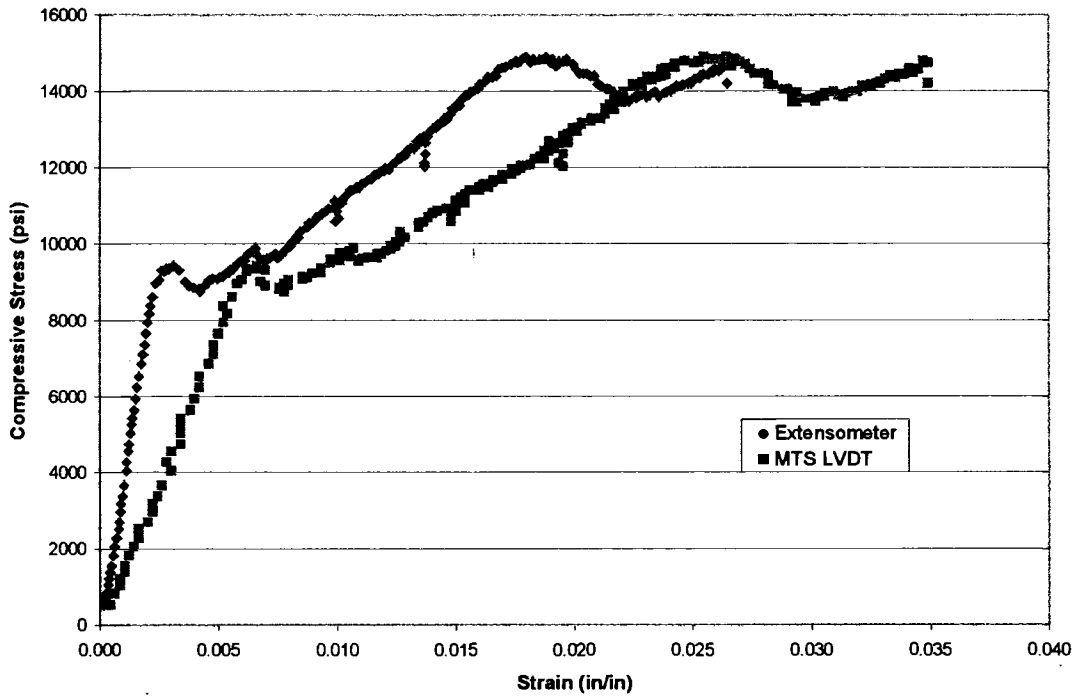
**i. Test Specimen ATS-13-y**



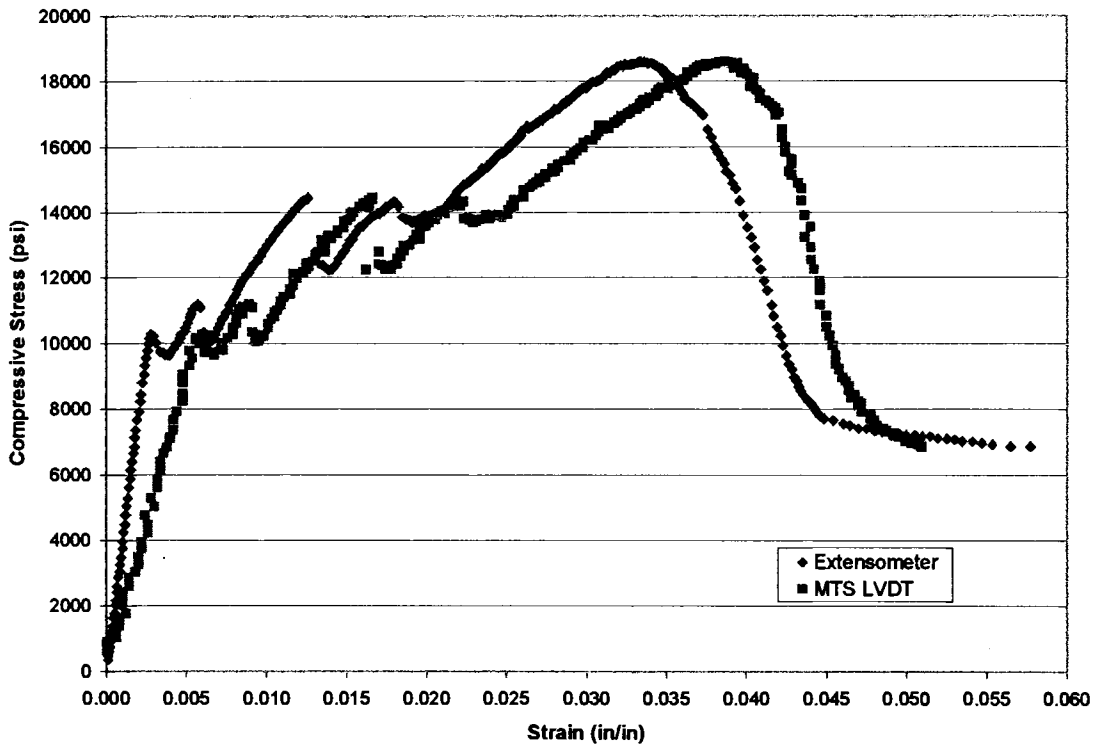
**j. Test Specimen ATS-14-y**



**Figure G.2 – Y-Direction Stress-Strain Curves (Continued)**

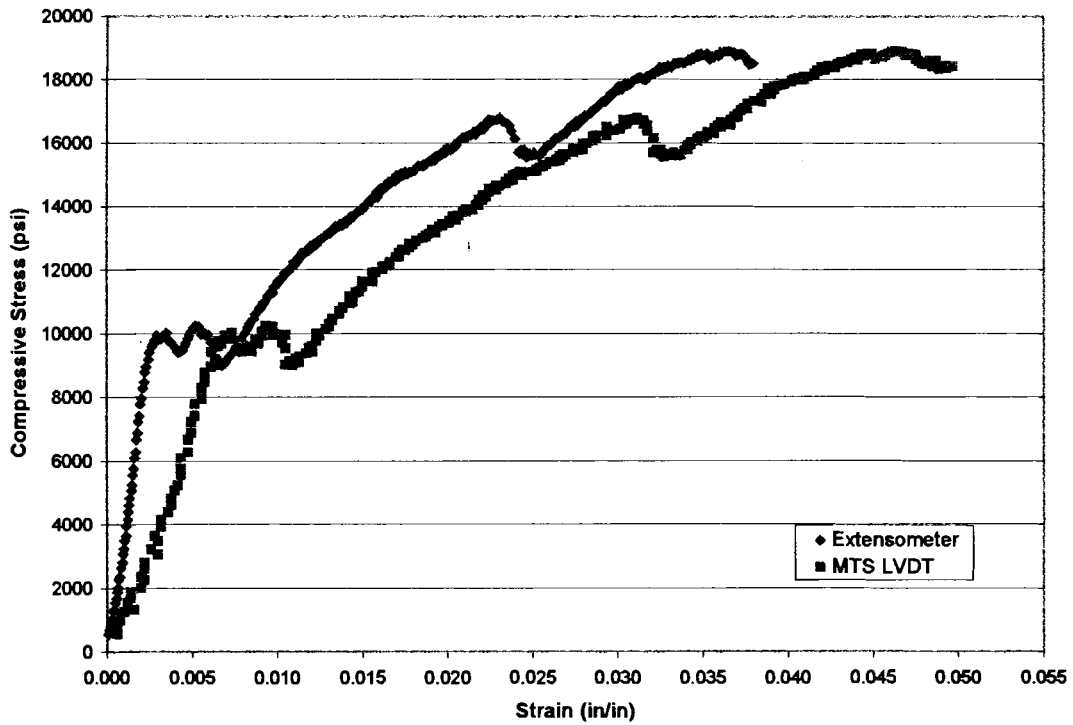


**k. Test Specimen ATS-16-y**

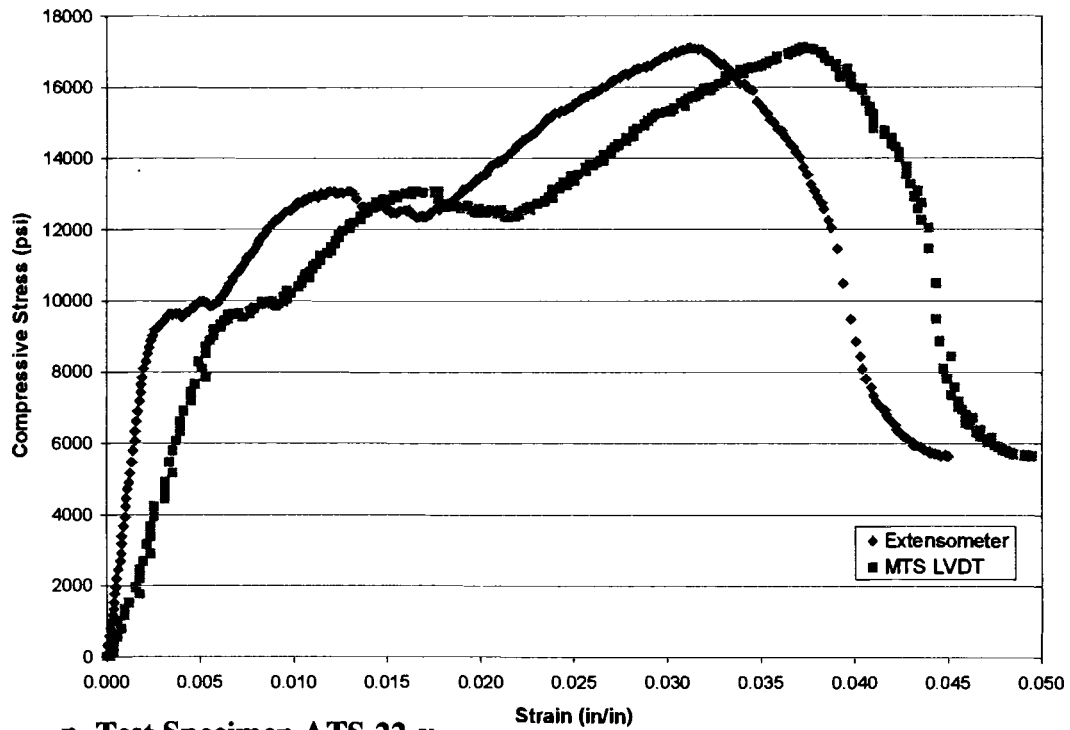


**l. Test Specimen ATS-17-y**

**Figure G.2 – Y-Direction Stress-Strain Curves (Continued)**

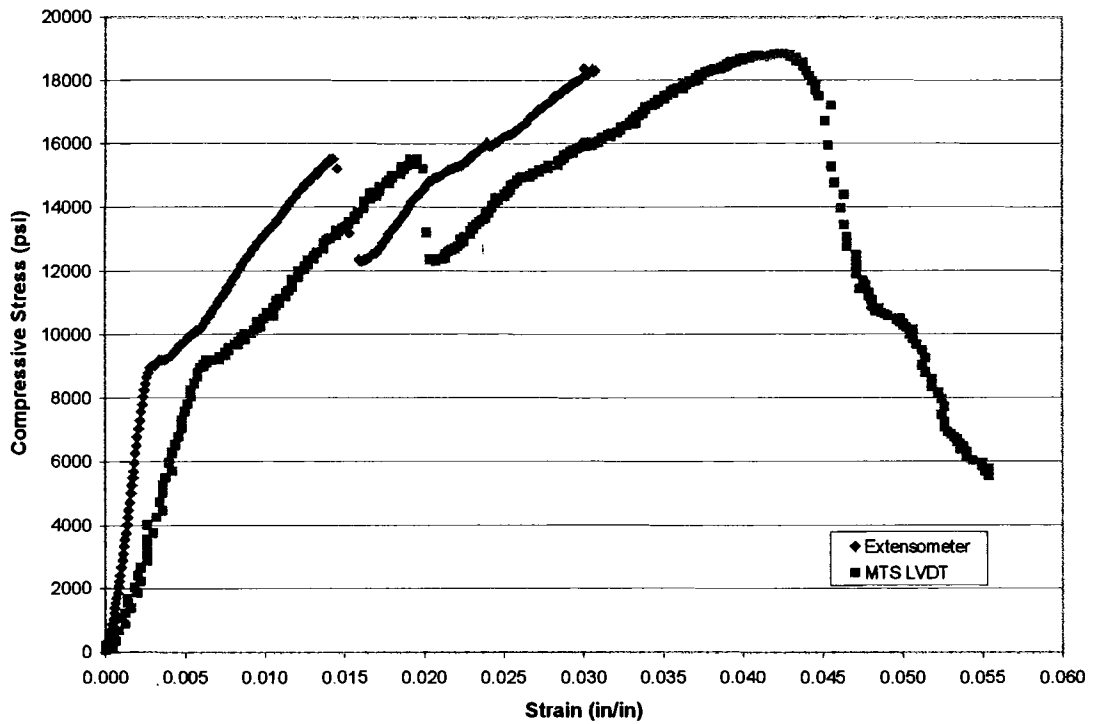


**m. Test Specimen ATS-18-y**

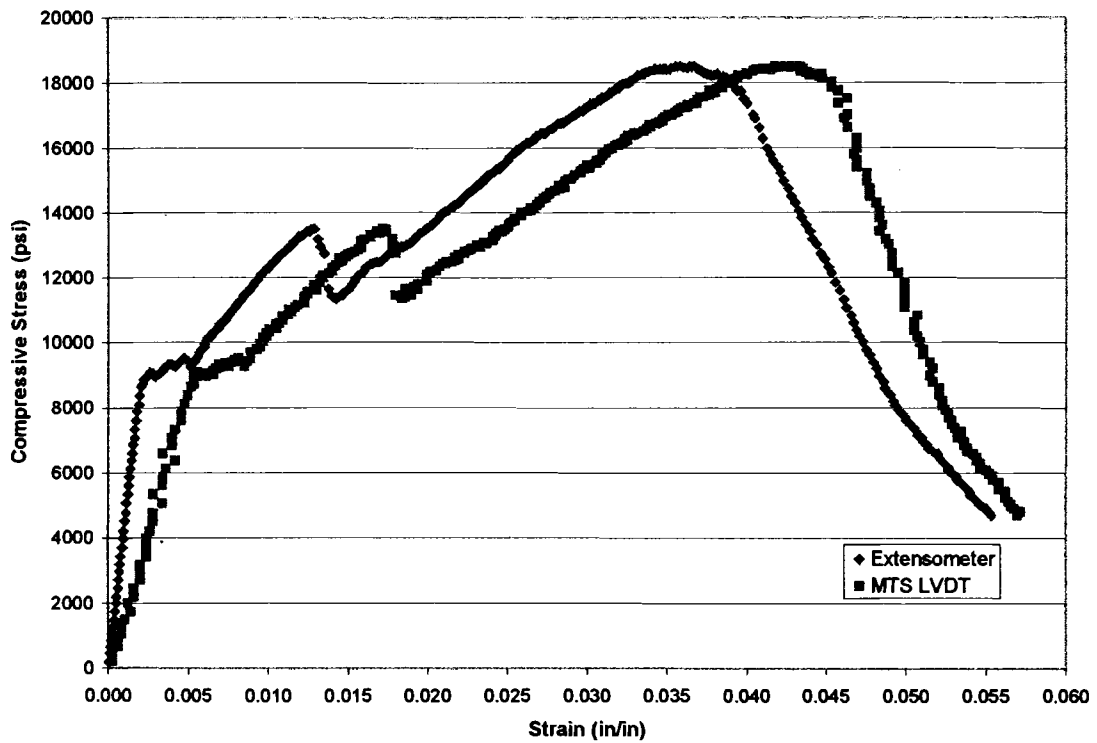


**n. Test Specimen ATS-22-y**

**Figure G.2 – Y-Direction Stress-Strain Curves (Continued)**

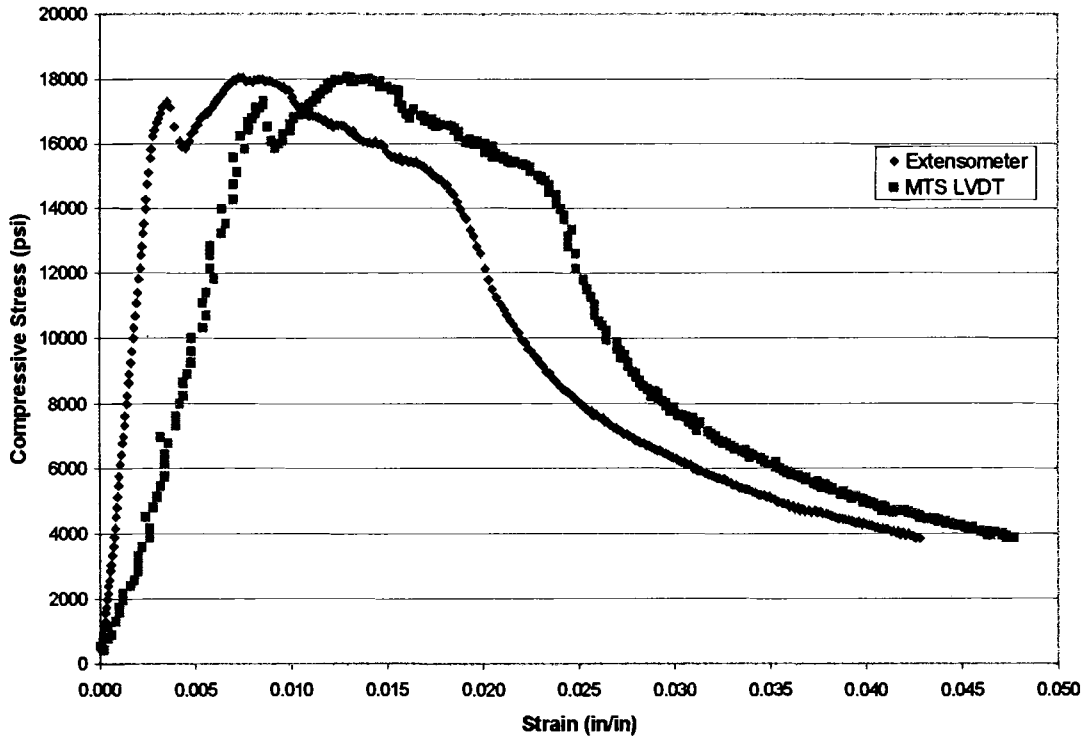


**o. Test Specimen ATS-24-y**

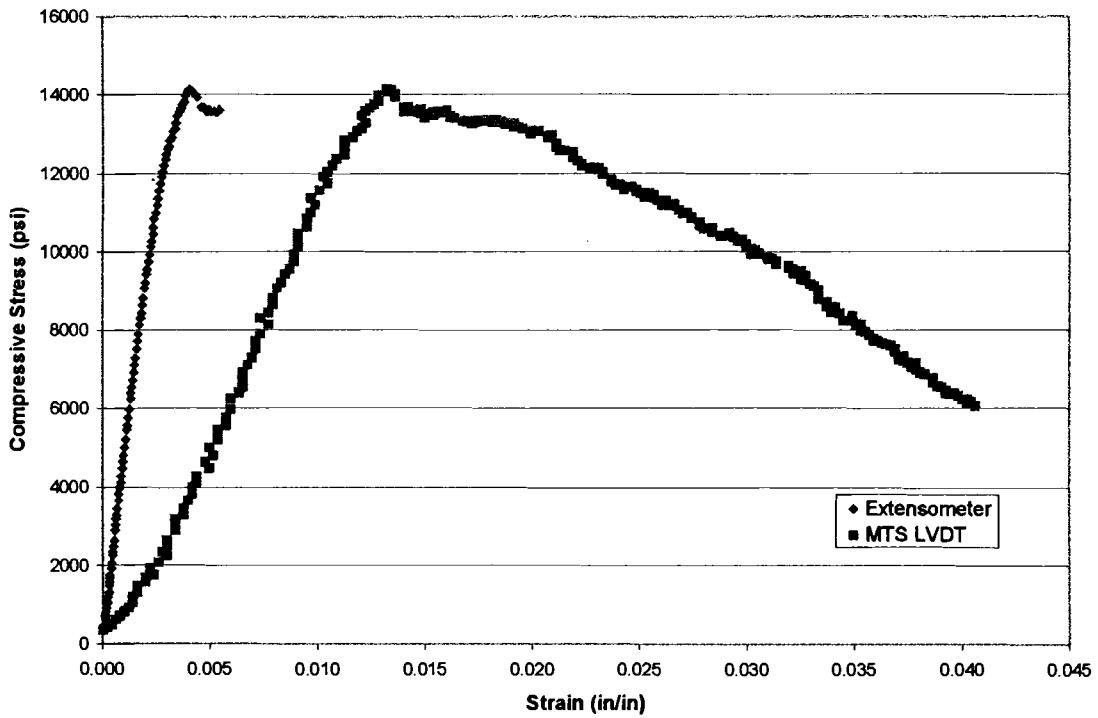


**p. Test Specimen ATS-25-y**

**Figure G.3 – Z-Direction Stress-Strain Curves**

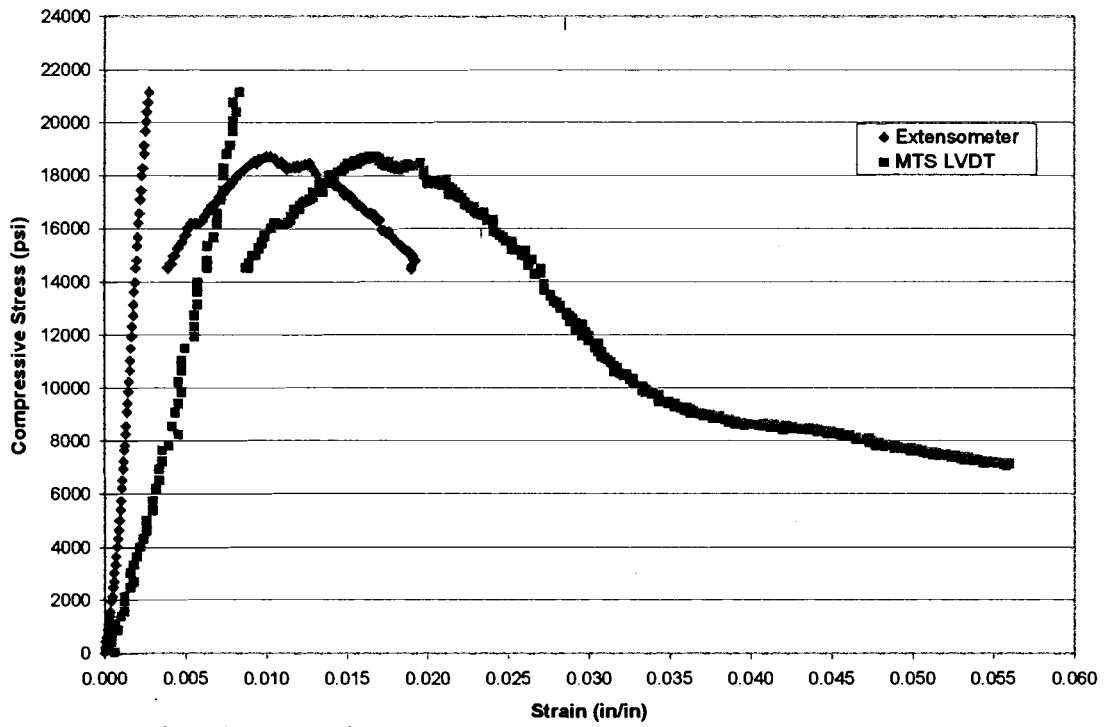


**a. Test Specimen ATS-01-z**

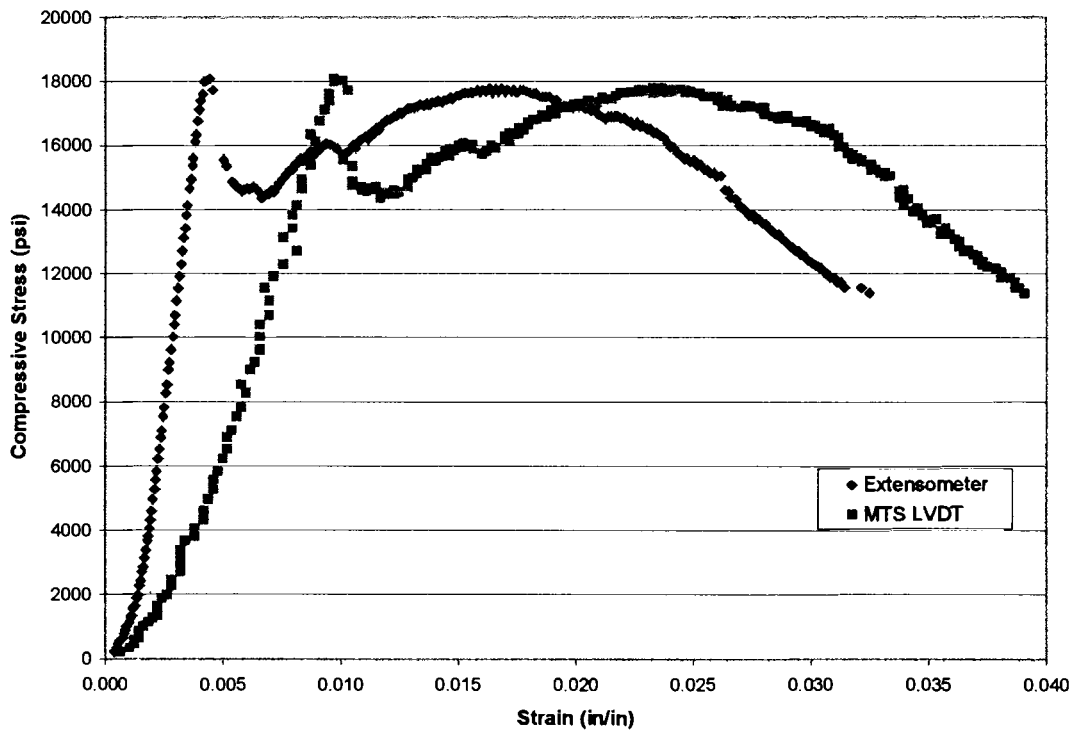


**b. Test Specimen ATS-03-z**

**Figure G.3 – Z-Direction Stress-Strain Curves (Continued)**

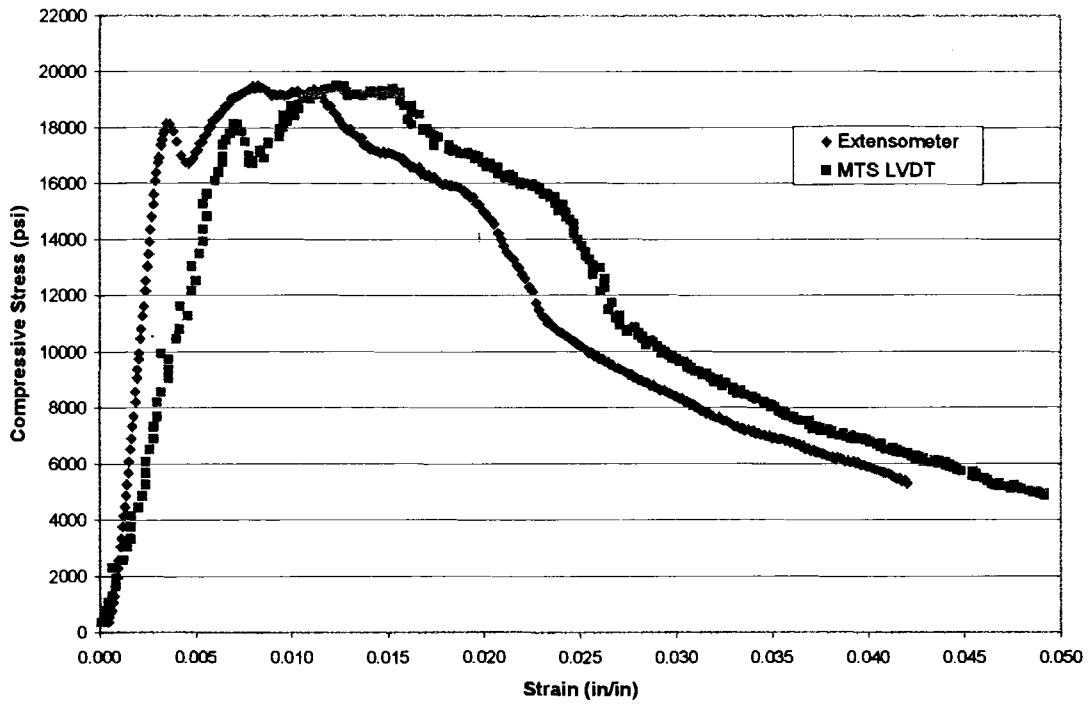


**c. Test Specimen ATS-05-z**

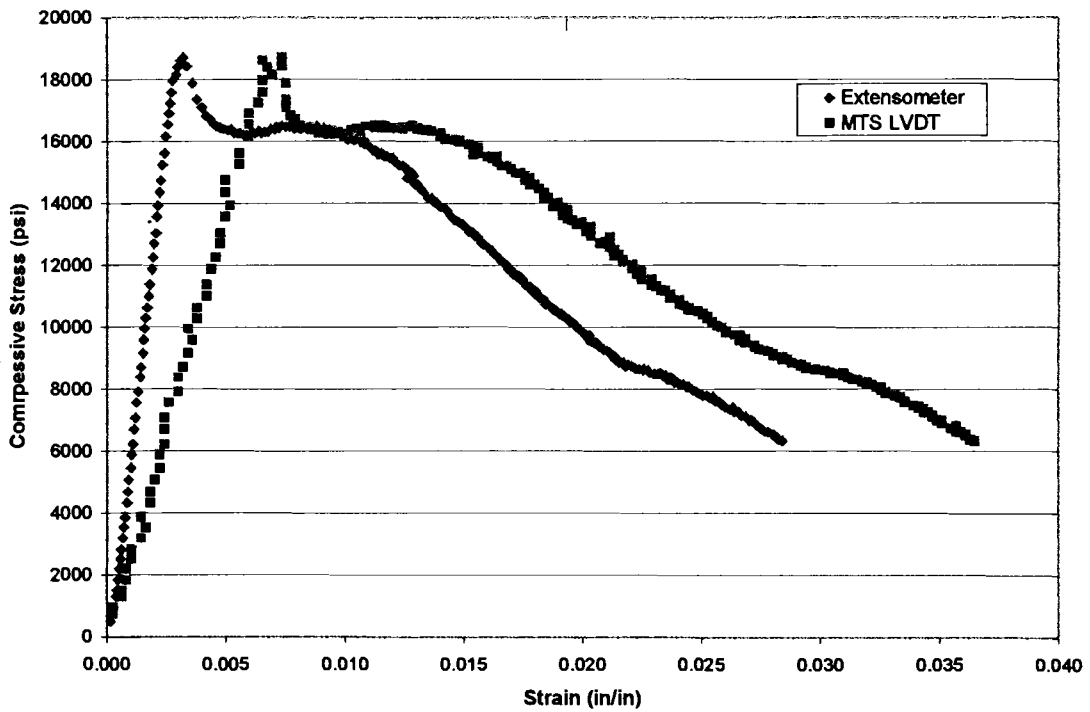


**d. Test Specimen ATS-06-z**

**Figure G.3 – Z-Direction Stress-Strain Curves (Continued)**

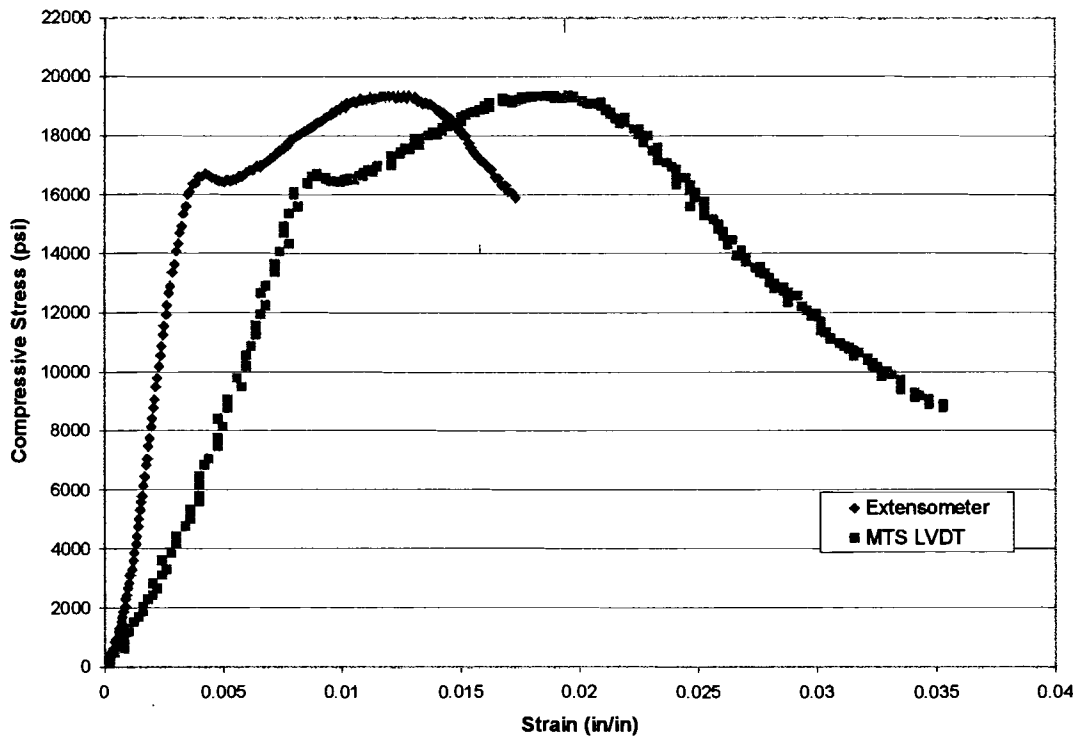


**e. Test Specimen ATS-07-z**

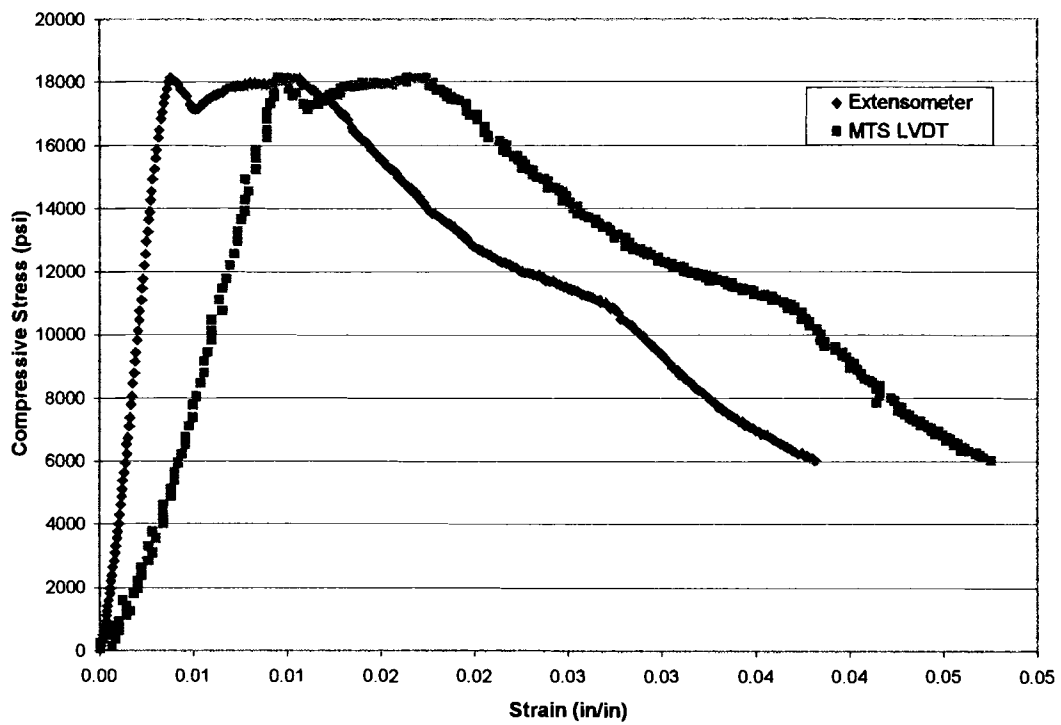


**f. Test Specimen ATS-08-z**

**Figure G.3 – Z-Direction Stress-Strain Curves (Continued)**

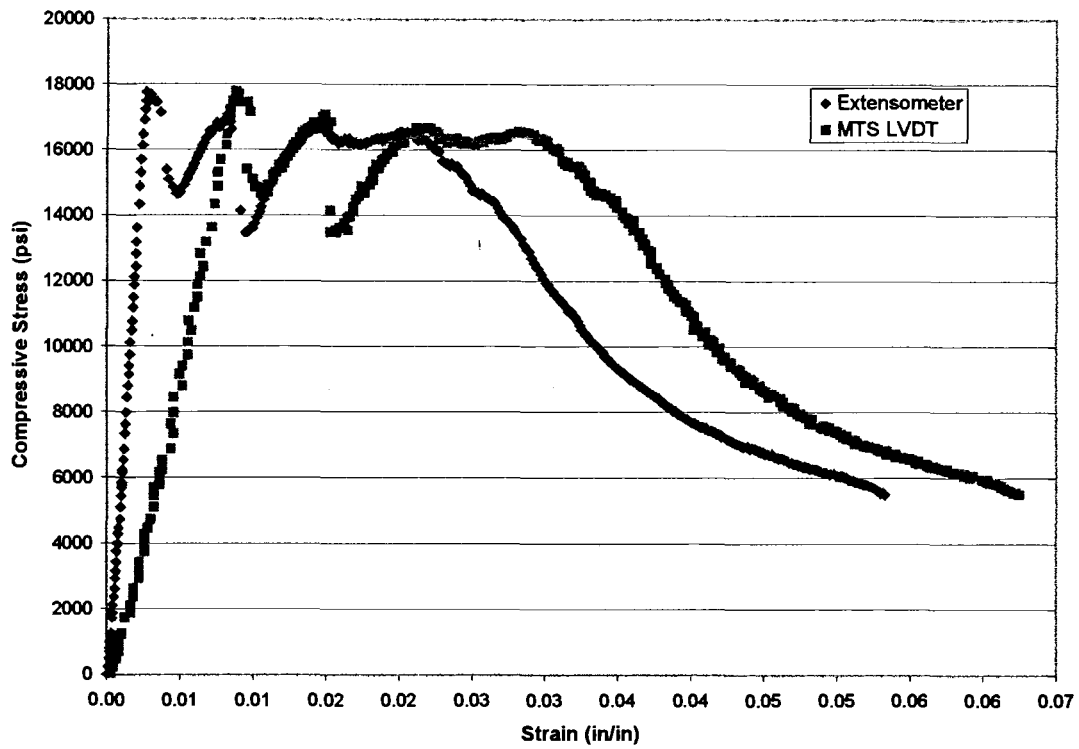


**g. Test Specimen ATS-09-z**

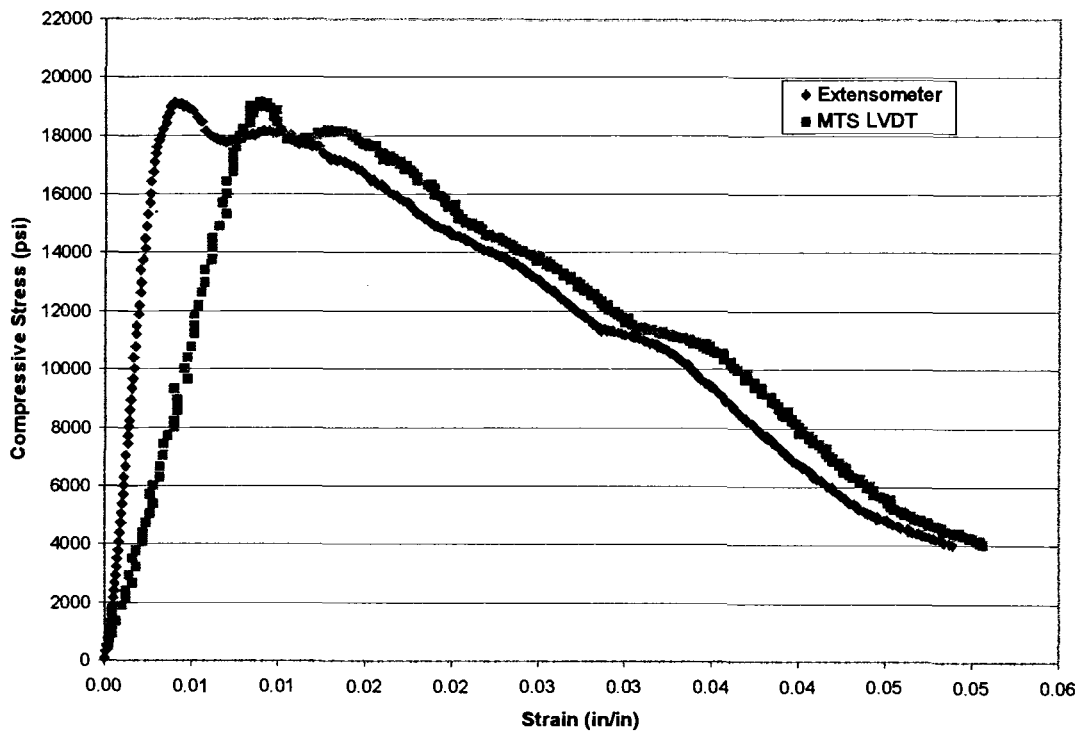


**h. Test Specimen ATS-11-z**

**Figure G.3 – Z-Direction Stress-Strain Curves (Continued)**



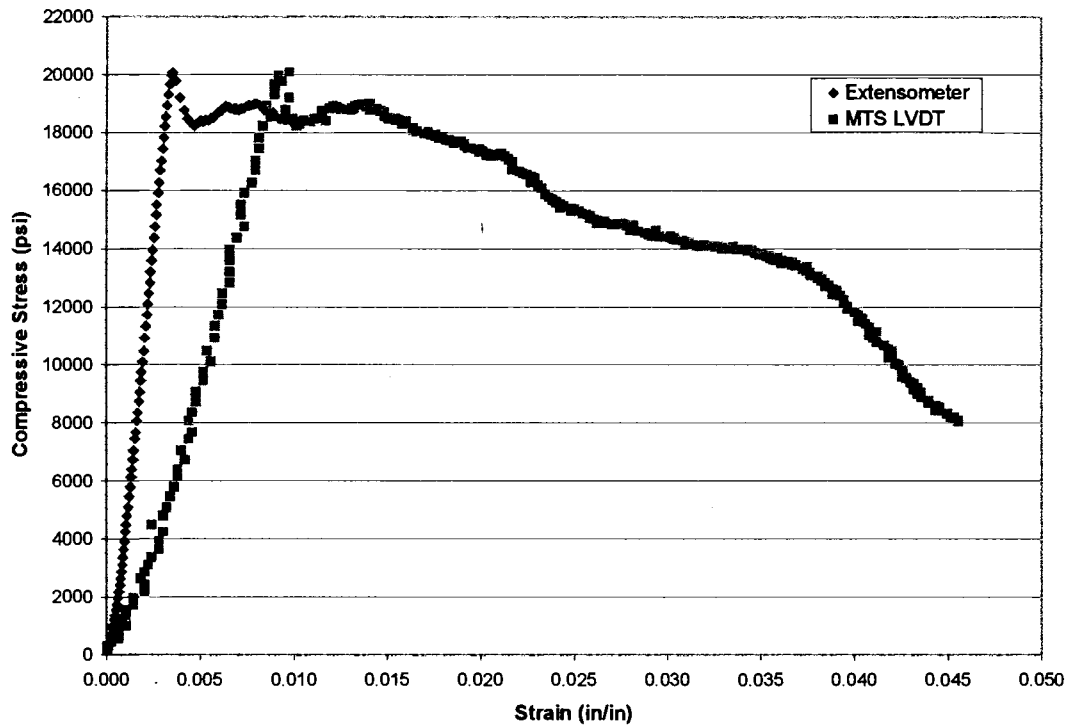
**i. Test Specimen ATS-13-z**



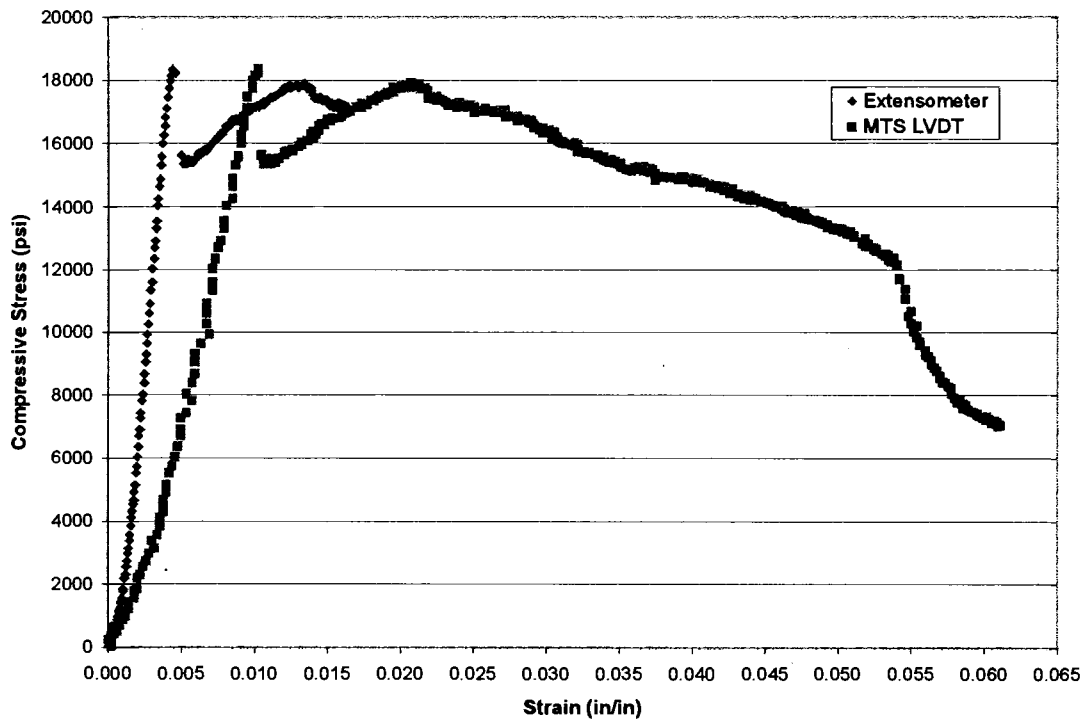
**j. Test Specimen ATS-15-z**



**Figure G.3 – Z-Direction Stress-Strain Curves (Continued)**

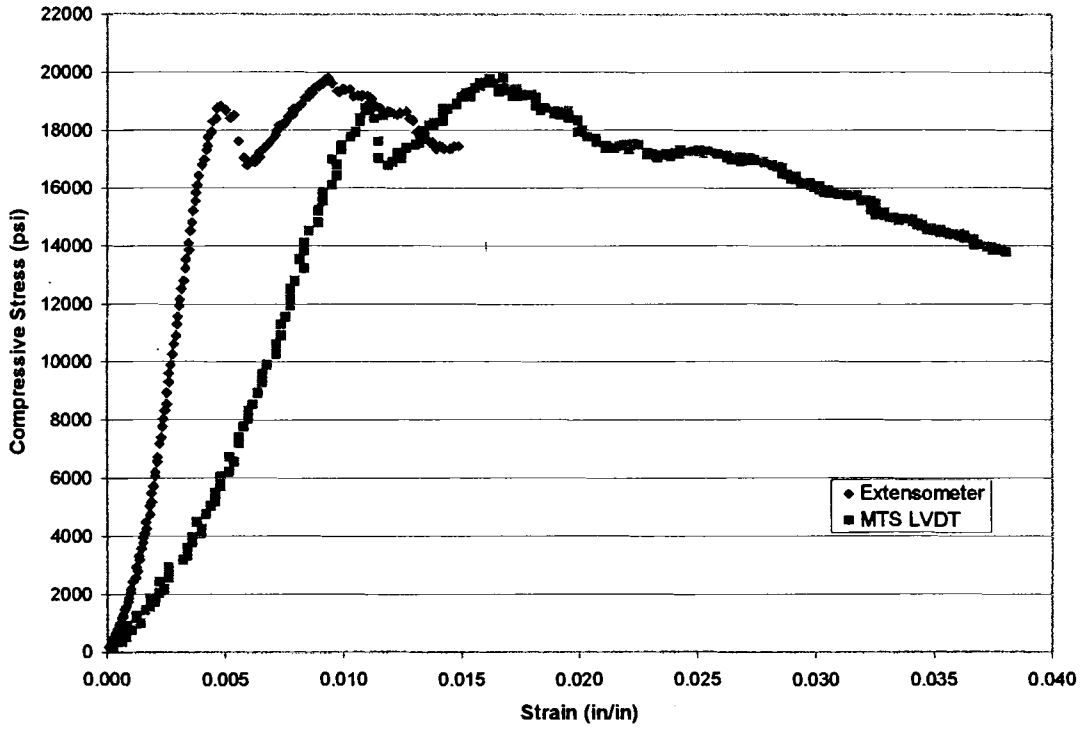


**k. Test Specimen ATS-16-z**

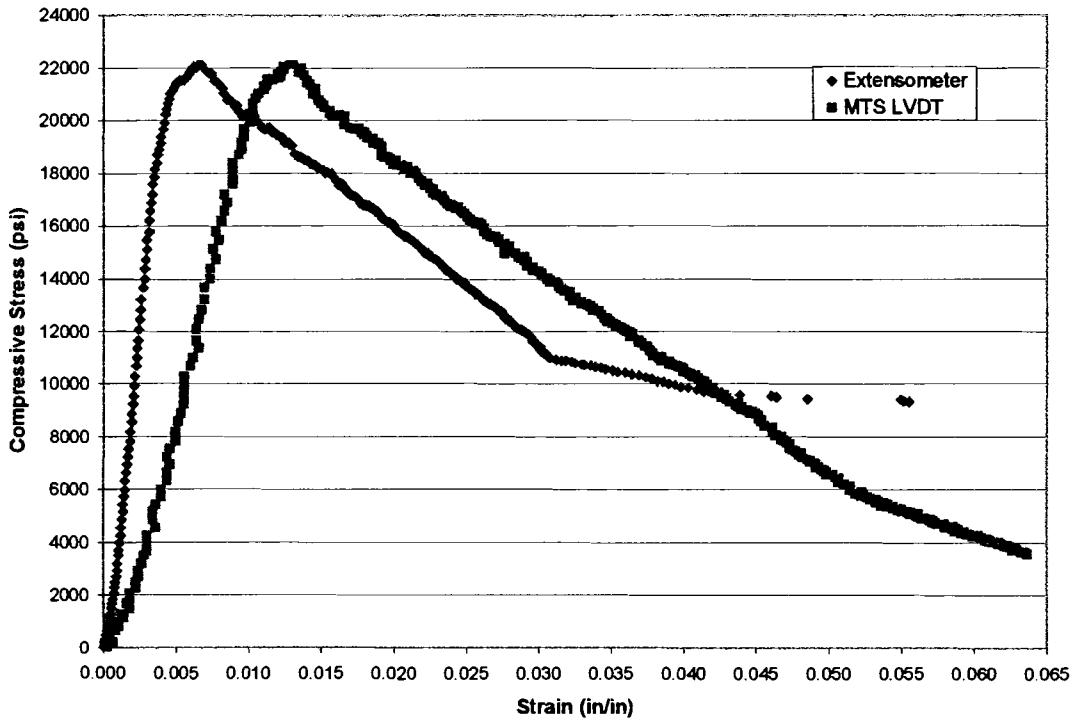


**l. Test Specimen ATS-19-z**

**Figure G.3 – Z-Direction Stress-Strain Curves (Continued)**

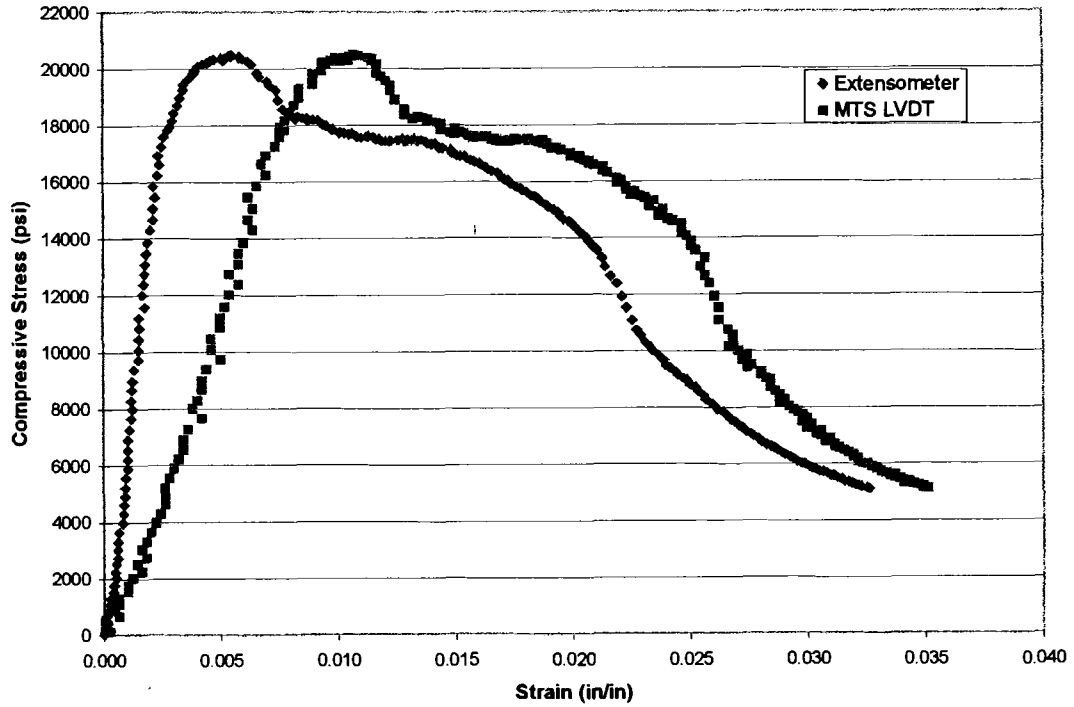


**m. Test Specimen ATS-21b-z**

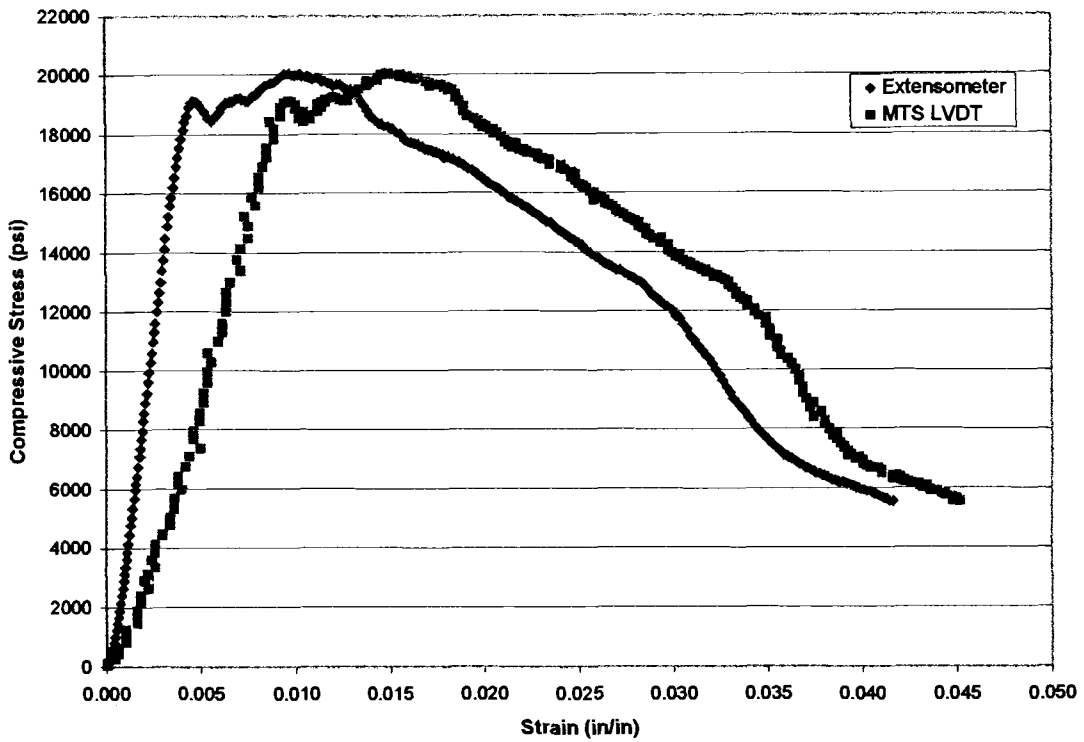


**n. Test Specimen ATS-22-z**

**Figure G.3 – Z-Direction Stress-Strain Curves (Continued)**



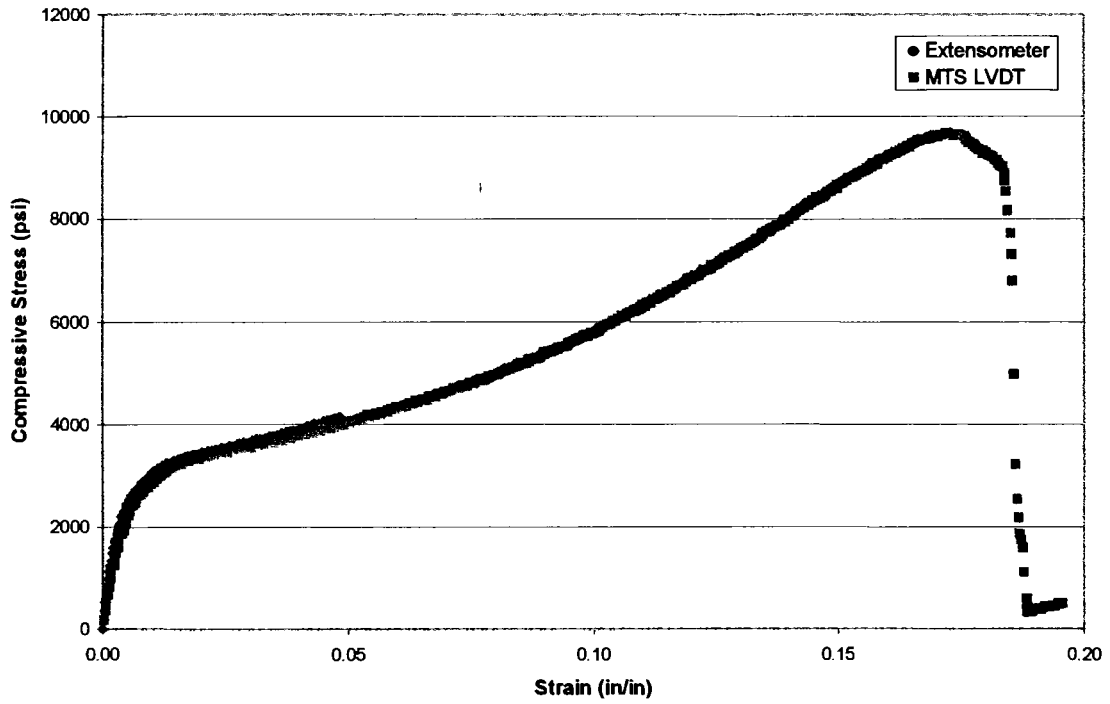
**o. Test Specimen ATS-27-z**



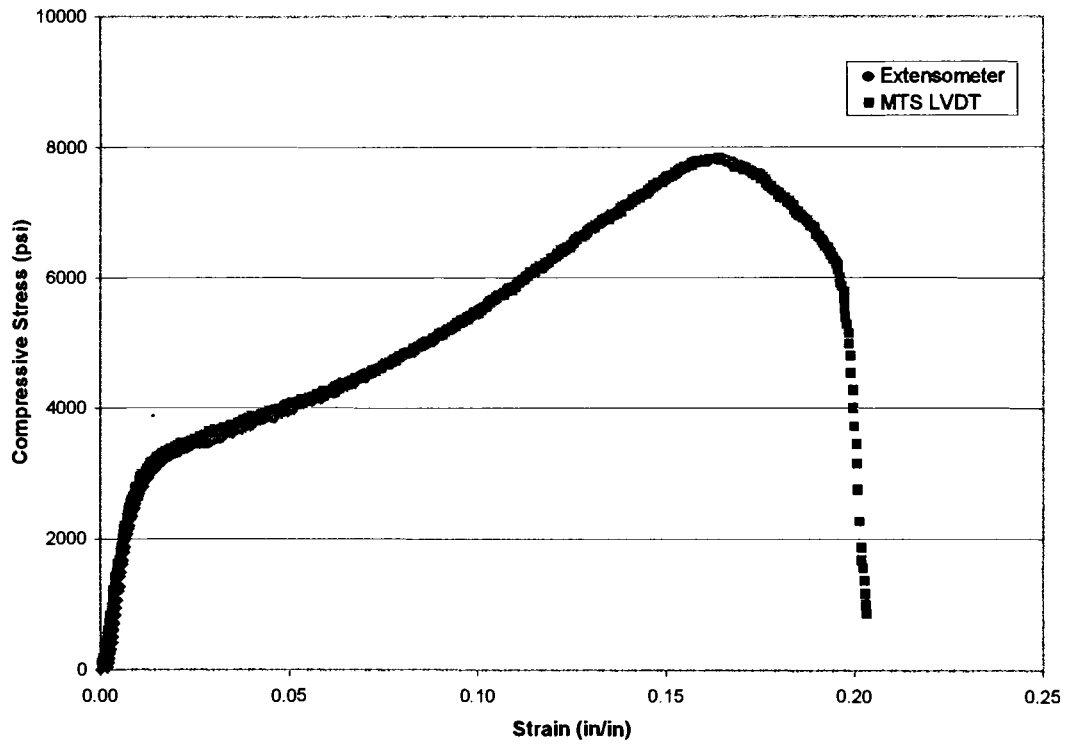
**p. Test Specimen ATS-28-z**

## Appendix H – Individual Off-Axis Compression Test Results

Figure H.1 – XZ-Plane Stress-Strain Curves

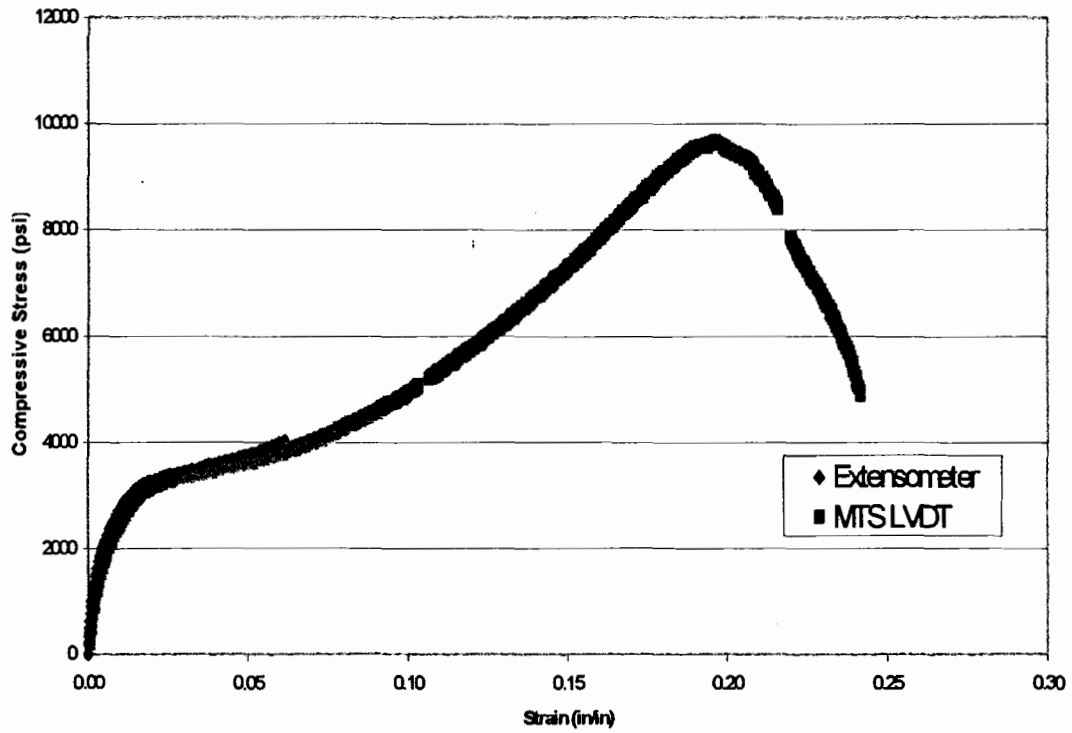


a. Test Specimen ATS-01-xz

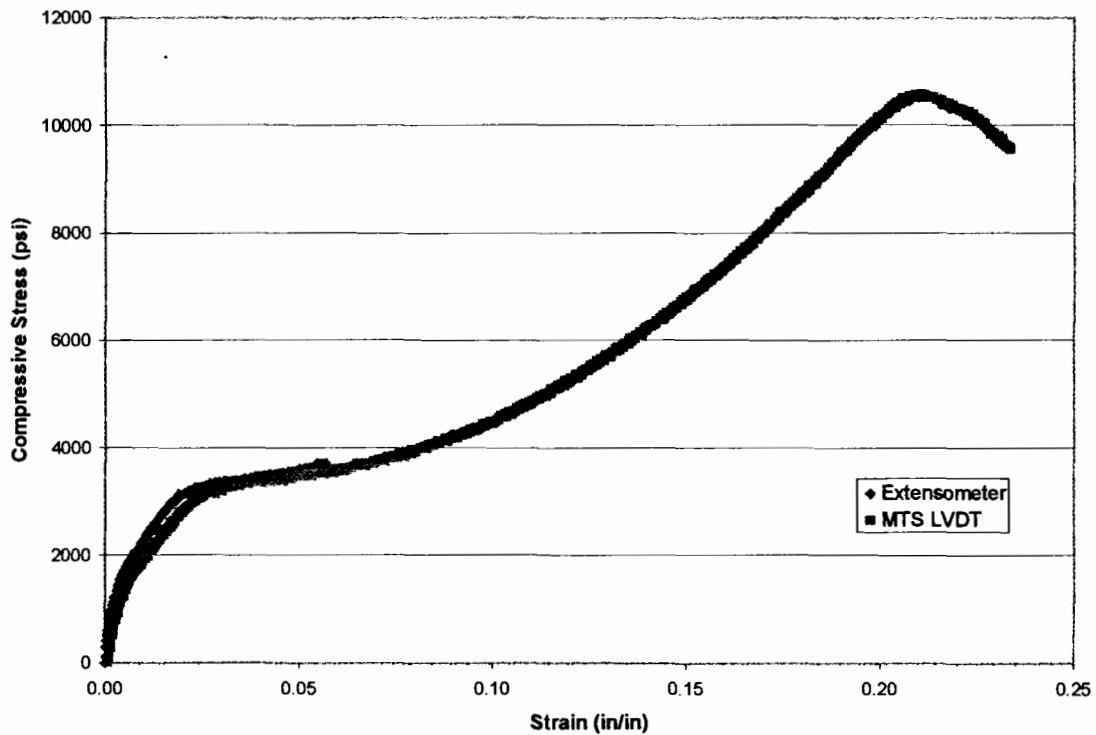


b. Test Specimen ATS-02-xz

**Figure H.1 – XZ-Plane Stress-Strain Curves (Continued)**

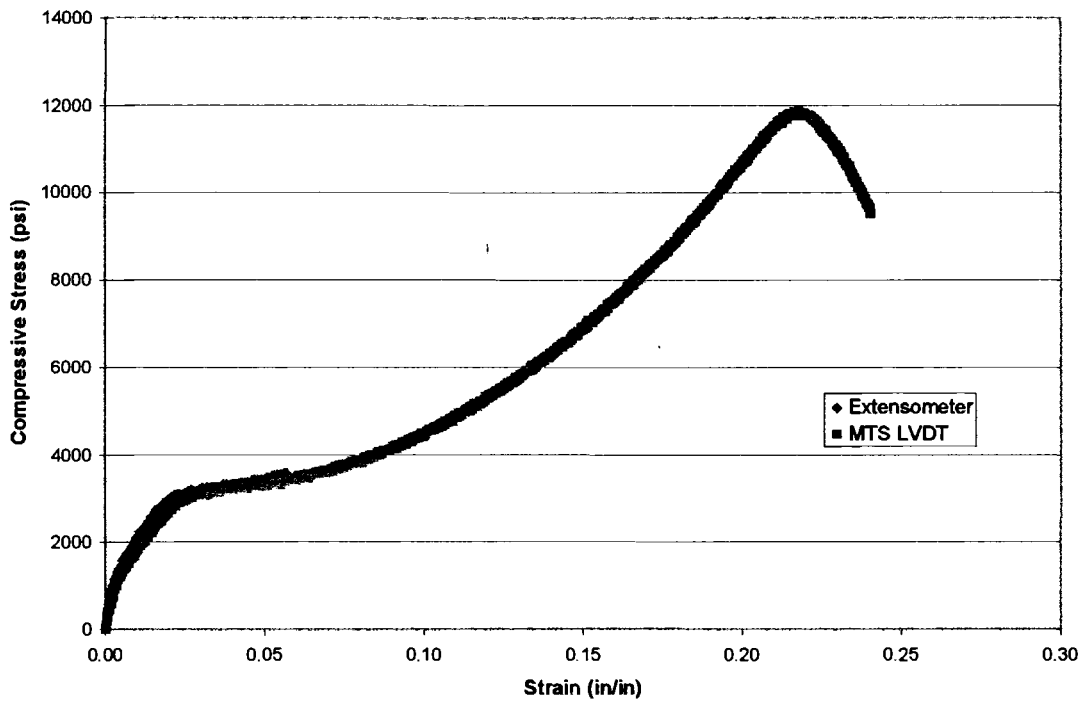


**c. Test Specimen ATS-03-xz**

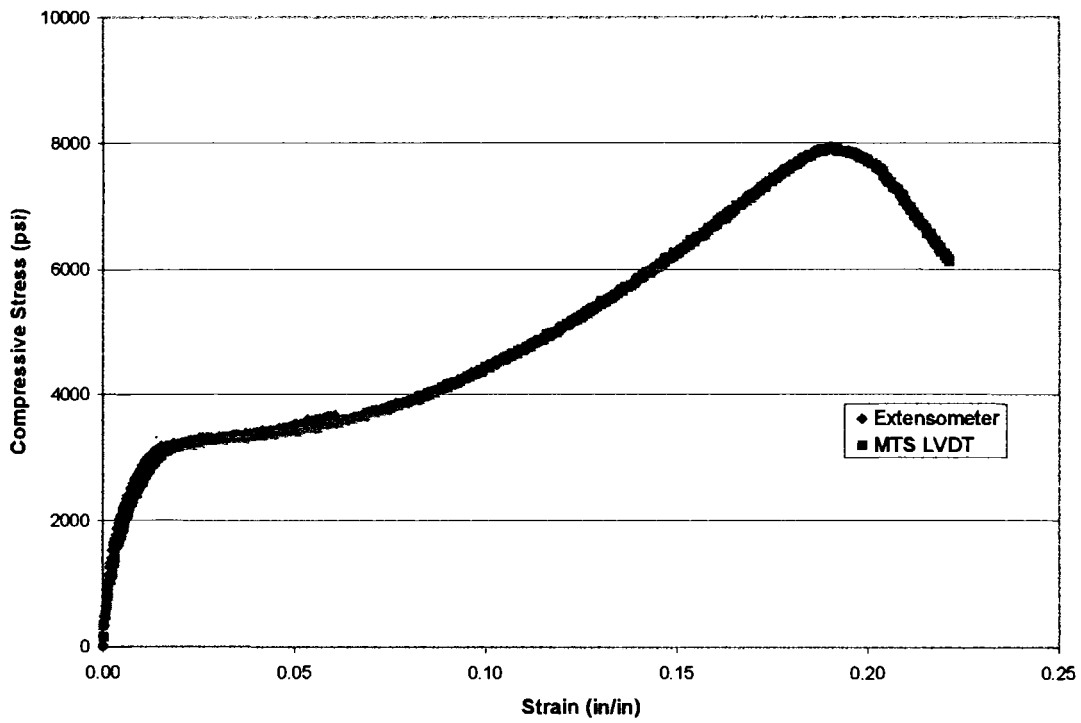


**d. Test Specimen ATS-05-xz**

**Figure H.1 – XZ-Plane Stress-Strain Curves (Continued)**

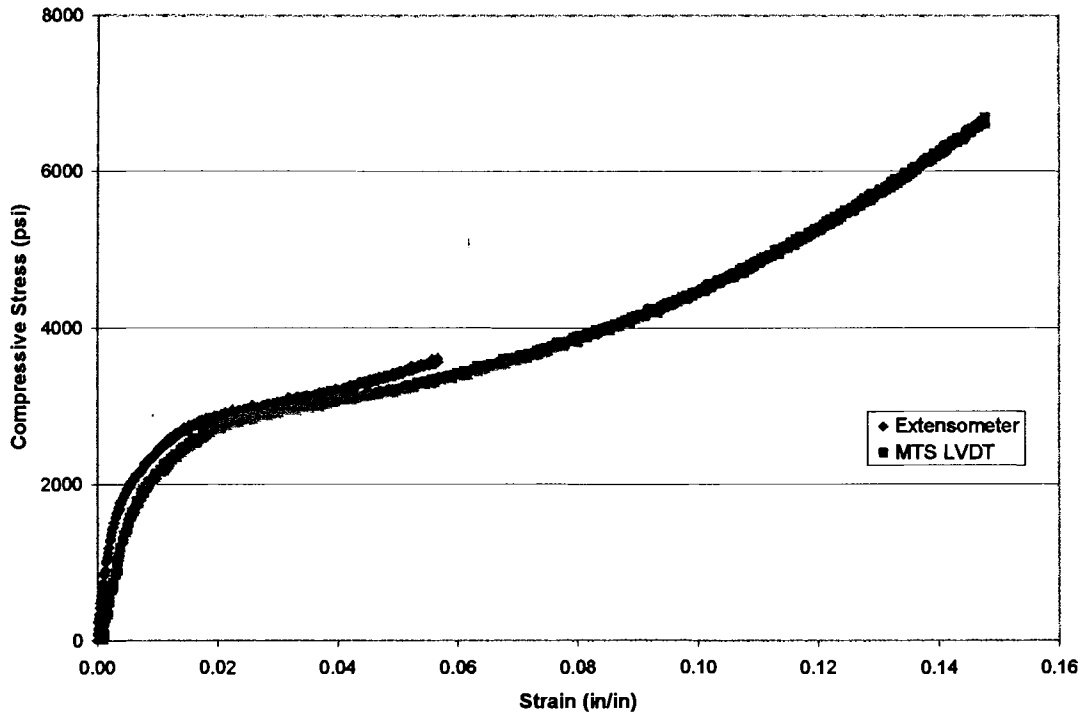


**e. Test Specimen ATS-06-xz**

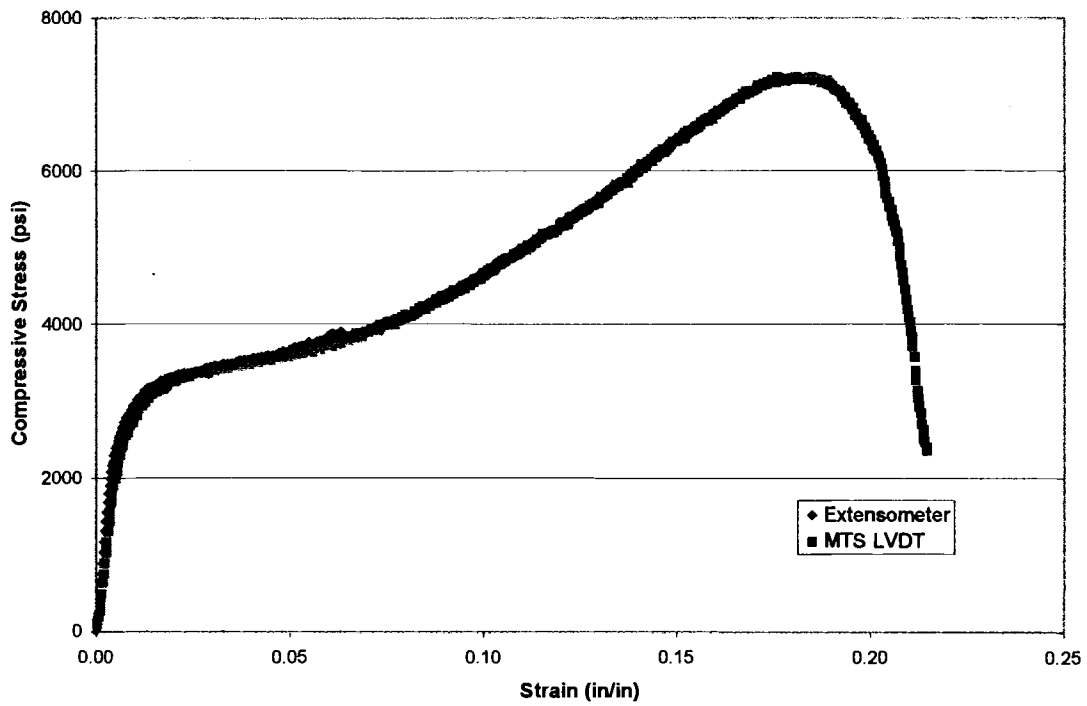


**f. Test Specimen ATS-09-xz**

**Figure H.2 – YZ-Plane Stress-Strain Curves**

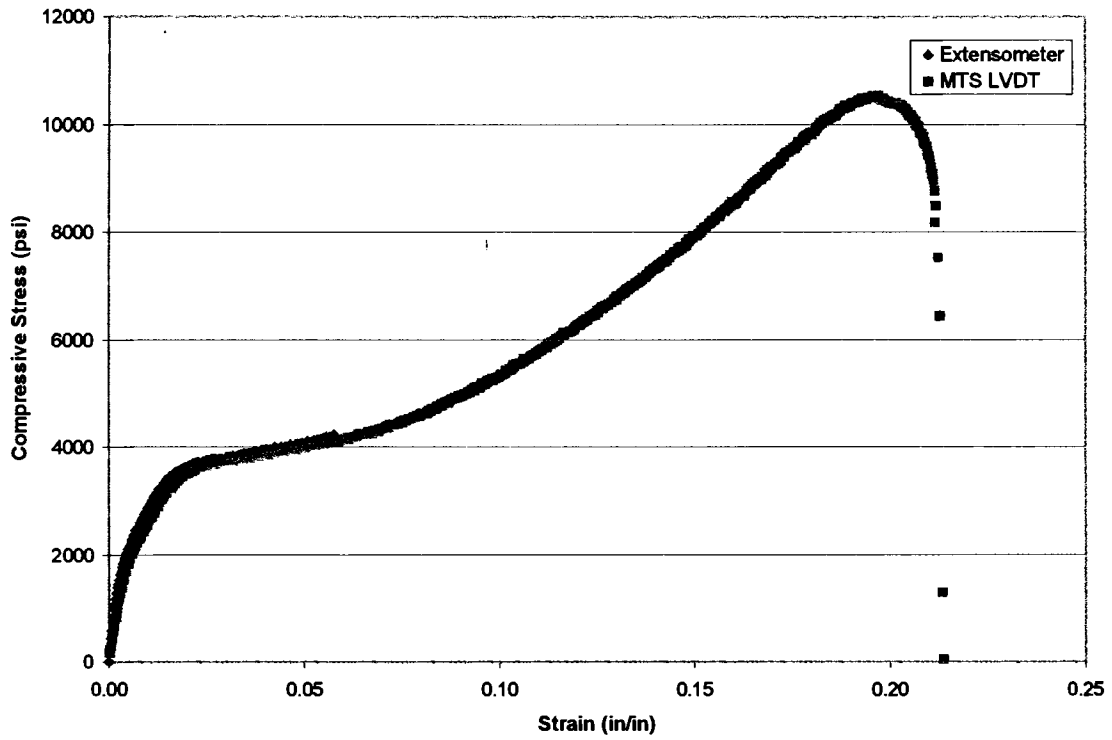


**a. Test Specimen ATS-01-yz**

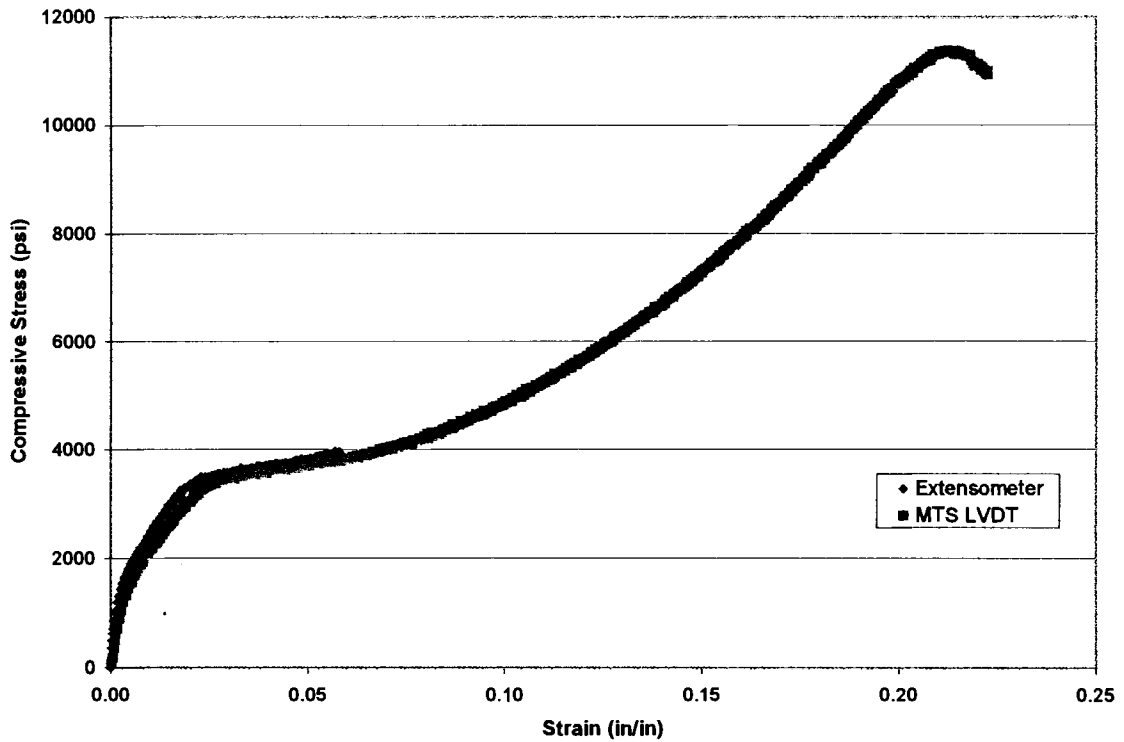


**b. Test Specimen ATS-04-yz**

**Figure H.2 – YZ-Plane Stress-Strain Curves (continued)**



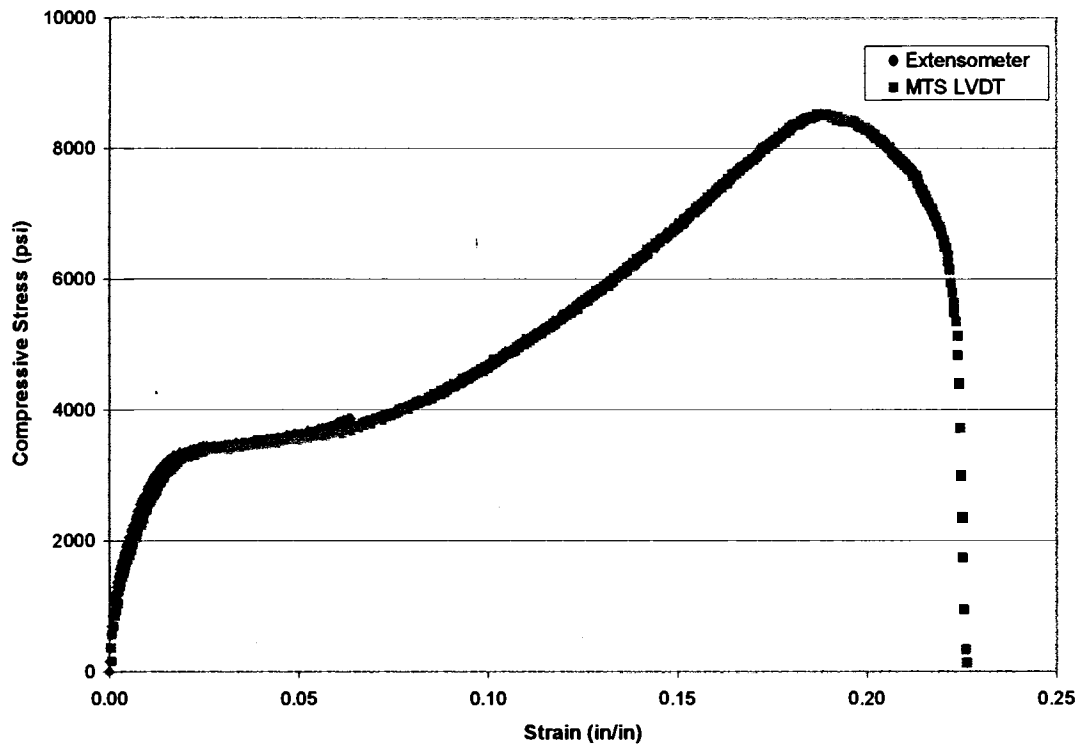
**c. Test Specimen ATS-06-yz**



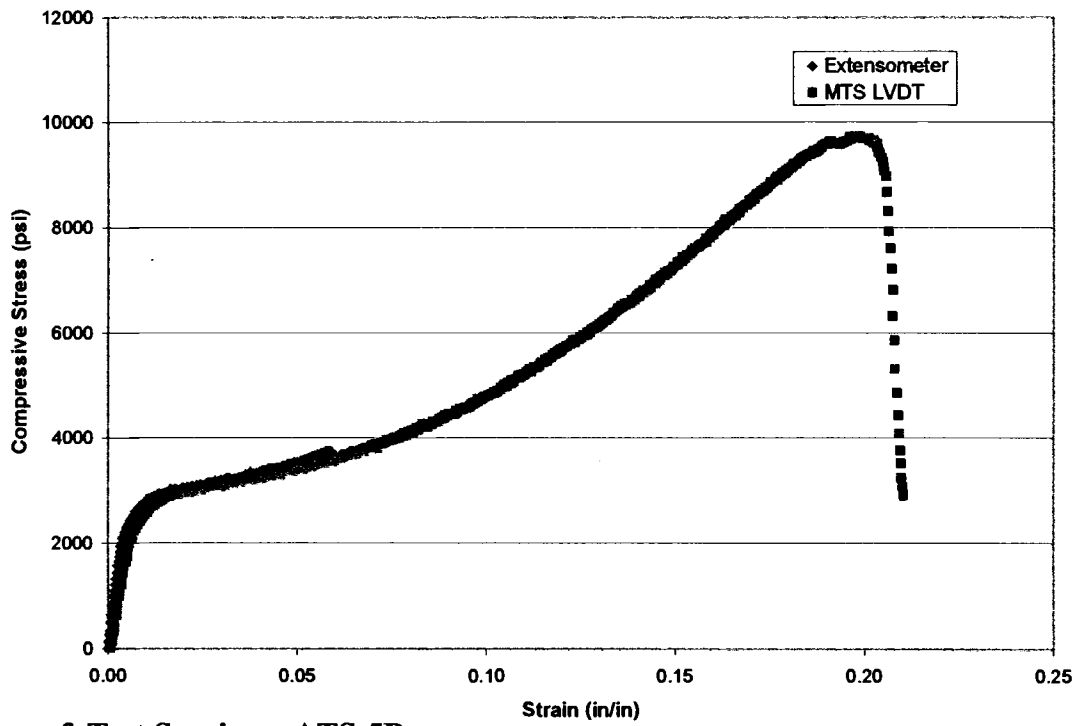
**d. Test Specimen ATS-07-yz**



Figure H.2 – YZ-Plane Stress-Strain Curves (continued)

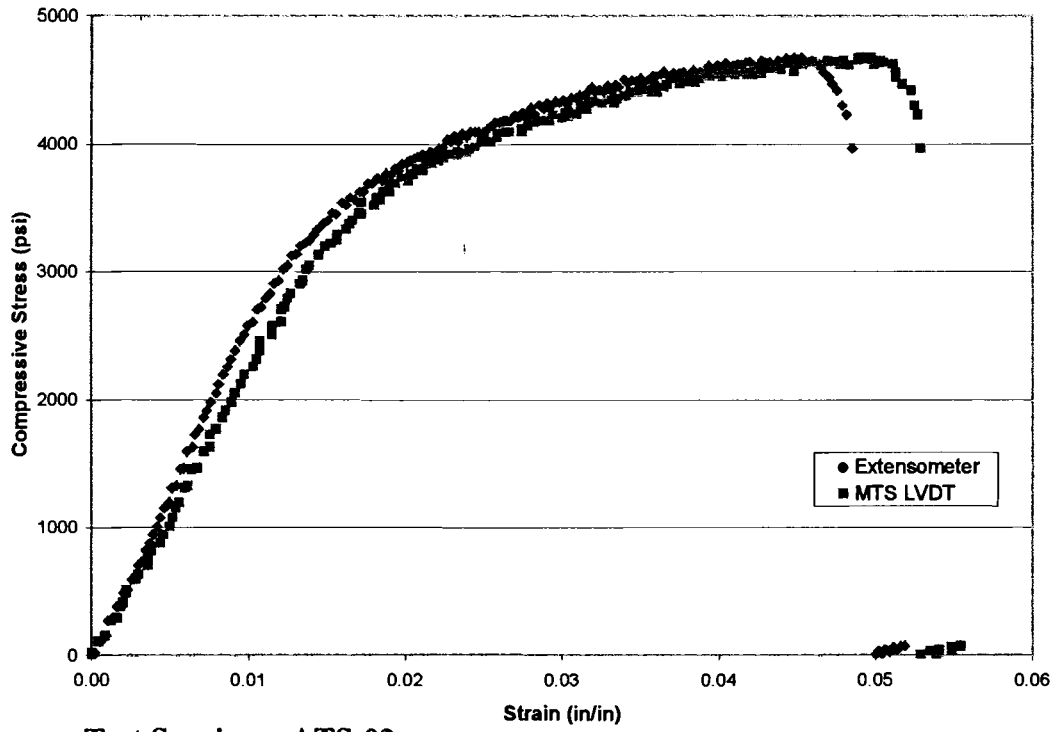


e. Test Specimen ATS-09-yz

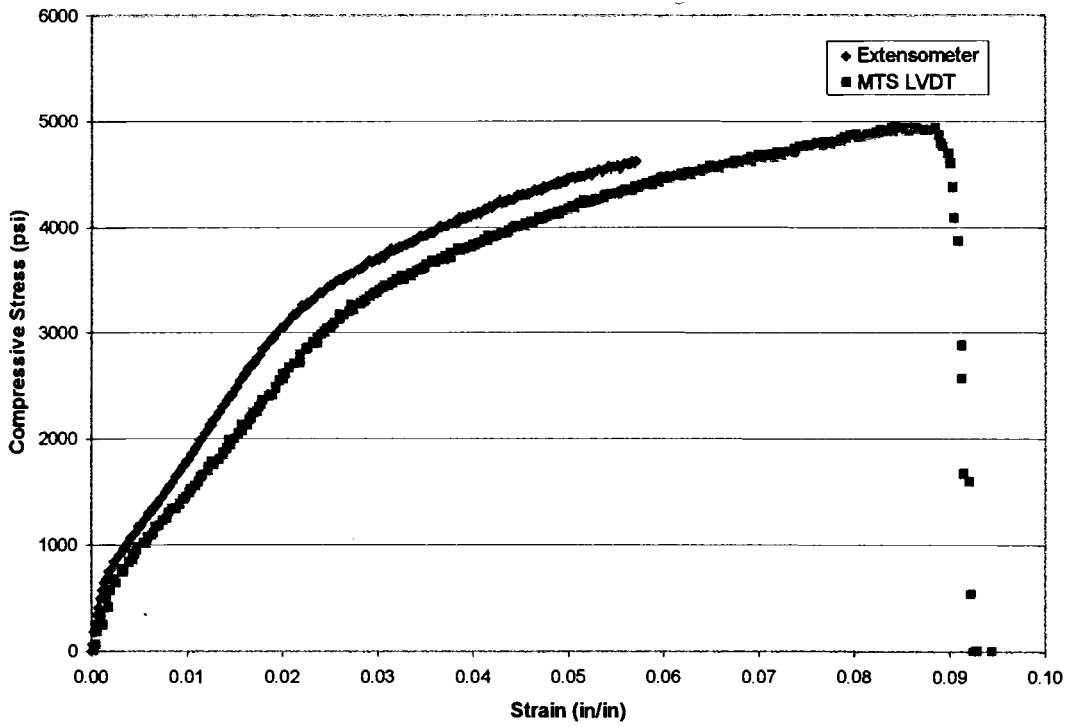


f. Test Specimen ATS-5B-yz

**Figure H.3 – XY-Plane Stress-Strain Curves**

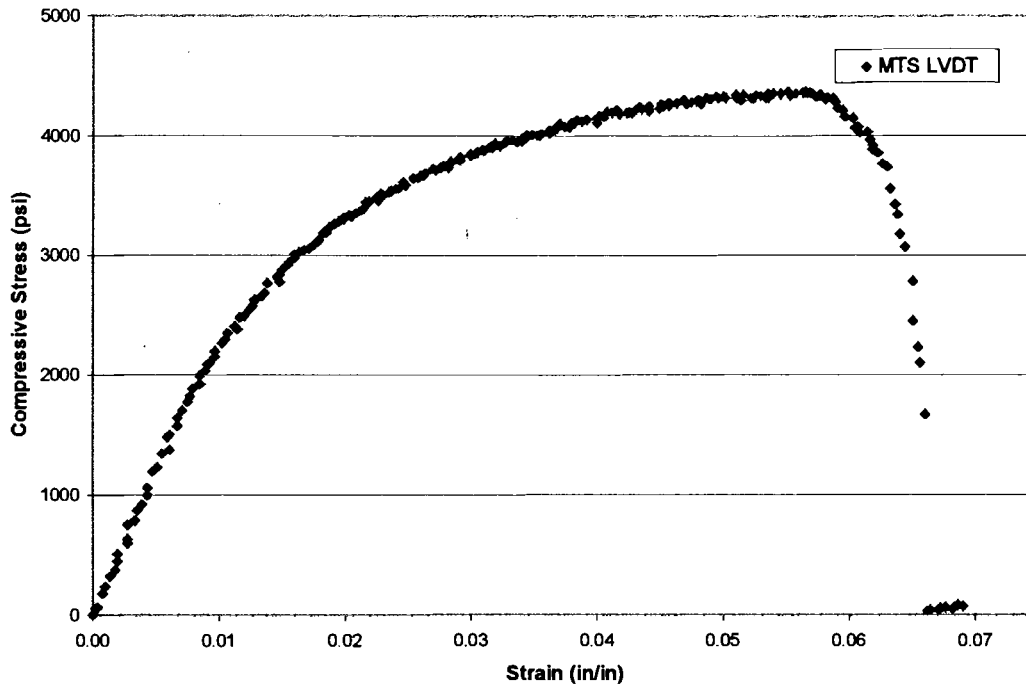


**a. Test Specimen ATS-03-xy**

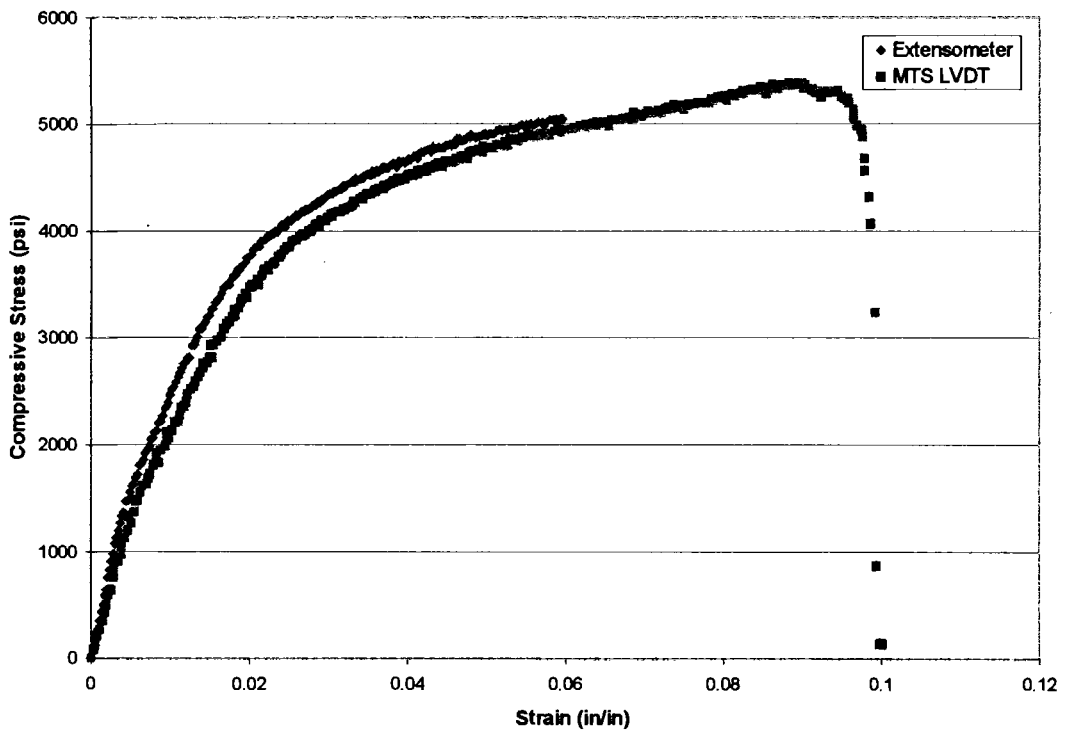


**b. Test Specimen ATS-04-xy**

**Figure H.3 – XY-Plane Stress-Strain Curves (continued)**

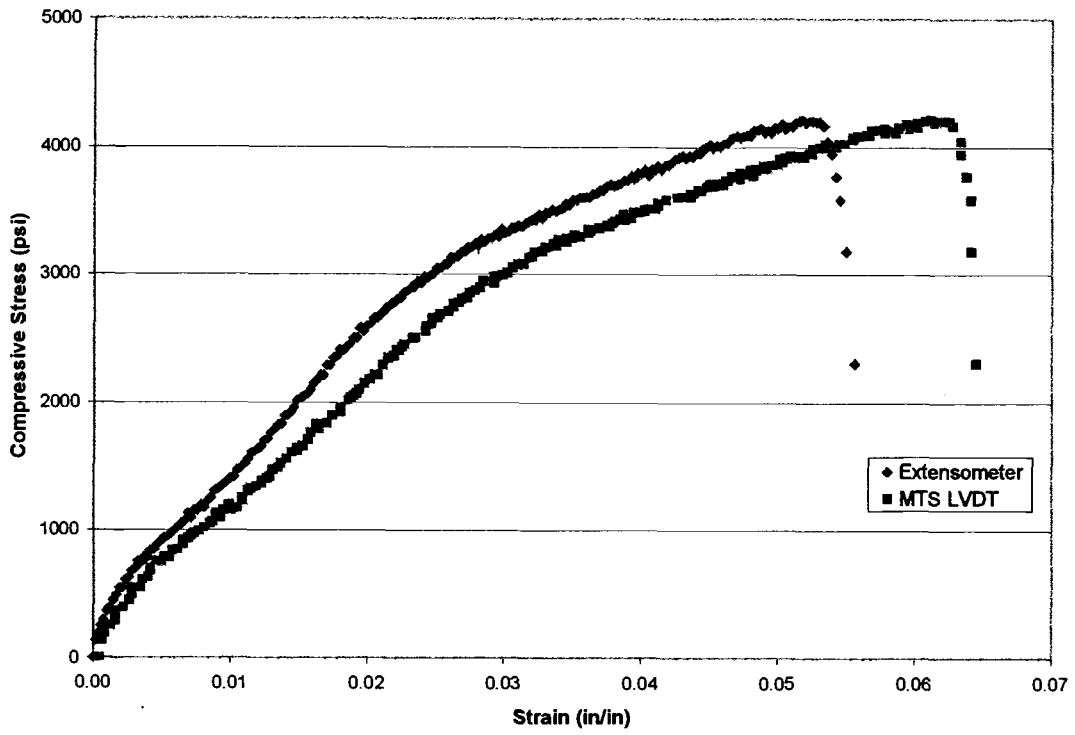


**c. Test Specimen ATS-05-xy**

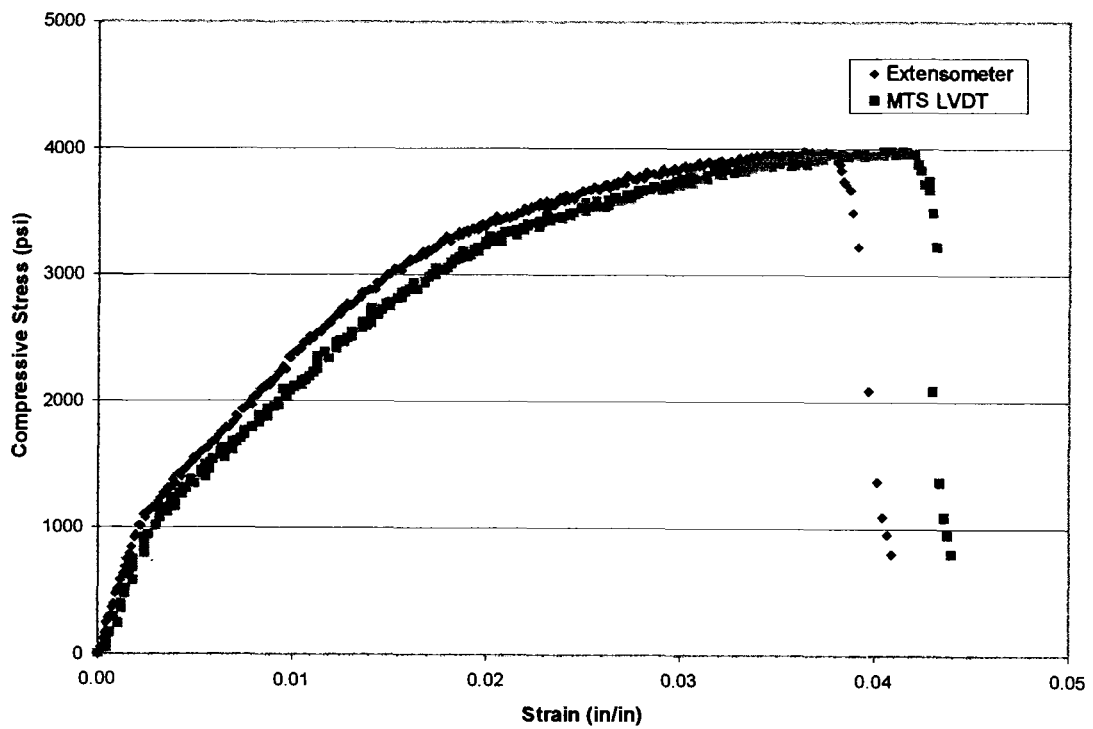


**d. Test Specimen ATS-07-xy**

**Figure H.3 – XY-Plane Stress-Strain Curves (continued)**



**e. Test Specimen ATS-08-xy**



**f. Test Specimen ATS-09-xy**

## **Biography of The Author**

Josh Walls was born in Portland, Maine on November 2, 1975. He was raised on Cousins Island, Yarmouth, Maine and graduated from Yarmouth High School in 1995. He attended the University of Maine and graduated in May, 2000 with a Bachelor's degree in Mechanical Engineering. Josh is a candidate for the Master of Science degree in Mechanical Engineering from The University of Maine in May, 2002.